Étude des facteurs de la biogenèse des ribosomes dans les progéniteurs neuraux de poisson zèbre

Stéphanie Bouffard

UNIVERSITÉ PARIS SUD

Study of ribosome biogenesis factors in zebrafish neural progenitors

Thèse de doctorat de l'Université Paris-Saclay
préparée à l'Université Paris Sud

École doctorale n°577
Structure et dynamique des systèmes vivants (SDSV)
Spécialité de doctorat: Sciences de la vie et de la santé

Thèse présentée et soutenue à Gif-sur-Yvette, le 22 septembre 2017, par

Stéphanie Bouffard

Composition du Jury :

Sébastien Bloyer — Président
Professeur, Université Paris Sud (Institut de Biologie Intégrative de la Cellule)

Filippo Del Bene — Rapporteur
Directeur de recherche, Institut Curie (Génétique et biologie du développement)

Paul Trainor — Rapporteur
Professeur, The University of Kansas School of Medicine (Stowers Institute for Medical research)

Virginie Marcel — Examinatrice
Chargée de recherche, INSERM (Centre de recherche en cancérologie de Lyon)

Sylvie Schneider-Maunoury — Examinatrice
Directrice de recherche, INSERM (Institut de Biologie Paris Seine)

Jean-Stéphane Joly — Directeur de thèse
Directeur de recherche, INRA (Paris-Saclay Institute of Neuroscience)

Françoise Jamen — Invitée
Maître de conférences, Université Paris Sud (Paris-Saclay Institute of Neuroscience)

A ma mamie, j'aurais tant aimé que tu sois là…

REMERCIEMENTS

Comme tout étudiant en thèse ayant terminé l'écriture de son manuscrit, ce n'est pas sans émotion ou nostalgie que j'écris ces remerciements. Ces trois années de thèse furent remplies d'une multitude de petits moments de bonheur, de peur, de stress et d'excitation. Ce serait mentir que de dire que je n'ai pas eu envie de tout lâcher à certains moments ou que je n'ai pas eu peur de l'échec de ce projet. Cependant, j'ai eu la chance d'être entourée par des personnes exceptionnelles, qui ont su me remotiver, me conseiller, m'épauler tout au long de cette aventure, à la fois à la fois dans ma sphère professionnelle et dans ma vie privée.

Mes premiers remerciements vont vers le Dr Jean-Stéphane Joly, sans qui cette aventure n'aurait jamais été possible. Il a su me faire confiance à la sortie de mon master en me confiant un projet intéressant et ambitieux. Jean-Stéphane, je tiens à t'exprimer toute ma gratitude. Tu as su me soutenir aux moments clés et tu as toujours été très présent malgré la grande quantité de choses que tu dois gérer tous les jours. J'ai particulièrement apprécié ton investissement à la fois professionnel mais aussi et surtout personnel. Tu as su déceler les moments où j'avais besoin de me confier et tu as su me redonner le moral. Pour toutes ces qualités humaines, travailler à tes cotés a été plus qu'agréable. Je garderai un excellent souvenir de ta bonne humeur, en particulier lors de notre petit voyage en Suède.

Je tiens également à remercier Françoise Jamen, qui m'a donné l'opportunité de travailler sur ce projet de recherche.

Je tiens à remercier le Dr. Filippo Del Bene et le Dr Paul Trainor d'avoir accepté d'être les rapporteurs de mon travail de thèse. Je remercie également le Dr. Virginie Marcel, le Dr. Sylvie Schneider-Maunoury et le Dr. Sébastien Bloyer d'avoir accepté d'être examinateurs lors de ma soutenance de thèse.

Je suis aussi très reconnaissante envers les membres de mon comité de thèse : Paula Alexandre, Pierre-Emmanuel Gleizes, Georges Lutfalla et Jean-Paul Concordet, qui ont pris de leur temps pour m'aiguiller et me prodiguer des conseils avisés. Par ailleurs, je tiens à spécialement rendre honneur à Nicolas David qui a joué le rôle de tuteur pendant ma deuxième année. Tes recommandations et ta vision du projet m'ont aidé à avancer et à évoluer.

Cette thèse n'aurait pas été la même sans le soutien immensurable de mes proches que ce soit au laboratoire ou dans ma vie privée.

Tout d'abord, c'est grâce aux membres de l'équipe CASBAH que j'ai réussi à avancer pendant ces trois années. En particulier, mes colocataires de bureau qui m'ont supportée, conseillée, soutenue et rassurée à chaque fois que j'en avais besoin.

Aurélie, tous ces moments de partage, de rigolades, de discussions entre filles vont terriblement me manquer. J'ai adoré partager le bureau avec toi, que ce soit nos moment d'hystérie et de stress, nos discussions scientifiques indispensables, ou toutes les petites histoires et nombreux potins qu'on a partagés. Je te souhaite beaucoup de courage pour l'écriture de ta thèse et j'espère être aussi présente pour toi que tu l'as été pour moi.

Matthieu, malgré ton obsession sur l'évolution, j'ai beaucoup apprécié travailler à tes côtés. Tu m'as beaucoup aidée, que ce soit à l'animalerie, dans la finalisation de mes travaux ou avec les nombreuses discussions professionnelles que nous avons eues et qui m'ont fait évoluer scientifiquement. En particulier, je tiens à te remercier sincèrement pour tout le temps passé à la relecture de mon manuscrit. Sans tes conseils précieux et tes remarques précises je n'aurais jamais réussi à rendre un manuscrit dont je suis fière. Ta joie de vivre et ta bonne humeur ont été un rayon de soleil pendant ces trois années.

Emilie et Alessandro, anciens membres de l'équipe, j'ai eu la chance de travailler avec vous au début de ma thèse et de rester en contact régulièrement. Vous êtes restés dans mon cœur malgré l'éloignement. Alessandro, merci pour ton soutien à distance, ton oreille attentive sur Skype et ta grande implication pour la relecture de mon manuscrit de thèse.

Rosaria, j'ai passé d'excellents moments à tes côtés. Nos pauses café me manquent terriblement, ainsi que nos conversations sur toute une diversité de sujets. Cette année de cohabitation dans le bureau m'a apporté énormément à la fois du point de vue professionnel que personnel. Tu es une amie formidable que je garderai je l'espère pour très longtemps.

Jean-Michel, merci pour ta sagesse scientifique et tes conseils précieux sur mon projet.

Que serait une thèse dans le département DevEvo, sans la joie de vivre apportée par les équipes voisines : AMAGEN (Sosthène le roi du clonage, qui trouve toujours le surnom flatteur, Naïma pour son sourire et sa joie de vivre, Joanne pour sa gentillesse et sa douceur), DECA (Lucie, qui connait le même stress de thésarde que moi, Victor avec qui j'ai beaucoup ri dans le couloir, Maryline pour ces conseils avisés et son soutien, Carole

pour son oreille attentive (et pas qu'aux Astyanax), Jorge pour sa bonne humeur, Sylvie, et Stéphane) et TCF. Mon cœur est rempli d'émotions en pensant à tous ces bons moments et ces franches rigolades qui ont eu lieu dans le couloir.

Je voudrais spécialement rendre hommage à tous les membres du TCF. Vous m'avez tous apporté à la fois humainement, scientifiquement et techniquement : Pierre pour ton expertise technique et ton humour (parfois effrayant) ; Arnim pour le partage de ta connaissance très étendue et les chamailleries dans le laboratoire ; Sylvain pour ces longues conversations sur toutes les choses de la vie et pour ton aide sur mon projet (grâce à moi tu sais monter les embryons en agarose comme personne !) ; Lionel pour toutes les infos inutiles que tu nous donnes chaque jour, et les vidéos étranges que tu trouves sur internet ; Elodie pour tout ton soutien dans cette fin de thèse, ton aide précieuse dans les expériences et ta présence à mes côtés pendant les derniers moments de l'écriture de manuscrit (comme ton aide a été si précieuse !); Johanna (ma jojo, ma grande sœur de cœur) pour toutes ces conversations dans la voiture, pour ton épaule sur laquelle j'ai beaucoup pleuré, pour tes conseils sages et ton soutien, malgré que tu sois obsédée par la langue française (malgré que !) et notre phobie partagée.

Ma myrtille et ma framboise, mes rayons de soleil du laboratoire. Qu'auraient été ces années sans vous à mes côtés, sans votre amitié si précieuse, sans nos sorties entre filles, sans nos rigolades et nos bêtises. Aucun mot n'est assez fort pour vous exprimer tout ce que je ressens pour vous.

Mes copines de facs, qui pour la plupart se sont également lancées dans l'aventure de la thèse, merci pour ces bières et ces repas partagés, en discutant de la vie, de la thèse et de notre avenir.

Je n'aurais jamais effectué cette thèse si je n'avais croisé le chemin d'une personne admirable et exceptionnelle : Raphaëlle, tu m'as inspirée et donné l'envie de faire de la recherche.

Enfin je souhaite remercier de tout cœur ma famille sans qui tout ça n'aurait jamais été possible. Tout d'abord, ma maman et ma grande sœur chérie. Vous avez été présentes et m'avez beaucoup soutenue depuis le début de mes études. Vous avez été compréhensives et avez su me remonter le moral quand ça n'allait pas, me motiver, me montrer votre fierté et m'épauler tout au long de ces années universitaires, et pas seulement lors de cette thèse. J'ai une chance inouïe d'avoir une famille si amante et si soudée. Tous les remerciements

du monde ne feront jamais assez honneur à l'importance que vous avez pour moi et à la valeur de ce que vous m'apportez chaque jour de ma vie. J'ai également une grosse pensée pour mon papi, qui malgré son éloignement, me soutient. J'ai une pensée particulière pour ma grand-mère, partie avant de pouvoir assister à la finalisation de tant d'années de travail. Mamie, je sais à quel point tu étais fière de moi, et j'aurais tant aimé avoir ta présence pour cette nouvelle page qui se tourne.

Et pour finir, je tiens tout particulièrement à remercier Vanou qui partage mon quotidien. Sans toi la vie n'aurait pas le même goût, sans toi ces deux dernières années n'auraient pas été les mêmes. Tu as su me soutenir, me supporter (le mot est faible car vivre avez une thésarde en phase d'écriture n'est pas facile tous les jours), me redonner confiance en moi, me motiver et me consoler tout au long de ce périple. Tu as donné un sens à ma vie, et ma permis de grandir, d'évoluer, de mûrir et de savoir ce que je voulais pour notre vie future. Je pense que je te ne remercierai jamais assez de tout ce que tu fais pour moi et du bonheur que tu apportes dans ma petite vie. Tout simplement et sincèrement merci de tout cœur. Je suis impatiente de commencer cette nouvelle vie avec toi.

ABSTRACT

Ribosome biogenesis is a highly complex process leading to the formation of the translational machinery. While this process has been considered as a "house-keeping" mechanism, recent highlights have stressed out the specificity of this process. Hence, translation has emerged as an essential regulation step of gene expression.

Zebrafish optic tectum (OT) is a suitable model to study cell proliferation since cells at different differentiation states are spatially partitioned. Slow-amplifying progenitors (SAPs), fastly-amplifying progenitors (FAPs) and differentiated cells are found in adjacent domains of the OT, as a consequence of its oriented growth. Interestingly, around 50 genes display restricted expression in the external tectal marginal zone (TMZe) where SAPs are localized. Strikingly, many "TMZe genes" code ribosome biogenesis factors.

Such an accumulation of transcripts for ubiquitously expressed genes in SAPs is a very surprising feature. Thus, during my PhD, I examined whether ribosome biogenesis may have specific roles in TMZe cells focusing on their involvement in cell cycle regulation. Taking advantage of a previous transcriptomic analysis, I screened for new candidates accumulated in SAPs.

To study the link between ribosome biogenesis and cell cycle regulation, I decided to focus on the *proliferation-associated 2G4* (*pa2g4)*, which has been shown so far to promote or repress cell proliferation in several species. In particular, it is involved in tumorigenesis either as a tumor suppressor, or as an oncogene. I designed a strategy for the inducible and specific over-expression of this gene using the UAS/ERT2-GAL4 system.

In addition, Fibrillarin (Fbl), a small nucleolar proteins involved in the methylation of pre-ribosomal RNAs (rRNAs) and the histone in ribosomal DNA (rDNA) loci, was also preferentially expressed in SAPs. Fbl also plays an important role in stem cell identity and cycle regulation as demonstrated by its involvement in cancer. I performed a functional study of Fbl using a zebrafish mutant line. I showed that mutant embryos displayed specific midbrain defects linked to a massive apoptosis and disruption of neural differentiation in the OT. I also demonstrated deficiencies in ribosome biogenesis and a decrease of the ribosome translational activity. Furthermore, *fbl* mutants showed severe deregulation of the cell cycle in the whole tectum with impaired S-phase progression. Taken together, our data suggest an essential role for Fbl in zebrafish neural progenitors, *via* the regulation of cell cycle proliferation.

Collectively, these data highlight how ribosome biogenesis factors contribute to the fine regulation of progenitor cell proliferation thereby contributing to the regulation of cell cycle progression.

RESUME

La biogenèse des ribosomes est un processus extrêmement complexe permettant la mise en place de la machinerie traductionnelle. Alors que ce processus a été considéré comme un mécanisme ubiquiste pendant des années, de nouvelles études ont mis en avant la spécificité cellulaire de ce processus. Ainsi, la traduction des protéines est apparue comme une étape essentielle de régulation de l'expression génique.

Le toit optique (TO) du poisson-zèbre est un modèle idéal pour étudier la régulation de l'identité cellulaire compte tenu de la répartition spatiale des cellules qui se trouvent à différents stades de détermination. Les progéniteurs lents (SAPs), les progéniteurs rapides (FAPs) et les cellules différenciées sont localisés dans des domaines adjacents du TO, conséquence de sa croissance orientée. Environ 50 gènes sont fortement exprimés dans les cellules de la zone marginale externe du toit optique (TMZe), où se trouvent les SAPs. De manière intéressante, beaucoup de gènes exprimés préférentiellement dans la TMZe codent des facteurs de la biogenèse des ribosomes.

Ainsi, au cours de mon doctorat, j'ai étudié le rôle spécifique que pourraient avoir les facteurs de biogenèse des ribosomes dans les cellules de la TMZe, en me concentrant sur leur implication dans la régulation du cycle cellulaire. Tirant profit d'une précédente analyse transcriptomique, j'ai criblé de nouveaux candidats accumulés dans les SAPs.

Parmi ces candidats, j'ai décidé de me concentrer sur le gène *pa2g4* (*proliferation-associated 2G4)* qui joue un rôle dans la promotion ou la répression de la prolifération cellulaire dans plusieurs espèces. En particulier, *pa2g4* est impliqué dans la tumorigenèse, en tant que suppresseur de tumeur, ou au contraire en tant qu'oncogène. J'ai mis en place une stratégie d'étude fonctionnelle permettant l'étude inductible et spécifique de ce gène dans les différents types cellulaire du TO, en utilisant le système UAS/ERT2-GAL4.

D'autre part, Fibrillarin (Fbl), une protéine nucléolaire impliquée dans la méthylation des ARN ribosomiques (« ribosomal RNAs », rRNAs) et des histones de l'ADN ribosomique (« ribosomal DNA », rDNA), est également préférentiellement exprimée dans les SAPs. De plus, la surexpression de Fbl dans les cellules cancéreuses, démontre son rôle important dans la régulation du cycle cellulaire. J'ai ainsi réalisé une étude fonctionnelle de Fbl en utilisant une lignée de poisson-zèbre mutée pour ce gène. J'ai montré que les embryons mutants affichent des défauts spécifiques du cerveau moyen liés à une apoptose massive et à une perturbation de la différenciation neurale du TO. J'ai également montré des défauts de biogenèse des ribosomes et une diminution de l'activité traductionnelle de ces derniers. En outre, les mutants *fbl* montrent une dérégulation sévère du cycle cellulaire dans l'ensemble du TO, avec une progression de la phase S perturbée. Cette étude suggère un rôle essentiel de Fbl dans les progéniteurs neuraux du poisson zèbre, *via* une régulation de la prolifération cellulaire.

L'ensemble de ces résultats montre comment les facteurs de la biogenèse des ribosomes contribuent à la régulation fine de la prolifération cellulaire des progéniteurs, et donc à la régulation de la progression du cycle cellulaire.

SYNTHESE

La biogenèse des ribosomes est un processus très conservé et longtemps considéré comme ubiquitaire. Cependant, de nombreuses études récentes ont démontré l'importance de cette voie dans la régulation de l'expression génique. En effet, bien que l'étude de la régulation de l'identité cellulaire a longtemps été focalisée sur les mécanismes transcriptionnels, l'idée émerge que la régulation de la traduction joue également un rôle dans la détermination et le devenir des cellules. En particulier, les cellules souches présenteraient une biogenèse des ribosomes particulière avec des facteurs de biogenèse des ribosomes (RBF) qui leur sont propres (**Brombin et al., 2015**). Ainsi, ces « ribosomes spécialisés » contribueraient au contrôle de l'expression des gènes de par leur affinité sélective pour certaines catégories d'ARNm. L'existence de ribosomopathies, désignant un groupe de maladies causées par une mutation sur les gènes codant pour les protéines ribosomiques ou les protéines nécessaires à la synthèse de ribosomes, représentent un élément supplémentaire en faveur de cette notion de spécificité. Néanmoins, cette notion de ribosomes filtreurs (**Mauro and Edelman, 2007**) a été principalement mise en évidence *in vitro*. L'identité des cellules souches et des progéniteurs, comme celle de tout type cellulaire est caractérisée par des signatures moléculaires spécifiques qui dépendent de l'environnement dans lequel les cellules se trouvent. Ainsi, il est primordial d'étudier ces cellules dans un contexte *in vivo*.

Au cours de mon doctorat, j'ai utilisé le toit optique (TO), structure dorsale du cerveau moyen, du poisson-zèbre comme modèle pour étudier le rôle des RBFs dans la régulation de l'identité et le devenir cellulaire des progéniteurs neuraux. En effet, cette structure présente un mode de croissance en « tapis roulant cellulaire », lui conférant une organisation cellulaire idéale. Ainsi, les progéniteurs neuroépithéliaux à cycle court (SAPs) sont présents dans la zone

marginale externe du toit optique (TMZe; **Joly et al., 2016**). Les progéniteurs à cycle rapide (FAPs), les cellules post-mitotiques et les neurones différenciés sont situés au centre de la structure. Chaque population cellulaire est marquée par des profils d'expression particuliers. Ainsi, une recherche dans la base de ZFIN nous a permis d'identifier environ 50 gènes dont le transcrit est accumulé dans les cellules de la TMZe (SAPs). De manière intéressante, une vingtaine de ces gènes codent pour des facteurs de la biogenèse des ribosomes.

L'accumulation de ce type de transcrits dans les progéniteurs lents étaient surprenantes. Ainsi, au cours de mon doctorat, j'ai étudié le rôle spécifique de facteurs de biogenèse des ribosomes dans le maintien des progéniteurs neuroépithéliaux de la TMZe. En particulier, les transcrits de *fibrillarin* (*fbl*), un gène codant une protéine nucléolaire impliquée dans la biogenèse des ribosomes, sont préférentiellement accumulés dans les progéniteurs lents du toit optique. Fbl correspond au centre catalytique du complexe ribonucléoprotéique box C/D, responsable une de la méthylation des ARN ribosomiques (ARNr). D'autre part, Fbl intervient également joue dans la méthylation des histones des loci d'ADN ribosomique (ADNr) et joue un rôle dans la régulation de la transcription et du clivage des ARNr (**Tessarz et al. 2014**).

Au cours des dernières décennies, de nombreuses études fonctionnelles ont souligné l'important de Fbl dans divers processus cellulaire. En particulier, des études fonctionnelles de perte de fonction effectuées chez la levure et la souris, ont montré que Fbl jouait un rôle crucial dans la survie cellulaire et le développement précoce. En outre, **Watanabe-Susaki et al**. ont mis en évidence l'importance de Fbl dans l'homéostasie cellulaire et l'identité des cellules souches, à travers la régulation de la pluripotence et l'alibilité des cellules souches pluripotentes de se différencier (**Watanabe-Susaki et al. 2014**). Fbl intervient également dans la régulation du cycle cellulaire, comme démontré par le niveau anormalement élevée de la

protéine dans plusieurs cancers (**Marcel et al. 2013; Su et al. 2014**), tels que le cancer du sein, le carcinome cervical à cellules squameuses (**Choi et al. 2007**) et le néoplasie intra-épithéliale prostatique (**Koh et al. 2011**). En particulier, **Marcel et al.** ont montré que la surexpression de FBL contribuait à la tumorigenèse. En effet, dans les lignées de cellules cancéreuses de sein, la surexpression de FBL conduit à une méthylation d'ARNr aberrante, une modification de l'activité ribosomique, une fidélité de traduction réduite et une augmentation de la traduction dépendante des sites d'initiation interne (IRES; **Marcel et al., 2013**). Inversement, la répression de *fbl* par siARN réduit la prolifération des cellules de lignées cancéreuses de sein (**Su et al., 2014**). La compréhension des rôles intégrés de Fbl dans la régulation du cycle cellulaire, la prolifération cellulaire et la biogenèse des ribosomes est donc devenue un réel challenge.

Mon projet de doctorat consistait donc à étudier le rôle de Fbl dans le développement du cerveau moyen, et en particulier du toit optique du poisson-zèbre. Ainsi, j'ai effectué une étude fonctionnelle en utilisant des poissons mutés pour le gène *fbl*. J'ai montré que les embryons mutants affichent des défauts spécifiques du cerveau moyen liés à une apoptose massive et à une perturbation de la différenciation neurale du TO. J'ai également montré des défauts de biogenèse des ribosomes et une diminution de l'activité traductionnelle des ribosomes. En outre, les mutants *fbl*^{hi2581} montrent une dérégulation sévère du cycle cellulaire dans l'ensemble du toit optique, avec une progression de la phase S perturbée. Ce défaut est surprenant car les défauts de biogenèse des ribosomes, menant souvent à un stress ribosomiques, provoquent un blocage du cycle à la transition G1-S ou G2-M mais à ce jour aucun arrêt en phase S après mutation d'un facteur de biogenèse des ribosomes n'a été mis en évidence. Cette étude suggère donc un rôle essentiel de Fbl dans les progéniteurs neuraux du poisson-zèbre, via une régulation de la prolifération cellulaire.

En parallèle, j'ai tiré profit d'une étude transcriptomique afin de cribler de nouveaux candidats accumulés dans les SAPs. Parmi ces candidats, j'ai décidé de me concentrer sur le gène *pa2g4* qui jour un rôle dans la promotion ou la répression de la prolifération cellulaire dans plusieurs espèces. En particulier *pa2g4* est impliqué dans la tumorigenèse en tant que suppresseur de tumeur ou au contraire qu'oncogène. Afin d'effectuer l'étude fonctionnelle de *pa2g4* j'ai mis en place une stratégie permettant la surexpression inductible et spécifique de ce gène dans les différents types cellulaires du TO, en utilisant le système UAS/ERT2-GAL4. J'ai caractérisé finement le patron d'expression de pa2g4 chez la larve de 2 et 3 jours post fécondation (dpf) ainsi que dans le cerveau de juvénile de 1 mois. Les transcrits comme la protéine codés par *pa2g4*, sont accumulés dans les progéniteurs neuroépithéliaux du toit optique. J'ai également mis en place les lignées transgéniques nécessaires à la surexpression de ce gène.

L'ensemble de ces résultats mettent en évidence l'importance de la biogenèse des ribosomes dans la régulation fine de l'homéostasie cellulaire, et dans la détermination de l'identité des progéniteurs neuroépithéliaux.

Introduction

1. La biogenèse des ribosomes, voie ubiquitaire considérée maintenant comme régulatrice.

Chez les eucaryotes, les ribosomes sont formés par l'association de deux sous-unités : la petite sous-unité appelée 40S et la grande sous-unité appelée 60S. Chacune de ces sous-unités est composée d'ARN ribosomiques (ARNr) et de protéines ribosomiques.

La biogenèse des ribosomes, et en particulier la synthèse des ARN ribosomiques, commencent par la transcription de l'ADN ribosomique par l'ARN polymérase I, dans le nucléole, en un ARN polycistronique. Cet ARN est ensuite modifié (méthylé et pseudo-uridinylé) et clivé pour donner naissance aux divers ARN ribosomiques formant les deux sous-unités ribosomiques. En parallèle, dans le cytoplasme, les protéines ribosomiques sont synthétisées. Elles s'associent progressivement, au cours de la maturation des ARNr, à différentes étapes du processus.

Cette voie est hautement régulée et coordonnée. Ainsi, elle requiert l'action de plus de 200 facteurs appelés « facteurs de biogenèse des ribosomes ». Ces derniers jouent un rôle à toutes les étapes de maturation, de la transcription jusqu'à l'exportation dans le cytoplasme des sous-unités et à l'assemblage d'un ribosome mature et fonctionnelle.

La biogenèse des ribosomes, malgré son apparente fonction ubiquiste, apparait maintenant comme spécifique en fonction du type cellulaire ou tissulaire. En effet, de nombreuses études, en particulier chez les téléostéens, ont démontré que les facteurs de biogenèse des ribosomes étaient exprimés préférentiellement dans certains types cellulaires. En particulier, la spécificité de la voie a été mise en évidence dans les cellules souches, en comparaison avec les cellules différenciées. Dans ces cellules souches, la voie de biogenèse, légèrement différente, serait responsable de la formation de ribosomes spécialisés. La notion de

ribosomes spécialisés ou ribosomes filtreur, encore débattue aujourd'hui, présente le ribosome comme un régulateur, choisissant les ARNm qui seront traduits. Ainsi, pour une même quantité d'ARNm entre deux cellules, une régulation traductionnelle s'ajouterait, afin de produire un traductome spécifique qui pourrait avoir un rôle dans l'homéostasie des cellules souches.

2. Le toit optique du poisson-zèbre comme modèle d'étude de l'homéostasie des cellules souches

Dans notre laboratoire, nous utilisons le toit optique du poisson-zèbre afin d'étudier l'homéostasie des cellules progénitrices, en prolifération. Le toit optique est une structure dorsale, appartenant au cerveau moyen. Il est composé de deux lobes, dont la croissance se fait en tapis roulant, par addition de colonnes de cellules à la périphérie de chaque lobe. Cette croissance originale produit un gradient de différenciation de la périphérie vers le centre de la structure. La population de cellules en prolifération se restreint progressivement au cours du développement du poisson-zèbre. Alors que dans les stades précoces de somitogenèse, la population en prolifération se trouve dans l'intégralité du tube neural, elle est progressivement restreinte à deux jours de développement à la périphérie du toit optique. En particulier, la couche cellulaire située à la périphérie du toit optique est composée de cellules neuroépithéliales caractérisées par leur polarité apico-basale et leur absence de marqueurs gliaux. En revanche, la signature moléculaire de ces progéniteurs neuro-épithéliaux n'a pas encore été identifiée. Ainsi, dans le laboratoire, deux analyses parallèles ont été utilisées afin de déterminer la signature moléculaire. Dans un premier temps, une analyse de patron d'expression a été faite chez l'embryon de poisson-zèbre. Environ 50 gènes semblent exprimés préférentiellement dans les cellules progénitrices de la périphérie du toit optique,

où se trouvent les cellules neuro-épithéliales. Dans un second temps, une analyse transcriptomique, dans les cerveaux de medaka juvénile, a été réalisée. De manière similaire, 500 gènes ont été identifiés comme étant surexprimés dans les cellules neuroépithéliales.
De manière intéressante, parmi ces gènes, plusieurs gènes de biogenèse des ribosomes sont présents.

3. But de la thèse

Sachant que le biogenèse des ribosomes a été montré comme spécifique, et que plusieurs facteurs de biogenèse sont préférentiellement exprimés dans les cellules neuro-épithéliales du toit optique du poisson-zèbre, le but de ma thèse était de comprendre comment les facteurs de biogenèse des ribosomes étaient impliqués dans le contrôle du cycle cellulaire et de l'identité cellulaire. En particulier, j'avais pour but de comprendre pourquoi ces facteurs étaient préférentiellement exprimés dans notre population d'intérêt, et s'ils avaient un rôle spécifique.

Pour cela j'ai travaillé sur deux projets pendant lesquels j'ai étudié le rôle spécifique de ces facteurs dans le développement du toit optique du poisson-zèbre.

Résultats

1. Identification d'un gène candidat pouvant jouer un rôle dans la biogenèse des ribosomes et dans le contrôle du cycle cellulaire.

Dans la première partie de mon doctorat, j'ai utilisé les données provenant de l'analyse transcriptomique performée dans le cerveau de médaka. Parmi les gènes surexprimés dans les cellules neuroépithéliales, 17 gènes ont un rôle dans la biogenèse des ribosomes. De plus, parmi ces 17 candidats, 9 n'étaient pas identifiés au préalable. J'ai donc commencé ce projet

en validant le patron d'expression restreint de ces 9 candidats. Parmi eux, 4 gènes montraient une expression préférentielle dans la zone où les cellules neuroépithéliales sont localisées.

J'ai ensuite concentré mon attention sur *pa2g4*, un gène associé à la prolifération. En effet, une analyse du contexte scientifique a permis de mettre en évidence le rôle potentiel de *pa2g4* dans la biogenèse des ribosomes, par son association avec des précurseurs d'ARN ribosomiques et les deux sous-unités des ribosomes. Une analyse plus précise du patron d'expression de pa2g4 au niveau de l'ARNm et de la protéine, pendant l'embryogenèse et à l'état juvénile a mis en évidence une expression préférentielle dans la zone de prolifération du toit optique. De plus, la caractérisation des cellules dans lesquelles la protéine Pa2g4 s'accumule, a permis de démontrer que Pa2g4 est préférentiellement exprimées dans les cellules neuroépithéliales de la zone de prolifération du toit optique.

Ainsi *pa2g4* semble être un candidat idéal impliqué dans la biogenèse des ribosomes et la prolifération cellulaire des cellules neuroépithéliales du toit optique. L'étude du rôle spécifique de ce gène sera faite par surexpression dans les différents types cellulaires du toit optique. Pour cela, nous souhaitons utiliser le système UAS/GAL4. J'ai ainsi commencé la génération et caractérisation de plusieurs lignées transgéniques nécessaires pour cette surexpression. Cette analyse spécifique mettrait en évidence le rôle spécifique de *pa2g4* dans la régulation du cycle cellulaire.

2. Fibrillarine est essentielle dans la progression de la phase S et dans la spécification neuronale dans le cerveau moyen du poisson-zèbre.

Dans la deuxième partie de mon doctorat, j'ai étudié le rôle de Fibrillarine (Fbl) dans le développement embryonnaire du poisson-zèbre. Fibrillarine, est une méthyltransférase responsable de la méthylation des ARNr et des histones de l'ADNr. Elle fait partie du complexe

box C/D. Afin d'étudier le rôle de Fbl, j'ai en premier lieu étudié son patron d'expression pendant le développement. fbl est exprimé de manière ubiquitaire aux stades de gastrulation et de somitogenèse. Son expression se restreint à partir de 24 heures de développement. A ce stade, l'ARNm est présent dans la totalité du toit optique où les cellules prolifératrices sont présentes. A 2 et 3 jours de développement, son expression dans le toit optique se restreint davantage, avec une expression à la périphérie de la structure, où les cellules neuroépithéliales sont localisées.

Afin d'étudier le rôle de Fbl, j'ai utilisé un mutant, généré par insertion rétroviral et fournit par le ZIRC. Ce mutant présente un phénotype morphologique dès 1 jour de développement. En particulier, on peut distinguer une désorganisation du cerveau et une réduction apparente de la taille des yeux. A 2 jours de développement, le phénotype s'amplifie. On peut distinguer une réduction apparente de la taille de la tête et des yeux, une augmentation de la taille du vitellus, et un œdème péri-cardiaque.

La Fbl ayant un rôle dans la biogenèse des ribosomes, j'ai tout d'abord étudié la voie dans les embryons mutants à 3 jours de développement. Pour cela, j'ai utilisé deux approches. Dans la première approche, j'ai performé de PCR quantitative en utilisant des amorces spécifiques de différentes séquences permettant de distinguer les différents états de maturation des ARNr. Cette analyse a mis en évidence une réduction massive de la quantité de l'ARN 18S, sans modification significative de la quantité des séquences internes progressivement clivées pendant cette voie. Ceci montre un défaut de biogenèse, dans les étapes tardives de la voie. J'ai également performé une étude du profil des polysomes dans ces embryons mutants. Cette technique permet d'estimer la quantité des deux sous-unités, des ribosomes et aussi des polysomes qui correspondent à l'association des ribosomes sur les ARNm. J'ai ainsi mis en

évidence un défaut quantitatif des polysomes, représentant l'activité traductionnelle de ces unités fonctionnelles.

Les mutants *fbl* montrent un défaut morphologique principalement localisé dans la région de la tête. Ainsi, j'ai quantifié l'apparente réduction de la taille du système nerveux central (SNC) et des yeux. Pour cela, j'ai utilisé un marquage DiI permettant de marquer les fibres, suivi d'une segmentation. La quantification des régions segmentées a permis de mettre en évidence une réduction massive de la taille du SNC et des yeux.

Afin d'étudier plus précisément les défauts observées dans le cerveau de nos mutant, j'ai performé une étude histologique qui a mis en évidence un défaut dans la taille du toit optique, contenant des trous acellulaire. De plus, une étude au niveau nucléaire du toit optique a démontré un défaut dans la forme et la taille des noyaux. En effet, alors que les noyaux dans le centre du toit optique des embryons sauvages apparaissent ronds, ils sont allongés et orientés dans le centre du toit optique des embryons mutants. Ce changement de forme pourrait être dù à un changement d'état de la chromatine dans nos mutants, et à un changement d'état de différenciation de nos cellules. Ainsi, j'ai étudié la différenciation cellulaire dans le cerveau d'embryons. J'ai pu détecter une absence de différenciation dans la partie dorsale du toit optique, avec un maintien de la différenciation dans les parties antérieure et ventrale du cerveau. Ceci montre un rôle spécifique de la Fibrillarine dans la croissance et la différenciation de la partie dorsale du cerveau moyen.

La réduction du volume du SNC pourrait être due à une apoptose massive ou à des défauts de prolifération. J'ai donc tout d'abord étudié l'apoptose dans nos mutants en utilisant le marquage TUNEL. A un jour de développement, on peut identifier une augmentation des cellules en apoptose dans les embryons mutants.

J'ai également étudié la prolifération cellulaire dans nos mutants. Pour cela j'ai marqué les cellules en prolifération, en phase S et en phase de mitoses. Pour chacun de ces marquages, dans l'embryon sauvage, les cellules en prolifération peuvent être détectées dans la périphérie du toit optique. En revanche, dans les embryons mutants, les cellules en prolifération sont localisée dans le centre et la périphérie du toit optique ce qui démontre un défaut dans la distribution spatiale des cellules progénitrices.

Des analyses par cytométrie en flux de la distribution de ces cellules dans les différentes phases du cycle n'ont pas mis en évidence de blocage dans une des phases du cycle. En revanche, le profil de cytométrie en flux a mis en évidence un défaut dans la phase S. La quantification de cellules dans les différentes phases de la phase S, démontre une diminution du nombre de cellule en phase S précoce et une augmentation des cellules dans les phase S moyenne et tardive. Ainsi, ceci démontre que fbl a un rôle dans la progression de la phase S.

Conclusion

Lors de ma thèse, j'avais pour but d'étudier le rôle de la biogenèse des ribosomes dans la régulation du cycle cellulaire et de l'identité cellulaire. Par mes deux projets j'ai mis en évidence un rôle dans la progression du cycle cellulaire ainsi qu'un rôle tissu spécifique. Cette analyse ouvre un nouveau domaine d'étude de la régulation génique au niveau traductionnelle et démontre un rôle dans le control du devenir cellulaire des cellules neuronales.

TABLE OF CONTENTS

LIST OF FIGURES INTRODUCTION

LIST OF FIGURES RESULTS

Chapter 2

Chapter 3

LIST OF TABLES

LIST OF ABBREVIATIONS

5'TOP: 5' Terminal OligoPyrimidine

AC: acaete

AdoMet: S-adenosyl-L-methionine

ANB: anterior neural boundary

aPKC: atypical protein kinase C

Arf: alternative reading frame protein

AS: asense

AS-C: achaete-scute

Ato: atonal

Bag1: BCL2-associated anathogene 1

Bcl: B Cell Lymphoma

bp: base pair

bHLH: basic helix-loop-helix

BLBP: brain lipid binding protein

BMP: Bone Morphogenetic Protein

CB: Cajal body

CC: *corpus callosum*

CCB: Cellular Conveyor Belt

CCe: corpus cerebelli

Cdk: cyclin dependent kinase

CHH: Cartilage Hair Hypoplasia

Chk1: checkpoint kinase 1

CMZ: ciliary marginal zone

CNS: Central Nervous System

CRM: *cis*-regulatory module

Csde1: cold shock containing domain E1

Ctec: Commissura tecti

DBA: Diamond-Blackfan anemia

DC: decoding center

DFC: dense fibrillar centers

DG: *dentate gyrus*

Di: Diencephalon

DIC: differential interference contrast

DKC: dyskeratosis congenita

Dkk1: Dickkopf-related protein

Dll1: Delta-like 1

E2F-1: E2 transcription factor 1

eEF1a: eukaryotic translation elongation factor 1 alpha

EG: eminentia granularis

eIF: eukaryotic initiation factor

EM: electron microscopy

ER: endoplasmic reticulum

ERK: extracellular signal-regulated kinase

ESC: embryonic stem cell

ETS: External transcribed sequence

FACS: fluorescent activated cell sorting

FACT: Facilitator of Chromatin Transcription

FAP: fastly-amplifying progenitor

Fbl: Fibrillarin

FC: fibrillar center

Fgf: fibroblast growth factor

FISH: fluorescent *in situ* hybridization

FRAP: fluorescence recovery after photobleaching

Frzb1: frizzled-related protein

GAR: glycine and arginine rich

Gbx2: gastrulation brain homeobox 2

GC: granular component

GFP: green fluorescent protein

GFAP: glial fibrillary acidic protein

GLAST: Glutamate aspartate transporter

GMC: ganglion mother cell

Gs: glutamine synthetase

GSC: germinal stem cell

GTP: guanosine triphosphate

H2A: Histone 2A

Ha: habenula

Hipp: hippocampus

hnRNP: heterogeneous ribo-nucleoproteins

HSC: Hematopoietic stem cell

IGS: long intergenic spacer

INM: Interkinetic Nuclear Migration

IPC: intermediate progenitor cells

IPZ:isthmic proliferation zone

IRES: Internal Ribosome Entry Site

IsO: isthmic organizer

ITAF: IRES Trans Acting Factor

ITS: Internal transcribed sequence

IZ: intervening zone

Jag1: Jagged 1

K-turn: kink-turn

Lsc: lethal of scute

LSU: large subunit

LV: lateral ventricle

MAPK: Mitogen-Activated Protein Kinase

Mbm: Mushroom body miniature

Mdm2: Mouse double minute 2 homolog

MDS: mylodysplastic syndrome

Mes: mesencephalon

Met: methionine

MHB: midbrain/hindbrain boundary

MTase: methyltransferase

mTORC1: mammalian target of rapamycin complex 1

My: Myelencephalon

NAIC: North American Indian childhood cirrhosis

NePC: Neuroepithelial progenitor cell

NHP2l: Non-Histone Protein Like 1

NOP: nucleolar protein

NOR: nucleolus organizer region

NoRC: nucleolar chromatin remodeling complex

NP: neural progenitors

Npm1: Nucleophosmin

NS: Nucleostemin

NS1: non-structural protein 1

OB: olfactory bulb

ORF: Open reading frame

ORR: optic recess region

OT: optic tectum

Otx2: orthodenticle homologue 2

p53: tumor suppressor 53

PABP: PolyA Binding Protein

PFA: paraformaldehyde

Pa2g4: Proliferation-associated 2G4

Pax6: Paired Box 6

PBN: prenuclear bodies

PCNA: proliferating cell nuclear antigen

PCT: Peptidyl Transferase Center

Pes: Pescadillo

PGZ: periventricular grey zone

pH3: phospho-histone 3

PI3K: phosphoinositide 3-kinase

PIC: pre-initiation complex

Pi: phosphatidylinositol

PIP2 phosphatidylinositol-4.5-bisphosphate

PML: posterior mesencephalic lamina

PNB: prenucleolar bodies

PolI: Polymerase I

PolR1A: RNA Polymerase I Subunit A

PPAN: Peter Pan

pRb: retinoblastoma protein

PRMT: Protein arginine N-methylatransferase

Pro: prosencephalon

PTC: peptidyl transferase center

PTRF: Pol-I Transcript-Release Factor factors

RBF: ribosomal biogenesis factor

rDNA: ribosomal desoxyribonucleic acid

RGC: radial glial cell

Rhomb: Rhombencephalon

RMS: rostral migratory stream

RNA: ribonucleic acid

RNAse MRP: RNA component of the mitochondrial RNA processing complex

RNP: ribonucleoprotein

RP: ribosomal protein

RPL: Ribosomal Protein of the Large subunit

RPS: Ribosomal Protein of the Small subunit

rRNA: ribosomal ribonucleic acid

SAC: *stratum album centrale*

SAM: Rossmann-fold-S-adenosylmethionine

SAP: slowly-amplifying progenitor

Sc: scute

SC: stem cell

ScaRNA: small Cajal body-specific RNA

SFGC: *stratum fibrosum et griseum superficiale*

SG: synexpression group

SGC: *stratum griseum centrale*

SGZ: subgranular zone

siRNA: small interfering RNA

SL1: selectivity factor 1

SM: *stratum marginale*

SMN1: Survival of motor neurons 1

snoRNA: small nucleolar RNA

snRNA: small nuclear RNA

SO: *stratum opticum*

SoxB: SRY-related HMG box B

Sp: spacer

SPV: stratum periventriculare

SSU: small subunit

St: striatum

SVZ: subventricular zone

TAF: TATA box binding protein associated factor

TBP : TATA-box-binding protein

TCS : Treacher Collins syndrome

Tel : Telencephalon

TF: transcription factor

TIE: Translation Inhibitory Element

TMZ: tectal marginal zone

TPZ: tectal proliferation zone

tRNA: transfer RNA

TS: *torus semicircularis*

TTF-I: Transcription Termination Factor

UAF: upstream activating factor

UBF: upstream binding factor

uORF: upstream open reading frame

VZ: ventricular zone

Wnt: wingless-integrated

Zic1: Zinc finger of the cerebellum 1

Zo-1: Zonula occludens-1

GENERAL INTRODUCTION

CHAPTER 1: RIBOSOME BIOGENESIS

Part 1-Ribosome and translation

I. Structure, composition and function of ribosomes

Ribosomes have been described for the first time in 1955 by George E. Palade as small granular particles through microscopic observations of rat cells (**Palade, 1955**). Following this description, a series of important studies have revealed the ribonucleoproteic nature of those particles which have, therefore, been baptized "ribosomes" during the 1960s.

Ribosomes form the core of the translational machinery converting the genetic information encoded in messenger RNAs (mRNA) into chains of aminoacids (polypeptides or proteins). Ribosomes are composed of two subunits: the large subunit (LSU) with a sedimentation coefficient of 60S in eukaryotes (50S in prokaryotes) and the small subunit (SSU) with a sedimentation coefficient of 40S (30S in prokaryotes). Their association leads to the production of functional ribosomes 80S (70S in prokaryotes) which composition is species-specific. They have two main functions- decoding of the mRNA (established by the small subunit) and formation of the peptide bonds (catalyzed by the large subunit through a peptidyl-transferase activity) **(Lafontaine and Tollervey, 2001)**. In eukaryotes, these highly complex structures are composed of four ribosomal RNAs (rRNAs) and at least 80 ribosomal proteins (RPs). Association of rRNAs and RP gives rise to the two ribosomal subunits. The core of the 40S subunit is formed by the 18S rRNA associated with 32 proteins while the 60S subunit formation requires the association of three rRNAs (28S, 5S and 5.8S) and 47 proteins.

II. Translation

II.1. Role of the different components of ribosomes in translation

Once the structure of ribosome was solved through x-ray crystallography and electron microscopy analyzes, the way the ribosome reads the mRNA code and accordingly form polypeptides has been studied. Indeed, the role of the components of ribosomes, proteic or nucleic, has not been investigated until the early 2000s. Hence, several studies have tried to reconstitute the enzymatic activity of those molecular machines by separation of the different components. Surprisingly, isolated components are not able to produce any translational activity. This highlighted the importance of the structure of ribosomes. Further surveys have followed in order to understand the structural basis of the mechanism. During

translation, three events are repeated for every single codon: (1) recognition of the current codon with the help of a transfer RNA (tRNA); (2) peptidyl transfer allowing the new-coming amino acid to be linked to the nascent polypeptide; and (3) mRNA-tRNA translocation permitting the ribosome to move on to the next codon. Each ribosome possesses three bond sites for tRNA: the A-site in which the aminoacyl-tRNA lodges itself, the P-site where the peptidyl-tRNA is situated and the E-site in which the unloaded tRNA waits, ready to leave the ribosome. tRNA are stabilized within the ribosome through numerous contacts with the RPs and rRNAs. These interactions guarantee a correct positioning facing the mRNA in the SSU, and the peptidyl transferase center (PTC) in the LSU. At the level of the A-site, the tRNA is positioned in order to allow the correct contact between the mRNA codon and the anticodon in a zone of the SSU called the decoding center (DC) (*fig 1A*). The tRNA is loaded to the A site associated with the eukaryotic translation elongation factor 1 alpha (eEF1a) and a GTP molecule. During one cycle of translation elongation, a ribosome recruits an aminoacyl-tRNA, verifies the pairing between the mRNA codon and the tRNA anticodon, transfers the peptide bond and finally recovers to a conformation suitable for a new cycle of translation (*fig 1B*).

II.2. Regulation of translation

Gene expression is a multistep process that involves the transcription, translation and turnover of messenger RNAs and proteins. In the past, analyzes of gene expression regulation have been principally focused on promoter activity modulation. However, it is now clear that each step of this cascade is controlled by gene-regulatory events in order to obtain a specific cellular proteome. Indeed, recent studies have highlighted the predominant role of translation in the control of protein abundance (**Schwanhäusser et al., 2011**). Translational regulation involves several signaling pathways which would allow the adjustment of the proteome depending on the environmental conditions (nutrient availability, oxygen, hormones, stress, etc.), on the cell type or even on the cell cycle phase. The involvement of various factors enables a regulation of the global protein synthesis level but also an activation or inhibition of the translation of specific mRNAs. Among the four steps of translation (i.e initiation, elongation, termination and recycling of the ribosomes), initiation is most probably the step which plays the more determinant role. This step includes the recruitment of ribosomes and recognition of the initiation codon, and requires dozen of translation initiation factors (eukaryotic initiation factors eIF). In this section, I will briefly describe the mechanisms of translation initiation and its regulation.

A

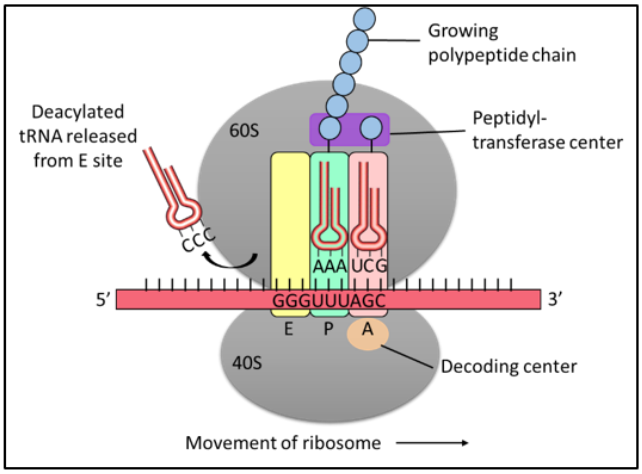

B

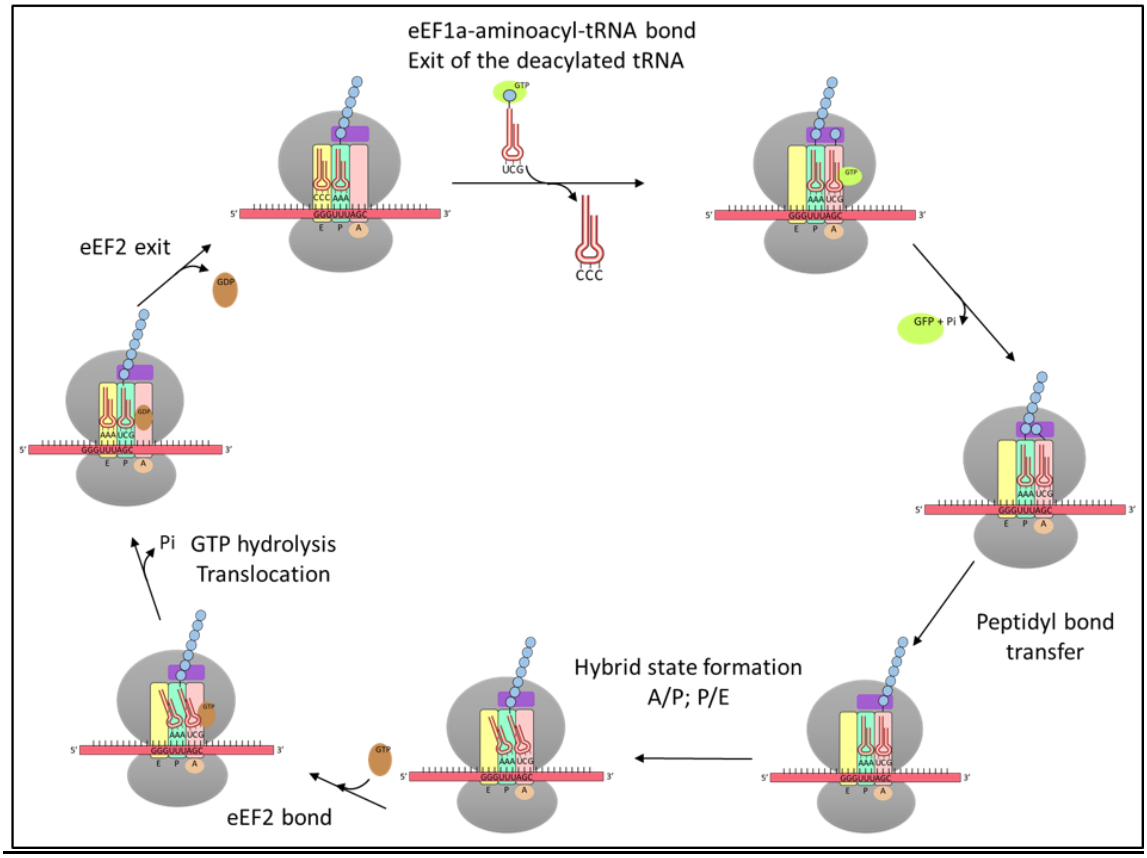

Figure 1: The numerous components of ribosomes allow a tightly organized translation.
A. Schematic representation of the three functional sites of ribosomes. The decoding center of mRNA (DC) is represented as an orange circle, and is located in the A site. A, P and E site are respectively indicated in pink, green and yellow. The peptidyl transferase center (PTC) is highlighted with a purple rectangle. The growing polypeptide chain is represented in blue. mRNA (in red), is located between the two subunits.
B. Translation elongation cycle. During the translation of mRNA, the ribosome first recruits an aminoacyl-tRNA in the A site and binds to the elongation factor eEF1a (green disc). Following this first crucial step, the tRNA hybridizes by complementarity its anticodon to the mRNA codon, releasing eEF1a. The peptide bond is transferred to the pre-existing polypeptide chains. The tRNA is translocated to the P sites after an intermediate hybrid state with the help of the eEF2 (brown disc). The deacylated tRNA located in the E site exits from the ribosomes and a new cycle begins.

II.2.1. Cap-dependent initiation

The predominant form of eukaryotic translation initiation depend on the m7G cap structure, present at the 5'end of the mRNA, and on ribosomal scanning. Translation initiation begins with formation of the 43S preinitiation complex (PIC) that is assembled from the eIF2–GTP–Met–tRNA complex, several initiation factors including eIF1, eIF1A, eIF13 and eIF15 and the 40S small ribosomal subunit. The 43S PIC, through eIF3 and eIF1, then, attaches the cap-proximal region of activated mRNAs. mRNA activation is driven by eIF4F which is composed of eIF4E - the cap-binding protein, eIF4G- a scaffold protein and eIF4A – a DEAD-box ATPase and RNA dependent helicase. The first step of activation occurs when eIF4E binds the cap structure. Subsequently eIF4A unwinds the cap-proximal secondary structure. Subsequently, the PolyA Binding Protein (PABP) interacts on one hand with the polyA sequence, and on the other hand with the eIF4G factor (*fig 2*). This interaction allows the formation of a "closed-loop" by connecting the 5' and 3' extremities of the mRNA. After mRNA binding, the 43S PIC travels along the mRNA 5′ Untrasletd region (UTR) in a 5′ to 3′ direction, looking for an AUG start coding in the RNA sequence (**Haimov et al., 2015**).

However, recent studies highlighting the position of ribosome on mRNA ("Ribosome Profiling") have revealed numerous translation "non-AUG" initiation sites such as CUG or GUG codons (**Ingolia et al., 2011**).

In addition to protein coding regions, another class of short open reading frames called "upstream open reading frames" (uORFs) are located in the 5'UTR region of the mRNA. In eukaryotes, almost 50% of the mRNAs contain those uORFs which can serve as regulators of translation (**Young and Wek, 2016**).

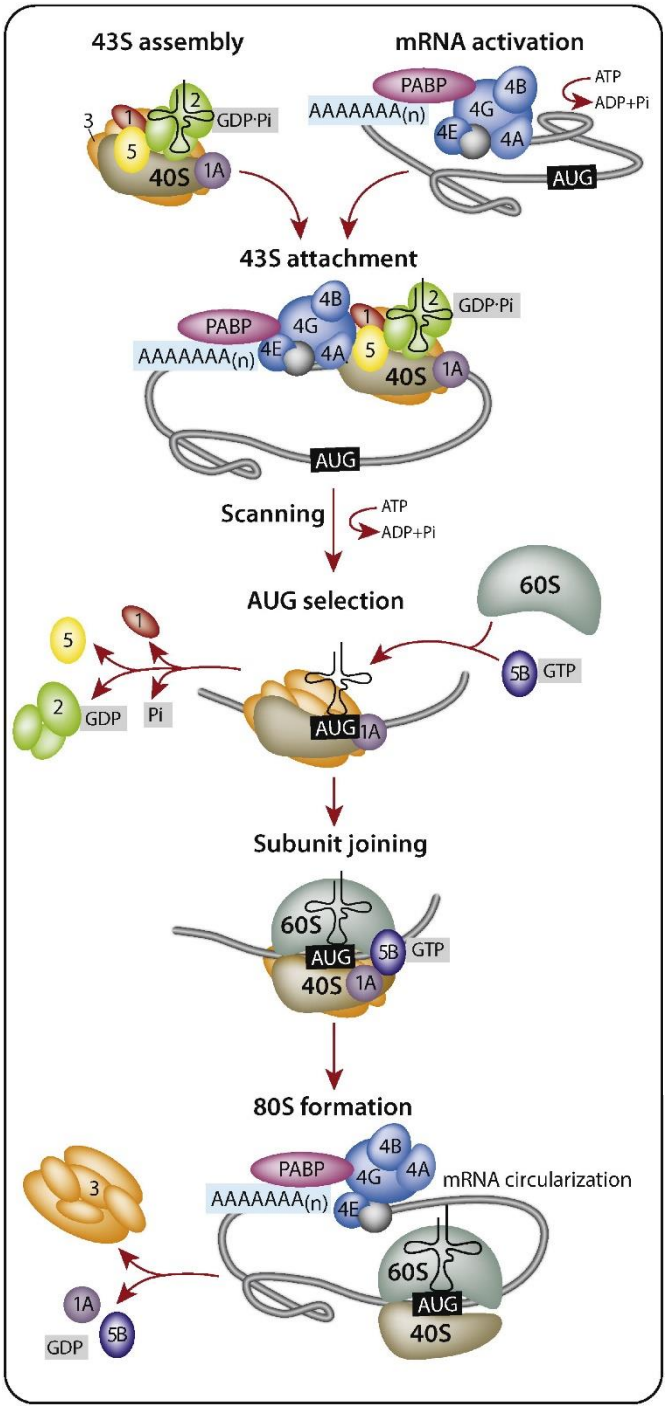

Figure 2: Schematic representation of the eukaryotic cap-dependent translation initiation mechanism. (*Haimov et al., 2015*)

The translation initiation is divided into several stages as indicated. The 43S PIC is assembled from the 40S subunit, a ternary complex consisting of eIF2–GTP–Met-tRNA, eIF1, eIF1A, eIF3 and eIF5. The mRNA activation stage involves cap-binding and unwinding of cap-proximal region by eIF4F subunits. Attachment of the PIC to the mRNA is mediated by the cap complex and is followed by an ATP-dependent scanning of the 5′ UTR in a 5′ to 3′ direction until an AUG is selected through codon-anti-codon base pairing with the Met-tRNAi. AUG recognition switches the scanning complex to a "closed" conformation and is accompanied by eIF5-assisted hydrolysis of eIF2-bound GTP, Pi release and eIF1 displacement. The 60S subunit joining to the 48S complex is associated with release of eIF2–GDP, eIF3, eIF4F and eIF5 and is mediated by eIF5B and eIF1A. GTP hydrolysis by eIF5B triggers its own and eIF1A release rendering the 80S ribosome ready to elongate. RNA circularization, mostly occurring in polysomes, is mediated by PABP–eIF4GI interaction.

II.2.2 IRES-dependent initiation

For a long time the "cap-dependent" mode of initiation was considered the only possible mechanism through which translation of eukaryotic mRNAs could be initiated. However, studies of viral gene expression in the late 1980s led to the discovery of an alternative mode of translation initiation in eukaryotic cells that bypasses the requirement for cap-dependent scanning and allows the 40S ribosome to be directly recruited to the vicinity of the initiation

codon. The mRNA regions required for this direct recruitment of the SSU were termed Internal Ribosome Entry Sites (IRESs) to emphasize that the process is independent of 5'-end recognition. The vast majority of cellular IRES elements are located within the 5'-UTRs immediately upstream of the initiation codon. Nevertheless, there are cases in which the IRES is downstream of the initiation codon or located in the coding regions, thereby triggering synthesis of a truncated protein.

It has been shown that viral IRES-driven translation initiation is typically used when cap-dependent initiation is compromised. Numerous IRES have been discovered in viruses, and a classification in four groups have been established depending on their secondary structures and on the initiation factors required for their activities (**Jackson et al., 2010**). IRES-mediated translation of cellular transcripts was not widely recognized or extensively studied until recently. Indeed, the common methods used to identify IRES activity are still debated and stringent test has questioned some of these claims (**Baranick et al., 2008**). Yet, the IRESite database presents evidence of many eukaryotic IRES elements and the list is growing (in 2009, at least 115 eukaryotic cellular mRNAs were reported) (**Mokrejs et al., 2010**). Importantly, IRES-containing mRNAs can also be translated by the cap-dependent mechanism. Hence, one should wonder how the switch between these two modes of initiation is regulated. In fact, mRNA synthesized by RNA polymerase I (PolI) are capped and, therefore, likely to be translated following the two initiation types. Other mRNAs have highly structured 5'UTR sequences, preventing the scanning by the PIC and allowing an IRES-mediated translation. Interestingly, it has been demonstrated that many physiological, pathophysiological and stress conditions that lead to inhibition of cap-dependent translation cause a substantial increase in cellular IRES-mediated translation (**Komar and Hatzoglou, 2005**). Such conditions include endoplasmic reticulum stress, hypoxia, nutrient limitation, mitosis and cell differentiation. It is striking that many of the cellular mRNAs that contain IRES elements encode proteins that are involved in protection of cells from stress or, alternatively, induction of programmed cell death (apoptosis). Therefore, it is currently believed that cellular IRES-mediated translation plays an important role in cell-fate decisions under a variety of conditions.

II.2.3. TOP mRNA translation

Biogenesis of the protein synthesis machinery and particularly the ribosome, is a highly resource-consuming process (**Granneman and Tollervey, 2007**). Thus, cells that encounter unfavorable conditions attenuate the production of components of the translational machinery and cease to grow. This coordinated translational control is carried through a common *cis*-regulatory element, the 5' Terminal OligoPyrimidine motif (5'TOP). mRNAs presenting this motif are referred as TOP mRNAs. These mRNAs alternate between repressed and active states.

Part II- Ribosome biogenesis

The highly coordinated mechanism leading to the formation of these molecular machines is called the ribosome biogenesis pathway. It takes mainly place in the nucleolus, but additional maturation events occur in the nucleoplasm and the cytoplasm. It requires the activities of three polymerases, 75 small nucleolar RNAs (snoRNAs) and more than 250 ribosomal biogenesis factors (RBFs) (**Brombin et al., 2015**). RBFs are involved in the synthesis and maturation of rRNA as well as the folding and association of RPs. Therefore, this process consumes the major part of the cellular energy **(Warner, 1999)** and requires a tight regulation.

There are six important steps in eukaryotes ribosome assembly: synthesis of the components (rRNAs, RPs, RBFs and snoRNA), pre-rRNA processing (cleavage), covalent modifications of the pre-RNAs, RPs, and RBFs, assembly, transport and quality controls (*fig 3*). Despite the ubiquitous nature of this process, ribosome formation and protein translation need to be adapted according to the cell type and the cell environment. Cells do not have the same proteome depending on their differentiation status or the organism requirements. As mentioned earlier, proteome composition can be regulated either at the mRNA or at the protein level. It has been suggested that proteome composition can differ between cells with identical translatome (**Buszczak et al., 2014**). Hence, ribosome biogenesis would need to be adjusted and regulated leading to ribosome heterogeneity within the same species, the same organism or the same tissue.

The objective of this chapter is to give an overview of the different steps of the pathway in eukaryotes to describe ribosome heterogeneity and its importance in cell cycle regulation and embryonic development.

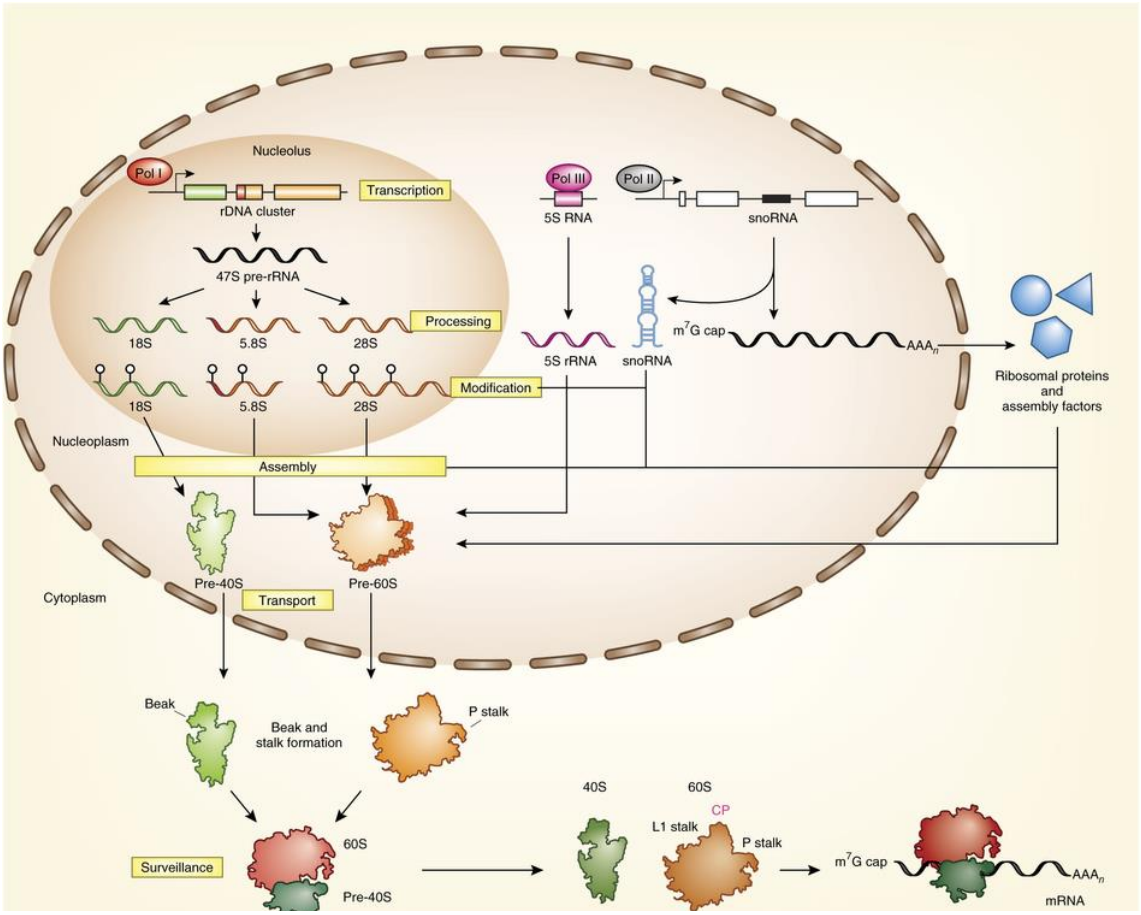

<u>Figure 3:</u> Eukaryotic ribosome biogenesis at a glance. ***(Lafontaine, 2015)***
Ribosome biogenesis encompasses six important steps (yellow boxes): (i) transcription of components (rRNAs, mRNAs encoding ribosomal proteins (RPs) and ribosome biogenesis factors (RBFs), and snoRNAs); (ii) processing (cleavage of pre-rRNAs); (iii) modification of pre-RNAs, RPs and RBFs; (iv) assembly; (v) transport (nuclear import of RPs and RBFs; pre-ribosome export to the cytoplasm); and (vi) quality control and surveillance. Three out of four rRNAs are transcribed in the nucleolus by Pol I as a long 47S precursor (47S pre-rRNA), which is then processed and modified to yield the 18S, 5.8S and 28S rRNAs that are assembled into the pre-40S (green) and pre-60S (orange) ribosomal subunits. 5S rRNA (pink) is transcribed by PolIII in the nucleoplasm and incorporated into maturing 60S subunits, forming the central protuberance (CP). 80 RPs, more than 250 RBFs and 200 snoRNAs are transcribed by PolII. The proteins are synthesized in the cytoplasm and reimported to the nucleus for assembly. Pre-40S subunits are exported to the cytoplasm more rapidly than pre-60S subunits, which require numerous nuclear maturation steps. Several structures important for ribosome function are formed only in the cytoplasm, including the beak on the 40S subunit and the stalk on the 60S subunit; both are protruding features that could obstruct subunit export if formed prematurely. Pre-40S subunits undergo a 'test drive' to prove functionality before final maturation.

I. rDNA transcription

I.1 Ribosomal DNA

Ribosomal DNA (rDNA) is organized in repeated sequences -200 copies in yeast **(Nomura et al., 2013)** and 400 copies in human cells **(Henras et al., 2015)**. Although the number and size of these repeats vary among species, the general layout of each repeat is conserved (*fig 4A*). The presence of many strongly transcribed rDNA genes allows the generation of an elevated number of rRNAs, fulfilling the massive demand of ribosome production.

However, only a fraction of these repeats is actively transcribed **(Birch and Zomerdijk, 2008)**, and the inactive part having a potential role in the maintenance of genome integrity **(Ide et al., 2010; Kobayashi, 2011)**. In mammalian cells, rDNA chromatin can exist in at least four distinct states (**Hamperl et al., 2013**). Among them, we can distinguish the open/accessible chromatin structure and the silent methylated and non-methylated rDNA. The epigenetic silencing of rDNA copies seems to play a role in nucleolar integrity, genomic stability, DNA repair and global regulation of gene expression**.** Particularly, heterochromatic rRNA genes would mediate the formation and inheritance of nuclear heterochromatic regions **(Guetg and Santoro, 2012)**. Moreover, rDNA instability has been associated with several human pathological conditions such as Bloom syndrome **(Killen et al., 2009)** or neurodegenerative syndromes **(Hallgren et al., 2014)** including Alzheimer.

Eukaryotic cells contain thousands of ribosomal genes, tandemly repeated and clustered in one or several chromosomes **(Long and Dawid, 1980)**. These clusters, called the nucleolus organizer region (NOR) play a role in nucleolus formation during interphase (reviewed in the chapter 1, Part II, I.4.Nucleolus) **(Anastassova-Kristeva, 1977).** They are isolated from the polymerases I and III because of their positioning and the presence of heterochromatic repetitive satellite DNA. Each single unit contains the sequence of rRNA polycistronic precursors (47S in human, 45S in mammals and 35S in yeast) organized in transcribed sequence and non-transcribed sequences (long intergenic spacer, IGSs). rRNA genes are composed of the three rRNAs (18S, 5.8S and 25/28S) distinguishable from internal and external sequences (ITS and ETS) (*fig 4B,C*). In mammals, rRNA genes are encompassed by diverse regulatory elements including promoter and enhancers. rRNA gene promoter is comprises of a core element essential for accurate transcription and an upstream core element (UCE). In addition, distal enhancer-like elements are present near the gene **(Russell and Zomerdijk, 2005)** (*fig 5B*).

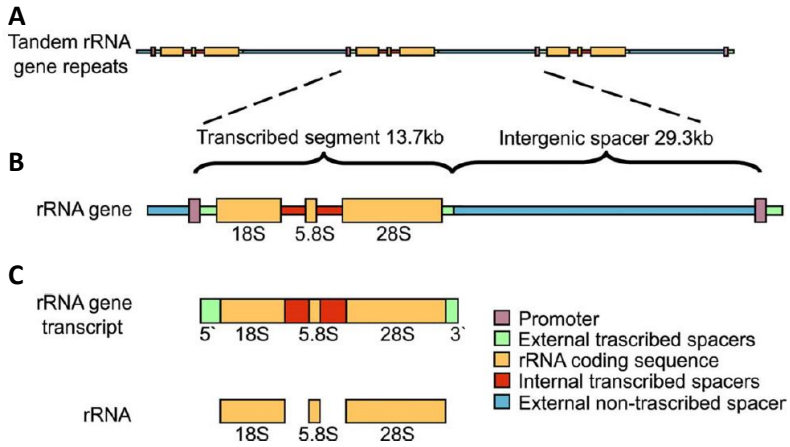

Figure 4: Scheme of human ribosomal genes and their transcripts *(Raska et al., 2004)*.
A. Ribosomal genes, tandemly repeated, are organized in transcribed sequences and intergenic spacers. **B.** rRNA gene (corresponding to one gene of the rDNA) is transcribed to give rise to a polycistronic rRNA. **C.** Maturation of the rRNA leads to the production of 18S, 5.8S, and 28S rRNA.

I.2 rDNA transcription

Ribosome synthesis starts with the transcription of three rRNAs from ribosomal DNAs. 45S/35S rDNA is specifically transcribed by the RNA polymerase I (RNA PolI) in the nucleolus whereas the precursor of the fourth rRNA (5S) is synthesized independently in the nucleoplasm from multiple genes by the RNA PolIII **(Ciganda and Williams, 2011)**. As the two mechanisms are distinct, 5S transcription will not be detailed in this manuscript.

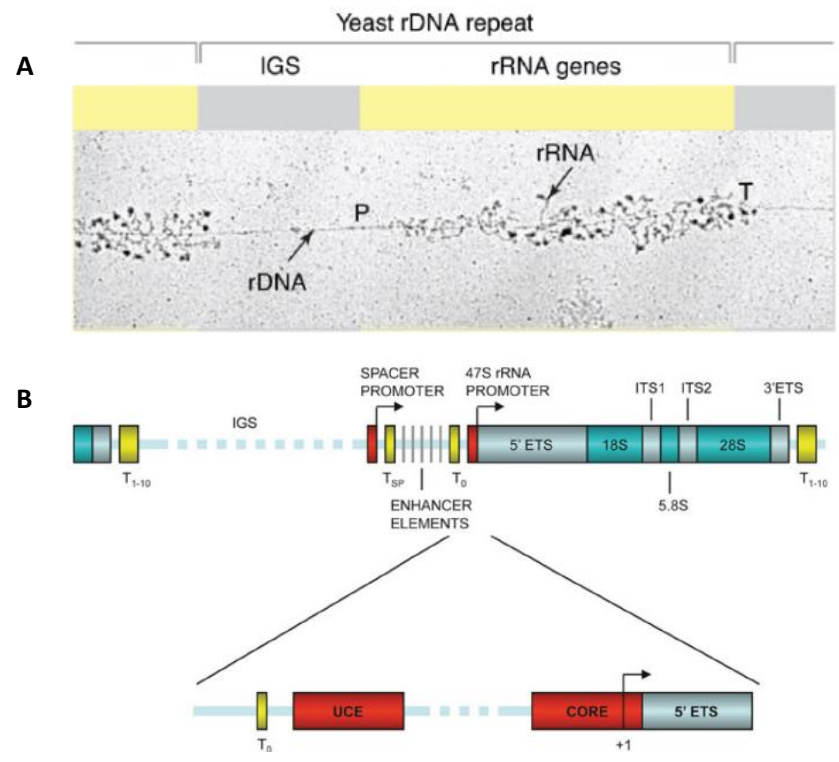

Figure 5: Organization of the rRNA genes
A. Illustration of the repetitive nature of rDNA in Yeast. Progressively longer rRNAs (stained for associated proteins) emanate from the many pol I complexes as they transcribe the rDNA, beginning at the promoter (P) and finishing at the terminator (T). **(*Russell and Zomerdijk, 2005*)**
B. Scheme of mammalian rDNA repeat. Each rRNA gene are preceded by a promoter (P), containing a core element and an upstream core element (UCE), and a spacer promoter (SP) upstream of the promoter.

As previously described, rDNA is transcribed as a polycistronic pre-rRNA which will give rise to the three rRNAs (18S, 5.8S and 28S).(***Goodfellow and Zomerdijk*, *2013***).

RNA PolI-mediated 45S /35S rDNA transcription is a key point in the regulation of the ribosome biogenesis process. This event comprises a series of coordinated steps including transcription initiation, promoter escape, elongation, and termination.

rDNA transcription starts with the formation of a transcriptionally competent complex formed through the recruitment and assembly of RNA PolI, with several transcription factors, into a pre-initiation complex (PIC) at the rRNA gene promoter. In mammal cells, the complex is composed of Polymerase I and the selectivity factor termed SL1 in human and TIF-IB in mouse (**Clos et al., 1986; Learned et al., 1986**). SL1 consists of at least 4 subunits including the TATA-box-binding protein (TBP) and associated factors. Activated transcription requires, in addition to PolI and SL1, the upstream binding factor UBF (*fig 6*) **(Russell and Zomerdijk, 2005; Schneider, 2012)**. UBF through its high mobility group (HMG) boxes, homodimerizes and loop approximately 140 base pairs (bp) of DNA into a single turn (**Stefanovsky et al., 2001**). This factor allows the activation of the transcription by recruiting PolI to the promoter and displacing nonspecific DNA binding proteins (e.g histone H1) from rDNA (**Kuhn et al., 1993**). UBF and SL1 act in synergistically to confer promoter selectivity to PolI. PIC assembly is conserved across evolution. In particular, in yeast, four factors are involved in the pre-initiation complex formation (UAF non-analog to UBF, TBP, the core factor analog to SL1 and Rrn3) (*fig6*).

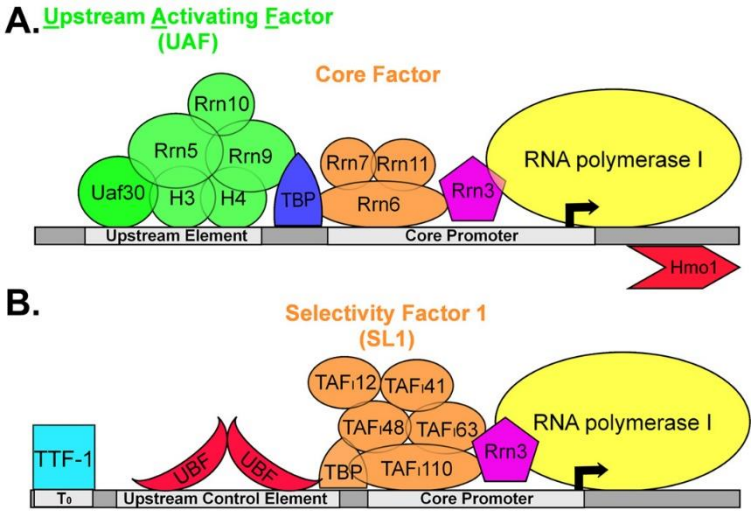

Figure 6: Comparative scheme of factors required for transcription initiation by PolI in yeast and mammals cells (*Schneider, 2012*).

A. Pre-initiation complex formation in yeast. Four factors are essential (Rrn3, core factor, TBP and UAF) to initiate polI-mediated transcription.
B. Pre-initiation complex formation in mammals. As in yeast, four components (SL1, UBF, Rn3 and TTF-I) are key for the initiation complex. (UBF, SL1 and Rrn3).

Once the pre-initiation complex is formed and the promoter chromatin is opened, the first nucleotide starts to be incorporated and transcription initiated. RNA PolI escapes the promoter through several inhibiting interactions, to engage the elongation of the transcription.

As PolI escapes from the promoter, the diverse transcription factors (SL1 and UBF in mammals) can re-initiate transcription allowing multiples rounds of transcription in parallel **(Panov et al., 2001**) (*fig 7*). In yeast, the Miller chromatin spreading technique for electron microscopy (EM) highlights perfectly this high density of loading of RNA PolI (*fig 5*). Finally, rDNA transcription termination occurs through the release of PolI by TTF- (Transcription Termination Factor) and PTRF (Pol-I Transcript-Release Factor) factors at the 3' end of the transcribed region (*fig 7*).

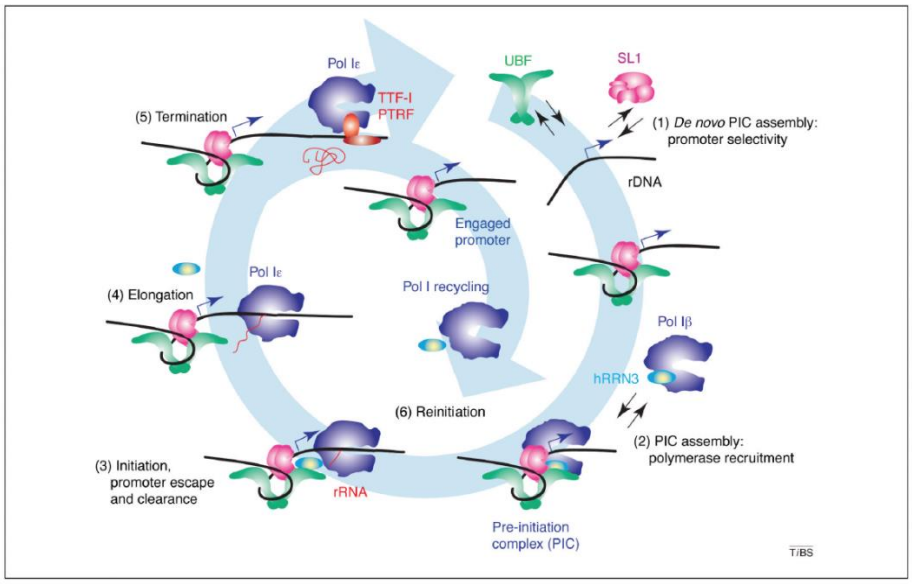

Figure 7: The RNA polymerase I (PolI) transcription cycle (*Russell and Zomerdijk, 2005*)

1. *De novo* PIC formation involves the selective binding of selectivity factor 1 (SL1) to the rDNA promoter and the incorporation of activator upstream binding protein (UBF)

2. Homodimerization of UBF allow the recruitment of PolI by SL1.

3. PolI initiates transcription upon promoter opening, followed by promoter escape.

5. Transcription by PolI terminates at the 3' end of the gene at specific sequences bound TTF-I and PTRF, with the concomitant release of PolI and the nascent rRNA.

6. Reinitiation of transcription is possible through the remaining bounding of SL1 and UBF.

PolI is composed of two subunits PolIα and PolIβ. The latter is associated with numerous proteins including DNA repair and replication proteins, topoisomerases and the transcription factor IIH (TFIIH). However, PolI transcription machinery is highly dynamic and assembles in a stochastic fashion, individually or in subcomplexes (**Dundr et al., 2002**).

I.3 Regulation of rDNA transcription

Transcription of rRNA genes is efficiently regulated to be responsive to both general metabolism and specific environmental challenges (**Grummt, 2010**). Regulations of ribosome biogenesis in general, and of rRNA transcription in particular, are both essential to control ribosome production therefore cell cycle and cell proliferation. rRNA synthesis can be modulated by varying the transcription rate per gene or by varying the number of active genes. Although there are evidences for both types of regulation, the majority of short term regulation affects the rDNA transcription rate following different environmental cues. However, it is now accepted that the fraction of active gene copies changes during development and differentiation (**Haaf et al., 1991**). This regulation acts as a long-term change in rDNA transcription. In this paragraph, I will give an overview of the mechanisms responsible for these two types of regulation.

As previously mentioned in the description of ribosomal DNA, only half of the rDNA copies are active and transcribed. Moreover, individual rDNA loci are not equally active in different cell types in mammals. For example, in mouse, several rDNA variants can be distinguished thanks to the length of the IGS and the sequence polymorphism (**Tseng, 2006**). In addition, Tseng et al. showed that rDNA variants are regulated independently in a tissue specific manner (**Tseng et al., 2008**).

As reported earlier, long term regulation involves control of the active and inactive status of rDNA loci through epigenetic modifications. In particular, active genes are characterized by an "opened" euchromatic structure whereas silent genes exhibit a more compact heterochromatic structure. These modifications of the chromatin states are associated with specific histone modifications including acetylation and methylation (*fig 8*). Surprisingly, even proliferating cells display a significant fraction of silent rRNA genes, implying that specific epigenetic modifications are maintained throughout the cell cycle and propagated to daughter cells upon division.

Despite this epigenetic maintenance, the switching between active silent state of rRNA genes is mediated by a chromatin remodeling complex termed NoRC (*fig 8*). NoRC allows the recruitment of the enzymes necessary for histone methylation and acetylation. It acts through two mechanisms: it positions the nucleosome on the rDNA promoter, and coordinates the machinery which establish a "closed" heterochromatic state (**Mayer et al., 2006; Santoro et al., 2002**). Moreover, the methylation of histone H2 by the

methyltransferase Fibrillarin (Fbl) seems to play a role in the ratio of active/inactive rDNA loci in yeast and plants (**Loza-Muller et al., 2015; Tessarz et al., 2014**).

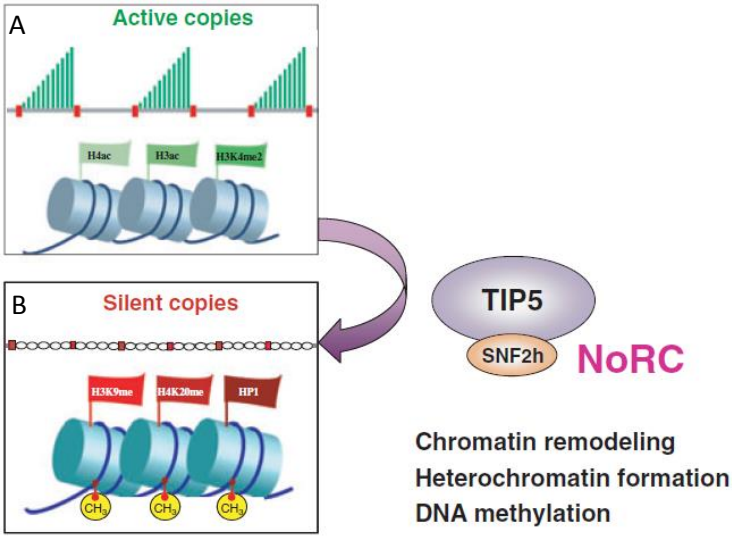

Figure 8: NoRC triggers the establishment of the silent, heterochromatic state of rRNA genes (*Grummt, 2010*)
A. Active chromatin copies are characterized by DNA hypomethylation, acetylation of histone H4 (H4ac), and demethylation of histone H3 Lys4 (H3K4me2).
B. Epigenetically silenced rRNA genes are demarcated by histone H4 hypoacetylation, methylation of histone H3K9 (H3K9me) histone H4 Lys20 (H4K20me), association with heterochromatin protein 1 (HP1) and CpG methylation (CH3).

On the other hand, short-term regulation is triggered in response to environmental changes leading to modifications of the transcription rate. Indeed, as the ribosome biogenesis adapts depending on cell needs, conditions that impair cellular metabolism such as nutrient starvation, oxidative stress, inhibition of protein synthesis and cell confluence will downregulate rDNA transcription. On the contrary growth factors and agents that stimulate growth and proliferation will upregulate RNA PolI-mediated transcription (*fig 9A*) (**Grummt, 2010**). For example, several growth factors, such as the phosphoinositide 3-kinase (PI3K)/AKT/mammalian target of rapamycin complex 1 (mTORC1) and RAS/RAF/extracellular signal-regulated kinase (ERK) pathways form an intricate control network with the transcription factor MYC (*fig 9B*).

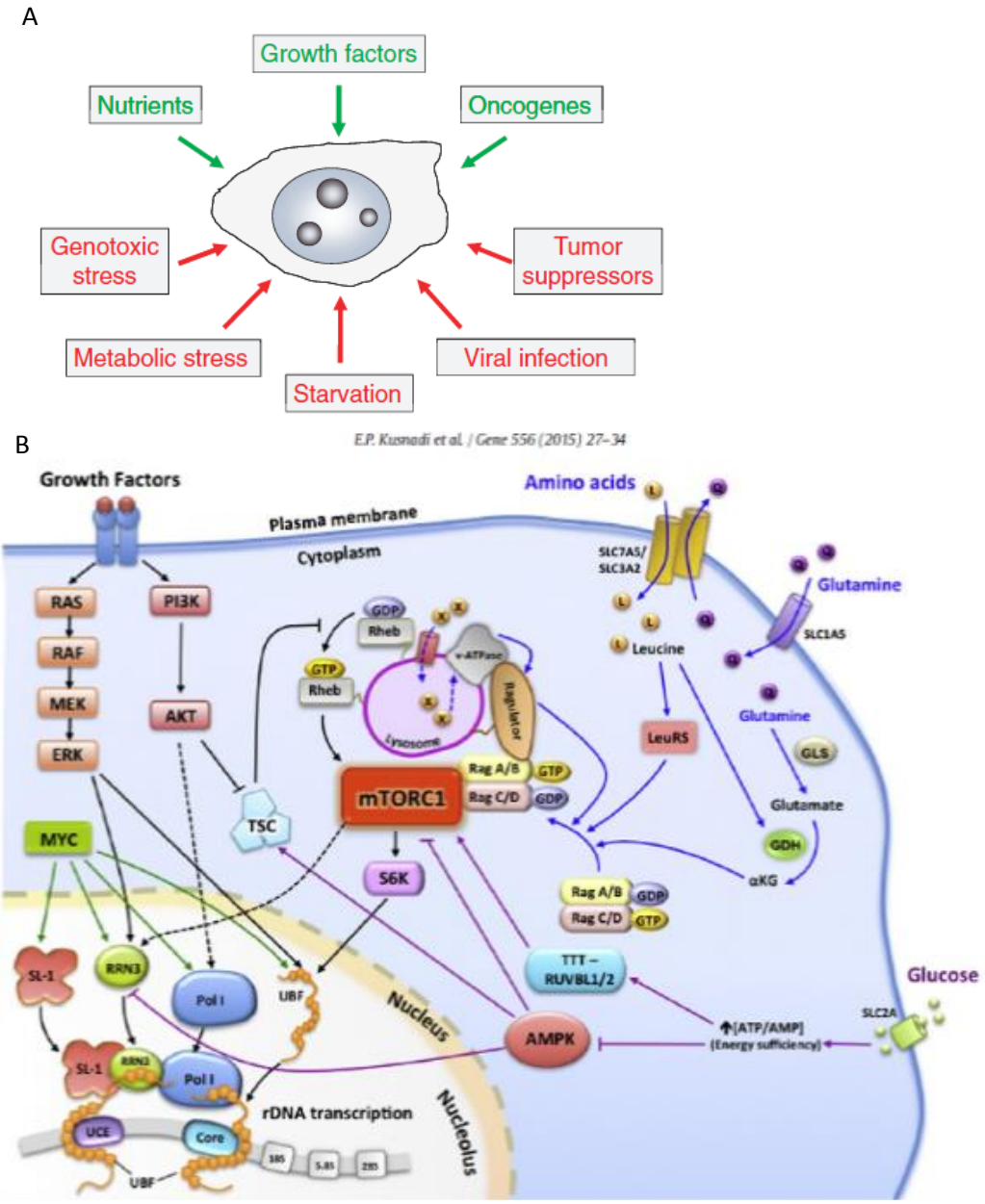

Figure 9: Short term regulation of rDNA transcription is mediated by extracellular cues and implies different signaling pathways

A. Schematic representation of the different extracellular signals acting on rRNA transcription (upregulation in green and downregulation in red). **(*Grummt, 2010*)**

B. Intracellular mechanism responsible for the activation or inhibition of rDNA transcription. mTORC1 links the availability of growth factors, amino acids and glucose. PI3K/AKT/mTORC1 and RAS/RAF/ERK pathways form an intricate control network with the transcription of MYC to regulate the rate or rDNA transcription. **(*Kusnadi et al., 2015*)**

Furthermore, in mammals, PolI regulation is directly linked to the cell cycle allowing the fine tuning of ribosome production depending on the cell cycle phase (*fig 10*). During mitosis, the upstream binding factor (UBF) is inactivated in order to silence RNA PolI-dependent transcription while during G1 phase, transcription is re-activated through TIF-IA and UBF. Cyclin-dependent kinases (Cdk), as well as the previously mentioned

signaling pathways, phosphorylate differently UBF and TIF-IA, linking cell cycle and rDNA transcription.

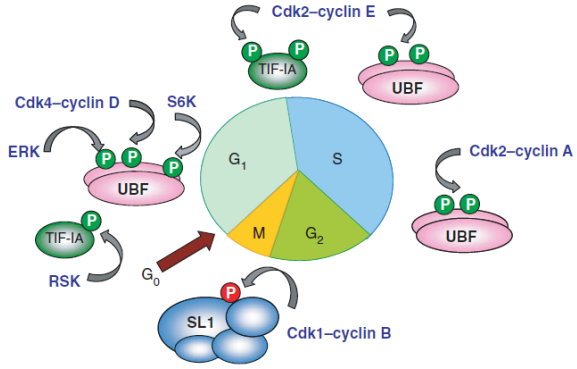

Figure 10: Regulation of PolI transcription during the cell cycle. (*Grummt, 2010*)
1. During G1/S phase, UBF is activated by phosphorylation by Cdk4-cyclinB and Cdk2-cyclinE/A. In addition, mTORC1-dependent and ERK-dependent pathways activate TIF-IA through its phosphorylation leading to the activation of PolI mediated transcription.
2. At entry in mitosis, Cdk1-cyclinB phosphorylates SL1 allowing the repression of PolI transcription.
Activating phosphorylation are marked in green, and inhibiting ones in red.

I.4 Nucleolus

Nucleoli are distinct subnuclear compartments which form at the end of mitosis around the rDNA genes. These structures are responsible for the generation of ribosomes via the localized rDNA transcription and processing. Nucleoli have been mainly observed and described by EM. With this technic, different subregions have been characterized by their morphology (**Hernandez-Verdun et al., 2010**). We can then distinguish the fibrillar centers (FCs), the dense fibrillar centers (DFCs) and the granular components (GCs) (*fig 11A*). FCs are fibrillar areas of different size containing fibrils. They are partly surrounded by the highly contrasted DFCs. FCs and DFCs are embedded in the GCs that mainly consist of granules in a loosely organized distribution. Complementary approaches allowed to go further into details and obtain a spatiotemporal map of ribosome biogenesis. Therefore, the localization of rDNAs, snoRNAs and several proteins of the machinery. For example, the site of active RNA PolI-mediated transcription are localized at the interface between the FCs and the DFCs while the non-transcribed part of rDNA is localized in the FCs (**Goessens, 1984**). The DFC consists of newly transcribed rRNAs bound to ribosomal proteins, while the GC contains rRNAs bound to ribosomal proteins that are being assembled into immature ribosomes. Hence, clusters of rDNA repeats are considered as the founders of nucleoli. However, this role may be shared with the regions of the same chromosome adjacent to NORs (**Kaplan et al., 1993**) (*fig 11C*). Nucleoli are visible with light microscopy as well (*fig 11B*). Besides, with new technics, it is now possible to label specifically the various subregions of the nucleoli (*fig 11B*) using immunohistochemistry or reporter proteins fused to fluorescent protein tags. Surprisingly, it has been proposed

that, during evolution, a third nucleolar compartment emerged at the transition between the anamniotes and the amniotes, following a substantial increase in size of the rDNA intergenic region.

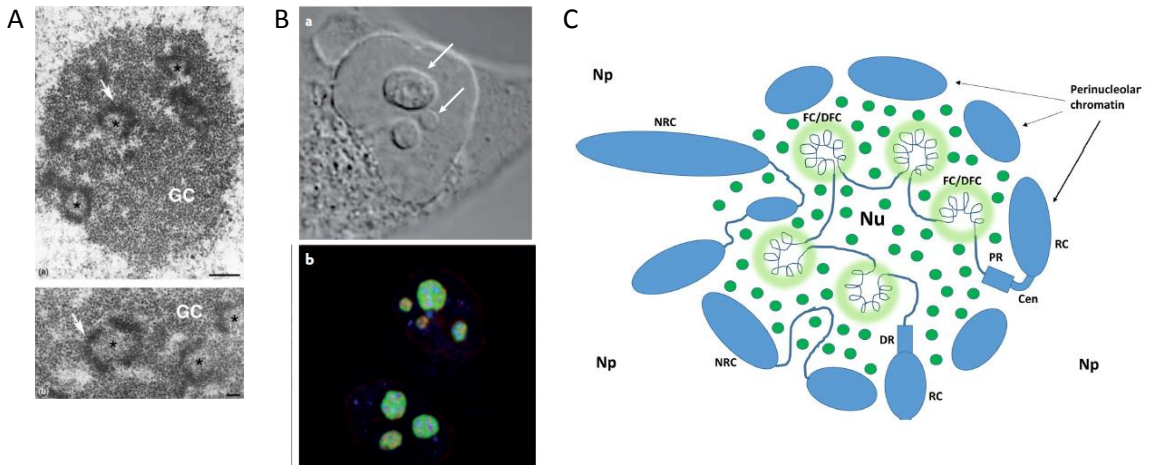

Figure 11: Nucleolar organization of eukaryotic cells

A. Nucleolar organization of a human Hela cell using electron microscopy standard preparation. The three nucleolar components are visible due to their different contrast: the fibrillar centers (FC, asterisks), the dense fibrillar component (white arrow) and the GC. (**Hernandez-Verdun et al., 2010**)

B. Visualization of nucleolar morphology and composition using light (a) and fluorescent (b) microscopy.

(a) Differential interference contrast (DIC) images of the Hela cells highlight the prominent nucleoli within the nuclei (white arrows) - (b) Immunofluorescent labelling of Hela cell with specific antibodies against proteins in the GC (B23 in green), DFC (Fbl in red) and FC (RPA39 in blue). (**Boisvert et al., 2007**)

C. Schematic representation of the nucleolus associated DNA. Nu nucleolus, Np nucleoplasm, RC chromosome carrying ribosomal genes (ribosomal chromosome), Cen centromere, PR proximal flanking region, DR distal flanking region, NRC non-ribosomal chromosome, FC/DFC FC/DFC unit. The center of rDNA transcription consists of FC surrounded with dense fibrillar component (DFC). Green dots represent granular component of the nucleolus. (**Smirnov et al., 2016**)

Nucleoli are characterized by a great variability in size, number, and position within the nuclear volume and this variability depends on the cellular metabolism. For example, in cycling cells, the volume of the nucleoli increases between the G1 and G2 phases and the number of FC doubles during G2 (**Junéra et al., 1995**). Terminally differentiated quiescent cells, ribosome biogenesis is stopped and nucleolar remnants are observed. Moreover, upon transcription or rRNA synthesis arrest, cells show nucleolar segregation. This peculiar reorganization of nucleoli is also observed upon treatment by low doses of actinomycin D. Indeed this intercalant agent affects particularly PolI transcription through its high binding affinity for GpC sites on rDNA and this observation highlights the link between PolI transcriptional activity and nucleolar organization. Several studies such as the inhibition of

Cdk (**Amin et al., 2008; Apicelli et al., 2008; Romanova et al., 2009; Sirri et al., 2002**) or the nucleolar protein depletion (**Yuan et al., 2005**) support this feature.

In multicellular eukaryotes, nucleolar assembly directly depends on pre-existing machineries and complexes inherited through mitosis. This processing machinery directly derives from the nucleolar disassembly to become building blocks for the new nucleoli. More precisely, at the onset of mitosis, the pre-rRNA processing complexes are released from the nucleoli concomitantly with condensation of chromatin into mitotic chromosomes and before the arrest of PolI-dependent transcription (**Gautier et al., 1994; Hernandez-Verdun et al., 1993**). Additionally, during mitosis, PolI-mediated transcription machinery remains associated with rDNA within NORs that were transcriptionally active during the previous interphase (**Roussel et al., 1996**). Nucleolar disassembly is highly governed by the cell cycle as this mechanism is linked to the repression of PolI-dependent transcription. In particular, Cdk1-cyclinB complex plays a critical role in the dynamic of assembly/disassembly of the nucleolus (*fig 12*). Particularly, during embryonic development pre-rRNAs of maternal origins, stored in the cytoplasm, participate in the structural organization of the nucleolus prior acquisition of its translation competence. They are localized in foci called prenucleolar bodies (PNBs) and are associated with the NORs.

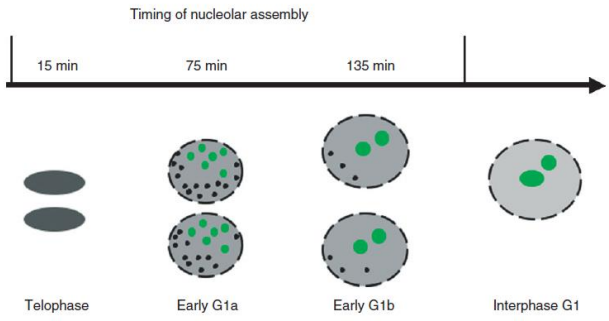

Figure 12: Timing of nucleolar assembly during cell cycle
(*Hernandez-Verdun et al., 2010*)
In HeLa cells, transcription by PolI starts in telophase in the six active NORs, whereas the mitotic chromatin is still condensed (oval dark structure). In early G1a, the mitotic chromatin decondenses (grey), the nuclear envelope (broken line) is assembled, numerous PNBs (dark foci) are formed, and the active NORs recruits the processing proteins in DFC (green). In early G1b, the processing proteins are almost completely transferred from prenucleolar bodies (PNBs) to GC, and NORs regrouped in two to three nucleoli.

II. rRNA maturation

Maturation of the nascent pre-rRNA begins while PolI-mediated transcription is still on going, with the help of maturation factors called ribosome biogenesis factors. These factors transiently interact with pre-rRNAs leading to the formation of the so called pre-ribosomal particles. Following transcription, pre-rRNAs are cleaved, post-transcriptionally modified

and assembled with ribosomal proteins. Most of the rRNA cleavages and post-transcriptional modifications are processed simultaneously. While the sequence of events is now well understood, the particularities and the regulation of each step are still not fully known. Many researches have been performed in yeast and human cells. Beside some analyzes on mice, very few studies have been performed on other vertebrates such as zebrafish. In this chapter, I will give an overview of the process.

II.1 rRNA cleavages

As previously mentioned, in eukaryotes nascent pre-rRNAs (35 S in S.Cerevisae or 47S rRNA in human cells) contains the sequences for the 18S, 5.8S and 25S/28S rRNA separated by ITSs and flanked by the 5' and 3' ETSs (*fig 4*). Along rRNA cleavages, the transcribed spacers are sequentially eliminated through a complex series of endonucleolytic and exonucleolytic cleavages giving rise to the mature rRNAs. The sequence of events differs depending on the species. In particular, in yeast, the 18S rRNA is exclusively generated by a series of endonucleolytic cleavages within the 5′-ETS and ITS1 sequences, whereas a combination of endonucleolytic and exonucleolytic processing steps in the ITS1 is involved in mammalian cells **(Mullineux and Lafontaine, 2012)**. Specifically, in human cells, the 47S rRNA is first cleaved at its extremities, giving rise to the pre-mature 45S intermediate rRNA. 45S rRNA can then be maturated through alternative pathways with variable kinetics and orders producing different intermediates but leading to the same mature rRNAs. In pathway 1, the initial cleavage occurs in the 5'ETS at site A0 (or A' in mouse) and is soon followed by cleavage at site 1. On the other hand, in pathway 2, the first cleavage event takes places at site 2 within ITS1 (*fig 13*). If cleavage of the 5'ETS occurs first (pathway 1), subsequent cleavage in the ITS1 takes place at site 2. These two important first cleavages allow the separation of the 90S pre-particle into pre-60S and pre-40S. The two subunits follow thereafter distinct maturation pathways. In both pathways, the majority of cleavage events take place in the nucleus. Yet, the final cleavage step of 18S maturation occurs in the cytoplasm after nuclear export. In parallel, the 32S pre-rRNA is cleaved in the ITS2, generating the 12S pre-rRNA and the 28S rRNA. 12S will thereafter give rise to the mature 5.8S rRNA **(Mullineux and Lafontaine, 2012)**.

These alternative processing pathways vary according to species, cell types, physiological and developmental stages and even pathological conditions (**Belin et al., 2009; Eichler and Craig, 1994; Gerbi and Borovjagin, 2013; Hadjiolova et al., 1993**). Studies showed that both alternative pathways in coexist in *Xenopus* in a single cell. It is worth noting that

there are conditions that favor alternative pre-RNA processing pathways (**Savino and Gerbi, 1990**). Moreover, it has been hypothesized, that in mammals, as in yeast, rRNA cleavage occurs co-transcriptionally and/or post-transcriptionally. This might be particularly relevant to cells with enhanced growth properties such as aggressive cancer cells.

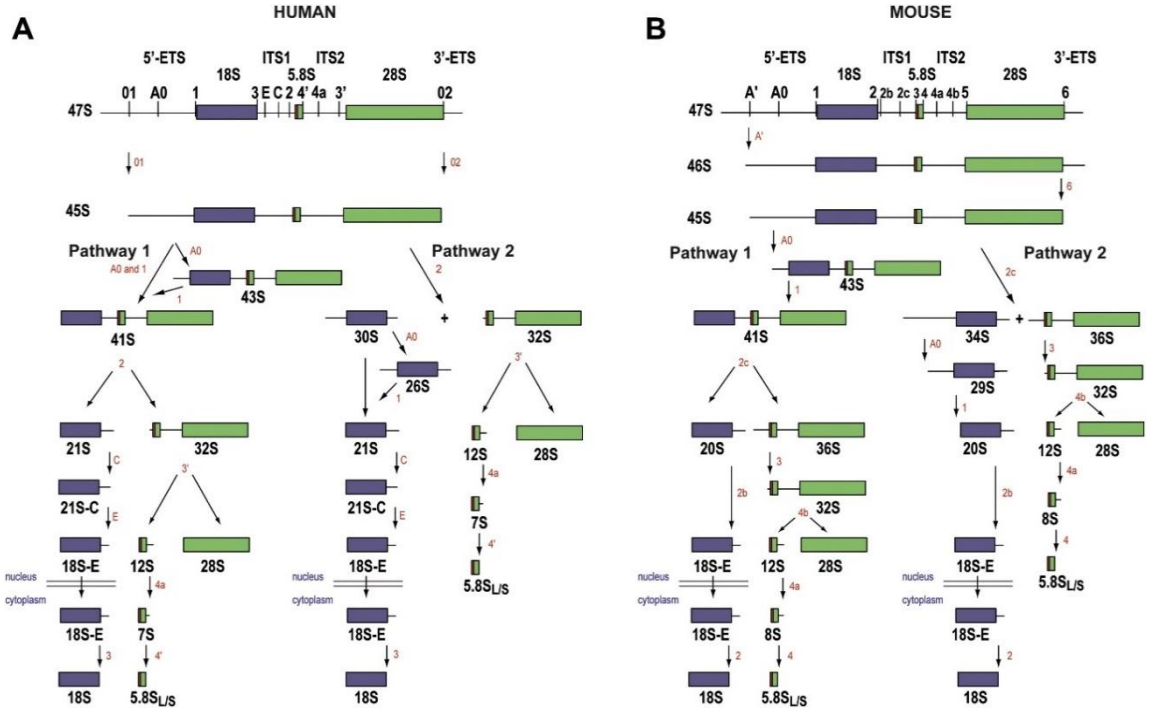

Figure 13: Overview of the pre-rRNA processing in mammals. ***(Mullineux and Lafontaine, 2012)***
A. Pre-rRNA processing in human cells. 47S pre-rRNA is first cleaved at the 5' and 3' ETS giving rise to the 45S pre-rRNA. Following this first cleavage, 45S pre-rRNA can follow two alternative pathways, diverging by the sites of cleavages producing therefore different intermediates. Both pathways mostly take place within the nucleus, beside the final cleavage steps of 18S maturation.
B. Pre-rRNA processing in mouse. As in human cells, the primary 47S transcript is first cleaved in the 5'ETS. However, contrary to human cells, supplementary intermediates are generated before the 45S pre-rRNA. Indeed, the cleavages in the 5' and 3' ends is performed in several steps in mouse cells. After obtaining the 45S rRNA, the latest undergoes further cleavages following two alternative pathways.

As shown above, immature rRNA cleavage sites are precisely located on the pre-rRNA and strictly ordered. A default in the location or the progression of these cleavages, independently of the chosen pathway, can lead to aberrant mature rRNAs and therefore defective ribosomes. Hence, the pre-rRNA cleavage steps are tightly regulated. Indeed, several rRNA modifying enzymes and factors as endo-and exonucleases and putative RNA helicases are required for the pre-rRNA processing. In particular, 5'-ETS processing necessitates ribosomal proteins **(Ferreira-Cerca et al., 2005; O'Donohue et al., 2010**), snoRNAs and the small subunit (SSU) processome U3 (**Dragon et al., 2002; Osheim et al., 2004; Phipps et al., 2011**) in mammals, and the exosome in yeast **(de la Cruz et al.,**

1998; Sloan et al., 2012). These factors not only play a role in the cleavage itself but also in the RNA folding and chaperoning through hybridization to the rRNAs (**Gerbi and Borovjagin, 2013; Hughes, 1996; Marmier-Gourrier et al., 2011; Sharma and Tollervey, 1999**) allowing to obtain the proper conformation needed. Similarly, ITS1 processing is mediated by a large number of factors including PES1, BOP1, NOL12 and ribosomal proteins of the large subunit **(Lapik et al., 2004; Preti et al., 2013; Sloan et al., 2013**). Functional mutation or removal of one of these factors affects processing leading to accumulation of the intermediates and to disrupted ribosomes. For example, in *Xenopus*, the order of cleavages is altered after mutation in U3 or U8 snoRNAs (**Peculis and Steitz, 1993**).

II.2 Post-transcriptional modifications

Maturation of rRNA is accompanied by the addition of a large number of post-transcriptional covalent modifications such as 2'-O- ribose methylation, pseudouridylation, or rRNA base methylations. These post-transcriptional modifications occur simultaneously to pre-rRNA cleavages. More specifically, 2'-O-methylation and pseudouridylation are performed early during ribosome biogenesis and co-transcriptionally whereas rRNA base modifications are formed later on during the process. The number of modified sites increases with the complexity of the organism, although modifications patterns show evolutionary conservation, and most sites modified in yeast rRNA are also modified in vertebrates. Pre-rRNA modifications are mostly located within the most conserved functionally important domain of mature RNAs, particularly into the structural elements contributing to the peptidyl-transferase region and its vicinity (**Brimacombe et al., 1993**). This functional studies, as well as the precise location allow to speculate that rRNA modifications are necessary for efficient and faithful translation (**Jack et al., 2011; Liang et al., 2007)**. In particular, both in yeast and bacteria, rRNA modifications are important for translational fidelity (**Liang et al., 2009; Watkins and Bohnsack, 2012**) and 60S stability therefore ribosome function **(Demirci et al., 2010; Gigova et al., 2014; Knippenberg, 1986**). Moreover, knockdown of a single snoRNA is sufficient to alter development of zebrafish embryos highlighting the importance of rRNA modifications during development (**Higa-Nakamine et al., 2012**). In addition, rRNA base modification, 2'-O-methylation and pseudouridylation have been linked to diseases such as cancers, autoimmune syndromes or genetic diseases (**Armistead et al., 2009; Jangani et al., 2014; McMahon et al., 2015; Nakazawa et al., 2011; Oie et al., 2014**). To date, however, it

remains unclear in most cases whether the disease is due to loss of RNA-modifying activity, or failure to assemble sufficient ribosomes. Indeed, ribosomal RNA-modification enzymes are known to perform additional functions in diverse processes, including pre-rRNA processing, rRNA synthesis regulation and rRNA surveillance **(Jobert et al., 2013; Oie et al., 2014; Tessarz et al., 2014; Yang et al., 2013**). Moreover, in mice, mutation of Dyskerin, therefore global decrease of pseudouridine, leads to a disruption of the IRES-dependent translation of cellular mRNA such as p27, XIAP or Bcl-xl (B Cell Lymphoma; **Bellodi et al., 2010; Yoon et al., 2006**). Surprisingly, cap-dependent translation is not affected by this mutation. Indeed, pre-initiation complex formation on IRES sequences is decreased of 50% in dyskerin mutants. In addition, decrease of the 2'-O-methylation leads to a decrease IRES dependent translation of a subset of mRNA such as p53, p27 and SNAT2 while global translation is not affected (**Chaudhuri et al., 2007**).

II.2.1. SnoRNP mediated modifications

The major chemical modifications are mostly guided by snoRNAs which are small, abundant and stable RNAs acting through the ribonucleoprotein (RNP) complex. Within this complex, snoRNAs base-pair (bp) to rRNAs allowing the correct positioning of the modification enzymes. On the basis of associated proteins and conserved RNA sequence elements, the snoRNAs can be divided into two major classes: the box C/D and box H/ACA. The conserved boxes are bound by proteins important for snoRNA stability, nucleolar targeting and snoRNA function. Box C/D and H/ACA snoRNAs ranging from 60 to 200 nt and 120 to 250 nt, respectively, are associated with four core proteins including the enzymes mediating the rRNA modifications. In particular, box C/D snoRNAs are involved in the 2'-O-methylation of the pre-rRNA and are associated with proteins such as the methyltransferase Fibrillarin (Nop1p in yeast), Nop56, Nop58 and Nhp2l1. 2'-O-methylation corresponds to the transfer of one methyl group at the 2' position of the ribose on the nucleoside (*fig 14*). Methylation of rRNA is carried out at more than one hundred sites. Box H/ACA snoRNAs are associated with the core proteins Nhp2p, Nop10p, Gar1p and dyskerin (Cbf5p in yeast). The latter is responsible for the isomerization of the uridine residue. As I worked on fibrillarin during my thesis, further details on the box C/D complex will be given in the Chapter 1, Part II, II.3. Box C/D complex.

It is noteworthy, however, that a subset of snoRNAs has an independent role in processing of pre-rRNA and is involved instead of rRNA modifications in pre-rRNA cleavages (**Tollervey, 1996**). These include the box C/D snoRNAs U3 and U14 and the box H/ACA snoRNAs snR10 and snR30. Indeed, as mentioned above, the U3 snoRNA is not a 2'-O-methylation guide but is involved in the cleavage steps leading to the maturation of the 18S rRNA (**Peculis and Steitz, 1993**).

II.2.2. rRNA base modifications

In addition to the box H/ACA mediated uridine isomerization, some rRNA bases are also modified. These modifications occur through the addition of one, or sometimes two, methyl groups onto specific atoms. A subset of bases can also be either aminocarboxypropylated or acetylated (**Sharma and Lafontaine, 2015**). These modifications are nearly all produced enzymatically by autonomous proteins interacting with their substrate, for which the site specificity does not require any snoRNA hybridization (**Mullineux and Lafontaine, 2012**). These enzymes have a particularly important role in rRNA processing as cleavage is reduced (or does not occur) when the enzymes do not assemble onto precursor ribosomes at the right time. Thus, by making binding of the modification enzyme to pre-rRNA a prerequisite for cleavage, cells have selected a strategy through which, in principle, only modified molecules are produced (**Mullineux and Lafontaine, 2012**).

II.3 Box C/D complex

As mentioned above, snoRNP particles are found in complexes consisting of snoRNAs and a few associated proteins. In particular, the box C/D complex comprises C/D guide snoRNAs with four core proteins. One part of my thesis project relies on the functional study of the box C/D complex. Therefore, in this chapter, I will describe the different components of this complex as well as its assembly and function.

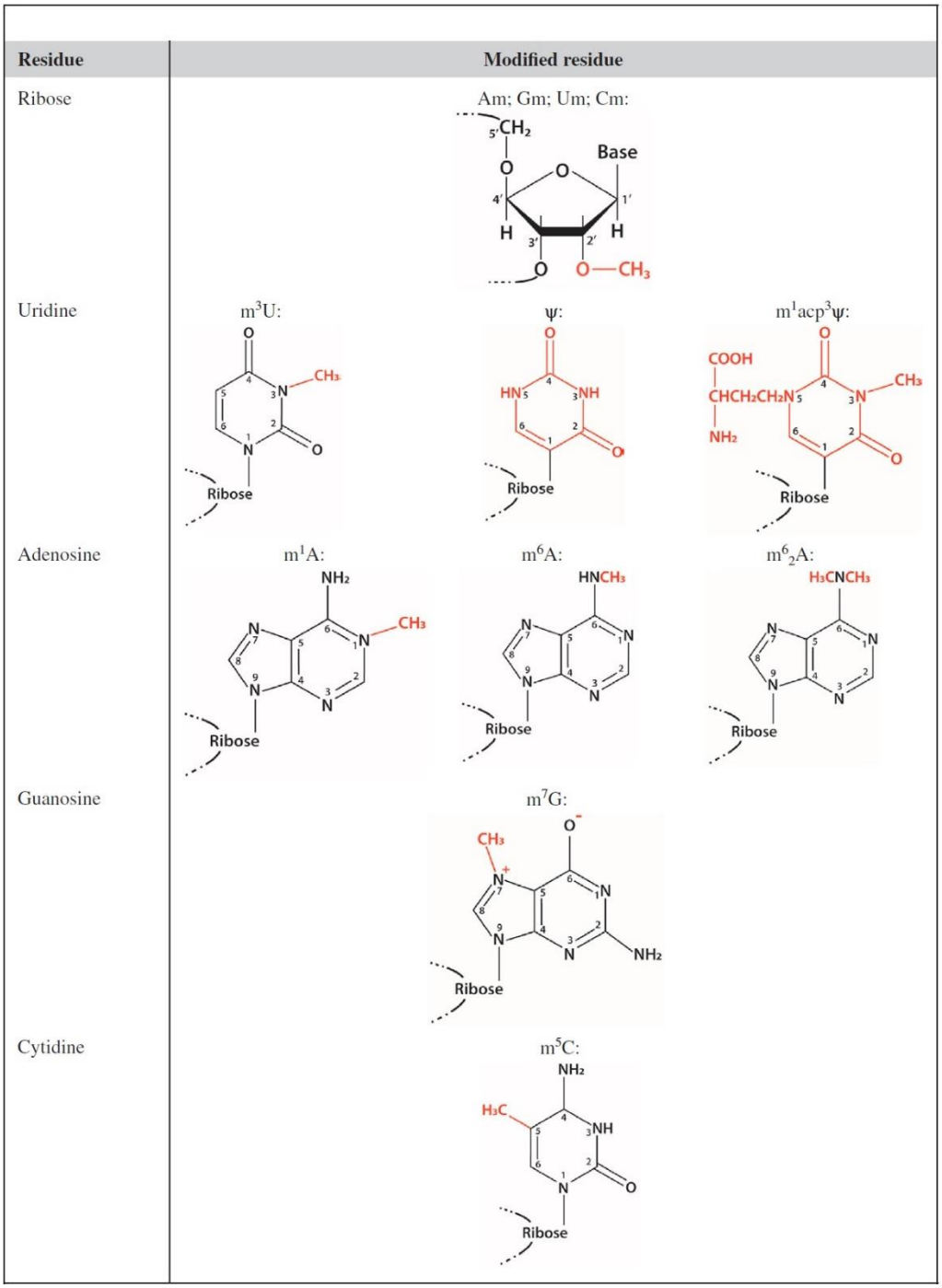

Figure 14: rRNA post-transcriptional modifications (*Therizols et al., 2015*)
Modified and/or added chemicals groups are highlighted in red; m3U,
A. Ribose methylation Am, 2′-O-methyladenosine; Gm, 2′-O methylguanosine; Um, 2′-O methyluridine; Cm, 2′-O methylcytosine, **B. Base pseudouridylation** ψ, pseudouridine**,**
C-E. Other base modifications.

II.3.1. snoRNA

The role of snoRNAs is to provide a scaffold onto which partner proteins assemble, and to function as guides for specific rRNAs sequence recognition and tethering of target RNAs, thereby specifying the modification sites. In eukaryotes, cells use different strategies to synthesize snoRNAs. Some vertebrate snoRNAs such as processing snoRNAs U3, U8 and Mitochondrial RNA processing (MRP), and most snoRNAs in yeast are transcribed from independent genes, mostly by RNA polymerase II (PolII). Another strategy, in plants and yeast, involves processing from polycistronic transcripts containing as many as nine different snoRNAs (**Terns and Terns, 2002; Weinstein and Steitz, 1999**). However, all known guide snoRNAs in vertebrates are encoded in introns of genes transcribed by PolII while in yeast and plants it is less common. Interestingly, most snoRNA host genes encode housekeeping proteins essential for ribosome biogenesis or function, suggesting that the host genes had been selected to allow coordinated accumulation or snoRNAs and encoded proteins (**Filipowicz and Pogacić, 2002**).

Following transcription most snoRNAs require processing to produce mature molecules. Polycistronic transcripts need to be excised through the catalysis by an endoribonuclease. Intronic snoRNAs can mature by two alternative pathways. Usually, these RNAs are processed from excised introns by the action of exonucleases. More rarely, snoRNAs are excised from introns by endonucleases and mature ends are then generated through exonucleolytic digestion. Interestingly, specific signals centered around boxes C and D, acting as binding sites for snoRNP proteins, are required for faithful processing of snoRNAs (**Terns and Terns, 2002; Weinstein and Steitz, 1999**). Moreover, core proteins interactions with their snoRNAs might provide protection from over-digestion by exonucleases (**Shaw et al., 1998**).

Box C/D snoRNAs contain two short sequence motifs box C (5'PuUGAUGA3') and box D (5'CUGA3'), located only a few nucleotides away from the 5' and 3' ends, respectively (*fig 15A*). The two motifs are generally brought together in a typical 5'-3' terminal stem-box structure, involving the 4–5 nucleotides at both termini, which is critical for snoRNA biogenesis and nucleolar localization (**Bachellerie et al., 2002**). The internal part of C/D box snoRNA often contains imperfect copies of C and D boxes, respectively called C′ and D′ which are less conserved in eukaryotes (**Kiss-László et al., 1998; Tycowski et al., 1996**). Characteristic sequence motifs, boxes C and D, and the neighboring structures play an essential role in the assembly of the snoRNPs and consequently, are also important for

the stability and proper localization of snoRNAs (**Terns and Terns, 2002)**. Indeed, the C/D box and C'/D' box form a characteristic stem-bulge-stem structure called the kink-turn, allowing the snoRNA to recruit the core snoRNP proteins. Upstream D and D′ boxes are complementary rRNA guide sequences able to form base pair with the rRNA, thus allowing the snoRNA to bind the rRNA substrate in a site-specific manner. The 2′-O-ribose-methylation occurs invariably on the fifth nucleotide upstream D or D′ box (**Cavaillé et al., 1996; Kiss-László et al., 1996**).

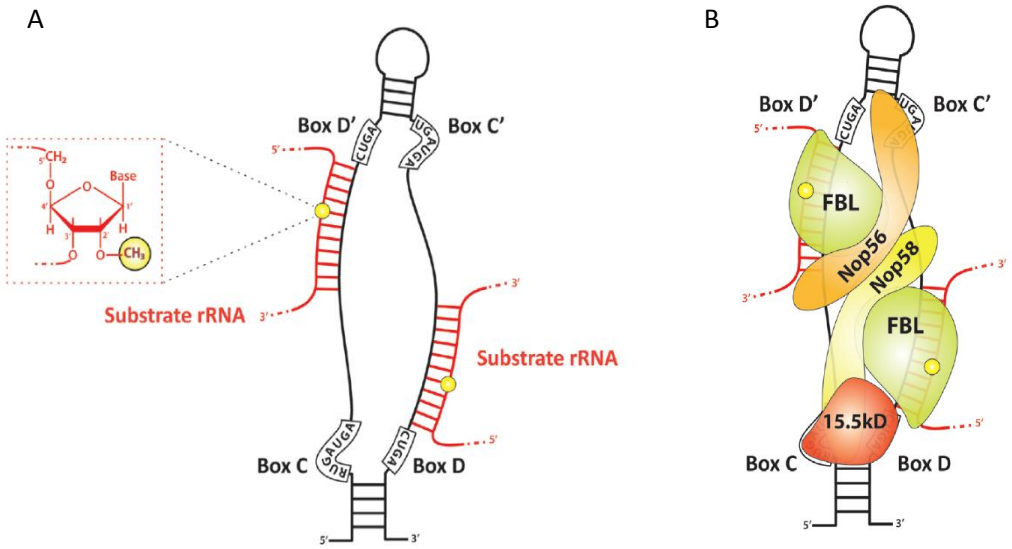

Figure 15: Eukaryotic C/D box snoRNA and snoRNPs organization. ***Adapted from (Therizols et al., 2015)***
A. Schematic representation of a C/D box snoRNA. SnoRNAs are represented in black with box C and D consensus sequences, shown in white boxes, respectively close to 5' and 3' ends. Substrate rRNAs are indicated in red. Methylated residues are highlighted in yellow.
B. Schematic representation of eukaryotic C/D box snoRNPs. 15.5kD (red) is recruited to the C/D box motif. Two copies of Fbl (green), each interacting with either one copy of Nop56 (orange) or one copy of Nop58 (yellow). Nop56 and Nop58 heterodimerize.

II.3.2. Proteins

Box C/D snoRNPs contain four evolutionary conserved, essential proteins: Fibrillarin, Nop56, Nop58 and Nhp2l1 (15.5kD/Snu13p). Beside the main methylation role, association with the core box C/D proteins is crucial for the accumulation of the snoRNA, as well as snoRNA processing and nucleolar localization. In this chapter, I will briefly give an overview of the different proteins of the complex and their association to give rise to a functional complex.

II.3.2.a Fibrillarin

Fibrillarin belongs to the superfamily of the Rossmann-fold-S-adenosylmethionine (SAM) methyltransferases (MTases). Within the snoRNP complex fibrillarin transfers the methyl group of SAM to 2-hydroxyl group of ribose targets. Fbl also contains site rich in arginine and glycine residues and a specific motif to bind RNA. Fbl seems to be involved in additional functions such as pre-RNA cleavage, rRNA transcription regulation or ribosome assembly (**Beltrame and Tollervey, 1995; Koh et al., 2011a; Tessarz et al., 2014; Tollervey et al., 1993**). Fibrillarin structure and functions will be described in more details in the Chapter 1, Part II, II.4.Fibrillarin.

II.3.2.b Nop56/Nop58

Nop56 for nucleolar protein (NOP) of 56kDa (also called Nol5A) and Nop58 for nucleolar protein of 58kDa (also called Nop5 in fruit fly) are two paralog proteins. They belong to a family of conserved proteins which all share a conserved central NOP domain that is proposed to function in the binding of these proteins, a C-terminal α-helical domain and a N-terminal a/b domain. NOP proteins heterodimerize in order to scaffold the whole complex and are responsible for the correct positioning of Fbl to the target rRNA. Indeed, they contact the guide regions of the snoRNAs and have been shown to cross-link to rRNA *in vitro*. In particular, Nop58 and Nop56 preferentially associate with the C/D and C'/D' motifs, respectively. In archaea, only one Nop homolog called Nop5 is responsible for the scaffolding of the complex through homodimerization via their coiled-coil domains (**Watkins and Bohnsack, 2012**).

II.3.2.c 15.5 kD/ Nhp2l1

The 15.5K protein (also called NHP2l in mammals, snu13p in yeast, L7Ae in archaea) was first characterized as a component of the U4/U6.U5 tri-snRNPs that directly binds to the 5'stem-loop of the U4 small nuclear RNA (snRNA). The structural protein binds directly to the box C/D core motif, initiating formation of the box C/D snoRNP core complex. It contains a conserved RNA binding domain allowing the binding of the snoRNA and therefore, the recruitment of the snoRNP.

II.3.3. Function and assembly of the complex

In vitro, Fbl is not able to catalyze nucleotide modifications of the rRNA targets in the absence of the other core RNP proteins, even when the guide is present (**Baker et al., 2005; Omer et al., 2002**). Hence, the assembly of the box C/D complex is a crucial process which

needs to be tightly regulated and ordered. The recruitment of the core snoRNP proteins to their respective snoRNAs is initiated co-transcriptionally. As mentioned above, initiation of the formation of the box C/D snoRNP complex involves the RNA binding protein 15.5k. Indeed, 15.5k directly recognizes kink-turn (K-turn) motifs, a common protein-binding site (**Klein et al., 2001**) present in the snoRNA. The specificity of 15.5k allows binding at only the more conserved C/D box motif of the snoRNA, but not at the C'/D' boxes, because these second sites often lack identifiable K-turns (**Szewczak et al., 2002**). This box C/D initiation complex formed by 15.5k is likely important for stabilizing the snoRNA in a conformation that favors the recruitment of the other proteins (**Reichow et al., 2007**). In archaea, the formation of the initiation complex enables the recruitment of Nop5 to the assembling RNP, which in turn facilitates the association of fibrillarin to the catalytically active complex *in vitro* (**Omer et al., 2002**). However, Nop5 can also directly associate with Fbl in the absence of RNA (**Aittaleb et al., 2003**). In eukaryotes, Nop58 and Fbl are independently recruited to the snoRNA, suggesting a direct interaction with rRNA. However, the association of Nop56 requires the presence of Fbl, suggesting that the interaction with the enzyme mediates its recruitment to the snoRNP (**Lafontaine and Tollervey, 2000**). While interacting with Fbl, Nop56 and Nop58 heterodimerize through their coiled-coil domains to allow communication between the C/D and C'/D' structural units. This interaction locks the RNP into the proper conformation leading to the formation of a functional snoRNP complex (**Aittaleb et al., 2003; Lin et al., 2011; Rashid et al., 2003**). Furthermore, 15.5k might be recruited to the C'/D' domain through protein-protein interactions, in particular Nop56/Nop58 **(Schultz et al., 2006**). Nop56/Nop58 interaction role in the formation of the complex has been demonstrated by the fact that snoRNA containing only the box C/D motif can still be associated with all four core proteins (**Newman et al., 2000; Watkins et al., 1998**). Interestingly, studies of C/D snoRNPs reconstituted in *Xenopus* oocyte nuclei highlighted a crosslink of Fbl to both D and D' boxes, leading to the hypothesis that one copy of the enzyme is associated with each guide domain of the snoRNA (*fig 15B*) (**Cahill et al., 2002**). Assembly of box C/D complex (as H/ACA complex) requires the HSP90/R2TP chaperone-cochaperone system (**Boulon et al., 2008; Zhao et al., 2008**). This system plays essential roles in the biogenesis of snoRNPs, and appears to use specific adaptors to interact with C/D snoRNPs (reviewed in **Massenet et al., 2016**).

II.4 Fibrillarin

Originally described in *Physarum polycephalum*, Fbl was subsequently identified in the dense fibrillar component of vertebrate nucleoli (hence its name) (**Christensen et al., 1977**). Fibrillarin is an essential nucleolar protein having a conserved sequence and function throughout evolution (**Jansen et al., 1991; Ochs et al., 1985**). It is one of the most abundant protein of the nucleolus, and it is therefore commonly used as a marker for this sub-compartment of the nucleus. During interphase, Fbl can be detected in the transition between FC and DFC, where rDNA transcription occurs, and in the DFC, where the pre-rRNA processing takes place in eukaryotic cells (**Ochs et al., 1985; Sobol et al., 2013**). Besides, Fbl can also accumulate in sub-organelles of the nucleus called the Cajal bodies (CBs) (**Snaar et al., 2000**). Several synonyms can be found in the literature depending on the organism and the time when the reference was published. In this manuscript I will use the term "Fibrillarin" for all eukaryotic Fbl, with the exception of yeast Fbl which is called Nop1. In this chapter, I will give an overview on the evolution, structure and functions of Fbl.

II.4.1 Fibrillarin structure

The Fbl protein sequence can be divided into two big domains: the N-terminal domain and the methyltransferase domain. In particular, eukaryotic Fbl consists of three major structural domains: N-terminal glycine and arginine rich (GAR) domain, a central domain with presumed RNA-binding capacity, and C-terminal α-helical domain (**Aris and Blobel, 1991**) separated by two short spacer sequences Sp1 and Sp2. The RNA-binding and the α-helical domains form the methyltransferase domain (*fig 16A*). The GAR domain is responsible for the interaction with different cellular and viral proteins. Moreover, it directs the protein to the nucleus and is involved in nucleoli retention. However, it should be emphasized that specific nucleolar localization of Fbl in the DFC does not depend on the GAR domain (**Snaar et al., 2000**). This domain is methylated on several arginine residues by the protein arginine N-methyltransferase 1 and 7 (PRMT1 and PRMT7) (**Yanagida et al., 2004; Zurita-Lopez et al., 2012**). This methylation might promote specific binding with some proteins such as survival of motor neurons 1 (SMN1), a protein located in the CBs and involved in the spinal muscular atrophy disease. The MTase domain is divided into two regions: the R or central region and the α-helix domain. The R region contains a characteristic RNA-binding motif GCVYAVCF specific of proteins that bind RNA (**Aris**

and Blobel, 1991). The C-terminal region of Fbl, composed of the α-helix domain, interacts with Nop56 **(Lechertier et al., 2009**).

II.4.2 Fibrillarin functions

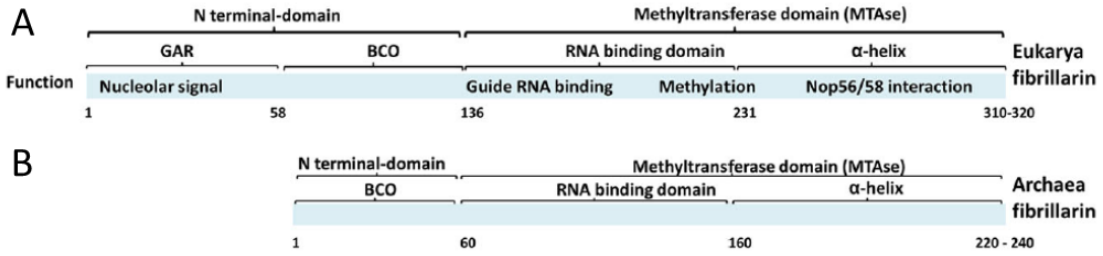

Figure 16: Structure of Fbl protein in eukaryotes and archaea. (*Rodriguez-Corona et al., 2015)*
A. In eukaryotes, the Fbl sequence is divided in four regions. The GAR domain is a sequence rich in glycine and arginine. The BCO domain is a sequence with undefined activity. The methyltransferase domain contains the enzymatic activity as well as the conserved RNA binding sequence. This MTase domain can be divided into two subdomains: the RNA binding domain and the α-helix. The latter allows interactions with the box C/D partner: Nop56.
B. In archaea, the GAR domain is lacking. N-terminal domain is composed of the BCO domain for which no defined activity has been highlighted so far.

Fibrillarin is nowadays considered as the rRNA methyltransferase. The rRNA 2'-O-methylation activity has been supported by the structure of the protein which is characteristic of methyltransferases (**Feder et al., 2003; Wang et al., 2000**), and by its ability to bind RNA **(Rakitina et al., 2011**). However, only a few studies show directly the enzymatic activity. In the early nineties, functional analyzes of Fbl have been performed in yeast. Especially, **Jansen et al.** demonstrated for the first time that vertebrate Fbl functions in rRNA processing *in vivo*. Furthermore, they highlighted the conservation of Fbl in eukaryotes since either human or *Xenopus* Fbl can complement a yeast *nop1* mutant. **Tollervey et al**. further characterized the function of Nop1 in yeast. Generating a point mutation in the putative methyltransferase domain of the protein, they stressed out the rRNA methylation activity of fibrillarin as well as its involvement in pre-rRNA processing and modifications, and ribosome assembly (**Tollervey et al., 1993**). Additional investigations showed that Nop1 binds AdoMet (S-adenosyl-L-methionine) which is necessary for the methylation reaction (**Galardi et al., 2002**). Besides, Fbl methylation activity is required and essential during embryonic development. Indeed, depletion of Fbl in mice leads to embryonic lethality (**Newton et al., 2003**).

Further analyzes demonstrated that 2'-O-methylation by Fbl can also be directed on distinct RNAs types such as snRNAs or mRNAs. Indeed, **Ganot et al. and Tycowski et al.** pointed out the existence of small RNAs able to target U6 snRNA in yeast (**Ganot et al., 1999**) and in higher eukaryotes such as *C.elegans*, *X.tropicalis* and *M.Musculus* (**Tycowski et al., 1998**). Particularly, in the latter, two small RNAs have been identified. They contain box C/C' and D/D', characteristics of box C/D snoRNAs associated with Fbl. Moreover, these RNAs co-immunoprecipitate with Fbl suggesting a snRNA methylation activity. Furthermore, small Cajal body-specific RNAs (scaRNAs) trigger the 2'-O-methylation and pseudouridylation of snRNA. ScaRNAs also co-immunoprecipitate with Fbl suggesting the involvement of the enzyme.

Surprisingly, in mice, a brain specific nucleolar RNA called HBII-52 displaying hallmarks of the family of ubiquitous snoRNAs that guide 2'-O-ribose methylation of rRNA, lacks any telltale rRNA complementarity. Instead, it has a conserved complementarity to a critical segment of the serotonin 2C receptor mRNA, pointing to a potential role in the processing or this mRNA (**Cavaillé et al., 2000**).

More recently, **Tessarz et al., 2014** showed that human FBL and its yeast orthologue Nop1 are also histone methyl-transferases. Indeed, they identified a single glutamine (Q104 in human and Q105 in yeast) in Histone 2A (H2A) as a site of methylation and showed that FBL/Nop1 is responsible for this enzymatic activity. Nop1 methylates *in vitro* H2AQ105 in the presence of of H2A and SAM but no other proteins, suggesting that Nop1 would function in a different molecular context than during rRNA methylation. Furthermore, *in vivo* studies using a temperature-sensitive mutant for Nop1, showed the involvement of Nop1 in this histone methylation. The same observation was made using human cells knocked down for FBL. This modification exclusively occurs within the nucleolus. More precisely Nop1 is particularly enriched in the 35S rDNA chromatin, in active rDNA sequences and results in the weakening of the interaction between H2A and the histone chaperone complex FACT (Facilitator of Chromatin Transcription) (**Tessarz et al., 2014**). Glutamine modification would therefore inhibit fixation of FACT, leading to the activation or PolI-mediated RNA transcription. Hence, FBL/Nop1, in human and yeast, regulates ribosome production by controlling PolI-mediated transcription and ribosome quality through its rRNA 2'-O-methylation activity.

Fbl is also involved in the rRNA maturation, more specifically in their cleavage. Indeed, a screen by **Tollervey et al**. allowed the identification of two mutants with maintained rRNA methyl-transferase activity, but defective in rRNA maturation. Indeed, they showed using western blot analyzes that in *NOP1* mutants, the 35S pre-rRNA was accumulating while the other pre-rRNA and mature 18S and 25S rRNA were not produced.

II.4.3 Fibrillarin localization during cycle

Fibrillarin localization, like other nucleolar proteins, is highly dynamic as shown with FRAP (Fluorescence Fecovery After Photobleaching) These observations showed that Fbl shuttles between the nucleoli and the nucleoplasm (**Phair and Misteli, 2000; Snaar et al., 2000**). Under these conditions Fbl molecules are present both in the CB and nucleoli only for a short time indicating that it may roam the nucleus in search of specific binding partners (**Phair and Misteli, 2000**).

The abundance and localization of Fbl during mitosis has also been studied in details using several models (**Amin et al., 2007**; **Hernandez-Verdun et al., 2013**). Particularly, in Hela cells, FBL is prominently found in the nucleoli during interphase (mainly in FCs and DFCs but also in the CBs). In prophase, when the nucleolus is dispersed, FBL is dispersed to the chromosomal periphery where it remains until anaphase. At the end of mitosis during telophase, FBL is considerably accumulated in prenuclear bodies (PNBs) which eventually form new nucleolus. This considerable accumulation supports the notion that the nucleolus is formed by recruited pre-rRNA processing factors followed by fusion of prepackaged PNBs into nucleolus (**Dousset et al., 2000; Savino et al., 1999**). In early G1, FBL localizes within the nuclear condensed chromatin **(Amin et al., 2007**). In addition, FBL seems to be actively involved in cell proliferation. Indeed, siRNA mediated knock-down experiments pointed out the role of FBL in maintaining normal nuclear morphology as well as contributing to cell growth.

In fact, siRNA treated Hela cells displayed an abnormal nuclear shape as well as a decreased cell proliferation. The link between ribosome biogenesis and cell cycle will be further detailed in the Chapter 1, Part II, III.1 Ribosome biogenesis and cell cycle progression are mutually regulated.

II.4.4 Fibrillarin and interacting partners

In yeast, mutations of *fbl* generated by **Tollervey et al**. showed that Fbl is essential for cell survival. The diverse mutations generated were located in different domain of the protein

and had different effects on ribosome biogenesis suggesting that different subsets of interacting partners can be involved (**Tollervey et al., 1993**). Over the past 20 years, many Fbl partners have been identified (*fig 17A*). As described above, FBL localization changes throughout the cell depending on the cell cycle phases. Hence, interactions may also depend on the cell environment or differentiation state. Results from sucrose and glycerol gradients show different sedimentation peaks of Fbl, suggesting that the protein is found in more than one complex in the cells (**Dragon et al., 2002; Sasano et al., 2008**). The typical Fbl interacting partners are Nop56/Nop58, 15.5K and snoRNAs, forming the snoRNP complex which is involved in rRNA methylation. However, Fbl protein interacts with a large variety of partners beside the snoRNP components. For example, in a large-scale analysis of protein complexes in yeast, **Krogan et al**. identified RPA49, a non-essential subunit of PolI, as one partner of Nop1.

Among other interacting proteins, p32 and Nop52 interact with Fbl at different times but probably at the same binding region. It has been suggested that p32 would associate with the pre-ribosomal 90S particles via Fbl in order to modify ribosome maturation. In its turn, Nop52 would replace Fbl and interact with p32 initiating the formation of the 60S and 28S ribosomal particle in the granular component **(Yoshikawa et al., 2011**).

The diversity and density of Fbl interactions (**Chatr-Aryamontri et al., 2013; Krogan et al., 2006**) highlight the extent of possible functions for Fbl such as post-translational modifications or regulation of the stability and localization of the protein. In particular, these interactions would be involved in many cellular processing. Depending on the interactions, Fbl could favor cell growth or growth inhibition (*fig17B*).

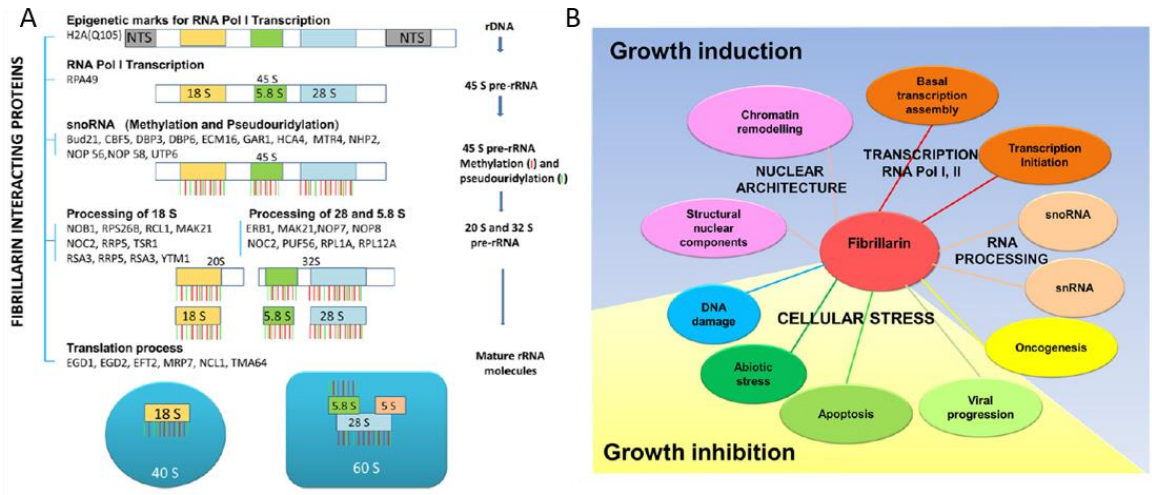

Figure 17: Fibrillarin interacts with a high diversity of partners, conferring several functions in cellular processes (*Rodriguez-Corona et al., 2015*)

A. Fibrillarin interacting proteins are involved at different stages of ribosomal processing from PolI mediated rDNA transcription to translation process.

B. Schematic drawing of fibrillarin involved in cellular processes.

II.4.5 Fibrillarin and pathology

The nucleolus is involved in biogenesis of the machinery necessary for overall protein translation and eventually cell growth and cell cycle progression (**Tsai and Pederson, 2014**). The specific alteration in many of the NOPs can result in growth behavior changes or altered cell viability. The involvement of ribosome biogenesis in general in pathologies will be further assessed in the Chapter 1, Part II, IV.3.Mutations of RP and RBF coding genes lead to tissue-specific phenotypes.

As described above, Fbl plays a regulatory role in many biological processes such as protein translation. Furthermore, its regulatory role is required during development or for the maintenance of the pluripotent state. Supporting this hypothesis, several observation show that dysregulation of Fbl is associate with pathological phenotypes. For example, Fibrillarin has been shown to be involved in cancer, viral infections or systemic scleroderma.

II.4.5.a. Fibrillarin is an oncogene

It is now well established that FBL is involved in cancer. Indeed, various studies measuring *FBL* expression in cancer, show an overexpression of the protein compared to healthy tissue. *FBL* expression level is significantly higher in human breast cancer **(Marcel et al., 2013; Su et al., 2014**), squamous cell cervical carcinoma (**Choi et al., 2007**) and prostatic intraepithelial neoplasia (**Koh et al., 2011b**). Moreover, *FBL* expression has been correlated to the expression of oncogenic or tumor suppressor genes, known to be involved in tumor development. In particular, *C-MYC* binds to *FBL* promoter (**Koh et al., 2011b**) in order to regulate its expression (**Schlosser et al., 2003; Coller et al., 2000**). Furthermore, a correlation between *FBL* and *C-MYC* expression is observed in breast cancer (**Su et al., 2014**), human B-cell line (**Schlosser et al., 2003**) and human fibroblasts (**Coller et al., 2000**). These studies demonstrate that *FBL* is a target of *C-MYC.*

In addition, **Marcel et al.,** showed that *FBL* is repressed by the tumor suppressor *P53*. In breast cancer cells, *P53* inactivation results in an increased level of FBL and higher level of aberrant rRNA methylation that leads to altered ribosome activity including impairment of translational fidelity and increased translation of key cancer genes (**Marcel et al., 2013**).

FBL expression has been correlated with cellular characteristics associated to cancer cells, such as proliferation. For example, diminution of *FBL* expression using siRNA leads to a diminished proliferation of prostatic and breast cancer cells (**Koh et al., 2011b**; **Su et al., 2014**).

II.4.5.b Fibrillarin is involved in viral infections

Several viruses with a nuclear phase interact with proteins localized both in the CBs and the nucleoli for their replication and transport inside the cells. Fbl shuttles between the CB and the nucleoli thereby explaining why this protein could be targeted by several viruses. One example, is Influenza A virus subtype H3N2 that causes flu. In this virus, a multi-functional protein (non-structural protein 1, NS1) inhibits the pre-mRNA processing in the host cells and counteracts cell antiviral responses. The NS1 protein interacts with both endogenous fibrillarin and nucleolin (**Melén et al., 2012)**. Similarly, the HIV Tat protein has been reported to interact with Fbl. This viral protein affects the ribosome rRNA maturation and the overall amount of 80S ribosome (**Ponti et al., 2008**) which could be involved in the modulation of the host response, therefore contributing to the apoptosis and protein shut-off in HIV-uninfected cells. Additionally, in plants, Fbl also interacts with viral proteins. Indeed, in the nut rosette virus, the encoded protein ORF3 interacts directly with Fbl (**Kim et al., 2007**) leading to the formation of viral RNPs able to move through the phloem resulting in complete infection of the plant. Therefore, this interaction is the key of systematic spread of the nut rosette virus (**Zheng et al., 2015**). However, the exact role of these interactions between fibrillarin and viral proteins remains unknown.

II.4.5.c Fibrillarin is targeted in systemic sclerosis

Systemic sclerosis is an autoimmune disease of the connective tissue. It is characterized by thickening of the skin caused by accumulation of collagen, and by injuries to small arteries. The systemic form of the disease affects not only the skin of the face, hands or feet, but can also progress to visceral organs such as kidneys, heart, lungs and gastrointestinal tracts. FBL autoantibodies were first identified in patients affected by systemic sclerosis (**Ochs et al., 1985**). In various population such as African descent and Native North American ethnicity, antibodies against FBL have been detected and correlated to shorter survival (**Mejia Otero et al., 2017**). Surprisingly, as in systemic sclerosis, autoantibodies against FBL develop in mercury-treated mice (**Reuter et al., 1989**). Moreover, mercury treatment leads to specific inhibition of PolI-mediated transcription and FBL cellular re-localization (**Chen and von Mikecz, 2000**). Upon treatment with mercury, FBL co-localizes with nucleoplasmic proteasome which might constitute the cell biological basis of autoimmune responses that specially target FBL in mercury-mouse models and sclerotome (**Chen et al., 2002**).

II.4.6 Fibrillarin evolution

Fibrillarin is present in archaea and eukaryotes which testify for the ancestral origin of Fbl. Sequence alignments and comparison of 10 model eukaryotic fibrillarins and all archaeal Fbls was carried out (**Rodriguez-Corona et al., 2015**). Archaeal Fbl lacks the GAR domain (*fig 16B*). These analyzes also revealed nine primary branches that separate groups of fungi, invertebrates, plants and vertebrates (*fig 18A*). The overall sequences vary significantly within each group. There are the greatest sequence similarities within plants (63%) and within vertebrates (61%), while invertebrates, fungi and Archaea show more sequence diversity (33, 27 and 20%, respectively). It remains to define if the differences account for some specific functions. For example, as described in the chapter Chapter 1, Part II, II.4.2 Fibrillarin functions, *Xenopus* and human Fbl are separated in the two different clades and they have a different complementation level in *NOP1* mutants (**Jansen et al., 1991**). Beside the variability of *fbl* sequence between clades, a particular signature, unique to the protein, has been highlighted. Furthermore, from the various X-ray crystallographic data which have been produced, the apparent sequence difference between *fibrillarins* only slightly alters the overall structure of the protein (*fig 18B*).

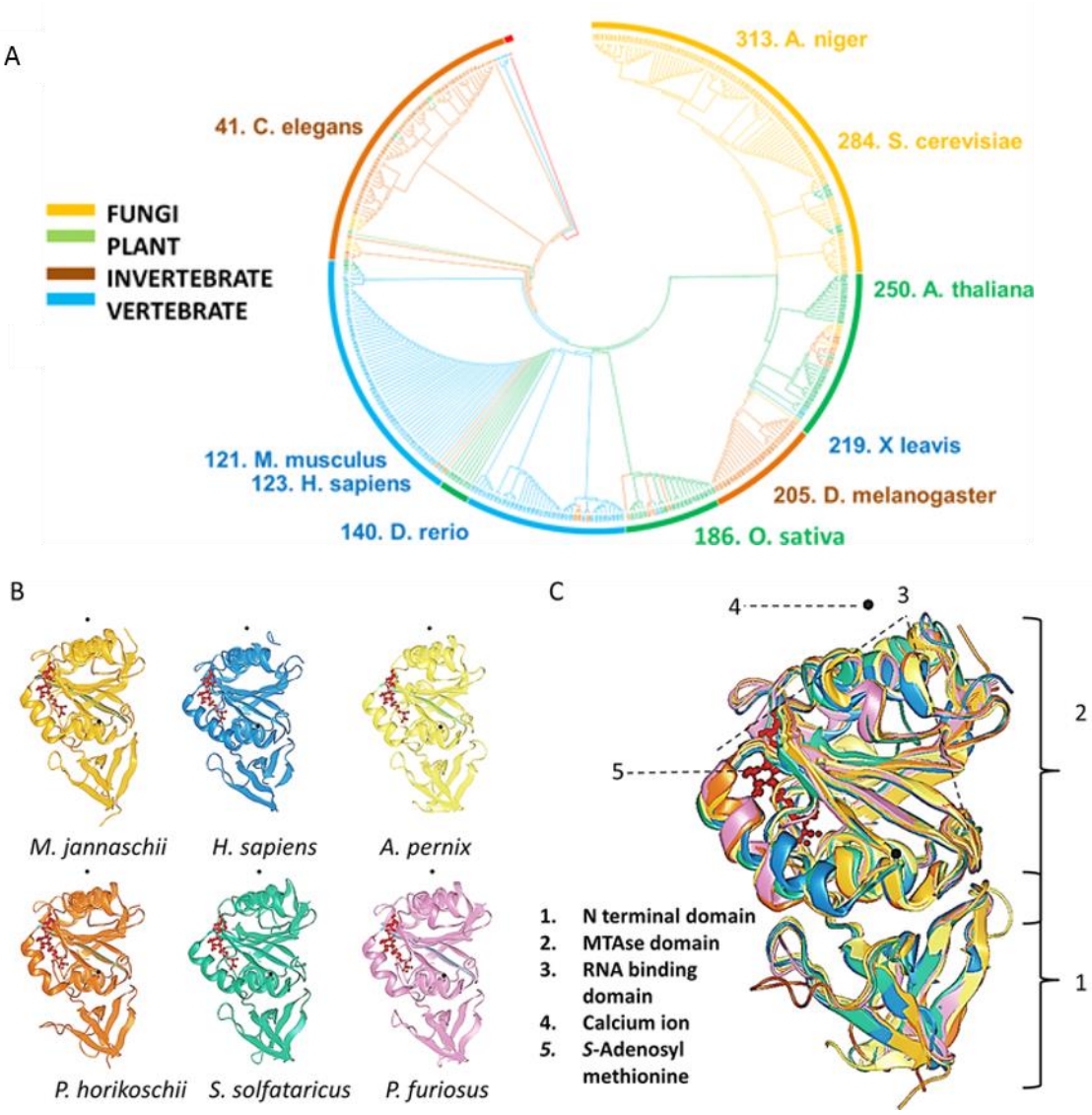

Figure 18: Evolution and conservation of Fibrillarin. ***(Rodriguez-Corona et al., 2015)***
A. Sequence comparison for all eukaryotic Fibrillarins.
The cladogram reveals nine primary branches separating fungi, plants, invertebrates and vertebrates. The analysis involved 212 amino acid sequences. All position contains gaps and missing data were eliminated.. **B**. Structural alignment of different Fbl. Six crystal structures of the Fbl from different organism were compared. Dark yellow: Methanococcus jannaschii; Blue: Homo sapiens Light yellow: Aeropyrum pernix; Orange: Pyrococcus horikoshii Green: Sulfolobus solfataricus; Purple from Pyrococcus furiosus **C**. The six crystal structures of Fbl were aligned to visualize the overlap of structures. The localisation of the calcium ion and the SAM are shown as well as the domain regions.

III Importance of ribosome biogenesis for cell homeostasis

Cell cycle progression and cell growth are highly energy-demanding steps and therefore require prodigious number of ribosomes. Several self-regulatory mechanisms controlling various aspects of ribosome biogenesis and functions have been uncovered and reveal new connections to cell cycle and cell-size control. In this chapter, I will describe the different ribosomal functions in the regulation of diverse cellular processes. In humans, alterations

of ribosome structure or function are involved in the development of cancer (**Montanaro et al., 2008**) as well as several different diseases. In fact, abnormal regulation of these key cellular mechanisms would lead to tumorigenesis through the deregulation of apoptosis, cell cycle arrest and cell proliferation (**Xu et al., 2016**). Consequently, a full understanding of the relationship between cell homeostasis and ribosomes may reveal new ways to induce cell cycle arrest in cancer cells. In addition, these analyzes may also provide new insights in the comprehension of the biology of stem and progenitor cells which are, by definition, strictly controlled-cycling cells. Furthermore, mutations of ribosomal proteins have been identified in several genetic diseases called ribosomopathies (**Yelick and Trainor, 2015**).

III.1 Ribosome biogenesis and cell cycle progression are mutually regulated

As previously mentioned, RNA PolI-mediated transcription level also oscillates during cell cycle progression (*fig 19*). In particular, Cyclin-Cdk complexes couple the ribosome biogenesis regulation with cell cycle progression. Transcription rate reaches its maximum during S and G2 phases and decreases during M phase. During G1 phase, rRNA transcription slowly recovers (**Klein and Grummt, 1999**). rRNA transcription fluctuations during cell cycle progression are generated by Cdk/cyclin-dependent phosphorylation of both UBF and TIF-1B/SL-1 (selectivity factor 1). More precisely, during mitosis, PolI-dependent transcription silencing is realized via Cdk1/cyclinB phosphorylation of TAF impairing the interaction of TIF-1B/SL1 with UBF (**Heix et al., 1998; Kuhn et al., 1998**). At the end of mitosis, Cdc14B, a phosphatase sequestered in an inactive state in the nucleolus during interphase, is released and dephosphorylate the TATA box binding protein associated factor (TAF), thereby activating SL1 and relieving mitotic repression of rRNA transcription. On the other hand, the quality of ribosomes itself can limit cell cycle progression. Indeed, it has been shown that the translation of cyclin E is specifically impaired upon ribosomal protein or rRNA haploinsufficiency. Hence, cells lacking a sufficient amount of ribosomal components fail to express cyclin E despite the formation of active Cdk4/cyclin D complexes. G1/S transition is therefore blocked and cells stop proliferating (**Derenzini et al., 2005; Volarevic et al., 2000**).

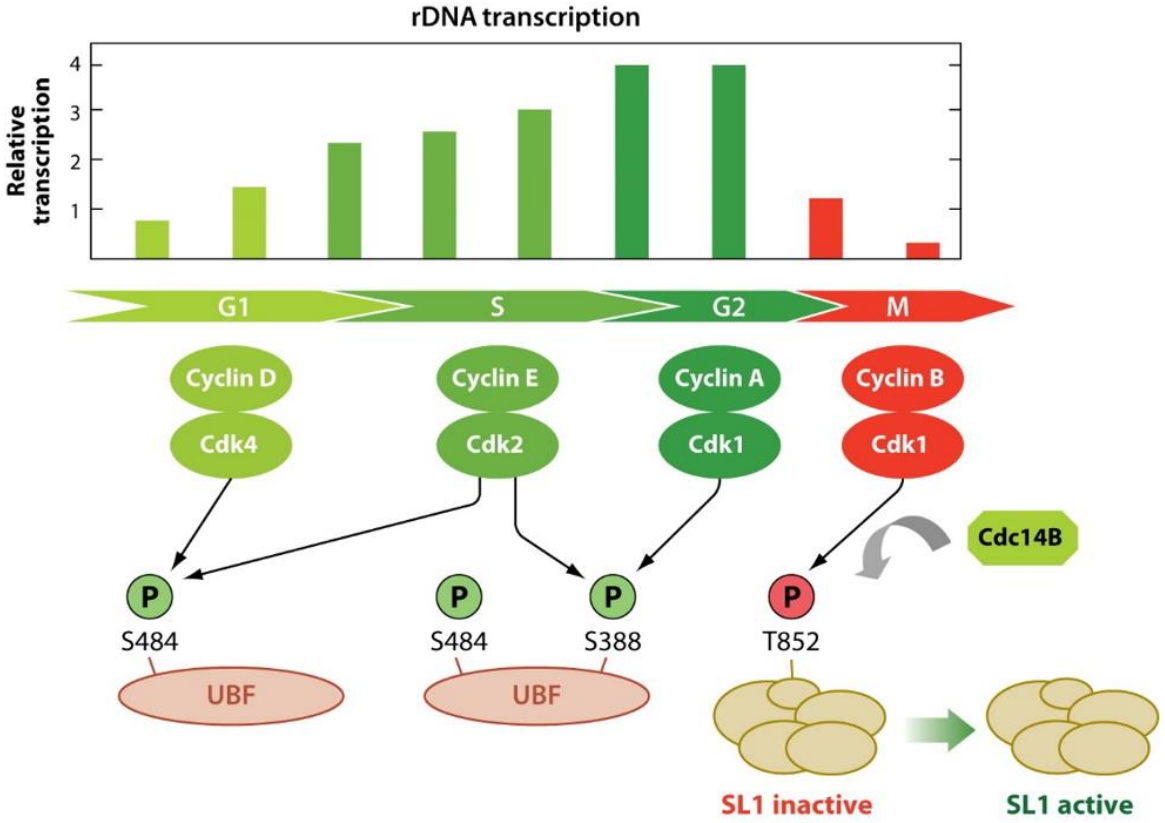

<u>Figure 19:</u> Regulation of RNA PolI-mediated transcription during cell cycle progression (*Drygin et al., 2010*)
UBF is activated during interphase by phosphorylation of serine 484 (S484) by Cdk4/cyclin D and phosphorylation of serine 388 (S388) by Cdk2/cyclin E and A. At the entry into mitosis, phosphorylation of TAFI110 at threonine 852 (T852) by Cdk1/cyclin B inactivates TIF-IB/SL1. At the exit from mitosis, Cdc14B dephosphorylates T852, leading to recovery of TIF-IB/SL1 activity. Activating phosphorylations are marked in green, inhibiting ones in red.

III.2 Nucleolar stress

In the last few years, it became evident that the nucleolus by using its huge reservoir of proteins, is able to regulate cellular processes such as cell cycle progression, cellular proliferation and differentiation, DNA damage repair, genome organization, ageing, cell stress response, protein degradation, protein folding and mRNA export (**Woods et al., 2015**). Thus the nucleolus is playing a very important role in maintaining cell homeostasis (**Pestov et al., 2001; Zhang and Lu, 2009**). In particular, upon ribosome biogenesis disruption via UV irradiation, nutrient deprivation or hypoxia, cellular processes regulated by the nucleolus are activated and cells are able to adapt to the new environment (**Boulon et al., 2010**). This condition, defined as the nucleolar stress, or ribosome biogenesis stress, is able to activate nucleolar stress signaling pathways mediated by several RPs. Some of these pathways involve the tumor suppressor 53 (Tp53, hereafter p53) activity while others

are p53-independent (**Deisenroth and Zhang, 2010; James et al., 2014; Pestov et al., 2001; Zhang and Lu, 2009**).

III.2.1. p53 dependent response pathways to nucleolar stress

P53 is a transcription factor which is able to induce cell cycle arrest and apoptosis by activating the transcription of several target genes and its own transcription. Under normal growth conditions, P53 is found in the nucleolus at a steady-state level under the control of the Mouse double minute 2 homolog (Mdm2). Mdm2 is the ubiquitin E3 ligase that negatively regulates *p53* by marking it for ubiquitin-mediated proteasomal degradation (*fig 20A*). In response to events inducing nucleolar stress, several RPs translocate to the nucleoplasm and bind to Mdm2, thus promoting P53 stabilization and subsequent activation of checkpoint genes (such as *p21/waf1/cip1*), DNA repair genes and pro-apoptotic factors (*Fig 20B*). In particular, RpL11, and RpL5 are essential for *p53* upregulation in response to impaired ribosome biogenesis. Furthermore, it has been shown that both ribosomal proteins of the large subunit can associate with each other via 5S rRNA to form a trimeric RNP complex (**Sloan et al., 2013b**).

Interestingly, when the 40S subunit is depleted in mouse hepatocytes, upon RpS6 conditional depletion, extra amounts of RpL11 were produced by a selective recruitment of the 5'TOP Rpl11 mRNA to actively translation polysomes. This transcript actually maintains translational activity upon loss of the small subunit, suggesting a de-repression of the 5'TOP (**Fumagalli et al., 2012**). Although most of the RPs interact with Mdm2 directly, some of them, such as Rps7 (**Zhu et al., 2009**), Rps15, Rps20, Rpl37 (**Daftuar et al., 2013**) and Rps25 (**Zhang et al., 2013**) have also been shown to bind Mdm2 partners contributing to the stabilization of P53. Moreover, Rpl26 not only interacts with Mdm2, but also associates with *p53* mRNA and enhances its translation (**Takagi et al., 2005**).

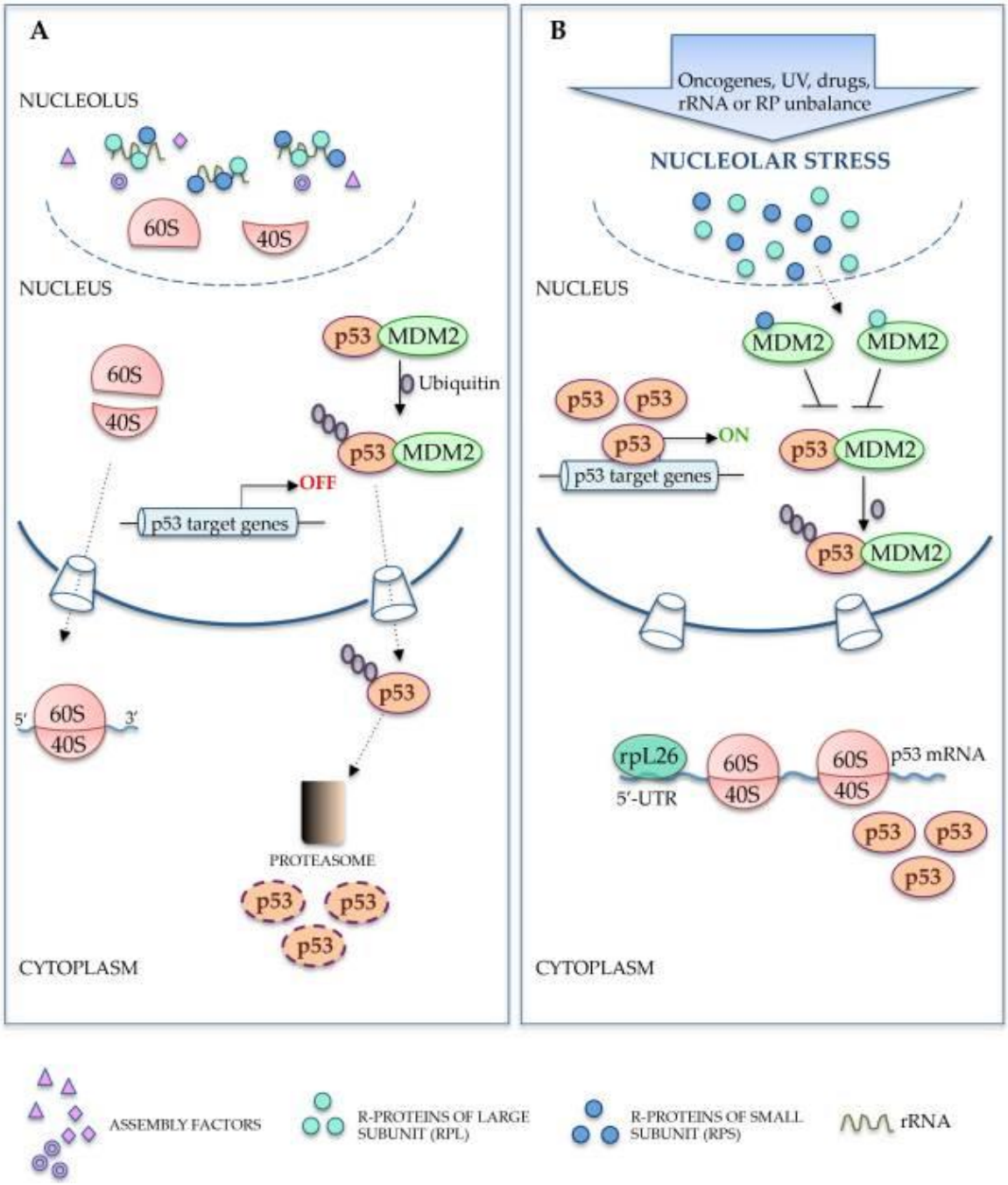

<u>Figure 20:</u> Role of ribosomal proteins in p53 activation upon nucleolar stress.
A. Under normal growth conditions, RPs are assembled with processed rRNAs into 40S and 60S subunits in the nucleolus. Mdm2 interacts with p53 and mediates its ubiquitinylation. p53 is sent to the proteasome and degraded.
B. During nucleolar stress, RPs are released into the nucleoplasm where they interact with Mdm2 inhibiting its ubiquitinylation activity and promoting the accumulation of p53. In the cytoplasm, ribosome-free RpL26 binds to the 5'UTR of p53 mRNA to induce its translation. Accumulated p53 activated the expression of target genes involved cell cycle arrest and apoptosis.

Beside ribosomal proteins, RBFs are also known to interact with Mdm2 in order to activate p53. Among these factors, which are normally segregated to the nucleoli, Nucleophosmin (Npm1) and Nucleostemin (Ns) are implicated in the nucleolar stress response. Npm1,

required for ITS2 cleavage in pre-rRNA processing is also involved in the nucleolar control of cell homeostasis. Indeed, it helps maintaining genome stability, blocks apoptosis when overexpressed, and participates in centrosome duplication (**Colombo et al., 2011**). Npm1 interacts with and segregates the alternative reading frame (Arf) protein, $p19^{Arf}$ in mouse and $p14^{Arf}$ in humans) in the nucleolus. Upon nucleolar stress, Arf is released in the nucleoplasm where it binds and blocks Mdm2 (*fig 21*) (**James et al., 2014**). When a dominant-negative (constitutively cytoplasmic) form of NPM1 (NPM1c+) is expressed, Arf is translocated to the cytoplasm as well. The subsequent activation of Mdm2 in the nucleoplasm induces the ubiquitylation of p53 and the activation of the proliferation. This has been proposed to be one of the causes of cell expansion in acute myeloid leukemia (**Falini et al., 2009**). Interestingly, when human NPM1c+ is overexpressed in zebrafish, it leads to the expansion of primitive myeloid cells. Moreover, cell expansion was extended to hematopoietic progenitors in p53-deficient zebrafish suggesting that NPM1 plays a conserved role across evolution and it might be particularly important for progenitor cell homeostasis *in vivo* (**Bolli et al., 2010**).

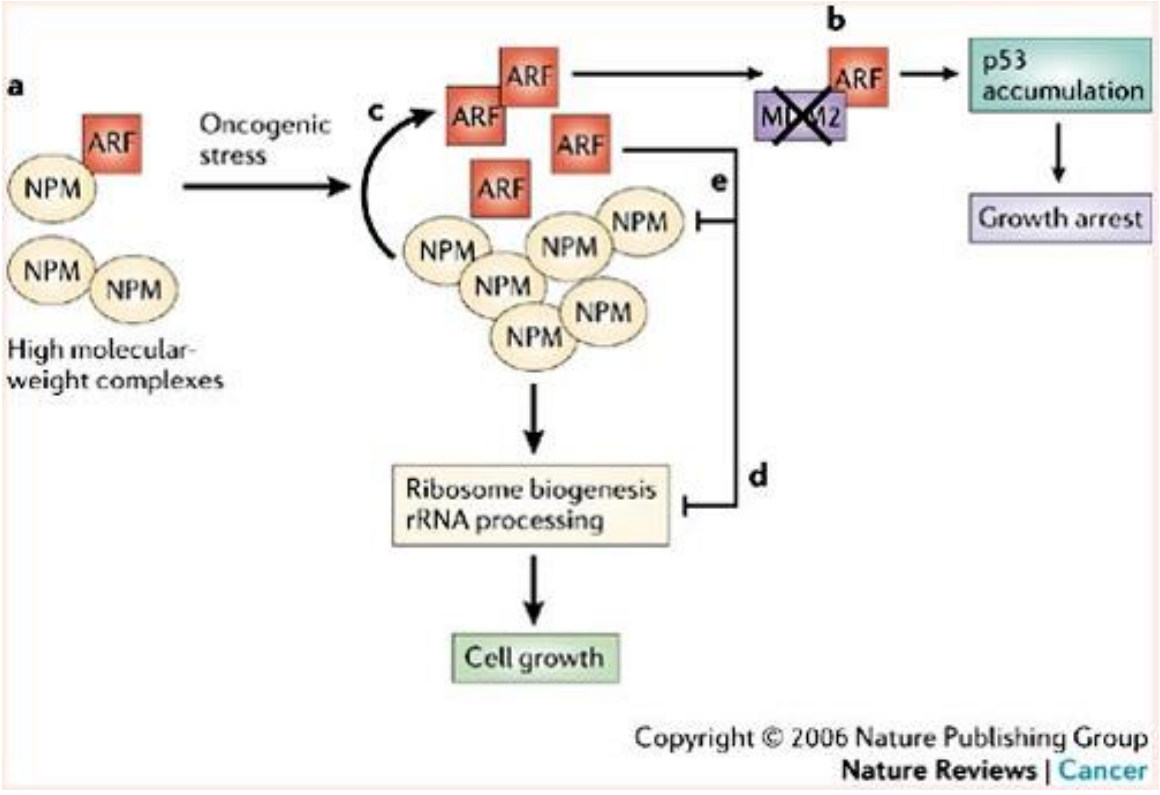

<u>Figure 21:</u> Npm1 and ARF couple ribosome biogenesis with cell cycle proliferation and cell growth. (*Grisendi et al., 2006*)

Npm1 segregate ARF in the nucleolus (a). Upon nucleolar stress and ribosome biogenesis blockage, ARF is released to the nucleoplasm where it can phosphorylate Mdm2 thereby preventing it to ubiquitylate p53. Hence, Npm1 and ARF couple ribosome biogenesis and cell cycle progression in a p53-dependent manner (b). Elevated levels of Npm1 lead to the accumulation and stabilization of ARF (c) that can negatively regulate ribosome biogenesis by inhibiting rRNA transcription (d) and destabilizing Npm1.

The role of Ns is less straightforward since both its overexpression and its down regulation lead to P53 activation and cell cycle arrest. When it is overexpressed and therefore more abundant in the cytoplasm, Ns binds the acidic domain of Mdm2 via its coiled-coil domain. This prevents the ligase activity of Mdm2 leading to the accumulation of p53 (**Dai et al., 2008**). On the other hand, the knockdown of Ns also leads to a p53-dependent cell cycle arrest. It is a side effect of Ns-dependent ribosome biogenesis disruption that leads to the accumulation of free RpL5 and RpL11 both *in vitro* (**Ma and Pederson, 2007**) and *in vivo* (**Essers et al., 2014**).

III.2.2. p53 independent response pathways to nucleolar stress

Although p53 stabilization is the major mechanism that induces cell cycle arrest and apoptosis during nucleolar stress, recent studies have highlighted new processes independent from p53. Similarly to the p53-dependent responses, ribosomal proteins and ribosome biogenesis also act as stress-sensors in a p53-independent manner. For example, upon nucleolar stress, ribosome-free Rpl5 and Rpl11 suppress cell proliferation through the negative regulation of c-Myc. Indeed, the two proteins of the large ribosomal subunit form a complex with *c-Myc* mRNA to repress its expression and/or induce its degradation (**Lindström, 2009**). Furthermore, Rpl11 released from the ribosome, binds to Mdm2 causing the release of E2F-1 (E2 transcription factor 1) and preventing its degradation (*fig 22A*). E2F-1 is a transcription factor which controls the expression of gene whose products are important for the entry and passage throughout the S-phase (**Dimova and Dyson, 2005**). In the p53-independent pathway, E2F-1, once activated, positively regulates several crucial pro-apoptotic genes such as *p73* (**Stiewe and Pützer, 2000**), *Apaf1, Puma or Noa*. Among RPs that can trigger nucleolar stress, Rpl3 is also one key players of the p53-independent response. Following ribosome stress, Rpl3 enters the nucleus where it acts as a co-transcription factor (*fig 22B* and *23C*). Together with Npm1, it activates the transcription of the *p21* gene thereby leading to cell cycle arrest at the G1/S phase transition (**Russo et al., 2013**).

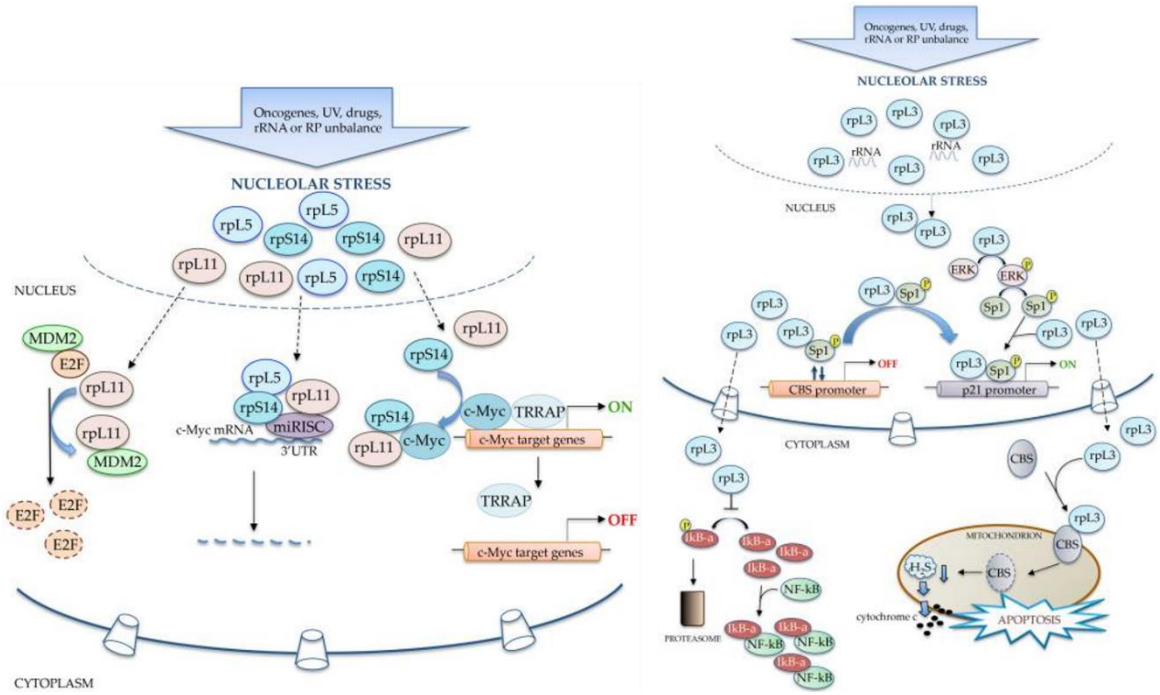

<u>Figure 22:</u> Models of p53-independent and RP-dependent response pathways to nucleolar stress (*Russo and Russo, 2017*).
A. Ribosome-free Rpl11 (pink) and Rpl5 (light blue) are translocated from the nucleolus to the nucleus upon nucleolar stress. Rpl11 specifically interacts with Mdm2 in order to prevent E2F-1 degradation. Rpl11 and Rpl5 form a complex with c-Myc to repress its expression and induce its degradation.
B. Following ribosome stress, Rpl3 enters the nucleus where it acts as a co-transcription factor. Together with Npm1 it activates the transcription of the *p21* gene thereby leading to cell cycle arrest at the G1/S phase transition.

Besides, there is now an emerging field of evidence suggesting the existence in the cells of a number of alternative nucleolar stress pathways involving RBFs that bypass p53 and directly play a crucial role in apoptosis. These p53-independent regulators of apoptosis include several nucleolar factors such as Npm1, Wnt target Peter Pan (PPAN) and ARF. In fact, as mentioned in the former section, Npm1 plays a crucial role in conditions of nucleolar stress in a p53-dependent manner. When Npm1 is translocated from the nucleolus to the cytoplasm, it complexes not only with Arf, but also with a Bcl2-associated X protein (Bax), a crucial effector of mitochondrial apoptosis (**Lo et al., 2013**). Arf proteins are also involved in both p53-dependent and independent pathways. Indeed, Arf may act independently of the Mdm2-p53 axis in tumor surveillance as its enforced expression induces cell cycle arrest and/or triggers apoptosis in cell lacking P53 (**Eymin et al., 2006**). Furthermore, following drug exposure, Arf negatively controls cell growth independently of p53 by activating ATM/ATR/CHK signaling pathways (**Eymin et al., 2006**). One last example of RBF involved in this p53-independent response is the well-known nucleolar factor PPAN playing a role in the large subunit maturation through its interaction with

Pescadillo (Pes) (**Bogengruber et al., 2003**). Interestingly, PPAN shuttles between the nucleolus, the cytoplasm and the mitochondria as different domains of PPAN are targeted to different cellular compartment. Following drug-induced nucleolar stress, PPAN translocates from the nucleolus and accumulates in the cytoplasm. This is accompanied by phosphorylation and subsequent cleavage of PPAN by caspases. PPAN depletion induces Npm1 and UBF degradation as well as Bax stabilization and activation, which is followed by depolarization of mitochondria and release of cytochrome c. Therefore, PPAN is required to inhibit mitochondrial apoptosis acting as a pro-survival factor (*fig 23D*) (**Pfister et al., 2015**).

In the Chapter 1, Part II I.rDNA transcription, I have widely described the processes and actors responsible for the transcription of rRNA genes. In particular, I have pointed out the fact that RNA PolI protein is the key polymerase involved in the nucleolar transcription of the majority of proteins necessary to build ribosomes. RNA Polymerase I Subunit A (PolR1A) encodes the catalytic subunit of RNA PolI. Silencing of this catalytic subunit leads to p53-dependent cell cycle arrest. Interestingly, p53-deficient cells also stop cycling (at the G1/S transition) after PolR1A knock-down and this phenotype can be rescued by protein retinoblastoma (*pRb*) silencing (**Donati et al., 2011**). Moreover, these cells displayed low levels of E2F-1. In resting cells, hypophosphorylated pRb binds E2F-1, preventing activation of its target genes. When the cell enters the cell cycle, phosphorylation of pRb by Cdk let E2F-1 free to activate the target genes involved in the synthesis of DNA. The reduction of E2F-1 expression after the inhibition of rRNA synthesis was observed in all the cell lines examined. This effect did not depend on p53 or pRb function, it was not due to changes in the cell cycle progression, and it was sufficient to decrease proliferation rates (*fig 23A*) (**Donati et al., 2011**).

Among the proteins that can be released upon nucleolar stress, there is also the serine-threonine kinase PIM1. This protein is normally associated to the ribosomes via RPS19. When ribosome biogenesis is impaired, PIM1 becomes free and can be degraded via the proteasome. This leads to the stabilization of p27 (which is not anymore phosphorylated and degraded) and to the p53-independent cell cycle arrest before the S phase (*fig 23B*) (**Iadevaia et al., 2010**).

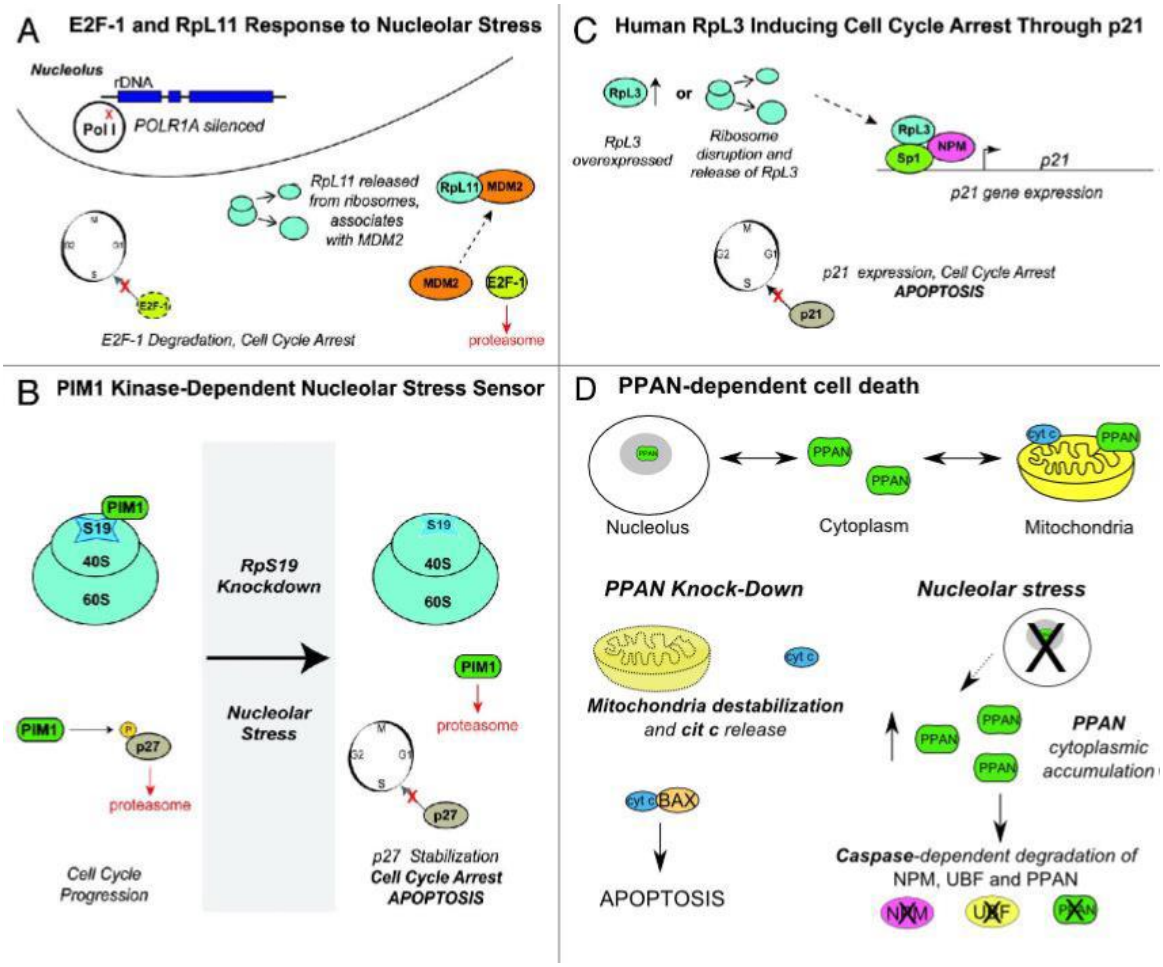

Figure 23: Examples of p53-independent apoptosis and cell cycle arrest mechanisms in metazoans- ***Adapted from James et al., 2014.***
A. E2F-1 and Prl11 response to nucleolar stress. **B.** Human RPL3 induces cell cycle arrest through p21. **C.** PIM 1 kinase-dependent nucleolar stress sensor. **D.** PPAN-dependent cell death.

IV Ribosome specificity and heterogeneity

Historically, ribosomes have been considered as homogeneous and constitutive "molecular machines" allowing the translation of every transcribed mRNAs into proteins. However, emerging studies have revealed that ribosome activity may be modulated between cells or depending on the developmental status of the organism. The heterogeneity of ribosome translational capacities depends on their variable internal composition. Indeed, differential expression and post-translational modifications of RPs, rRNAs diversity and the activity of ribosome-associated factors may generate "specialized ribosomes". Moreover, constitutive components of the ribosome may also exert more specialized activities by virtue of their interactions with specific mRNA regulatory elements such as IRESs or uORFs (**Xue and Barna, 2015**). Decades of research have highlighted several layers of regulation allowing the production of an important diversity of cell types. Nowadays, the existence of a

"ribosome code" is a new concept highlighting the additional layer of regulation at the translational level. In this chapter, I will examine the evidence for heterogeneity in ribosomes and its importance for cell identity and cell homeostasis. In addition, I will illustrate this contribution by using the examples of cancer and ribosomopathies in which mutations in RBF or RPs give rise to cell/tissue-specific phenotypes.

IV.1 Heterogeneity in ribosome functions rely on variability in ribosomal proteins

In the 1990s, attempts in delineating the minimal components necessary for ribosome activity have demonstrated that the peptidyl-transferase can be functional in the absence of most ribosomal proteins (**Noller et al., 1992**). This has raised the questions of ribosomal proteins functions. Despite the function of RPs in rRNA folding and function, it has been hypothesized that they might also bear greater specificity to the RNA-based translation machinery to control protein synthesis (**Xue and Barna, 2012**).

IV.1.1 Different paralogs of ribosomal proteins can exert different functions

Paralogs are genes that are separated by a duplication event in the same species and that can evolve new functions. In *S.Cerevisae*, multiple RP paralogues have raised from genome duplication. In particular, 59 out of the 78 RPs retained two genome copies (**Kellis et al., 2004**). Remarkably, despite having high sequence identity, the two RPs gene copies do not always seem to be functionally redundant. Integration of different paralogues within ribosomes can confer drug resistance (**Parenteau et al., 2011**), bud size selection (**Ni and Snyder, 2001**) or virus susceptibility (**Ohtake and Wickner, 1995**; **Carroll and Wickner, 1995**). Functional specificity of ribosomal proteins genes regulate the production and function of yeast ribosomes (**Komili et al., 2007**) .

In multicellular eukaryotes, similar specificity is observed. In particular, RPs paralogues can be expressed in different tissues in the same organism. For example, in *Arabidopsis thaliana*, many RP paralogues display sequence variations and are differentially expressed during development (**Falcone Ferreyra et al., 2010; Weijers et al., 2001**). In particular, *RPS5A* is strongly expressed in dividing cells, whereas *RPS5B* is expressed in cells undergoing differentiation (*fig 24A*). Furthermore, in *Drosophila melanogaster*, some paralogues such as *Rpl11/Rpl11l* show differential expression levels in the adult testes (*fig 24B*). Such heterogeneity in RP expression in the gonads suggests that the development of germ cells may require tissue-specific variations in the translational machinery (**Marygold et al., 2007**). In mammals, most ribosomal proteins are encoded by only a single gene copy.

However, notable exceptions exist. Indeed, similarly to *Drosophila*, RP paralogues expression is restricted to germ cells in human (*fig 24C*) or mice (**Lopes et al., 2010; Sugihara et al., 2010**). In human only a few other examples can be found, but the list is growing. Among them, the RPL39, RPL39L, is specifically expressed in embryonic stem cells (**Wong et al., 2014**). Interestingly, differential RP expression or/and functions between stem cells and differentiated cells has been also documented in zebrafish. Indeed, zebrafish *rpl7l1* is specifically expressed in neuroepithelial progenitors. By contrast, its paralogue *rpl7* has been shows to be strongly and ubiquitously expressed (**zfin.org**). Similarly, in *Drosophila*, RPL7 is specifically required in neuroblasts to maintain their proliferation whereas its counterpart (*Rpl7-like*) displays ubiquitous expression (**Neumüller et al., 2011**). Additional studies have showed that Rpl22l1 and Rpl22 play essential, distinct and antagonistic roles in hematopoietic stem cells (HSCs; **Zhang et al., 2013b**). Recently, it has been shown that the expression of ribosomal protein RPL22 controls ribosome composition by directly repressing expression of its own paralogue, *Rpl22l1* in mouse (**O'Leary et al., 2013**). Differentially expressed RP paralogues in progenitor and differentiated cells might indicate the existence of different ribosome biogenesis in stem/progenitor cells compared to differentiated cells.

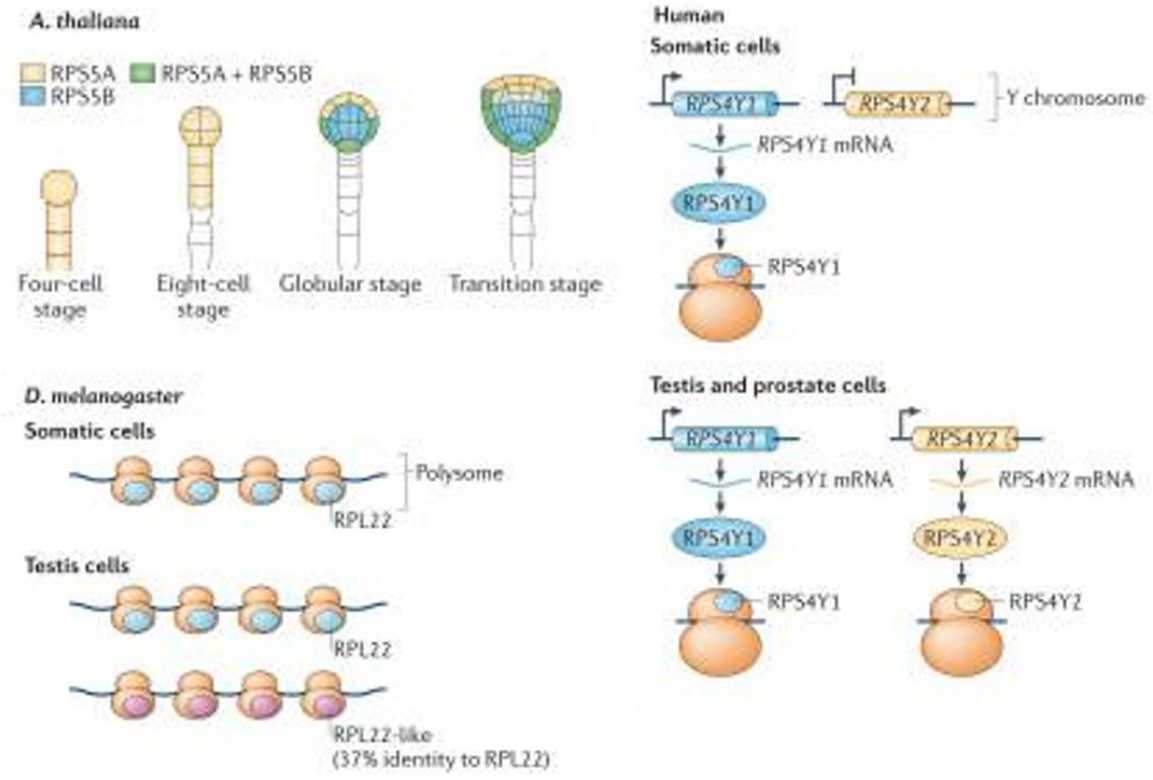

Figure 24: Heterogeneity of ribosomes can be due to differential expression of ribosomal proteins paralogs
A. In plants, ribosomal protein paralogues have different functions and different expression patterns. For example, in Arabidopsis thaliana, RPS5A is expressed in rapidly dividing cells early in embryonic development, whereas RPS5B is expressed in cells undergoing differentiation**. B.** In Drosophila melanogaster, ribosomal protein paralogues show different expression patterns in the adult testes. For example, RPL22 is expressed ubiquitously, but RPL22-like protein levels are specifically increased in the testes. Both proteins are incorporated into translationally active ribosomes (called the polysomes). **C.** In humans, only some ribosomal protein paralogues have been identified; however, notable examples exist. RPS4Y1 is expressed ubiquitously, whereas RPS4Y2 is restricted to the testis and prostate.

IV.1.2 Core ribosomal proteins are expressed at distinct levels in unique cells

Beside the involvement of RP paralogues in ribosome heterogeneity, core ribosomal proteins seem to be differentially expressed depending on the cell/tissue type considered. For example, in the social amoebae *Dictylostelium discoideum*, ribosomes are composed of different RPs at two different phases of its life cycle. This observation suggests that those RPs may be developmentally regulated during cell differentiation (**Ramagopal, 1990; Ramagopal and Ennis, 1981**). In mouse, the levels of *Rpl38* transcripts exhibit a tissue-specific expression pattern with an increased expression in developing somites and in specific subset of motor neurons (**Kondrashov et al., 2011**). Strikingly, this expression pattern mirrors, to a large extent, the tissues that are affected by the loss of function of RPL38 in mouse embryos. More precisely, *rpl38* mutant mice exhibit skeletal patterning defects including homeotic transformations and compromised neural tube patterning. Interestingly, polysome profiling analyzes revealed that RPL38 exerts a specialized function in translational control of a subset of Hox mRNA by facilitating 80S complex formation (*fig 25A*). More globally, a large-scale quantitate expression-profiling screen highlighted a restricted expression of 72 RPs in the developing vertebrate embryo. Taken together, these studies reveal that ribosome composition varies between cells and specialized ribosomes are required to determine cell identity in vertebrates. Further studies performed by **Barna et al**. completed the work on Rpl38 and the Hox genes. Indeed, they discovered the presence of specific RNA regulatory elements within the 5'UTR of the Hox transcripts translated by Rpl38-containing ribosomes (**Xue and Barna, 2015**). These regulatory elements called "Translation Inhibitory Element" (TIE) inhibits general cap-dependent translation (*fig 25B*). Moreover, these Hox mRNAs also contain an IRES element which allows the recruitment of ribosome through the cap-independent mechanism (see Chapter 1, part I, II.2.2 IRES-dependent initiation). This confirms that ribosomes with

specific composition can be specific for a subset of mRNAs, thereby adding a new level of complexity at the translational regulation of gene expression.

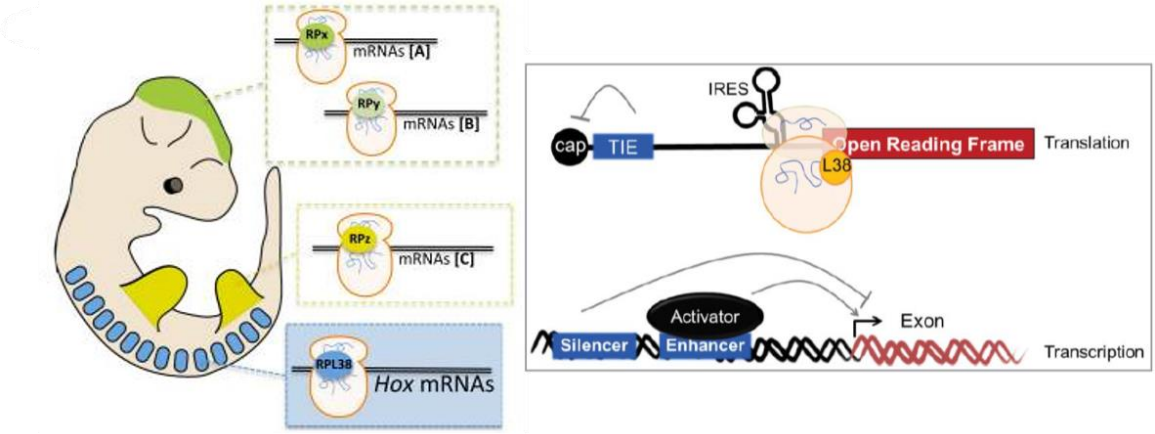

Figure 25: Rpl38 is rate limiting for the translation of Hox mRNAs. (*Xue and Barna, 2015*)
A. Processed model of RP specificity in control of gene expression during murine embryogenesis. The enriched expression of specific RP in different tissues may confer translational specificity to distinc classed of mRNAs (a,b,c). Brain: green, limbs: yellow, somites: blue.
B. A TIE in the 5'UTR of certains mRNA (as Hox) inhibits cap-dependent translation. An addition *cis*-regulatory element (IRES) can recruit the ribosome through a cap-independent mechanism. Translation from the IRES enables specialized regulation by the ribosome itself. For example, RPL38 is required for the translation of several TIE and IRES-containing Hox transcripts.

IV.2 Ribosome biogenesis variations lead to ribosome heterogeneity

Since the publication of the ribosome filter hypothesis which postulate that ribosomes function as regulatory elements that filter particular mRNAs (**Mauro and Edelman, 2007**), RPs have been considered as the major actors in the transitional control of gene expression. However, little attention has been given to the way ribosomes were built. Indeed, the ribosome biogenesis pathway has always been considered as a conserved and ubiquitous process. Therefore, results obtained in yeast were thought to reflect the situation in metazoans. Nevertheless, the repertoire of RBFs varies considerably among eukaryotes (**Ebersberger et al., 2014**). Hence, it has been hypothesized that these newly acquired RBFs could have tissue and/or cell-specific roles thereby finely regulating gene expression at the translational level. Particular attention has been given to the ribosome biogenesis pathway variations between stem cells and differentiated cells (**Brombin et al., 2015**).

IV.2.1 rDNA transcription

As fully described in the Chapter 1, Part II, I.3.Regulation of rDNA transcription, rDNA transcription can be modulated depending on the cell environment or via epigenetic modifications. More specifically, differences in rRNA synthesis between proliferative pluripotent cells, such as stem cells (SCs), and differentiated cells has been demonstrated

in several organism. Stem cells can undergo self-renewal while retaining ability to differentiate into several types of cells. SCs have unique nuclear properties such as hyperdynamic chromatin and condensed nucleoli. Moreover, stem cells display higher rates of rDNA transcription than their daughter cells. For example, in drosophila, female germinal stem cells (GSCs) display high levels of rRNA transcription. Reduction of rRNA synthesis in this cell type changes cell fate, growth and proliferation (**Zhang et al., 2014**). On the contrary, during differentiation, rRNA synthesis is down-regulated by phenotype specific-transcription factors such as MyoD or Runx2 (**Ali et al., 2008**). Although it is generally believed that the down-regulation of rRNA production is simply a consequence of the differentiation process, recent findings show that this event actually triggers differentiation (**Hayashi et al., 2014**). For example, in mouse HSCs rDNA transcription inhibition leads to the expression of differentiation markers and provokes differentiation. Moreover, silencing of rDNA genes and down-regulated ribosome biogenesis are associated with stem cell ageing, as shown recently in murine HSCs (**Flach et al., 2014**).

As described in the Chapter 1, Part II, II.4.2 Fibrillarin function, rDNA transcription can be modulated via the methylation of H2A by fibrillarin. Interestingly, Fbl is overrepresented in the proteome of murine embryonic stem cells (mESCs) (**Watanabe-Susaki et al., 2014**) and the neuroepithelial progenitors of the zebrafish midbrain (**Recher et al., 2013**).

Recent studies in zebrafish have also supported the "specialized" ribosome hypothesis (**Locati et al., 2017**). Indeed, it has been shown that rDNA transcription varies during development. Two distinct types of ribosomes (called maternal and somatic) exist with variable 18S, 5.8S and 28S sequences. In particular, sequence differences of the 5.8S are located in the central region of the rRNA which is responsible for protein binding and conformation. Similarly, sequence variations of the 28S are located in the functional center of the rRNA. In addition, 18S rRNA sequence diversity has been observed in the so called "sticky regions" responsible for the complementary binding of the mRNA 5'UTR. Therefore, in zebrafish, specific rRNA differentially expressed during development and in adulthood, would give rise to "specialized" ribosomes having different function and targeting specific mRNAs (**Locati et al., 2017**).

IV.2.2 RBFs

Beyond rDNA transcription, many RBFs appear to play cell-specific roles. Indeed, in *Drosophila*, the Mushroom body miniature factor (*Mbm*) is highly expressed in neuroblasts and is required for proper cell growth. Analyses of mutants for this gene showed that mbm is necessary for the maturation of the small subunits in neuroblasts, but is dispensable in ganglion mother cells (GMCs) and neurons (**Hovhanyan et al., 2014**). Another good example of the specific requirement of several RBFs for stem cell survival and homeostasis has been underlined in zebrafish. Cirh1a, a component of the small subunit processome is expressed in the developing liver (**Wilkins et al., 2013**). Knock-down of the gene leads to specific defects in the biliary system demonstrating a specific importance in liver progenitors. Likewise, conditional knock-out of Notchless, a murine orthologue of the yeast 60S subunit maturation factor *rsa4*, depletes HSCs and multipotent progenitors, but not mature hematopoietic cells (**Le Bouteiller et al., 2013**). *Nop56* and *Nop58* are also enriched in *Drosophila* neuroblasts and in zebrafish neuroepithelial-like progenitors of the midbrain (**Neumüller et al., 2011; Recher et al., 2013; Southall et al., 2013**). *Nop56* orthologue, in particular, has been described to play a major role in the maintenance of neuroepithelial stem cells of the optic lobe (**Wang et al., 2013**).

Similarly to ribosomal protein variations, RBF specificity would give rise to target translation of a subset of mRNAs. For example, FBL overexpression in *p53*-deficient cancer cells, triggers the hyper-methylation of rRNAs leading to the synthesis of ribosomes with modified translational specificity such that IRES-containing mRNAs (e.g cMYC, FGF1, VEGFA) are preferentially translated instead of 5'-capped transcripts (**Marcel et al., 2013**).

Interestingly, Fbl, Nop56 and Nop58 are up-regulated upon cold exposure induced stress (**Long et al., 2013**). Upon stress, IRES-mediated translation is favored over cap-dependent translation (**Spriggs et al., 2010**). Moreover, studies in flies, amphibians and mice show that stem cells respond better than other cell types to stress (**Love et al., 2014; McLeod et al., 2010; Yilmaz et al., 2012**). Therefore, it is possible that the capacity of stem cells to survive upon stress is linked to the type of RBFs they express, and thus to the type of mRNA that are translated. It is still unclear how differences in ribosome biogenesis contribute to the diversification of proteome among different types. Detailed functional analyses of the newly discovered RBFs are still lacking and the situation becomes more complicated when the diverse mechanisms of gene expression control are taken into account (**Buszczak et**

2014; Signer et al., 2014). For example, differentially expressed RBFs could contribute to the generation of the previously mentioned specialized ribosomes. Moreover, it was recently discovered that stem cells and differentiated cells express different subsets of tRNAs (**Gingold et al., 2014; Topisirovic and Sonenberg, 2014**) adding yet another mechanism contributing to the determination of cell identity.

IV.3 Mutations of RP and RBF coding genes lead to tissue-specific phenotypes

IV.3.1 Ribosomopathies

While the prevailing assumption for many years was that organisms bearing defects in making ribosomes would be non-viable, the notion was refuted by the discovery of ribosomopathies. Ribosomopathies are a diverse group of disorders which, despite their heterogeneity at a clinical level, affect the same biochemical process. They are each caused by mutations in a gene encoding either a ribosomal protein, or a component of the apparatus required for ribosome synthesis. Indeed, several common features of ribosomopathies such as small stature, cancer predisposition, and hematological defects, point to how these diverse diseases may be related at a molecular level. Surprisingly, this class of disease presents a wide range of distinct tissue-specific phenotypes. Several different mechanisms have been proposed to underlie the tissue specificity of ribosome biogenesis disorders, including the selective translation of specific mRNAs, the extra-ribosomal functions of RPs and RBFs, and the differential requirements for ribosomes in different tissues.

IV.3.1.a Selective translation of IRES mRNAs

As described earlier, ribosomes can preferentially translate certain mRNAs, depending on the cellular environment. Defects in RBFs and/or RPs lead to alterations in the ribosome itself, which change its ability to recognize and bind different IRES elements under various conditions. Several examples of the effect of disruption of IRES-mediated mRNAs translation have been highlighted by clinical studies and/or animal models as detailed in the following paragraphes.

Dyskeratosis congenita (DKC) is a rare inherited bone marrow-failure syndrome characterized by abnormal skin pigmentation, nail dystrophy, and mucosal leukoplasia (**Walne and Dokal, 2008**). The X-linked form of the disease is caused by a mutation in *DKC1* (**Heiss et al., 1998**), encoding DYSKERIN, responsible for the pseudouridylation of rRNA (**Lafontaine et al., 1998**). DYSKERIN is also a part of the telomerase complex, and defects in both ribosome biogenesis and telomere maintenance have been shown in

patient cells and in mouse models of the disease (**Mitchell et al., 1999; Mochizuki et al., 2004; Montanaro et al., 2002; Ruggero et al., 2003**). Alterations in rRNA pseudouridylation have been shown to be deleterious for ribosome biogenesis and function most likely by altering the affinity of the ribosome for mRNAs. More precisely, X-linked DKC results in a specific reduction of IRES-mediated mRNA translation in patient lymphoblasts and fibroblasts, without affecting global levels of protein synthesis (**Yoon et al., 2006**). In particular, translation of the tumor suppressor p27, and the anti-apoptotic proteins XIAP and Bcl-xL, is significantly reduced. Therefore, DKC patients show increased apoptosis in hematopoietic progenitors and stem cells, resulting in bone marrow defects. In addition, disruption of dyskerin leads to accumulation of cells in the G2/M phase of the cell cycle, resulting in reduced proliferation rates (**Alawi and Lin, 2011; Gu et al., 2013**). Given that IRES-containing mRNAs are expressed under particular conditions, it seems likely that these defects would only be present at specific times or in specific tissues.

Another good example of the role of IRES-mediated mRNA translation in tissue-specific disorders is the Diamond-Blackfan anemia (DBA). DBA is a congenital hypoplastic anemia caused by selective decrease or absence of erythroid precursors in the bone marrow (**Delaporta et al., 2014**). In addition to the bone marrow symptoms, patients present craniofacial defects, cardiac defects and thumb abnormalities (**Kim et al., 2012**). The syndrome is caused by the mutation of ribosomal proteins genes including most commonly *RPS19* (**Zhang et al., 2014b**), and also *RPL5* and *RPL11* (**Delaporta et al., 2014**). Knockdown of *RPS19* in healthy CD34+ cells reduces their proliferation capacity by stalling the cell cycle at G0, in addition to impairing erythroid differentiation. Moreover, in mice, mutation in *Rps19* and *Rpl11* result in deficient IRES-mediated translation of BCL2-associated anathogene 1 (BAG1) and cold shock containing domain E 1 (CSDE1) in erythroblasts. Reduced translation of BAG1 and CSDE1, due to an alteration in ribosome specificity for IRES-containing mRNAs, is also detected in DBA patient cells (**Horos et al., 2012**).

IV.3.1.b. Extra-ribosomal functions and binding partners

In addition to the specific affinity of ribosome towards IRES-containing mRNAs, RPs have been shown to have other functions that those related to ribosome. Furthermore, RPs can be differentially processed by RBFs leading to heterogeneity of the translation machinery (see Chapter 1, Part II, IV.Ribosome specificity and heterogeneity).

Treacher Collins syndrome (TCS) is a rare congenital disorder of craniofacial development. TCS is characterized by hypoplasia of the facial bones, particularly the mandible and zygomatic complex, together with cleft palate, downward slanting of the palpebral fissures, and anomalies of the external and middle ear. Patients often have complications from the craniofacial dystosis, including issues with airway, swallowing, brain development and hearing (**Sakai and Trainor, 2009**). In 1996, *TCOF1* was identified as the gene responsible for TCS (**Group et al., 1996**). *TCOF1* encodes for the protein TREACLE. TREACLE colocalizes with UBF1 and RNA PolI and plays an essential role in rDNA transcription and rRNA processing (**Valdez et al., 2004**). There is a clear temporal aspect to the disease, as Tcof1 expression in the mouse embryo is strong in embryonic development, particularly in the developing branchial arches, and diminishes to near background levels by embryonic day 10.0 (**Dixon et al., 1997**). Mouse and zebrafish models of the disease have revealed a deficiency specifically in migrating neural crest cells due to reduced proliferation rates and increased apoptosis (**Dixon et al., 2006; Weiner et al., 2012**). This defect in neural crest cells is proposed to underlie the hearing loss in Treacher Collins syndrome, as the affected middle ear is neural crest derived, while the unaffected inner ear does not originate from neural crest cells (**Richter et al., 2010**). In *Xenopus* oocytes, treacle was shown to interact with fbl (**Tessarz et al., 2014; Tollervey et al., 1993**), and nop56, both components of the RNP methyltransferase complex. TCOF1 knockdown therefore causes a reduction in 2'-OH methylation in nascent rRNA (**Gonzales et al., 2005**). Reduction of rRNA transcription and modification due to TREACLE haploinsufficiency is thus proposed to underlie the proliferation defect in neural crest cells, which in turn leads to hypoplasia of the facial bones. Recently, mutations in *POLR1C* and *POLR1D*, encoding subunits of RNA PolI and RNA PolIII respectively, were also found to underlie the etiology of TCS (**Dauwerse et al., 2011**). Mutant zebrafish models, homozygous for the mutations of polr1c or polr1d, exhibit cartilage hypoplasia and cranioskeletal anomalies. These mutants display neuroepithelial cell death and a deficiency of migrating neural crest cells, which underpins the cranioskeletal defects (**Noack Watt et al., 2016**).

The role of RBFs in ribosomopathy and ribosome heterogeneity can also be highlighted in the cartilage hair hypoplasia (CHH) disorder. Indeed, patients affected by the disease carry a mutation in the RMNP gene (**Hermanns et al., 2005; Reicherter et al., 2011**), which encodes the RNA component of the mitochondrial RNA processing complex (RNAse MRP). CHH is characterized by short-limb dwarfism, accompanied by sparse hair,

immunologic and hematological defects (**Boothby and Bower, 1973; Thiel et al., 2007**). One of the important functions of the RNase MRP complex is to cleave the precursor rRNA, which contributes to the maturation of the 5'end of the 5.8S rRNA. Strong evidence that CHH is a ribosomopathy is provided by studies in yeast, which demonstrate that RMRP gene mutations affect yeast cell growth and are directly proportional to the observed defects in 5.8S processing (**Shadel et al., 2000**).

IV.3.1.c. Differential requirement for ribosome biogenesis factors

Ribosomal proteins display heterogeneous and non-overlapping expression patterns. More precisely, RP paralogs seem more likely to develop tissue-specific variations. If the ribosomal proteins have variable expression, it seems likely that variation in ribosome biogenesis factor distribution among tissues and throughout development also contribute. One excellent example to illustrate this hypothesis is the North American Indian childhood cirrhosis (NAIC) disorder. NAIC is caused by a mutation in *CIRH1A* encoding the protein CIRHIN (**Chagnon et al., 2002**). The yeast homolog of *CIRHIN*, *Utp4*, is a member of the small ribosomal subunit processome and is essential for ribosomal RNA maturation (**Freed and Baserga, 2010; Freed et al., 2012**). During mouse development, Cirhin is highly expressed with much lower levels of expression in the somites, brain and craniofacial structures. Zebrafish show similar results with high expression in the liver, gallbladder, pancreas and anterior intestine (**Wilkins et al., 2013**). Morpholino injection targeting *cirh1a* leads to defects in the development of the biliary system, with no defects observed in the other tissues (**Wilkins et al., 2013**). In this case, it seems that the high requirement of Cirhin in the liver makes it most sensitive to a loss of Cirhin function.

Differential expression of the ribosomal protein RPL38 has also been shown to play a role in mediating the phenotype in mice deficient in ribosome biogenesis. This is demonstrated in the spontaneous dominant mouse mutant, Tail short, which is characterized by a short and kinky tail, homeotic transformations of the skeleton, facial malformations, and eye abnormalities. *Rpl38* expression is enriched in the somites along the entire anterior-posterior axis during somitogenesis, pointing to a role in axial vertebral patterning (**Kondrashov et al., 2011**).

Many other ribosome-related disorders are observed in patients. The list of these diseases is depicted in Table 1.

Human Ribosomopathy Disease	Human Ribosomal Gene mutations	Human Phenotype	Mouse Phenotype	Zebrafish Phenotype	Yeast Phenotype
Treacher Collins Syndrome (TCS) 1:50,000	Treacle/Tcof1 RNA Pol I RNA Pol III POLR1C, POLR1D	Severe craniofacial defects including dysmorphic: • Face • Eyes • Mandible • Ears	Craniofacial anomalies including: • agenesis of nasal passages • abnormal maxilla development • exencephaly • anophthalmia • increased apoptosis in pre-fusion neural folds	• Craniofacial defects • reduced cell proliferation	Inhibition of: • rDNA transcription • cell growth
Postaxial acrofacial dysostosis (POADS) Less than 1:1,000,000	DHODH	• Hypoplasia of the femora • Ossification defects in ischium and pubis • Bilobed tongue • Lung hypoplasia	• Dhodh expression in pharyngeal arch and limb buds • site and stage-specific requirement for de novo pyrimidine synthesis	• inhibitors of DHODH led to an almost complete abrogation of neural crest development	• Reduced pyrimidine synthesis • Reduced DHOdenase activity
Diamond-Blackfan anemia (DBA) (5–7 cases per Million live births 1:200,000 ete abrogati	At least 11 Ribosomal proteins including: RPS19, RPS26, RPS27, RPL27, TSR2, RPS28, L5, L11, GATA1	• Absent lower eyelashes • down slanting palpegral fissures • deformed external ears • malar hypoplasia • micrognathia • Pro-apoptotic hematopoiesis leading to bone marrow failure • congenital anomalies • predisposition to cancer	• Constitutive expression of RSP19 mutation results in lethality • Conditional expression resulted in growth retardation, mild anemia, inhibited terminal erythroid maturation	• Impaired erythrocyte production • Defects in tail and/or brain development	
Roberts syndrome (RBS)	ESCO2	• Acetylation defects • Mental retardation • Limb deformities • Craniofacial defects • Heterochromatic repulsion	• Reduced acetylation of cohesin • lagging chromosomes • Increased apoptosis • Lethality	• Disruption of cell cycle • high levels of apoptosis	• reduced rDNA transcription • transcriptional signature of starvation • deletion of FOB corrects genome-wide replication defects, nucleolar structure and rDNA segregation defects
Shwachman-Diamond syndrome (SDS)	SBDS, essential cofactor for elongation factor 1	Exocrine pancreatic dysfunction mild neutropenia metaphyseal dysostosis mild mental retardation organ dysfunctions	Early embryonic lethality in null animals,		Disruption of 60S subunit maturation at later stagerelatively stable pre-60S particles
Cartilage hair hypoplasia (CHH) Rare autosomal	RMRP, an RNA component of the mitochondrial RNA processing ribonuclease	• Disproportionate short stature • Sparse hair • metaphyseal dysplasia • anemia • immune deficiency • increased incidence of cancer • altered cytokine signaling • defects in cell cycle progression • differentiated lymphocytic and chondrocytic cell lineages	• embryonic lethality in either conditional or homozygous RMRP null mice		• Normal mitochondrial function • Normal chromosomal segregation • Normal cell cycle progression • Altered ribosomal processing and ratio of short versus long forms of the 5.8S rRNA • Cell cycle defects at end of mitosis
Bowen-Conradi syndrome (BCS) Autosomal recessive 1in 10 in Hutterite population	EMG1 Trisomy 18 Nep1 (Emg1) SPOUT-class methyltransferase	• Severe growth failure • Psychomotor retardation • Death in early childhood	• Early lethality prior to blastocyst stage development • Defects in cell lineage-specification • Nucleologenesis defects • Is not rescued by loss of p53		• Methylation defects • Defined dual Nep1 function as a as a methyltransferase and ribosome assembly factor • BCS mutation prevents nucleolar accumulation of Nep1
North American Indian Childhood Cirrhosis (NAIC)	CIRH1a/Utp4 NOL11	• Cirrhosis of the liver, liver disease • Neonatal cholestatic jaundice • Hepatosplenomegaly	• Expressed in embryonic mouse liver	• Upregulated transcriptional targets of p53 • Defects in canalicular and biliary morphology	• Stabilization and nuclear accumulation of p53 • p53-mediated cell cycle arrest • apoptosis

Table 1: Comparison of human and animal model of ribosomopathy. (*Yelick and Trainor, 2015*)

IV.3.2 Cancers

The history of the relationship between ribosome biogenesis and cancer begins long before the discovery of either ribosomes or the functions of the nucleolus in ribosome biogenesis. In fact, in 1896, Pianese observed that cells of malignant tumors were characterized by particularly larger nucleoli than normal cells (**Pianese and Teuscher, 1896**). Nucleoli hypertrophy was considered to be a cytological parameter useful for the diagnosis of malignancy. Further studies have revealed that normal proliferating cells were also characterized by larger nucleoli. However, the link between ribosome biogenesis and tumorigenesis exists as cancer cells require ribosome biogenesis and protein translation to maintain their high proliferation rate. Indeed, the rate of ribosome biogenesis controls the expression level of the tumor suppressor p53, and upregulation of ribosome biogenesis is often associated with increased cancer risk (**Montanaro et al., 2012**). In this chapter, I will give an overview of the recent advances made toward understanding how nucleolar functions may become corrupted in malignant cells.

IV.3.2.a Upregulation of ribosome biogenesis

As mentioned above, increase in nucleolar size has been for a long time one of the parameters used to characterize tumorigenic cells. Nucleolar size and number actually reflect upregulation of ribosome biogenesis. Recent studies have demonstrated the causal role of increased ribosome biogenesis in pathogenesis in malignant tumors. Upregulation of ribosome biogenesis may alter the pattern of translated mRNAs and thereby contribute to tumorigenesis. Indeed, mRNAs that have low affinity for the translational machinery are out-competed by message with high affinity when the number of ribosomes is limited. Interestingly, many mRNAs with low affinity for the ribosomes encode oncoproteins, growth factors, survival factors and cell cycle regulators (**Ruggero, 2013**). Moreover, it is also becoming apparent that upregulation of various steps of ribosome biogenesis is an essential component of tumorigenic programs. The strongest indication that increased ribosome biogenesis can be a direct cause of malignant transformation was provided by Barna et al, employing transgenic mice that express c-myc under the control of the immunoglobulin heavy chain promoter and enhancer and consequently develop B-cell lymphomas (**Barna et al., 2008**). In this study, the authors demonstrated how perturbations in translational control provide a highly specific outcome for gene expression, genome stability, and cancer initiation. More precisely, they observed an aberrant regulation of cap- and IRES-dependent translation during mitosis responsible for impairment of cytokinesis and increased centrosome numbers and genome instability. Moreover, overexpression of c-myc in Rpl24 heterozygous mice leads to the delayed onset of B-cell lymphoma, along with the re-establishment of accurate translational control and genome stability. This latest observation emphasizes the importance of increased ribosome biogenesis to the development of c-myc-driven B-cell lymphomas (**Barna et al., 2008**). In addition to changes in the patterns of translated mRNAs, increased ribosome biogenesis may upregulate global protein synthesis, leading to enhanced protein accumulation in the endoplasmic reticulum (ER). Following this protein accumulation, the cells activate a feedback mechanism which slows down protein synthesis. Furthermore, increased translation rates upon excessive ribosome biogenesis may decrease translational fidelity. Both phenomena might contribute to ER stress leading to uncontrolled cell proliferation. Moreover, upregulated ribosome biogenesis may inhibit cell differentiation as well, increasing cancer cell initiation. Ribosomal proteins variations can also play a major role in tumor formation. Indeed, several RPs are overexpressed in tumor cells and clinical tissue

samples obtained from cancer patients. For example, RPL36A, a tumor associated ribosomal protein, is highly expressed in hepatocellular carcinoma. Ectopic overexpression of RPL36A in liver cells enhances colony formation and increases cell proliferation by accelerating the cell cycle (**Kim et al., 2004**). Similarly, overexpression of another ribosomal protein RPS3a in NIH3T3 cells induces the characteristic features of malignant transformation (**Naora et al., 1998**).

Although these observations suggest that alteration of ribosome biogenesis increase the susceptibility to tumorigenesis, many evidence show that dysregulation of ribosome biogenesis can be explained as a consequence of malignant transformation. In particular, several oncogenic signaling pathway such as RAS/RAF/ERK and PI3K/AKT/mTORC1, are able to modulate the rDNA transcription (see Chapter 1, Part II, I.3.Regulation of rDNA transcription). Therefore, activation of these signaling pathways, following tumorigenesis, could enhance ribosome biogenesis.

IV.3.2.b Decreased ribosome biogenesis

In addition to a dysregulation leading to an overproduction of ribosomes, a decrease in the number of mature ribosomes may also contribute to tumorigenesis (**Bursac et al., 2014**). Reduction in ribosome biogenesis could decrease not only the rate of total protein synthesis, but also the translation of specific mRNAs with lower affinity for ribosomes such as those encoding for tumor suppressors (**Lodish, 1974; Ruggero, 2013**). Recent studies in model organisms and humans have suggested that both of these changes may contribute to the etiology of cancer. Deficiencies of 17 individual RPs in zebrafish led to the development of certain malignant peripheral nerve sheath tumors (**Amsterdam et al., 2004**). Subsequent work showed that RP-haploinsufficient zebrafish cells lose *p53* expression at the level of protein synthesis, suggesting that a decrease in the number of ribosomes impairs the selective translational upregulation of mRNAs encoding for this key tumor suppressor (**MacInnes et al., 2008**).

Moreover, most of the syndromes linked to ribosomal dysfunction appear to have an increased incidence of cancer, although the type and frequency vary considerably. In particular, RP-haploinsufficiency in DBA, leading to a decrease number of mature ribosomes, is associated with an increased risk of myelodysplastic syndrome (MDS) (**Mason and Bessler, 2011**).

IV.3.2.c Qualitative changes in ribosome biogenesis

Specific RPs have been found to be dysregulated at the mRNA or protein levels in a wide range of array of human cancer types, including liver, lung, colon, prostate as well as gynecologic tumors (**Zhou et al., 2015**). It is possible that the differential expression of RP genes may alter the stoichiometry of RPs in the ribosome. Therefore, over-and under-expression of individual RPs could potentially establish heterogeneity and specialized functions of ribosomes (see Chapter 1, Part II, IV.1.Heterogeneity in ribosome functions rely on variability in ribosomal proteins) that could mediate translational reprogramming during tumorigenesis and cancer progression (**Xue and Barna, 2012**). Moreover, it could be hypothesized that, in addition to variation in RP complement of the ribosome, many other qualitative ribosome changes that result from usage of alternative RP isoforms, post-translational modification of RPs, mutations of RPs genes, sequence diversity of rRNA and post-transcriptional chemical modification of rRNA might be associated with tumorigenesis and cancer progression (**Filipovska and Rackham, 2013; Xue and Barna, 2012**). To date, however, the only ribosomal heterogeneity that has been identified in malignant tumors arises from the presence of specific mutant RPs or aberrant chemical modification of rRNA (**De Keersmaecker et al., 2013; Xue and Barna, 2012**). Moreover, as described in the Chapter 1, Part II, II.4.5.a. Fibrillarin is an oncogene, recent studies by **Marcel et al**. have led to significant progress in expanding our understanding of the molecular mechanisms that regulated 2'-O-methylation of rRNA and their role in protein synthesis and tumorigenesis, illustrating the importance of rRNA post-transcriptional modifications in cancer generation (**Marcel et al., 2013**).

CHAPTER 2: ZEBRAFISH OPTIC TECTUM AS A MODEL OF NEUROGENESIS

I. Neurogenesis

The term "Neurogenesis" describes the process by which functional neurons are produced from neural progenitors. This event includes neural fate induction, proliferation and migration of neural progenitors, differentiation and functional integration of the newborn neurons within the nervous system. Neurogenesis has also been described in the adult brain of several species. In this chapter I will give an overview of the embryonic and adult neurogenesis in vertebrates, emphasizing some shared properties but also highlighting the heterogeneity of adult neurogenesis. One aspect of this heterogeneity resides on the progenitor cell type that sustains the neurogenic process. In particular, I will focus on some neurogenic regions of the adult zebrafish brain, neural progenitors retaining neuroepithelial characteristics (hereafter referred as neuroepithelial progenitor cells, NePCs). It is the case in the optic tectum (OT), the part of the teleost brain on which I focused my studies. Consequently, one part of this chapter will be dedicated to the description of the OT morphogenesis.

I.1 Embryonic neurogenesis

Embryonic neurogenesis starts with the neural induction. As mentioned above, this is followed by a sequence of events including proliferation, specification and differentiation. Each of these steps is spatially and temporally regulated generating the diversity of neural cells which will form the central nervous system (CNS).

I.1.1 Neural induction

The neural induction, initiated during early embryonic development and more exactly during gastrulation, allows the specification of the neuroectoderm. It is triggered by a series of signals emanating from the adjacent dorsal mesoderm (the "Organizer" in frog and fish and the "Node" in chick and mouse) and occurs according to the "default model" described in *Xenopus* **(Ozair *et al.*, 2013)**. Briefly, cells within the ectodermal layers differentiate into neural tissue unless exposed to Bone Morphogenetic Protein (BMP), secreted from the ventral side of the gastrula and diffused as a gradient along the dorso-ventral axis (**Weinstein and Hemmati-Brivanlou, 1999**). Dorsally, BMP antagonists such as Noggin, Chordin or Follistatin, protect the ectoderm from BMP signaling and trigger neural plate

formation from the dorsal ectoderm (**Pera et al., 2014**). Moreover, the wing-integrated (Wnt)/β-catenin proteins form an additional gradient along the antero-posterior axis allowing the regionalization of the CNS (*fig 26B*). The organizer secretes Wnt antagonists Frzb1 (frizzled-related protein), Cerberus and Dkk1 (Dickkopf-related protein 1), which during gastrulation translocate to the anterior pole of the embryo and establish a Wnt/β-catenin gradient that determine the antero-posterior polarity of the neural plate (*fig 26B;* **Niehrs, 2010**). At the onset of neural plate induction, the anterior part of the neural plate is already specified to form brain tissue whereas the most posterior part is committed to establish the spinal cord (**Ozair et al., 2013**). Perpendicular activity gradients of BMP and Wnt signals are conserved throughout evolution. Chordin and BMP have conserved functions in Bilateria for patterning the dorso-ventral axis during gastrulation. Key roles for anterior Wnt inhibition by Dkk and posterior Wnt signals have been validated in most Metazoans (**Niehrs, 2010; Ozair et al., 2013**). In addition, FGF (Fibroblast Growth Factor) can also inhibit BMP signaling in the early embryo through the binding to tyrosine kinase receptors and the signaling via the MAPK (Mitogen-Activated Protein Kinase) cascade. For example, FGF/MAPK pathway can promote phosphorylation of the BMP transducer Smad1 (**Eivers et al., 2009**) leading to neural fate induction. More precisely, the FGF pathway is involved in the caudalization of the tissue (**Pera et al., 2014**).

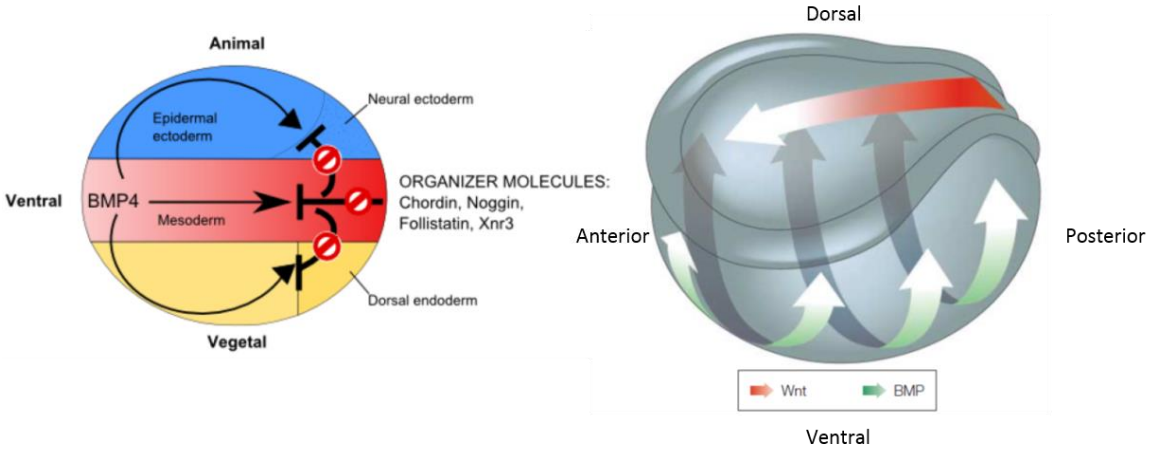

Figure 26: Neural induction and early patterning

A. In amphibians, BMP4 (along with certain other molecules) is a powerful ventralizing factor. Organizer proteins such as Chordin, Noggin and Follistatin, the block the action of BMP4; their inhibitory effects can be seen in all the three germ layers. Drawing depicts the classical model for organizer signaling developed in amphibians. This model applies to all vertebrates. From **(*Gilbert S., Developmental Biology, 9th edition*).**

B. The model shows how perpendicular activity gradients of Wnt and BMP regulate antero-posterior and dorso–ventral patterning. The color scales of the arrows indicate the signaling gradients; arrows indicate the spreading of the signals. Patterning begins at gastrula stages, but for clarity, it is depicted in an early amphibian neurula. The formation of head, trunk and tail requires increasing Wnt activity. **(*Niehrs, 2004*)**

I.1.2 Expansion of neural progenitors

To develop the CNS with the appropriate number of neural cells, it is essential that neural progenitors proliferate adequately before differentiating. Following neural induction by extrinsic factors, neural ectodermal precursors express a large number of neural transcription factors (TFs) which are co-expressed in overlapping domains. The so-called proneural domains arise following the coordinated activity of pre-pattern genes. The earliest transcription factors expressed are involved in the stabilization of the neural fate program. Indeed, once the neural ectoderm is induced, the tissue continues to be exposed to both BMP and Wnt signals from the surrounding mesoderm and ectoderm. Hence, the first TFs to be expressed in this cell population prevent them from reverting to a non-neural fate. For example, in *Xenopus*, Zic1 (Zinc finger of the cerebellum 1), induced by chordin (**Mizuseki et al., 1998**), sensitizes the ectoderm to neural inducers such as noggin (**Kuo et al., 1998**). Many other TFs expressed during early induction are involved in this mechanism. For instance, prepattern genes from the *Iroquois (iro/irx)* family such as Irx1/Xiro1, in frogs, downregulate BMP signaling and are, thereby, essential for neural fate stabilization (**Gómez-Skarmeta et al., 2001**). Once the neural ectoderm has been induced, and the neural fate stabilized, the cells become highly proliferative and form the neural plate. Several transcription factors expressed in those progenitors promote their proliferation and/or delay their differentiation into neural cells. Among the most important and conserved "prepattern genes" maintaining the neuroectoderm in a proliferative state, SRY-related HMG box B (SoxB) provide neurogenic potential but, at the same time, inhibit neural differentiation (**Hartenstein and Stollewerk, 2015**). Another TF involved, called Geminin, maintains neural progenitors proliferative state by inhibition of the basic helix-loop-helix (bHLH) neural differentiation genes (**Seo and Kroll, 2006**). *Fox* (*Forkhead boxes*) family genes such as *Foxd4* also increase the number of proliferating cells, and inhibit bHLH neural differentiation genes (**Moody et al., 2013**). Furthermore, neural progenitor cells are also maintained in an undifferentiated state through the action of bHLH factors such as Hes (Her in zebrafish), Hey and Id family members. In particular, *Hes* genes homologous of Drosophila *hairy* and *Enhancer of split* (**Kageyama et al., 2008**), are target of the Notch signaling pathway, and repress the bHLH proneural proteins (**Pierfelice et al., 2011**).

I.1.3 Neural tube formation

Following the neural plate formation by neural induction, the neural tissue folds in on itself to form the neural tube. In most vertebrates, the epithelial sheets fold into a tube. Specifically, in zebrafish embryos, the neural plate first forms a neural rod primordium which will then rearrange in order to generate a hollow tube.

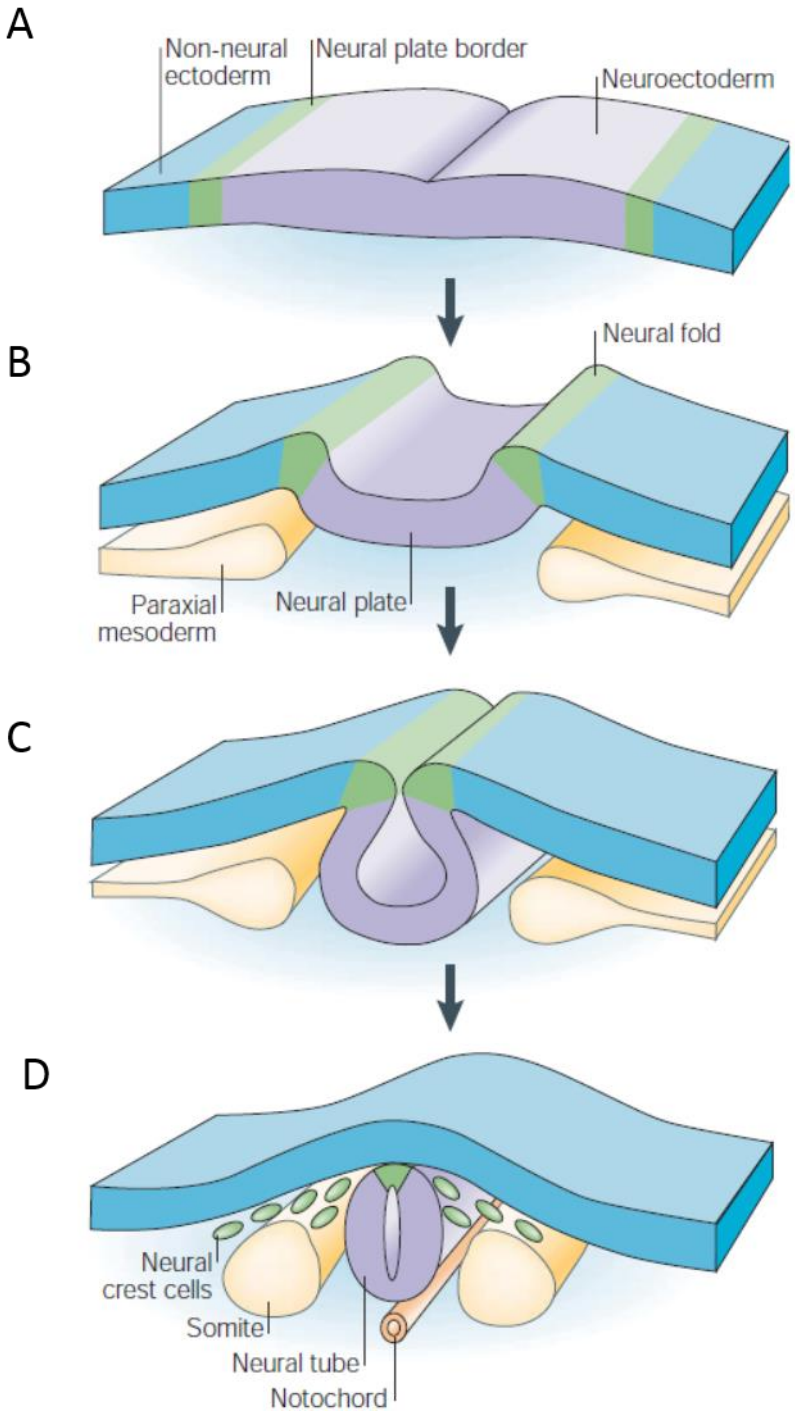

Figure 27: Neural tube formation (*Gammill and Bronner-Fraser, 2003*)
A. The neural plate border (green) is induced by signaling between the neuroectoderm (purple) and the non-neural ectoderm (blue) and from the underlying paraxial mesoderm (yellow). **B, C**. During neurulation, the neural plate borders (neural folds) elevate, causing the neural plate to roll into a neural tube. **D**. Neural crest cells (green) delaminate from the neural folds or the dorsal neural tube (shown), depending on the species and axial level.

This process called neurulation allows the subdivision of the neuroectoderm into the neural tube which will form the central nervous system (brain and spinal cord) and the neural crest cells which will migrate and give rise to peripheral neurons, pigment cells, facial bone cells and multiple other cell types (*fig 27*). As my work was focused on the central nervous system I will not detail neural crest cell specifications.

In the anterior region, the neural tube balloons into three primary vesicles: the prosencephalon (forebrain), the mesencephalon (midbrain), and the rhombencephalon (hindbrain). As development continues, the three primary vesicles divide and lead to the formation of the five secondary chambers, sources of all brain derivatives. In particular, the prosencephalon vesicle divides into the telencephalon and the diencephalon. The rhombencephalon vesicle divides into the metencephalon and the myelencephalon (*fig 28*).

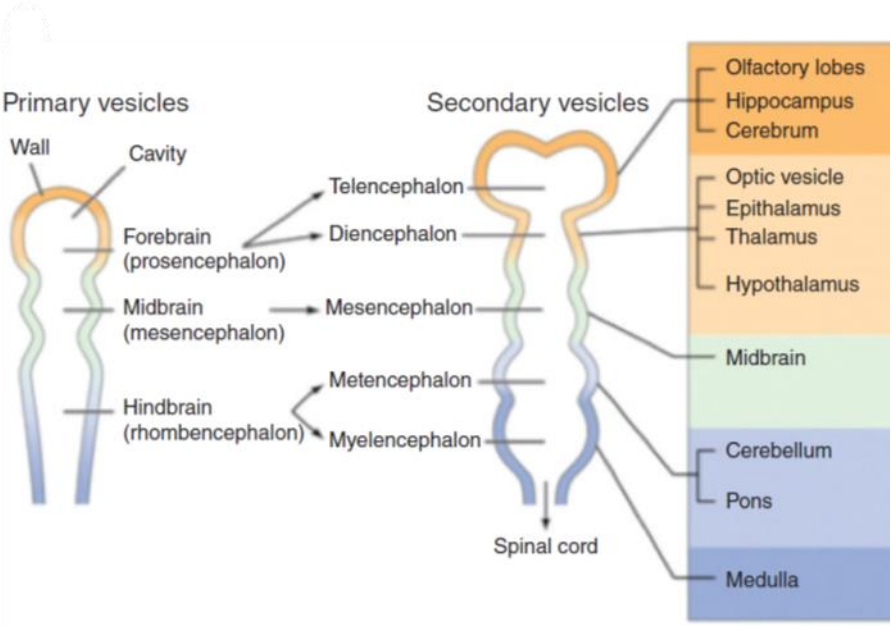

Figure 28: Differentiation of the neural tube in human. (*Darnell and Gilbert, 2017*)
The three primary vesicles become similarly subdivided as development continues and become functionally different from each other. The prosencephalon (orange) subdivides in the telencephalon (dark orange) and the diencephalon (light orange).
The mesencephalon (green) does not divide and give rise to different structures of the midbrain. The rhombencephalon (blue) subdivides to generate the metencephalon (source of the cerebellum in light blue, and the myelencephalon (dark blue).

I.1.4. Initiation of neural differentiation

The onset of neurogenesis in the vertebrate neural plate becomes apparent during late gastrulation by the expression of proneural genes. Indeed, once neural progenitors reach the proper number, a different category of TFs arises in order to promote the transition

towards differentiated neural cells. An example of master regulator at this stage is Paired Box 6 (Pax6) which is expressed in several brain regions, such as forebrain, retina and hindbrain (**Osumi et al., 2008**). Pax6 is a highly conserved transcription factor among vertebrates and is important in various developmental processes in the central nervous system. Beside the role of Pax6 in the maintenance of neural progenitor cells, it also has a major role in neural differentiation through the control of expression of different downstream molecules in a context dependent manner. For example, this master regulator gene control the expression of proneural genes. As previously mentioned, most proneural genes belong to the superfamily of bHLH genes. They induce neuronal differentiation and upregulate the expression of ligands for Notch signaling, such as the transmembrane protein Delta-like 1 (Dll1) and Jagged 1 (Jag1), which activate the transmembrane protein Notch in neighboring cells (**Castro et al., 2006; D'Souza et al., 2008; Henke et al., 2009**). Upon activation of Notch, a cascade of events leads to the expression of *Hes* genes. As previously described, Hes factors, then, repress the expression of proneural genes such as *Dll1*, thereby inhibiting neuronal differentiation and promoting the maintenance of neural progenitor cells. Hence, differentiating neurons inhibit neighboring cells from differentiating into the same type via Notch signaling lateral inhibition. This lateral inhibition prevents simultaneous differentiation of all NPCs, thereby achieving prolonged NPC maintenance into later stages of development (**Imayoshi et al., 2010**). Besides their role in neural differentiation, bHLH genes also contribute to the specification of distinct neuronal cell types. Proneural genes had been initially identified in Drosophila based on their ability to confer a neural identity onto naive ectodermal cells. The first proneural genes identified in *Drosophila* comprised the four genes *achaete* (*ac*), *scute* (*sc*), *lethal of scute* (*lsc*), and *asense* (*as*). Additional proneural genes were subsequently identified, including *atonal* (*ato*). This gene family is conserved throughout evolution. Mouse *ato* orthologs divide into three distinct gene families: Neurogenin genes (*Neurog1, Neurog2, Neurog3*), Neurogenic differentiation genes (*NeuroD1, NeuroD2, Neurod4/Math3/Atoh3, Neurod6/Math2/Atoh2, Atoh1/Math1, Atoh7/Math5*), and Olig genes (*Olig1, Olig2, Olig3*). Members of this family are even more numerous in zebrafish. In contrast, there are only two AS-C-related genes in mouse: *Ascl1/Mash1*, which is expressed in the nervous system, and *Ascl2/Mash2*, which is not. Vertebrate proneural genes are specifically expressed in neuroepithelial cells while they are also expressed in ectodermal cells in *Drosophila*. Besides this difference they act and are expressed similarly. Furthermore, their expression domains define several proneural domains along the antero-posterior axis in the embryo (**Huang et al., 2014**).

I.1.5 Neural progenitors

Neural progenitors are defined by their capacity of generating neurons and glia. Cell types that fulfill this definition are diverse and they change between species and between developmental stages. Mammalian neurogenesis and, more specifically, murine neurogenesis are considered as the "standard" in the field. In mammals, there are three main types of neural progenitors: the neuroepithelial cells, the radial glial cells and the basal progenitors (**Götz and Huttner, 2005**). They differ in terms of *in vivo* localization, *in vivo* behavior, potency, division mode and genetic markers. In particular, neural proliferative progenitors can divide following three different modes: symmetric proliferative, asymmetric proliferative, or symmetric differentiative. Asymmetric divisions are often defined as divisions resulting in daughter cells that adopt different fates. For example asymmetric divisions may result in one neuron or two neurons of different classes. However, asymmetric divisions can also occur without cell cycle exit, such as the generation of two proliferative daughter cells with different lineage restrictions. In this chapter, I will describe the main features of the different types of neural progenitors which are found during neurogenesis in vertebrates.

I.1.5.a. Neuroepithelial progenitor cells

At the end of neurulation, the neural plate and neural tube are composed of a single layer of cells derived from the ectoderm. The so-called neuroepithelial progenitor cells (NePCs) show typical epithelial cell features. Indeed, they are polarized along their apico-basal axis. Interestingly, apico-basal polarity is critical for many cellular mechanisms which regulate neurogenesis and when disrupted, the normal ratio between cell self-renewal and differentiation is often altered (**Willardsen and Link, 2011b**). NePCs are connected to each other at their apical and lateral surface by adherent junctions and tight junctions. Hence, they express different markers of those junctions at their apical domain (the ventricular contacting domain) such as zonula occludens-1 (Zo-1). As a consequence of the presence of junctional components, certain transmembrane proteins such as the atypical protein kinase C (aPKC) are specifically observed at the apical and lateral membranes (**Götz and Huttner, 2005**). Neuroepithelial cells form a pseudostratified epithelium called the neuroepithelium. Its apparent stratified organization is due to a cellular process called interkinetic nuclear migration (INM, *fig 29A*). During this process, cell nuclei move periodically in phase with cell-cycle progression (**Del Bene, 2011**). Before the onset of neurogenesis, the entire neuroepithelium consists of a single germinal layer, the ventricular

zone (VZ). As soon as neurogenesis begins, cells extend from the basal lamina to the ventricle and span the entire thickness of the neural tube (*fig 30*). However, nuclei are positioned in several layers depending on the cell cycle-phase. In particular, M-phase nuclei are positioned at the apical-most region while G1/S phase nuclei move to more basal locations. During G2 phase, nuclei rapidly move back to the apical surface to enter the M-phase (*fig 29A*). Although this phenomenon has been described over 80 years ago (**Sauer, 1935**), its function has remained controversial. Several studies support that INM would maximize the number of mitosis per apical surface available (**Fish et al., 2008**). Complementary data have suggested a potential role in cell fate determination, by regulating the time of exposure to ventricular factors (**Del Bene et al., 2008**). NePCs are highly proliferative cells and increase in number by symmetric proliferative divisions to produce a pool of progenitors necessary for CNS development (**Huttner and Kosodo, 2005**).

I.1.5.b. Radial glial cells

As development proceeds, NePCs undergo a series of changes in their gene expression profile, cytological characteristics and differentiation potential (Malatesta et al., 2008). They mature into regionally-specified progenitors and give rise to radial glial cells (RGCs) (**Guérout et al., 2014**). RGCs cell bodies are located along the ventricular zone. In addition to Nestin expression, already present in neuroepithelial cells, RGCs express glial marker such as GLAST (glutamate aspartate transporter), GS (glutamine synthetase), BLBP (brain lipid binding protein), GFAP (glial fibrillary acidic protein), the Ca^{2+} binding protein S100β and the intermediate filament Vimentin (*Table 2,* **Götz et al., 2015**). RGCs keep several features of NePCs such as apico-basal polarity, adherent junctions and INM. INM is different between NePCs and RGCs. In these latter, nuclei do not move along the whole apico-basal axis, but movements are confined to the portion of the cell between the apical surface and the basal boundary of the ventricular zone of the subventricular zone (*fig 29B;* **Götz and Huttner, 2005**).

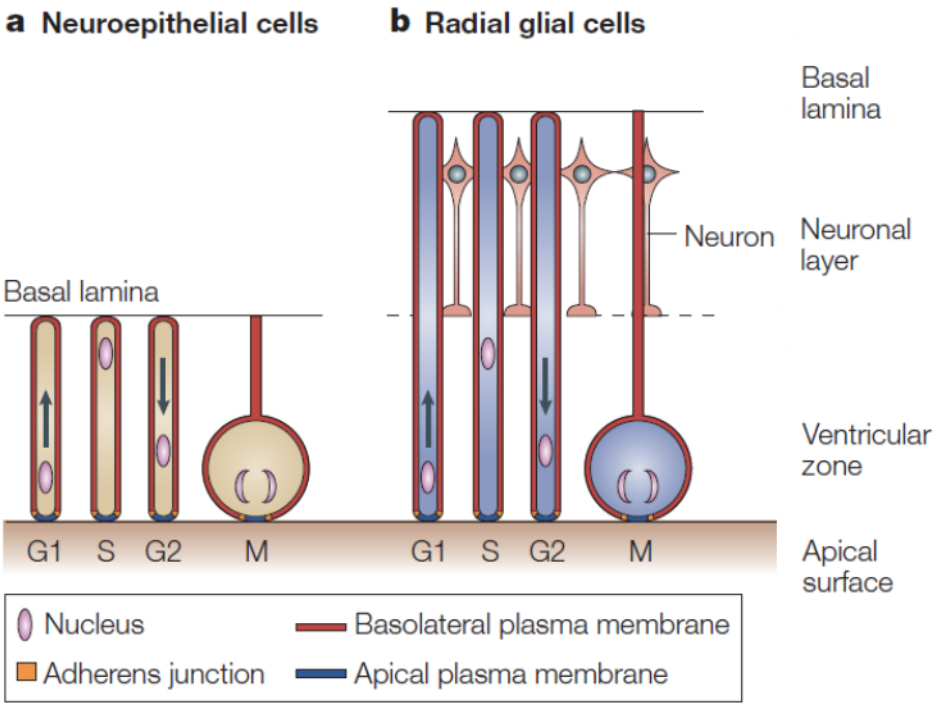

Figure 29: Apico-basal polarity in neuroepithelial and radial glial (*Götz and Huttner, 2005*).
A. In neuroepithelial cells, interkinetic nuclear migration spans the entire apico-basal axis of the cells. The nucleus migrates to the basal side during G1 phase. S phase occurs at the basal region. The nucleus rapidly moves back to the apical surface to enter the M-phase.
B. In radial glial cells, nuclear migration does not extend toward the basal side, but rather, stays confined to the portion of the cell between the apical surface and the basal boundary of the ventricular zone.

	Neuroepithelial cells	Radial Glia (early)	Radial Glia (late)	Mammalian aNSCs (Astrocyte-like stem cells)
GFAP	-	-/+	+	+++
GLAST	-	++	++	++
Glutamine synthetase	-	-	+	++
S100-β	-	-	+	+
Nestin	+++	+++	+++	+++
Vimentin	-	+	++	+++
BLBP	++	+++	+++	++
Sox2	+++	+++	+++	++
ZO-1	+	-	-	-
aPKC	+	+	+	ND

Table 2: Similarities and differences between the different kinds of neural progenitors in term of selected molecular markers. Adapted from *Götz et al., 2015*

	Neuroepithelial cells	Radial Glia (early)	Radial Glia (late)	Mammalian aNSCs (Astrocyte-like stem cells)
Glutamate uptake	-	+	++	+++
K-cunductance at rest	-	-	++	++
Glycogen storage	-	+	++	++
Blood vessel contact	-	+	++	+++
Interkinetic Nuclear Migration	+++	++	++	-
Cell division	+++	+++	++	++
Multipotency	+++	+++	++	+++
Self-renewal	++	++	+++	++

Table 3: **Similarities and differences between the different kinds of neural progenitors in term of cellular behavior. Adapted from *Götz et al., 2015***

Finally, the transition from NePCs to RGCs and their progression from proliferative to neurogenic divisions during embryonic development is associated with an increase in the lengths of their cell cycle and in particular of the G1 phase (**Takahashi et al., 1995**) . RGCs can be found in the entire CNS: in the brain, the spinal cord, the retina where they are called Müller glia, or even in the cerebellum where they are named Bergmann glia (**Pinto and Götz, 2007**). For decades, radial glial cells were considered as neural migration support cells. However, further studies have shown that these cells are multipotent progenitors able to produce any type of cells such as neurons, oligodendrocytes, intermediate progenitor cells (IPC), astrocytes or ependymal cells (*fig 30;* **Kriegstein and Alvarez-Buylla, 2009**). Surprisingly, radial glial cells are a heterogeneous population. Depending on the expressed markers, radial glial cells are differentially classified and possess divergent potency. At the end of embryonic development, radial glial cells disappear turning into ependymal cells or astrocytes supporting neuronal function and regulating metabolic activity.

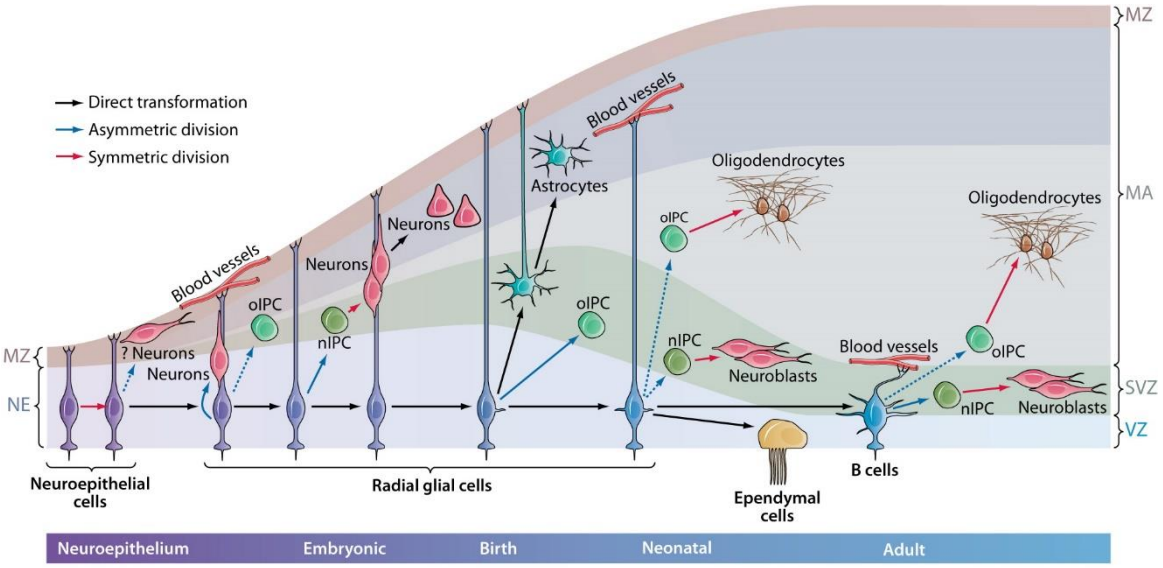

Figure 30: Neurogenesis and gliogenesis in proliferative zone of the embryo and adult rodent brain. (*Kriegstein and Alvarez-Buylla, 2009*)

Neuroepithelial cells firstly divide symmetrically to generate more neuroepithelial cells. Some neuroepithelial cells likely generate early neurons. As the developing brain epithelium thickens, neuroepithelial cells elongate and convert into radial glial cells. RGCs divide asymmetrically to generate neurons directly or indirectly through intermediate progenitor cells. Radial glial cells can also give rise to oligodendrocyte indirectly thought intermediate progenitors (oIPC). As the progeny from RGCs and IPCs move for differentiation, the brain thickens, further elongating the RGCs. At the end of embryonic development, most RG begin to detach from the apical side and convert into astrocytes while oIPC production continues. A subpopulation of RGCs retains apical contact and continue functioning as neural progenitors in the neonate. These neonatal RGCs continue to generate neurons and oligodendrocytes through nIPCs and oIPCS; some convert into ependymal cells, whereas others convert into adult subventricular zone (SVZ) astrocytes (type B cells) that continue to function as NSCs in the adult. B cells maintain an epithelial organization with apical contact at the ventricle and basal endings in blood vessels. They continue to generate neurons and oligodendrocytes through (n and o) IPCs. This illustration depicts some of what is known for the developing and adult rodent brain. Timing and number of divisions likely vary from one species to another, but the general principles of neural progenitor identity and lineages are likely to be preserved. Solid arrows are supported by experimental evidence; dashed arrows are hypothetical. Colors depict symmetric, asymmetric, or direct transformation. IPC, intermediate progenitor cell; MA, mantle; MZ, marginal zone; NE, neuroepithelium; nIPC, neurogenic progenitor cell; oIPC, oligodendrocytic progenitor cell; RG, radial glia; SVZ, subventricular zone; VZ, ventricular zone.

I.2 Adult neurogenesis

For decades, neurogenesis has been widely studied at embryonic stages. Indeed, the famous Spanish histologist Santiago Ramon y Cajal has described neuron formation in the embryonic brain. In particular, he observed mitotic figures only in the embryonic brain while he could not find any dividing cells in the adult. Therefore, he proclaimed that adult "nerve paths are something fixed and immutable" (**Cajal, 1913**). This dogma has been accepted for almost a century. However, as early as 1960s, Joseph Altman and collaborators demonstrated that new neurons could be generated in the adult hippocampus and the olfactory bulb of mammalian brain (**Altman, 1962**). Yet, it took more than 20 years and multiple researches in diverse species for adult neurogenesis to be accepted in the scientific

community. Indeed, adult neurogenesis is conserved throughout evolution. It has been highlighted in mammals, invertebrates and several non-mammals vertebrates such as reptiles, birds or fishes (**Grandel and Brand, 2013**). However, neurogenic abilities are highly different depending on the species and brain territories of interest. Moreover, while it was widely postulated that adult neurogenesis was only dedicated to the continuous growth of various brain regions, it is now clear that the biological significance of this life-long-lasting neurogenesis is less restricted. For example, regenerative territories in adult brain are much more numerous in teleost or amphibians than in mammals. Extended studies on the production of new neurons during adulthood showed that progenitors with embryonic features and signaling pathways are reused during adulthood upon injuries. Therefore, the study of both embryonic and adult neurogenesis would help deciphering the neural progenitor cell homeostasis. In this context, in this chapter, I will compare adult neurogenesis focusing on mammals and teleosts and I will stress out the potential importance of neuroepithelial cells.

I.2.1. Adult neurogenesis in mammals

In mammals, especially in rodents, two major neurogenic niches can be found: the subventricular zone (SVZ) lining the lateral ventricles and the subgranular zone (SGV) within the dentate gyrus of the hippocampus (*fig 31A, fig 32A*; **Lindsey and Tropepe, 2006**). The SVZ is directly derived from the embryonic ventricular zone. In adulthood, this neurogenic zone represents the most proliferative zone in the rodent brain. Indeed, about 30 000 new immatures neurons (neuroblasts) are formed every day from neural progenitors.

Four classes of cells have been identified in this niche: type A cells (NCAM and βIII-tubulin-positive neuroblasts), type B cells (GFAP-positive astrocytes), type C cells (transient-amplifying cells) and type E cells (ependymal cells). **Doetsch et al**. showed that type B cells are slowly dividing progenitor cells which then generate the fast dividing transient-amplifying cells type C cells. Then, the latter give rise to the neuroblasts (type A cells) (**Doetsch et al., 1999**). Newly generated neurons would thereafter, migrate towards the olfactory bulbs where they differentiate into interneurons. In addition, SVZ neural progenitors can also give rise to oligodendrocytes of the corpus callosum (*fig 32B*).

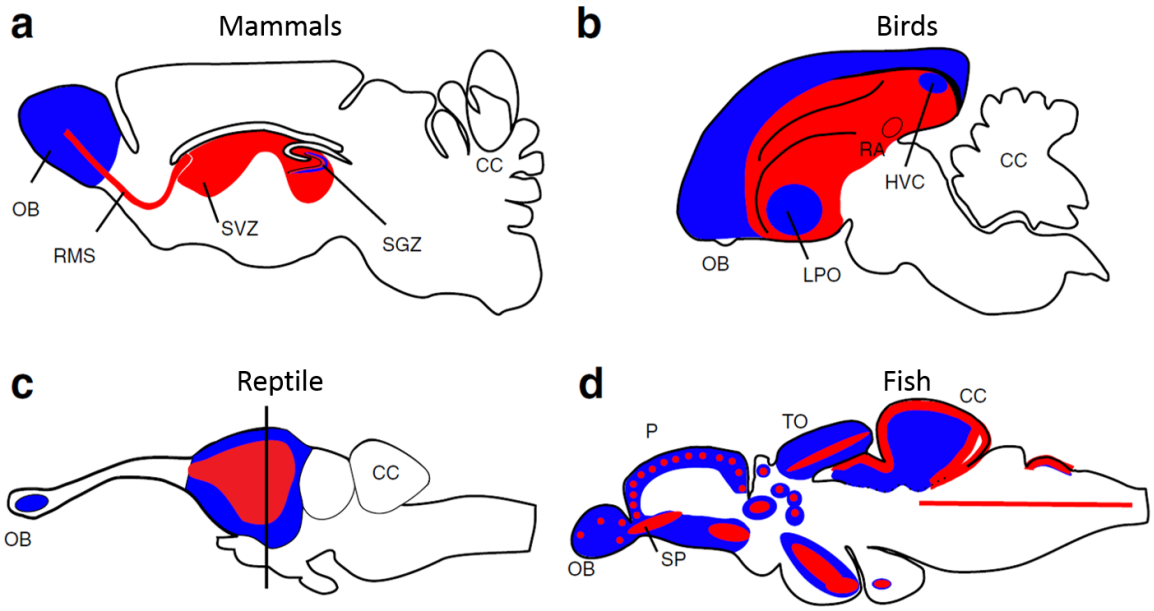

<u>Figure 31:</u> Comparative aspects of adult neural progenitor activity (Adapted from *Grandel and Brand, 2013*)

Parasagittal sections through the brains of an adult (**a)** rodent (mouse), (b) bird (canary), (c) reptile (lizard) and (d) fish (zebrafish) indicating regions of constitutive proliferation (red) and neurogenesis (blue).
CC: corpus cerebelli; HVC: nucleus engaged in song learning and production; LPO: lobus parolfactorius; OB: olfactory bulb; P: pallium (dorsal telencephalon); RA: robust nucleus of the archistriatum; RMS: rostral migratory stream; SGZ: subgranular zone; SP: subpallium (ventral telencephalon); SVZ: subventricular zone; TO: optic tectum.

The dentate gyrus is a substructure of the hippocampus, essential for the learning process. In this neurogenic zone, proliferation is more restricted. Indeed, around 3000 to 9000 neurons are formed every day in the rodent, depending on the age. Progenitors of the SGZ are also astrocytes expressing *Gfap* and *Nestin*. They can undergo two modes of division: symmetric or asymmetric. Following asymmetric divisions, SGZ astrocytes give rise to intermediate transient-amplifying progenitors (type D cells). Besides this peculiarity, the general lineage of adult neurogenesis in the SGZ and the SVZ is similar (**Seri et al., 2001, 2004**).

More recent analyzes have highlighted additional constitutive neurogenic zones such as the cortex or the hypothalamus. However, the neurogenesis activity in these structures remains discrete in comparison with the subventricular zone of the lateral ventricle and the dentate gyrus (**Abrous et al., 2005**).

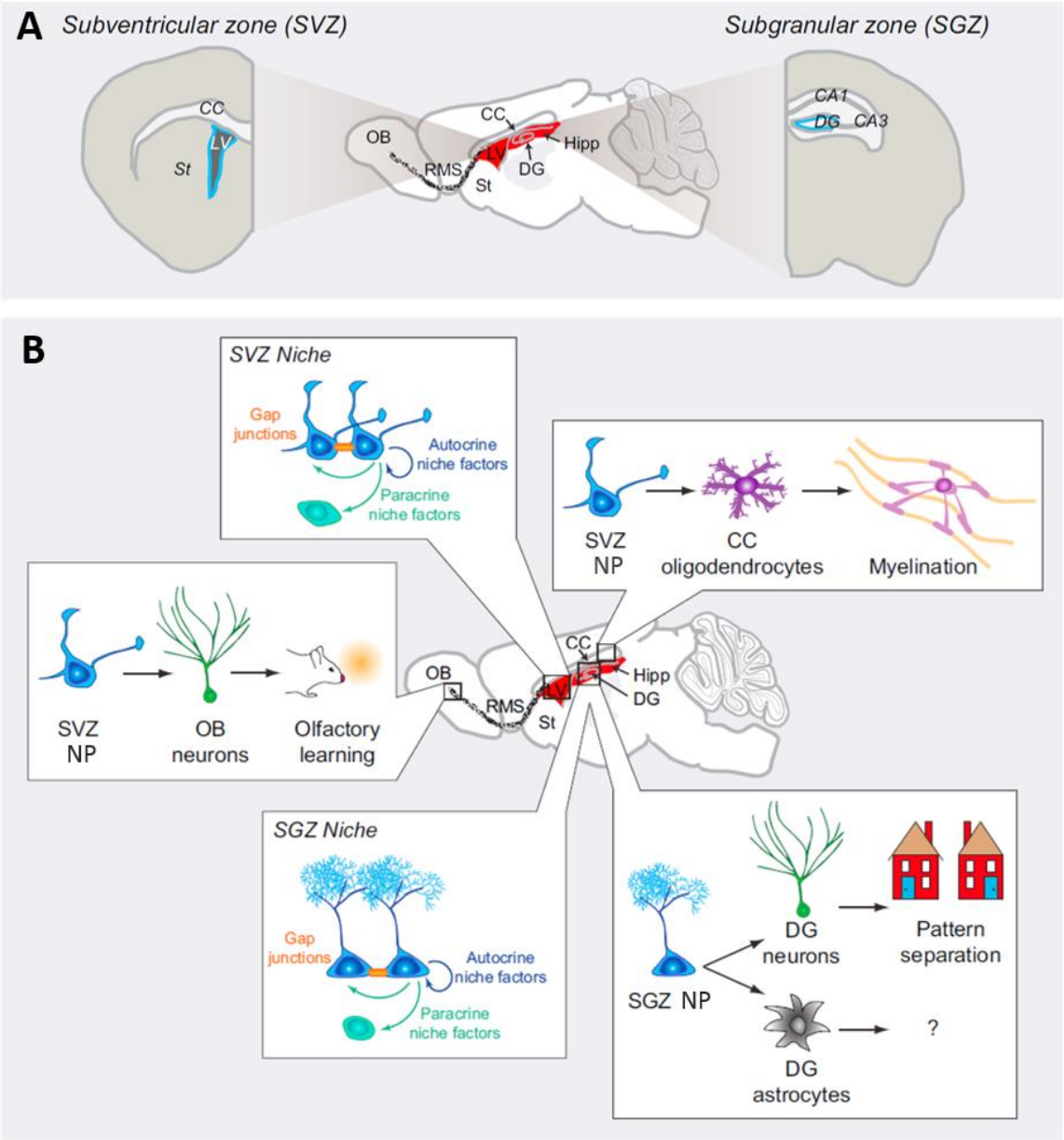

Figure 32: Adult mammalian neurogenesis (Adapted from *Bond et al., 2015*)
A. Sagittal view of the adult rodent brain. Two major niches can be found. The subventricular zone (SVZ) is located along the lateral ventricle in the forebrain, while the subgranular zone (SGZ) is located in the hippocampus along the dentate granule cell layer.
B. Impact of the neural progenitors in the adult mammalian brain. Neural progenitors in the SVZ and SGZ release autocrine and paracrine niche factors. In addition, neural progenitors form GAP junctions to directly communicate with each other. SVZ NPs generate OB neurons and CC oligodendrocytes. OB neurons contribute to olfactory learning, while CC oligodendrocytes myelinate CC axons. SGZ NPs generate DG neurons and astrocytes. DG neurons are important for pattern separation functions.
CC: corpus callosum; DG: dentate gyrus; Hipp: hippocampus; LV: lateral ventricle; NP: neural progenitors; OB: olfactory bulb; RMS: rostral migratory stream; St: striatum; SGZ: subgranular zone; SVZ: subventricular zone.

Neural progenitors are dynamically regulated by a number of factors. In particular, several signaling pathway involved in embryonic neurogenesis such as Noggin (see chapter 2, Part I, I.1 Embryonic neurogenesis) persist exclusively in the adult SVZ (**Gates et al., 1995**). Furthermore, additional morphogens such as BMPs, Notch, Wnt and SHH continue to

regulate adult neurogenesis (**Faigle and Song, 2013**). Interestingly, new methods have allowed to describe the molecular signature of quiescent adult progenitors. Upon activation of those neural progenitors and induction of neurogenesis, a molecular switch has been observed. For example, activation of several transcription factors expression, variation of the energy sources, changes in the niche signaling capacity and priming of protein translation machinery have been observed (**Llorens-Bobadilla et al., 2015; Luo et al., 2015; Shin et al., 2015**).

Many questions was raised following the identification of both SVZ and SGZ neurogenic niches. Indeed, when adult neural progenitors were initially discovered, it was hypothesized that they were activated for regeneration of new neurons following injuries. However, recent studies suggests that the primary function of endogenous adult neural progenitors is to confer an additional layer of plasticity to the brain via both direct and indirect mechanisms (**Christian et al., 2014**).

I.2.2 Adult neurogenesis in non-mammalian vertebrates

Adult neurogenesis has been widely studied and described in mammals and, more particularly, in rodent brains since mice and rats are closely related to humans. However, adult neurogenesis is not restricted to mammals, and is widely represented in other vertebrates such as birds, reptiles, amphibians and fish. In particular, adult neurogenesis has been widely studies and described in amphibians and fish since the first evidence in rodents (**Kirsche, 1967; Rahmann, 1968**). In amphibians, proliferation and neurogenesis has been observed in the telencephalon, the preoptic region, the hypothalamus, the midbrain and the cerebellum. Moreover, constitutive neurogenesis has been seen in the forebrain and midbrain of adult bullfrog (*Rana catesbeiana*) (**Simmons et al., 2008**). In teleost, between 12 and 16 distinct proliferation zones have been described (*fig 31D*) in several species such as stickleback (*Gasterosteus aculeatus*), brown ghost (*Apteronotus leptorhynchus*) and zebrafish (*Danio rerio*) (**Grandel and Brand, 2013**). In medaka (*Oryzias latipes*) and *Nothobranchius furzeri*, adult brain proliferation zones have been partially characterized and correspond to the general pattern published so far in teleost (**Kuroyanagi et al., 2010; Tozzini et al., 2012**). Interestingly, those proliferative/neurogenic zones are present along the whole rostro-caudal axis of the brain (*fig 31*). In particular, in zebrafish two distinct neurogenic proliferation zones have been detected in the telencephalon: a ventral proliferation zone along the ventricular side of the subpallium and a dorsal proliferation zone along the ventricular surface of the pallium (*fig 33B*; **Adolf et al., 2006; Byrd and**

Brunjes, 1998, 2001; Ekström et al., 2001; Grandel et al., 2006; Zupanc et al., 2005). In addition, widespread proliferation has been shown in the cerebellar molecular layer (*fig 33D*). Finally, in zebrafish, the optic tectum as well as the retina both possess prominent proliferative niches. More particularly, a proliferation zone is located around the posterior half of the OT, at the margin of the periventricular grey zone (PGZ) facing the tectal ventricle (*fig 33C*; **Grandel et al., 2006; Ito et al., 2010**). Similar niches are present in both goldfish and medaka. The peculiarity of adult neurogenesis in teleost and amphibian resides in the nature of the neural progenitors involved. Indeed, as mentioned in the previous sections, astrocytes contribute widely to neurogenesis in mammals. However, astroglial adult neural progenitors appear to be a mammalian-specific feature. Outside this group, astrocytes do not contribute to adult neurogenesis which is mainly supported by radial glial cells. Radial glial cells contribute to adult neurogenesis in anamniotes as well.

I.2.3 The underevaluated importance of neuroepithelial progenitors

As described above, mammalian and teleost adult neurogenesis are mostly different in terms of localization and underlying cellular activity. These specificities lead to differential regenerative abilities and neurogenic potential. Indeed, mammalian regeneration in the CNS appears to rely mostly on the reactivation of astrocytes (**Sabelström et al., 2013**; **Götz et al., 2015**). In non-mammalian vertebrates, regeneration is driven by RGCs activation. Nonetheless, both in amphibians and fish, neuroepithelial cells are maintained until adulthood. In particular, neuroepithelial cells have been found in the cerebellum of zebrafish, and in the visual system of both amphibians and fish where they contribute to the life-long neurogenesis in the optic tectum and in the retina (*fig 33A*). Indeed, the cells in the proliferative zone express progenitor markers such as *Sox2* or *Musashi* and do not show any radia glial phenotype in both zebrafish (**Ito et al., 2010**) and medaka (**Alunni et al., 2010**). They express polarity markers like z*o-1*, g*amma-tubulin* and *aPKC*. Additionally, in the anterior part of telencephalon, non-glial progenitors showing neuroepithelial characteristics have been found (**Ganz et al., 2010**). Recently **Dirian and colleagues** demonstrated that "a minute population of neuroepithelial progenitors persist throughout life ant the posterolateral edge of the pallial ventricular zone" (**Dirian et al., 2014** ; *fig 33B3*). Therefore, it has been hypothesized that these cells could contribute to constitutive neurogenesis and regeneration when Notch-dependent progenitors are depleted (**Ninkovic and Götz, 2014**). Moreover, a neuroepithelial progenitor cells population can be found in the cerebellum of zebrafish juvenile and adult brains (**Kaslin et al., 2013**). In

this region, NePCs have the capacity to produce granule cells and remain stable in the aging of the cerebellum. Moreover, in this region of the brain, RGCs seem to play only a minor role in regeneration (**Kaslin et al., 2017**). During embryogenesis, it is clear that all neurons derive directly or indirectly from neuroepithelial cells which are hardly accessible and poorly understood in mammals. These cells have an underestimated developmental importance. Thus, studies on zebrafish neuroepithelial cells are important for elucidating basic principles of neurogenesis from development to adulthood.

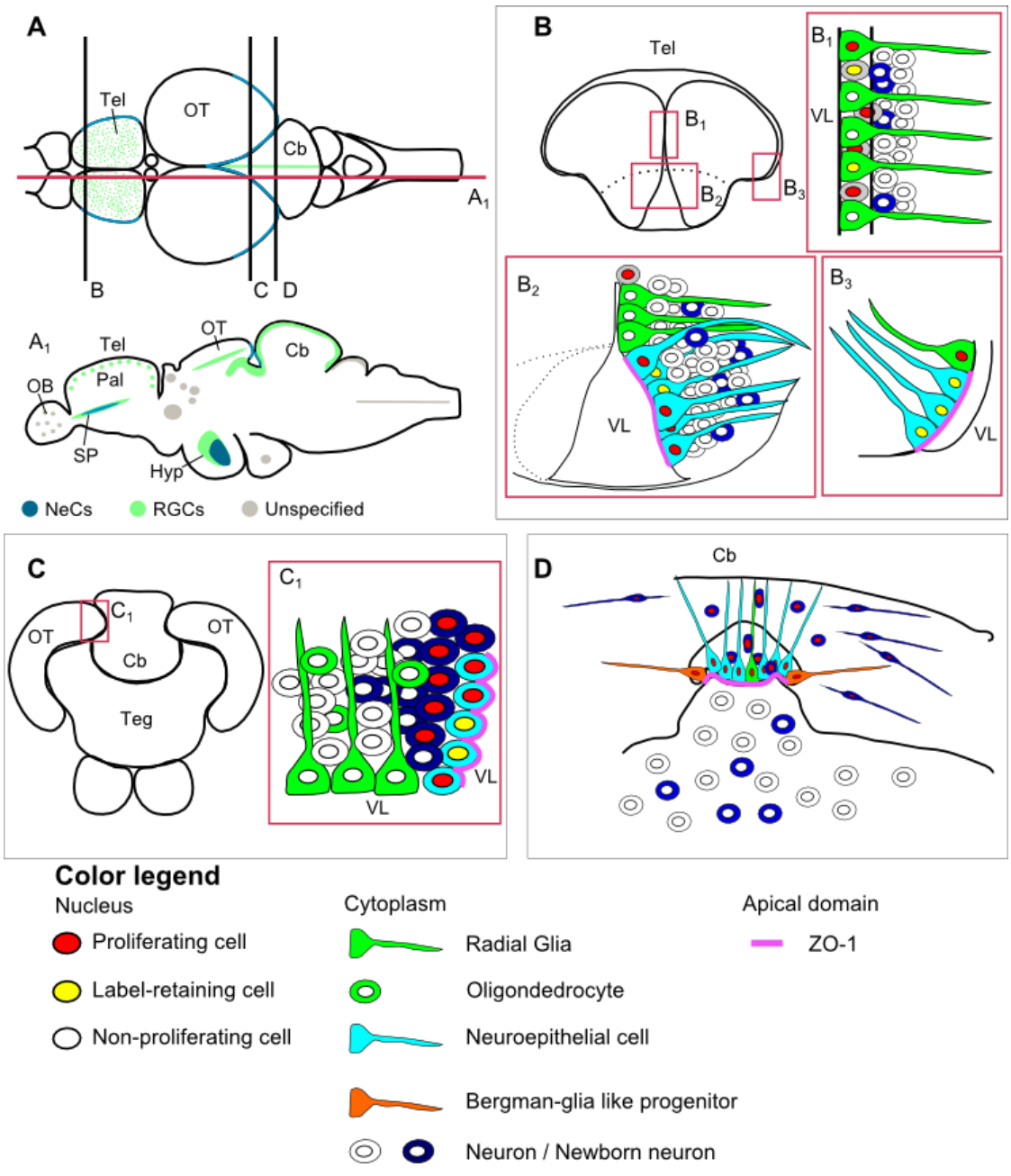

Figure 33: Overview of the progenitor niches in the zebrafish adult brain. Adapted from *Grandel and Brand, 2013*

The zebrafish adult brain contains at least fifteen neurogenic niches. Both radial glial cells (RGCs) and neuroepithelial cells contribute to neurogenesis at adulthood.

A. Dorsal view of the zebrafish brain. Red line indicates sagittal section. Black lines indicate section levels through (B) telencephalon, (C) optic tectum and (D) cerebellum.

B. Telencephalic cross section indicating neurogenic niches in the pallium/dorsal telencephalon (B1), subpallium/ventral telencephalon (B2) and lateral pallium (B3) that are magnified in the same panel. RGC support neurogenesis in the pallium (GFAP+, vimentin+, S100β+), whereas neuroepithelial cells support neurogenesis in the subpallium and in the lateral pallium (nestin+; ZO1+ in apical membrane).

C. Neurogenic niche in the tectum around the margin of the periventricular grey zone facing the tectal ventricle. Boxed area depicts location of the tectal neurogenic niche in C1: non-glia (GFAP−, BLBP−, S100β−) polarized (ZO-1+, γ-tubulin+, aPKC+ at apical membrane) progenitor cells give rise to neurons and periventricular radial glia.

D. The cerebellar neurogenic niche gives rise to granule cells and some Bergmann glia. Cerebellar stem/progenitor cells are non-glia (GFAP−, vimentin−, BLBP−, S100β−) but neuroepithelial-like polarized cells (nestin+; ZO-1+, β- catenin+, γ-tubulin+, aPKC+ at the apical membrane). VL indicates the position of the ventricle lumen in every structure.

II. The optic tectum

During my PhD, I have studied a small population of neuroepithelial progenitors located at the periphery of the zebrafish optic tectum. In this section I will provide a detailed description of the tectum, its anatomy, embryonic origin and growth mode.

II.1 Anatomy and organization of the optic tectum

One of the most studied region of the central nervous system in both embryos and adults, is the visual system. It is composed of the retina and the connected tissues in the brain. In teleost, the brain structure responsible for the processing of visual inputs is named the optic tectum (OT). In mammals, the homologous region of the OT is called the superior colliculus. The visual system in mammals is more complex and necessitates also the involvement of additional parts of the brain: the lateral geniculate and the visual cortex (**Sterling, 1988**). The OT is the dorsal part of the vertebrate midbrain (*fig 34*) which receives afferents from the retina. In particular, it mainly receives axons from the retinal ganglion cells, but also from the pretectum, the dorsal thalamus, the tegmentum, and the nucleus isthmi. (**Butler and Hodos, 2005**). It is noteworthy that the size of the tecta and their complexity change between fish species, depending on their behavior and ecological niches. Species that process more visual information have larger tecta (**Ito et al., 2007**). Particularly interesting in this context are the intraspecific variations that can be found in subpopulations adapted to live in constant darkness compared with river-adapted subpopulation (**Eifert et al., 2015**). The OT is a structure involved in the control of eye movements and the spatial orientation **(Krauzlis et al., 2013; Zénon and Krauzlis, 2014**).

In addition, it controls visual spatial attention and receives some auditory afferents as well (**Celesia, 2015**). Both components of the visual system (e.g the retina ant the OT) are organized similarly in several well organized layers.

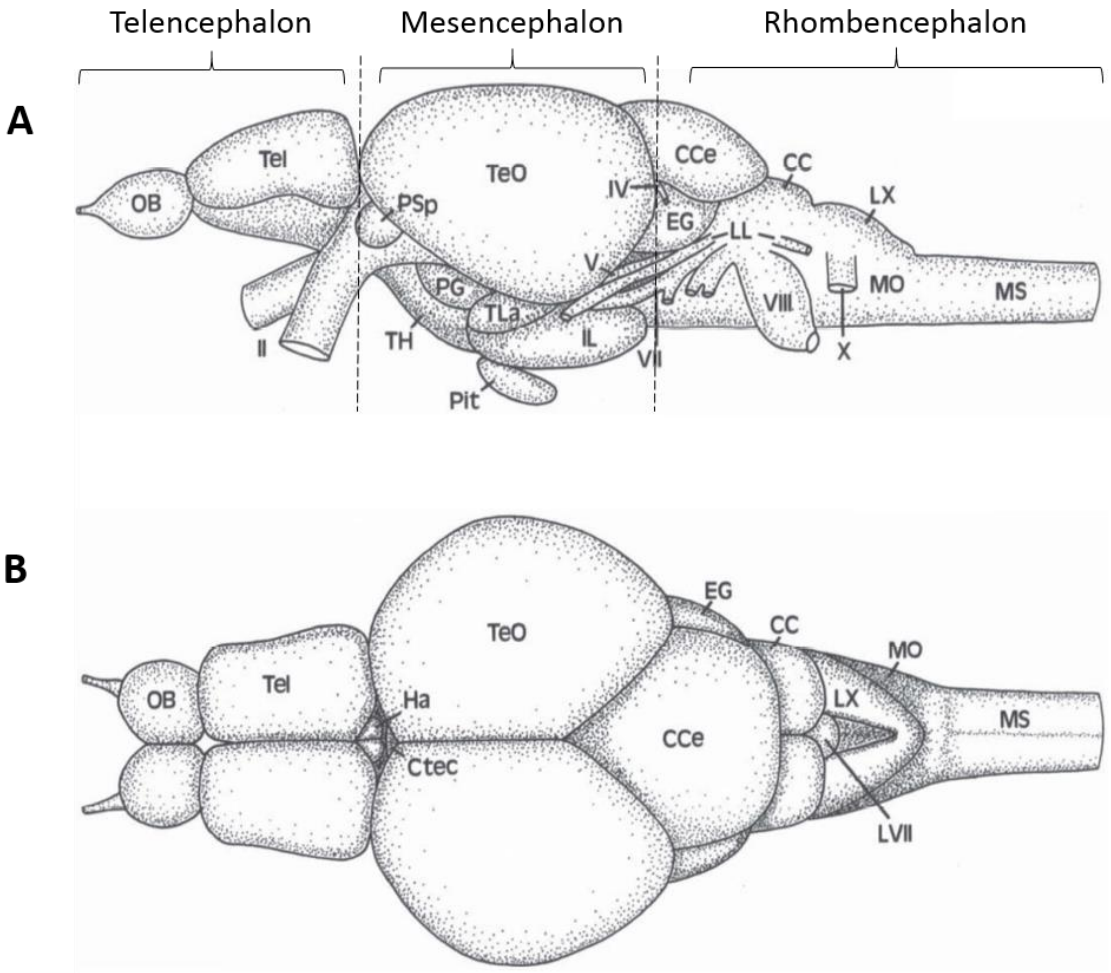

Figure 34: Localization of the optic tectum within the adult teleost brain. Adapted from *Wulliman et al., 2012*

Lateral (**A**) and dorsal (**B**) view of the adult zebrafish brain. Dotted lines delimit, from left (rostral) to right (caudal) the telencephalon (forebrain), mesencephalon (midbrain) and rhombencephalon (hindbrain). The optic tectum is the large structure, localized dorsally in the mesencephalon. The dorsal view of the brain highlight the existence of two lobes in the OT.

CC: crista cereballis; CCe: corpus cerebelli; Ctec: Commissura tecti; EG: eminentia granularis; Ha: habenula; IL: inferior lobe of hypothalamus; LL: lateral line nerves; MO: medulla oblongata; MS: medulla spinalis; OB : olfactory bulb; PG: periglomerular area; Pit: pituitary; PSp : parvorcellular superficial pretectal nucleus; Tel : telencephalon; TeO: optic tectum; TH: tuberal hypothalamus; TLa: *torus lateralis.*

The OT can be subdivided in three layers: the periventricular gray zone (PGZ) also called the *stratum periventriculare* (SPV) which contains most cell bodies of the tectal neurons; the superficial and central zones, which can be found within the neuropil and where the tectal afferents terminate (**Nguyen et al., 1999**). The superficial and central zone can further be subdivided into several layers (*fig 35A*). However, the number of these layers depends

on the considered species. In most teleost, the superficial zone includes the *stratum opticum* (SO) and the *stratum marginale* (SM), while the central zone is composed of the *stratum fibrosum et griseum superficiale* (SFGC), *stratum griseum centrale* (SGC) and *stratum album centrale* (SAC) (**Cerveny et al., 2012**). One of the particularity of the visual system resides in the topographic organization of the retina and the optic tectum. Indeed, tectal termini of retinal afferents reflect their body position in the retina (**Baier, 2013**; *fig 35A*). Retinal ganglion cells axons project from the retina to the contralateral or ipsilateral hemisphere of the tectum. Therefore, a retinotopic map is formed in the tectum (**Cerveny et al., 2012**).

As mentioned in the chapter "adult neurogenesis", the OT as well as the retina are growing throughout life. Thus, the retinotectal connections need to be continuously adjusted but they need to maintain the appropriate representation of the visual space (*fig 35B*).

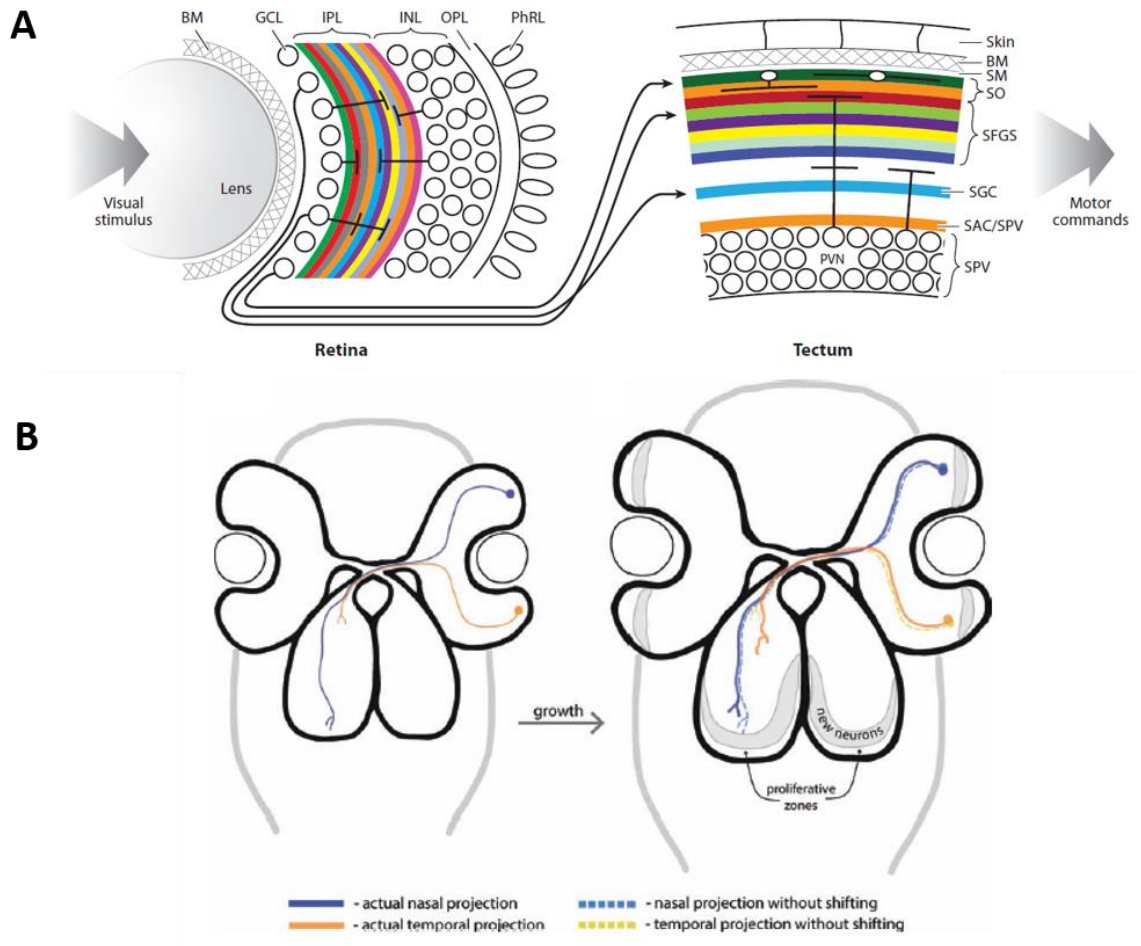

Figure 35: Retinotopic map in the optic tectum
A. Schematic representation of the topography and orientation of synaptic regions of the zebrafish visual pathway. In the retina, a ten layered structures is present, gathering several cell type afferents such as ganglions cells neurites and amacrine cells (colored bands on the left, IPL). Ganglion cells axons leave the eye via the optic nerve and project to the optic tectum. In the OT neuropil, each axons terminate in one of ten layers (colored band in the right). (***Baier, 2013***). **B.** Progression of the retinotectal connections shift over time. On the left panel, the retinotectal projections form a retinotopic map in the OT. Over time, when both retina and OT are growing, each tectal hemispheres are adding new cells in a crescent shape at the periphery. In the retina, the growth of the structure is triggered by the addition of cells circumferentially. Because new neurons are added in discordant patterns, the retino-tectal connections need to be remodeled to conserve the map. (***Cerveny et al., 2012***)
BM: basement membrane; GCL: ganglion cell layer; INL: inner nuclear layer; IPL: inner plexiform layer; OPL: outer plexiform layer; PhRL: photoreceptor layer; PVN: periventricular neurons; SAC: *stratum album centrale*; SAC/SPV, boundary between SAC and SPV; SFGS: *stratum fibrosum et griseum superficiale*; SGC: *stratum griseum centrale*; SM: *stratum marginale*; SO: *stratum opticum*; SPV: *stratum periventriculare* (also called periventricular grey zone, PGZ); PVN: Periventricular neurons.

II.2 Embryonic origins of the OT

As described in the chapter dedicated to embryonic neurogenesis, at the onset of gastrulation, the neural plate begins to form and to regionalize in order to give rise to the diverse regions of the brain. Morphogenesis of the brain is triggered by the generation of local signaling centers playing a major role in neural plate patterning and fate specification. In particular, OT determination and localization requires the involvement of different signaling centers, and is included in the general patterning of the neural plate. At present, two signaling centers have been identified: the anterior neural boundary (ANB) necessary for telencephalic fate, and the isthmic organizer (IsO) involved in the development of both mesencephalic and metencephalic structures and in the positioning of the MHB (**Wurst and Bally-Cuif, 2001**). In addition, **Affaticati et al**. showed that an additional region of the brain would act as a morphogenetic entity. This region, called the optic recess region (ORR) is situated in the forebrain around the optic recess, between the telencephalon and the hypothalamus. The identification of this zone has been based on the presence of bundles of fibers, radial glial cells and differentiating neurons (**Affaticati et al., 2015**). However, so far, no functional analyzes has been performed in order to identify the precise role of this region. One of the most studied signaling center in vertebrates is the IsO, the organizer responsible for the development of the midbrain/hindbrain boundary (MHB; **Raible and Brand, 2004**). Indeed, the MHB domain has retained many attention as it is required for patterning and differentiation of the midbrain and cerebellum. The IsO is largely conserved

in vertebrates and involves several molecular and cellular activities. Early during development, several steps are necessary for the correct positioning, induction, maintenance and morphogenesis of MHB and adjacent territories (**Rapacioli et al., 2016**). The first step corresponds to the positioning of the MHB via the spatial restriction of transcription factors expression along the rostro-caudal axis. In particular, the homeobox-domain-containing transcription factors Orthodenticle homologue 2 (*otx2*) and gastrulation brain homeobox 2 (*gbx2*) are expressed in the anterior and posterior epiblast, respectively. The boundary between the two expression domains is defined by the action of Wnt molecules secreted by the lateral mesendoderm (**Cavodeassi and Houart, 2012**). The interphase between *otx2* and *gbx2* expressions ultimately defines the position of the IsO and of the MHB lately. In zebrafish, *fgf8* and *wnt11*, expressed by both structures, are required for the definition of hindbrain vs midbrain identify. Indeed, **Foucher et al.** demonstrated that *fgf8* is required at the MHB to repress *otx* in the presumptive anterior hindbrain (*fig 36;* **Foucher et al., 2006**).

The expression of *fgf8* is induced, between the caudal limit of *otx2* and the rostral limit of *gbx2* in MHB. *fgf8* expression domain corresponds to a neuron-free neuroepithelial zone in which neurogenesis is delayed. This feature is conserved across evolution (**Vieira et al., 2010**). In zebrafish, this neuroepithelial zone had been named the intervening zone (IZ) and it has been demonstrated that, in this region, neurogenesis is inhibited by virtue of Her5 protein action (**Geling et al., 2003**). Moreover, it has been shown that *her5+* cells could contribute both to the midbrain and to the hindbrain formation until the end of the somitogenesis thereby highlighting that *her5* is the earliest marker of the MHB (**Tallafuss and Bally-Cuif, 2003**). *her5* expression characterizes some cells that will contribute to the midbrain growth until adulthood (**Chapouton et al., 2006**). In the second and third phases, the specific epigenetic program of the IsO is activated and maintained. Once established, the IsO starts to organize the adjacent territories which are the OT, anteriorly (dorsal midbrain) and the cerebellum posteriorly (metencephalon) (**Rapacioli et al., 2016**).

II.3 Morphogenesis of the optic tectum

II.3.1 The conveyor belt neurogenesis of the teleost optic tectum

Following the determination of the OT, this latter grows according to a tightly regulated process. Specifically, in teleost, OT neurogenesis is spatially and temporally regulated as it depends on how NePCs, post-mitotic cells and differentiating neurons are localized within the developing OT. In the early phase of morphogenesis, the whole tectal plate is composed of proliferating neural progenitors (*fig 37A*, zone a in red). Post-mitotic cells are generated during the first phase, and are restricted in a central zone (*fig 37B*, zone b in blue). Finally, those post-mitotic cells differentiate into neurons (*fig 37C*, zone c in yellow; **Rapacioli et al., 2016**). Once neurulation is achieved, proliferating cells become restricted to the medial, caudal and lateral margins of the structure (*fig 37E, 38C*).

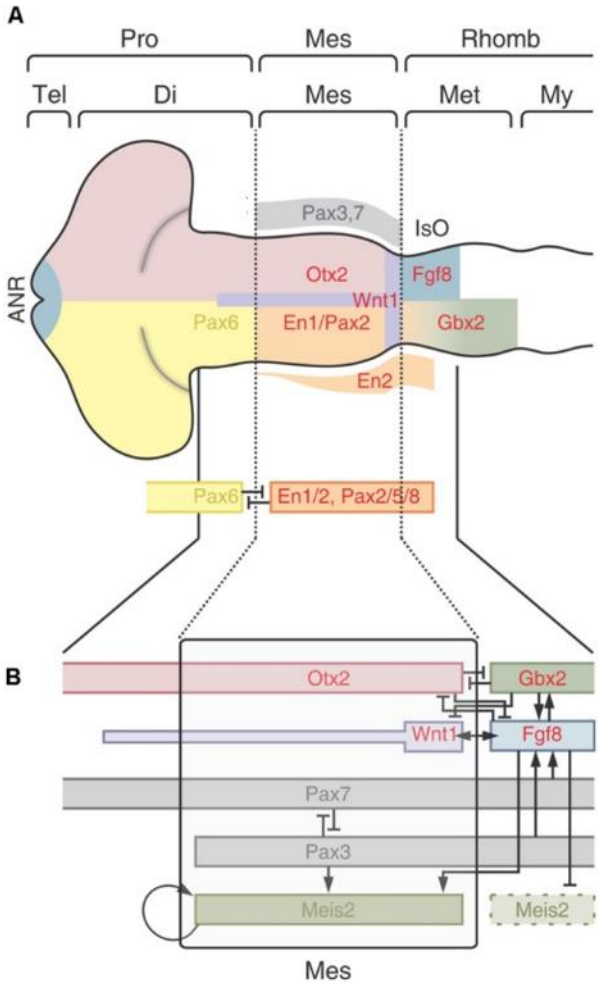

Figure 36: Establishment of the tectal territory (*Rapacioli et al., 2016*)
A. Patterning of the brain along the rostro-caudal axis. The prosencephalon (Pro), mesencephalon (Mes) and rhombencephalon (Rhomb) are divided in five territories along the antero-posterior axis. The prosencephalon is divided in two parts: the telencephalon (Tel) and the Diencephalon (Di). The rhombencephalon is composed of the metencephalon (Met) anteriorly and the Myelencephalon (My) posteriorly. Dotted lines represent the optic tectum rostral and caudal boundaries. Two signaling organizers are patterned in the developing brain: the anterior neural ridge (ANR) and the isthmic organizer (IsO). Different transcription factors are expressed along the rostro-caudal axis, defining several territories. **B.** Representation of the network of interactions between the diverse signaling pathways involved in the neural plate regionalization and patterning. A model proposes that Meis2 plays a role in the identity of the OT. The network of interactions allow the progressive restriction of Meis2 expression within the dorsal midbrain. Mutual repression between *otx* and *gbx* genes defines and refines the position of the IsO. Fgf and Wnt signaling pathways are both involved in the definition of metencephalon vs the mesencephalon. Otx2, Pax3 and Pax7 localize the tectal identity.

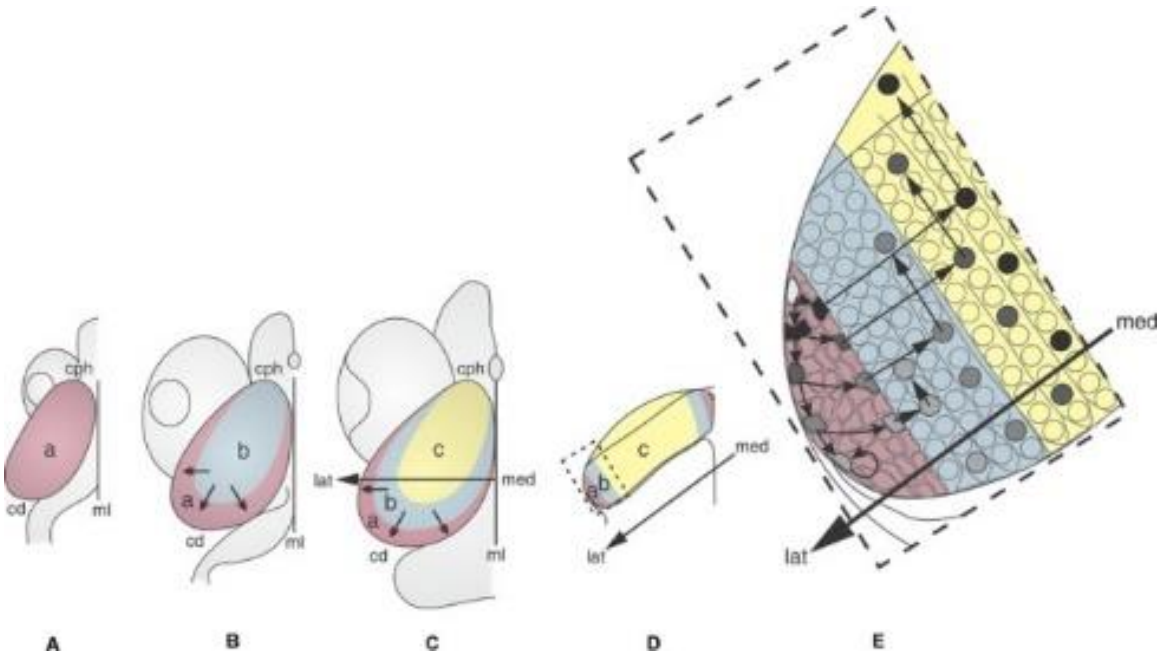

Figure 37: Dorsal representation of OT morphogenesis during medaka development. (*Rapacioli et al., 2016*)

A. Stage 22-26: The whole tectum is composed of proliferating neural progenitors (red). **B**. Stage 30: Post-mitotic cells born between the stage 22-26 and the stage 30 are now localized in the center of the OT while the proliferative cells are pushed to the periphery. **C**. Stage 32-39: Post-mitotic cells have differentiated in neural cells. The latter are localized in the center of the structure. **D**. Traverse section through the medio-lateral axis shown in (C). **E**. Higher magnification of the cell cycle and proliferation zone.

The growth of the OT will continue throughout life via the addition of columns of cells at its periphery in a zone called "the tectal marginal zone" (TMZ; **Joly et al., 2016**) and previously as peripheral midbrain layer (PML, **Recher et al., 2013**; **Than-Trong and Bally-Cuif, 2015**). Differentiated cells are localized in the most antero-central part of each lobe of the OT. Thus a gradient of differentiation is created from the periphery toward the center of the structure (**Cerveny et al., 2012; Devès and Bourrat, 2012**). This radial growth mode seems to be common in the OT of amphibians and teleosts (**Cerveny et al., 2012; Mansour-Robaey and Pinganaud, 1990; Nguyen et al., 1999; Raymond and Easter, 1983**). Moreover, this radial morphogenesis is shared between the tectum and the retina (*fig 38B*).

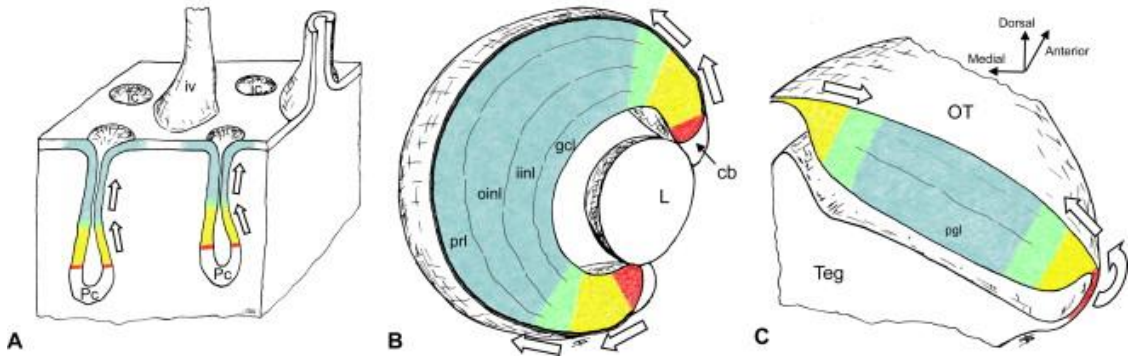

Figure 38: Schematic representation of three examples of cellular conveyor belts
A. Intestinal crypts of a mammal **B.** Retina of a teleost fish or a frog **C**. Optic tectum of a teleost fish
The progenitor zones are in red, the zone of actively dividing progenitors (or fast amplifying progenitors) are in yellow, the cell cycle exit zones are in green and the differentiated cells are in blue. The white arrow indicate the direction of the cellular conveyor belts movements.
cb: ciliary body; gcl: ganglion cell layer; iinl: inner part of the inner nuclear layer; ic: intestinal crypt (Lieberkühn crypt); iv: intestinal villosity; L: lens; oinl: outer part of the inner nuclear layer; OT: optic tectum; Pc: Paneth cells; pgz: periventricular grey layer; prl: photoreceptor layer; Teg: tegmentum (ventral midbrain)

The tectal and retinal marginal zones are homologous regions and are spatially and temporally coordinated during development (*fig 39*). Growth of the neural retina is supported by a long-lasting pool of neuroepithelial progenitors located in the ciliary marginal zone. Because cells at different differentiation states are present in an ordered manner, the OT and the retina can be considered as cellular conveyor belts (CCBs) and can be used to answer cell- cycle related questions (**Devès and Bourrat, 2012**). According to the definition "A CCB is an organ, or a part of an organ that has a balanced growth pattern so that, during development, there is no mixing between proliferative cells and cells that exit the cycle. Typically, these are polarized growing organs which bear at one pole (or extremity) a zone of actively dividing progenitors, followed by a zone of cells exiting the cycle, followed by a zone of differentiating cells" (**Devès and Bourrat, 2012**). In the OT there is a spatio-temporal correlation between the position of a cell and its differentiation state. Thus, the OT completely fulfills the definition of cellular conveyor belt. Interestingly, several examples of cellular conveyor belts have been described in vertebrate such as mammal's intestinal crypts (*fig 38A*), frog's retina or mammal's bone growth. Moreover, this mode of growth can also be found in non-vertebrates like in the growth of cnidarian tentacles or cerebral ganglion of some snails (**Devès and Bourrat, 2012**).

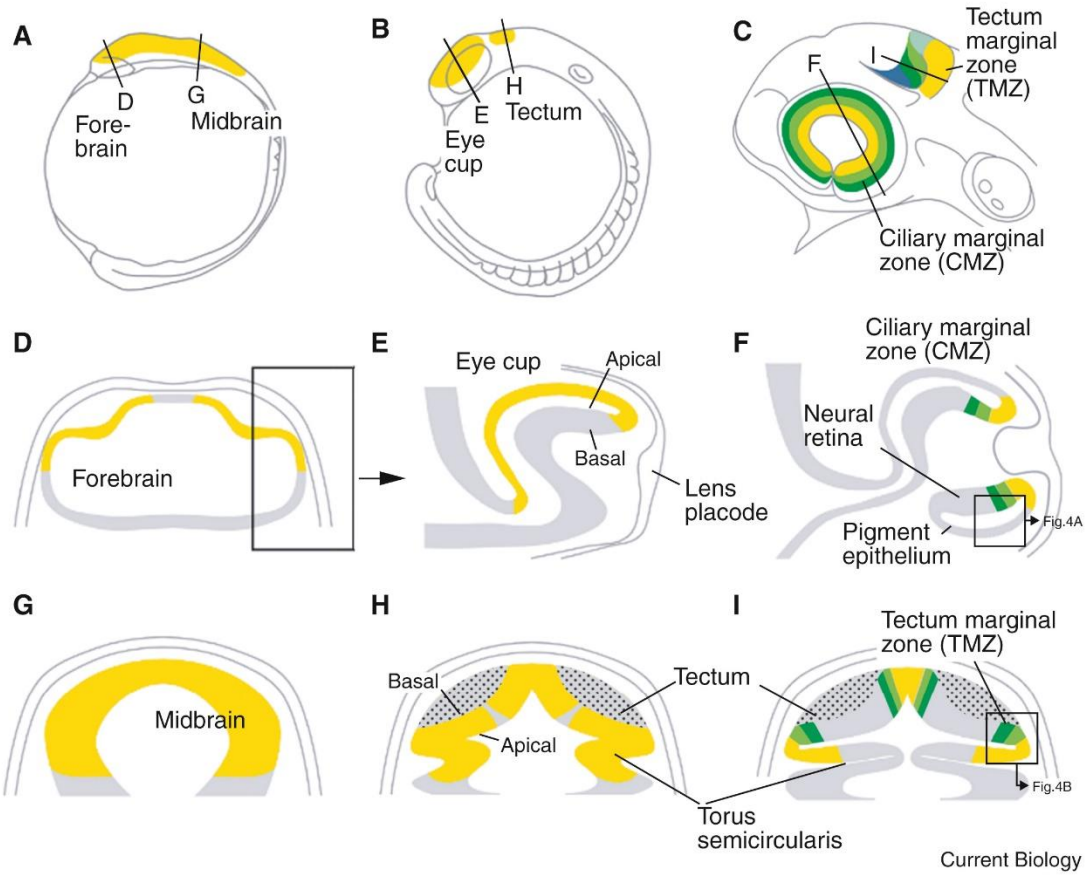

Figure 39: TMZ and CMZ are homologous structures (*Joly et al., 2016*)
Schematic lateral views (**A–C**) and cross sections (**D–I**) of zebrafish embryos. Proliferation genes (yellow) are first expressed in the entire alar part of the forebrain/midbrain, but then expression retreats to the progenitor zones of TMZ and the CMZ. **A,D,G.** At the 3-somites stage, expression of proliferation genes is in the dorsal part of the anterior neural tube. **B,E,H** At the 15-somite stage, the primordia of the tectum and retina become separated. The retina evaginates, forming the eye cup. Expression of proliferation genes becomes confined to the dorsal eye cup. In the midbrain, proliferation genes retreat towards the mid-dorsal and the ventral part of the alar plate, which invaginates to form the *torus semicircularis*. **C,F,I** At the 25-somite stage, expression of proliferation genes become restricted to the TMZ and CMZ. The CMZ forms a transitional domain between the neural retina and pigmented epithelium, encircling the lens. Similarly, the TMZ forms a narrow, hinge-like region encircling the lateral and posterior tectum.

II.3.2 Life-long growth of the optic tectum in teleost

Several studies demonstrated that, in the adult zebrafish OT, proliferating cells exist within the dorsal, caudal, and ventral margins of the periventricular gray zone (**Grandel et al., 2006; Marcus et al., 1999; Zupanc et al., 2005**). Interestingly, **Grandel and colleagues** using simple pulse BrdU experiments labeled a region that has been named PML (posterior mesencephalic lamina; *fig 40A* and *40B*). This thin layer of cells starts dorsally at the proliferative tectal margin, continues as non-proliferative lamina and becomes proliferative again as it touches the cerebellum in the medial region called the isthmus. Cells in the PML contribute to the formation of the OT at adulthood. Moreover, laterally, they contribute to the formation of the *torus semicircularis* (*TS*, *fig 40C*).

Adult tectal progenitors have been further characterized both in zebrafish (**Ito et al., 2010**) and medaka (**Alunni et al., 2010**). In both species slow-cycling label-retaining cells have been found at the caudal-most tip of the adult tecta. Interestingly, these cells express neural stem cells marker such as *sox2* and *musashi1*, but they do not express any radial glia marker such as *blbp* or *gfap*. Together these data highlight the fact that neuroepithelial cells persist until adulthood in teleosts and they actively contribute to neurogenesis in the OT. Slow cycling cells reported in these two works correspond to the dorsal most part of the PML identified by Grandel and colleagues (*fig 42***; Grandel et al., 2006**).

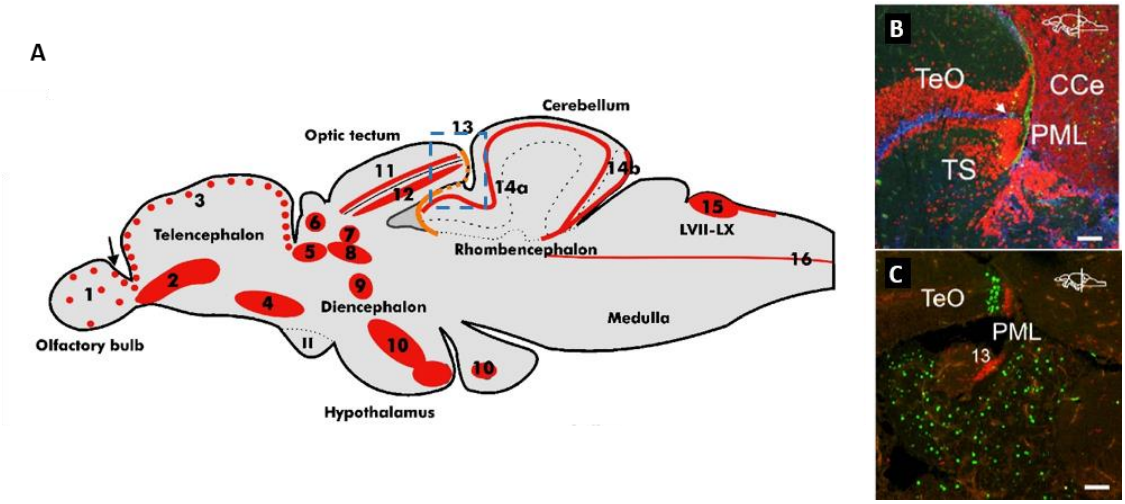

Figure 40: Proliferation cells are presents at the tectal margins in the adult zebrafish brains. Adapted from *Grandel et al., 2006*

A. Grandel and colleagues highlighted the presence of sixteen proliferation zones within the zebrafish adult brain which are depicted on the schematic drawing of a parasagittal section and indicated by numbers

B-C. The proliferation zone of the midbrain (zone 13, blue box) is particularly interesting. PML cells are actively proliferating as it can be seen in B on cross-sections of a brain of a 7-month-old adult zebrafish double stained for BrdU (green), 46 days after an initial 48 hours pulse, and PCNA (red) to visualize actively proliferating cells. Moreover, these cell contribute both to the optic tectum (TeO) and to the *torus semicircularis* (*TS*) as shown in C cross-sections of a brain of a 7-month-old adult zebrafish stained for BrdU (green) 46 days after an initial pulse, HuC/D (neuronal marker, red) and S100β (radial glia marker, blue). Indeed, adjacent to the PML, BrdU+ cells have moved into the HuC/D+ nuclear areas of the optic tectum and the *torus semicircularis* and into the S100β+ ventricular zone (arrow) of the OT.

Furthermore, it has been demonstrated, by fluorescent *in situ* hybridization (FISH) experiments, that these cells express three notch receptors (*notch1a/1b/3*; **de Oliveira-Carlos et al., 2013**). Notch signaling might thus be required to keep the progenitor niche as a neuron-free zone. It is noteworthy, that Notch signaling and, in particular, the activation of the Notch 3 receptor is required for the quiescence of the radial glial cells in the zebrafish telencephalon (**Chapouton et al., 2010; Alunni et al., 2013**). Further studies have tried to assess the characteristics of the adult proliferation zone in OT as well as their embryonic origins. Indeed, preliminary, **Chapouton et al.** showed that at adulthood, *her5*+ cells were located at the junction between the midbrain and the hindbrain barrier (**Chapouton et al.,**

2006, 2011). Those cells would contact the ventricle ventrally to the *torus semicircularis* and contribute to the neurogenesis in the tegmentum (ventral midbrain). Interestingly, **Galant et al.** identified *her5*-expressing cells as a TMZe subpopulation of NePCs. This cell population is at the origin of the adult proliferative TMZe cells and will progressively build the OT in an anterior to posterior sequence (**Galant et al., 2016**). In the post-embryonic brain, two different progenitor pools contribute to neurogenesis in zebrafish midbrain in a spatial and temporal manner. One population of radial glial cells contribute to neurogenesis in the ventral part of the midbrain (the tegmentum) and one population of neuroepithelial cells contribute to the neurogenesis in the OT (**Chapouton et al., 2011; Schmidt et al., 2013**). *her5*-positive cells are the most upstream progenitor pools giving rise to the TMZ cells. Then, transient neurogenic radial glial cells expressing *her4* act downstream in order to give rise to neurons. More precisely, *her5*-positive cells can either give rise to her4-positive radial glial cells, or, more rarely, directly participate in the tectal neurogenesis (**Galant et al., 2016**; **Dirian et al., 2014**).

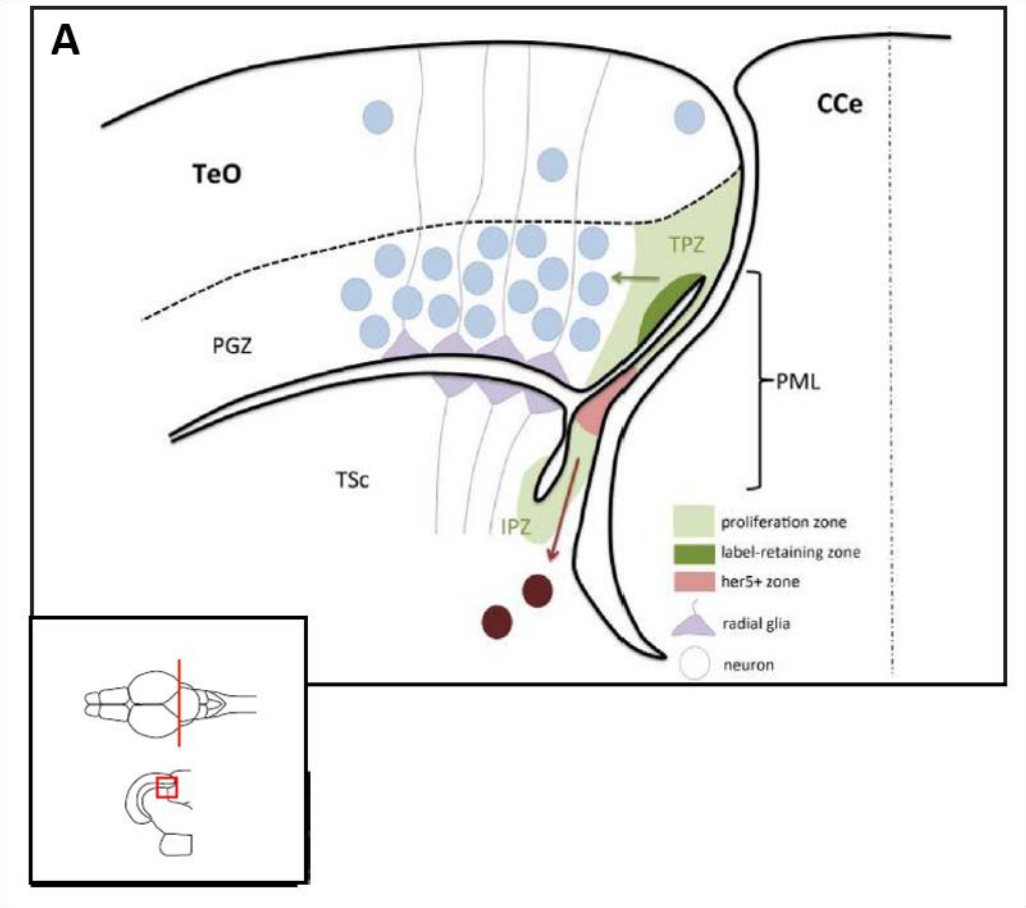
A
TeO
CCe
TPZ
PGZ
PML
TSc
IPZ
proliferation zone
label-retaining zone
her5+ zone
radial glia
neuron
B
Optic tectum
(ii)
(TPZ)
(PML)
(PML)
(i)
PCNA
her4
GFAP, GS
non-neurogenic RG
neurogenic RG
amplification pool
NE pool her5+
NE pool her5+
Adult
Embryo

Figure 41: Her5-positive cells of the TMZe express neuroepithelial characteristics and are at the origin of the adult neurogenic activity (*Galant et al., 2016*)
A. Schematic cross-section of one tectal hemisphere from an adult zebrafish showing the different cell populations. Arrows indicate the lineages, ie:green arrow: generation of PGZ neurons and radial glia from TPZ proliferating progenitors; dark red arrow: generation of tegmental neurons by her5-positive cells of the PML. **B.** Schematic representation of OT the neurogenic sequence. The arrows indicate hierarchical relationships; cell types and genes expression are color-coded. The indirect (i) and indirect (ii) neurogenic route evidences in the OT are indicated. OT territory maintain NePCs inherited from an embryonic NePCs pool expression her5 genes, and that serve both as a growth zone and as a RGCs source. RGCs are transiently neurogenic in the OT. They rapidly switch to a non-neurogenic stage (green, dark greys surrounding)
CCe:crista cerebellaris ; IPZ:isthmic proliferation zone, PGZ:periventricular grey zone ; TMZe : tectal marginal zone externe ; TeO:tectum opticum ; TPZ: tectal proliferation zone ; TSc: torus semicircularis.

II.3.3 The TMZ population is heterogeneous

In the OT and the retina, the TMZ and CMZ can be subdivided in two zones: the external edge (TMZe, CMZe) which are slowly-amplifying progenitors (SAPs), and the intermediate layer (TMZi, CMZi) which are fastly dividing progenitors cells (FAPs) (*fig 42*; **Joly et al., 2016; Recher et al., 2013**). In zebrafish, at long-pec stage (48hpf), the external layer of the TMZ (previously called the peripheral midbrain layer or PML) connects the OT to a ventral structure called *torus semicircularis*.

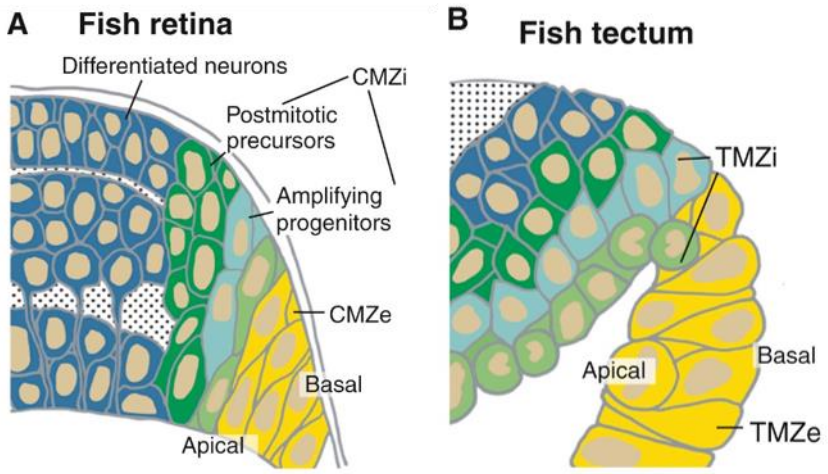

Figure 42: Conveyor belt neurogenesis in the visual system of teleosts (*Joly et al., 2016*)
Magnified view of schematic sections of the CMZ (**A**) and TMZ (**B**). Both CMZ and TMZ can be further subdivided, which is indicated by color coding. At their peripheral edge, the TMZ and CMZ contain stem cells (yellow). Away from this edge one finds the intermediate TMZ (TMZi) and intermediate CMZ (CMZi), both of which have fast amplifying progenitors (light green). Dark green indicates neural precursors exiting the cell cycle. In dark blue are differentiated neurons.

Formation of the TMZe can be divided in two steps: the initial formation before 48hpf, and the elongation of the sheet after 48hpf (*fig 43*). These slow amplifying progenitors are large polarized neuroepithelial cells. They contain larger nucleoli than more central cells of the

OT. In addition, their nuclei migrate toward the apical side of the layer to divide (INM). TMZe progenitors give rise to the fast amplifying progenitors of the TMZi that subsequently differentiate in different tectal cell types (**Recher et al., 2013**).

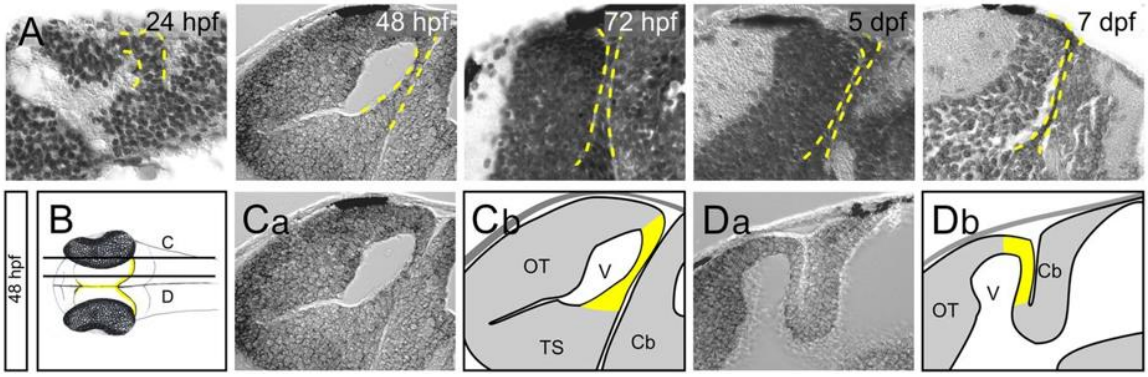

Figure 43: TMZe morphogenesis in zebrafish from 1 to 7dpf (*Recher et al., 2013*)
A. Parasagittal sections of zebrafish from 1dpf to 7 dpf. As development proceeds, the TMZe (delineated by a yellow dashed line) becomes thinner and tightly apposed to the OT. **B**. Schematic dorsal view of an embryo at 48 hpf. Planes of the sagittal sections in C (parasagittal) and D (sagittal) are indicated. The TMZe is found at the margin of the OT (yellow). **C**. On parasagittal sections, the TMZe connects the OT to the TS. **D**. On sagittal sections, the TMZe connects the OT to the cerebellum.

II.3.4 A specific molecular signature defines the proliferation zone of the OT

Interestingly, cells at similar differentiation states located either in the tectum or in the retina share common gene expression patterns. Thus, growth and cell identity in the two structures are regulated by a common subset of genetic determinants (**Cerveny et al., 2012)**. Such groups of genes, sharing the same spatiotemporal expression pattern and acting in similar biological processes are called synexpression groups (SGs). **Ramialison et al**. demonstrated that a subset of those groups shared common *cis*-regulatory modules (CRMs) allowing the synexpression of the concerned genes (**Ramialison et al., 2012**). Furthermore, some SGs of genes expressed in proliferative tissues are clustered at the same genomic locus. Most often, they are expressed ubiquitously early during development and become restricted at later stages. This is particularly observed in the developing neural tissue and CNS. For example, in the OT proliferative zone, TMZe cells display specific gene expression profiles compared to TMZi. Strikingly, TMZe cell transcriptome is enriched in transcripts previously considered as housekeeping such as genes coding for nucleotide biosynthesis and ribosome biogenesis associated factors. More precisely, TMZe-specific gene network encode for nucleolar proteins such as protein of the box C/D complex (Nop56/58, Fbl; see Chapter 1, Part II, II.3.Box C/D complex). Transcripts encoding *nop56/58* are also a signature of the fish and frog retina (**Parain et al., 2012**). Additional

RBF mRNAs are also preferentially accumulated in the TMZe like Wdr12, Pescadillo and Bop1 (**Recher et al., 2013**). Similarly, in *Oryzias latipes*, different groups of housekeeping genes involved in ribosome biogenesis or DNA replication are preferentially co-expressed in the CMZ of the retina. One hypothesis for the preferential expression of such gene family could be that slow cycling cells would function as "storage chambers" for fast subsequent cell divisions in the early embryo. On the other hand, as mentioned in detailed in the chapter 1, nucleolar proteins are involved in the control of cell proliferation (**Ruggero et al., 2003**). Therefore, specific ribosome biogenesis factors expressed in our cell population could lead to the production of specialized ribosomes playing a specific role in the regulation of the cell cycle. The accumulation of those factors within our cell population is striking and need further investigations to understand their role in the OT neural progenitor cell-cycle control. Moreover, important overlaps between the TMZe specific gene list and other progenitor datasets have been obtained independently. Interestingly, the TMZe gene-network dataset display many genes in common with a Drosophila neuroblasts-specific network or with related to human pluripotent stem cells or cancer associate gene-networks (**Recher et al., 2013**). Similarly, SGs involved in ribosome biogenesis are also specifically expressed in *Xenopus* suggesting a conservation throughout evolution.

AIM OF THE PHD

Cell identity regulation studies have been, for decades, focused on transcriptional mechanisms. However, the idea that translation regulation could be crucial for cell identify and cell fate is arising. Not only gene expression would be controlled by targeting promotor activity, but also, it would be regulated through the tuning of ribosome quality and quantity.

In the CASBAH group, we use zebrafish optic tectum (OT) as a model to study cell fate determination and cell cycle regulation. Indeed, the oriented mode of growth of the structure allows to predict the role of genes expressed in the region of interest. In particular, we are interested in understanding the molecular cues that contribute to determine progenitor cell identity. To this aim, the group has investigated the molecular signature of the neuroepithelial progenitors that support the life-long growth of the teleost OT. Interestingly, the expression of some genes appeared to be restricted to the proliferative cells, and more precisely to the neuroepithelial progenitor cells of the optic tectum. What does make these cells so different from the adjacent cells? The team first observed a preferential expression of genes coding for factors involved in nucleotide and ribosome biogenesis pathways in the progenitor population. Why are these general factors expressed in such a restricted manner? Do they play specific roles in neuroepithelial cell biology?

We made the hypothesis that, in those tectal neuroepithelial progenitor cells, specialized ribosomes and/or various pathways or ribosome biogenesis would lead to slightly different ribosomes allowing a regulation of cell cycle progression and cell identity.

In this context, I performed a functional study of Fibrillarin, the methyltransferase of the box C/D snoRNP complex to understand the relationship between ribosome biogenesis factor coding genes and cell cycle regulation. In particular I analyzed zebrafish null mutant for *fbl*. *fbl* mutants display specific midbrain defects, massive apoptosis, impaired translational activity and cell cycle progression defaults. I devoted a paper to this work which will be submitted very soon.

A transcriptomic approach has been performed by a post-doctoral researcher of the group (**Dambroise et al., 2017**). Indeed, new pathways involved in adult neural progenitor homeostasis were highlighted by this transcriptomic analysis, including new ribosome biogenesis factor genes. Quantitative analyzes of the various genes expressed in the different cell types of the OT and *in situ* hybridization screen allowed to point out the new candidate *pa2g4* which could be involved in the regulation of cell cycle. I first characterized

its expression pattern during zebrafish development. Moreover, to investigate the putative specific role of *pa2g4* in the highly proliferative population of the OT, I generated several transgenic lines necessary for the functional study of the gene.

Since my first arrival in the group, we have witnessed a veritable explosion of papers highlighting the intimate relationship between ribosome biogenesis and progenitor cell biology. Not only ribosome biogenesis contributes to the homeostasis of these cells, but it also contributes to the determination of their identity. As described in the first chapter of the introduction, ribosome biogenesis is not anymore seen as a ubiquitous process, but it is now accepted that this process can be cell, tissue or organ specific.

RESULTS

Chapter 1: Finding the molecular signature of neuroepithelial progenitors

Publication 1: Postembryonic fish brain proliferation zones exhibit neuroepithelial-type gene expression profile

In order to analyze the molecular signature of the OT neuroepithelial progenitor cell (NePC) population, a medaka transgenic line with the *wdr12* promoter sequence driving the expression of GFP in NePCs has been generated in our group. Further characterization of this line demonstrated that NePC localization is widespread in the juvenile medaka brain. We reported the molecular signature of those cells by following cell sorting of three different cell populations (*wdr12:GFP+*, *wdr12:GFP-* and *ebf3:GFP+* labelling differentiated cells) and subsequent RNA-sequencing (RNA-seq). Gene ontology analyzes demonstrated a specific molecular fingerprint in the active neuroepithelial cells. In addition, comparative analysis of lists of genes expressed in the ventricular zone of the cortex in human fetuses and in mouse embryos with the list of genes overexpressed in tectal NePCs led to the identification of neuroepithelial markers. In particular, in this context I performed WMISH for six of those genes in zebrafish embryos and juvenile brains since zebrafish and medaka have a similar tectal mode of growth. Five of them, showing highly restricted pattern of expression in NePCs, could serve as markers of a putative conserved molecular signature.

STEM CELLS®

EPIGENETICS, GENOMICS, PROTEOMICS AND METABONOMICS

Postembryonic Fish Brain Proliferation Zones Exhibit Neuroepithelial-Type Gene Expression Profile

EMILIE DAMBROISE,[a] MATTHIEU SIMION,[a] THOMAS BOURQUARD,[b] STÉPHANIE BOUFFARD,[a] BARBARA RIZZI,[c] YAN JASZCZYSZYN,[d] MICKAËL BOURGE,[e] PIERRE AFFATICATI,[c] AURÉLIE HEUZÉ,[a] JULIA JOURALET,[f] JOANNE EDOUARD,[g] SPENCER BROWN,[e] CLAUDE THERMES,[d] ANNE POUPON,[b] ERIC REITER,[b] FRÉDÉRIC SOHM,[g] FRANCK BOURRAT,[a] JEAN-STÉPHANE JOLY[a]

[a]INRA CASBAH Group, Neuro-PSI, UMR 9197, CNRS, Gif-sur-Yvette, France; [b]BIOS UMR 7247, INRA PRC, Nouzilly, France; [c]Tefor Core Facility, TEFOR Infrastructure, Neuro-PSI, CNRS, Gif-sur-Yvette, France; [d]Plateforme de séquençage haut débit, [e]Plateforme de cytométrie, I2BC, and [f]Plateforme BM-Gif, Imagif, UMR 9198, CNRS, Gif-sur-Yvette, France; [g]UMS AMAGEN CNRS, INRA, Université Paris-Saclay, Gif-sur-Yvette, France

E.D. and M.S. contributed equally to this article.

Correspondence: Joly Jean-Stéphane, PhD, DR1, INRA CASBAH Group, Neuro PSI, UMR 9197, CNRS, 1 av de la Terrasse, 91198 Gif-sur-Yvette, France. Telephone: 33-1-69-82-41-38; Fax: 33-1-69-82-34-47; e-mail: joly@inaf.cnrs-gif.fr; or Dambroise Emilie, Ph.D., U1163 Institut Imagine, 24bd Montparnasse, 75015 Paris, France. Telephone: 33-1-42-75-42-50; Fax: 33-1-42-75-42-24, e-mail: emilie.dambroise@institutimagine.org

Received April 27, 2016; accepted for publication December 20, 2016; first published online in STEM CELLS *EXPRESS* February 9, 2017.

1066-5099/2017/$30.00/0

http://dx.doi.org/10.1002/stem.2588

This article was published online on 14 March 2017. An addition was made to the caption to Figure 2. This notice is included in the online and print versions to indicate that both have been corrected 12 April 2017.

Key Words. Neuroepithelial cell • DNA repair • Cell cycle • RNA seq • Optic tectum • Microcephaly

ABSTRACT

In mammals, neuroepithelial cells play an essential role in embryonic neurogenesis, whereas glial stem cells are the principal source of neurons at postembryonic stages. By contrast, neuroepithelial-like stem/progenitor (NE) cells have been shown to be present throughout life in teleosts. We used three-dimensional (3D) reconstructions of cleared transgenic *wdr12*:GFP medaka brains to demonstrate that this cell type is widespread in juvenile and to identify new regions containing NE cells. We established the gene expression profile of optic tectum (OT) NE cells by cell sorting followed by RNA-seq. Our results demonstrate that most OT NE cells are indeed active stem cells and that some of them exhibit long G2 phases. We identified several novel pathways (e.g., DNA repair pathways) potentially involved in NE cell homeostasis. In situ hybridization studies showed that all NE populations in the postembryonic medaka brain have a similar molecular signature. Our findings highlight the importance of NE progenitors in medaka and improve our understanding of NE-cell biology. These cells are potentially useful not only for neural stem cell studies but also for improving the characterization of neurodevelopmental diseases, such as microcephaly. STEM CELLS *2017; 00:000–000*

SIGNIFICANCE STATEMENT

This study provides an integrated view of neuroepithelial-like cells in the adult fish brain. In the field, our results challenge the widely accepted view that adult neurogenesis relies on radial glia and will fuel discussions on the nature of extensive cell proliferation observed in these animals. We adapted state-of-the-art clearing protocol which should be of interest for a large readership. Indeed, published protocols remain scarce, although they open tremendous perspectives in phenotyping. As never reported before in vertebrates, we show cells paused in G2, thereby pointing to novel pathways of quiescence control in stem cells, including for example the DNA repair machinery.

INTRODUCTION

Adult neurogenesis has long been known to occur in vertebrates [1], but interest in this process has recently increased. We need to identify the various cell types with stem properties in the adult brain, to be able to evaluate the heterogeneity of neurogenesis between niches and species. In the central nervous system (CNS) of amniotes, postembryonic stem/progenitor cell populations generally have a glial phenotype, either radial glial or astrocytic in nature [2]. In mammals, adult neural stem cells (aNSCs) are largely restricted to the telencephalon. They are derived from embryonic radial glial cells [3–5] and do not give rise directly to neurons; instead, they first generate intermediate progenitor cells [6]. The molecular fingerprints of these cells reveal their heterogeneity, in terms of active cycling or quiescence [7], and the combination of markers expressed [8–11]. Studies of aNSCS in organisms other than mammals have focused principally on the zebrafish telencephalon, in which radial glial neural stem cells and intermediate progenitors have been characterized [12–15]. However, the picture of adult neurogenesis based entirely on glial cells that has emerged from these studies needs to be refined, as it does not capture the complexity of vertebrate aNSCs.

Recent studies in mammals have shown that some ependymal cells have a potential "neural stem cell" role. Indeed, a subpopulation of ependymal cells has been shown to have

stem cell activity in mice [16], and administration of vascular endothelial growth factor can reactivate quiescent ependymal cells in non-neurogenic regions of the adult brain [17].

The situation in teleosts is far more complex. The adult teleost brain is a site of continuous, intense proliferative activity that is by no means restricted to the telencephalon [18, 19]. In some of the zones of proliferation in the teleost brain, the aNSCs have neuroepithelial, rather than radial glial, characteristics. In vertebrates, the neural tube is initially made up of neuroepithelial cells, which divide symmetrically to expand the neural progenitor pool. The resulting neural progenitors subsequently give rise to the neurons, glia, and ependymal cells collectively forming the CNS [3, 6, 20]. Several studies have demonstrated that some of proliferative aNSC populations are indeed neuroepithelial-like stem/progenitor (NE) cells rather than radial glial cells. This is particularly true in the optic tectum (OT) and cerebellum, which contain large populations of aNSCs [21–24]. Moreover, Dirian et al. [25] have identified a population of adult NE cells maintained from early developmental to postembryonic stages in the zebrafish lateral pallium.

All these results highlight the importance of nonradial glial stem cells in adult neurogenesis, at least in teleosts. However, the overall distribution, cell cycle properties, and molecular hallmarks of NE cells in these animals have been little studied at postembryonic stages. We focused on these aspects in this study.

Using the promoter of *wdr12*, which encodes a ribosome biogenesis factor, we established a fluorescent reporter line of NE cell in the medaka [26, 27]. Immunohistochemistry (IHC) on sections and 3D reconstructions of cleared brains show that NE cells populate most of the zones of proliferation in the postembryonic medaka brain.

We performed cell cycle and molecular studies on NE cells from the OT, the largest structure of the CNS, which accounts for a substantial proportion of the mitotic cells in the adult brain and the morphological features of which are well-characterized [21, 28].

We analyzed the transcriptome of OT *wdr12*:GFP$^+$ cells, to characterize their molecular profile, and to highlight pathways potentially involved in the homeostasis of NE cells. OT NE cells display a broad range of levels of proliferative activity (from slow cycling to rapid division), and at least some of the slowly dividing cells are in the G2 phase and strongly express DNA repair genes. Whole-mount in situ hybridization (WMISH) experiments showed that OT NE cells have several molecular features in common with NE populations from elsewhere in the brain. We then performed comparative analyses to identify neuroepithelial markers common to several animal species. We present here a detailed molecular and cellular description of an important stem/progenitor cell population from medaka brain. Our findings provide new insight into neural stem cell biology.

Materials and Methods

Animals and Transgenic Lines

Medaka lines were maintained at 27°C in our facility. Embryos were kept at 28°C and staged as described by Iwamatsu [29]. We used 1-month-old fish for this study. All procedures were performed in accordance with European Union Directive 2011/63/EU and were approved by the local ethics committee (no. 59 CEEA)

Immunohistochemistry and EdU Labeling

IHC was performed as previously described [21]; see the Supporting Information for a list of the antibodies used. For 5-Ethynyl-2'-deoxyuridine (EdU) experiments, fish were intraperitoneally injected with 10 mM EdU (1 μl/15 mg) and killed by over-anesthesia 1 hour later. Their brains were dissected out and treated as previously described for IHC. EdU was detected with the EdU Click-iT Plus EdU Alexa Fluor 594 Imaging Kit (Life Technologies, Rockville, MD, http://www.lifetech.com), according to the manufacturer's protocol.

Cell Dissociation, FACS, Sample Preparation, and RNA Sequencing

We followed a slightly modified version of a published protocol [30]. Cells were sorted on a MoFlo Astrios (Beckman Coulter) cytometer. RNA was isolated with the PicoPure Isolation kit, according to the manufacturer's protocol (Life Technologies, Rockville, MD, http://www.lifetech.com). Three *wdr12*:GFP$^+$, two *wdr12*:GFP$^-$, and three *ebf3*:GFP$^+$ samples were used for library construction (Epicentre, Madison, WI, http://www.epibio.com). Library construction was performed with the TotalScript RNA-Seq Kit, according to the manufacturer's protocol. Libraries were sequenced on an Illumina Hiseq 1000 instrument, with a TruSeq SR Cluster Kit v3-cBot-HS (Illumina, San Diego, CA, https://www.illumina.com) and TruSeq SBS Kit v3-HS—50 cycles (Illumina), and a 50 bp-single read protocol. See the Supporting Information for additional details.

Analysis of RNA-Seq Datasets

Data were demultiplexed with CASAVA software (CASAVA-1.8.2). Data quality was checked with FastQC 0.10.1. Reads were mapped to the genome of *Oryzias latipes* oryLat2 (downloaded from UCSC), with TopHat2. RNA-seq and gene expression profiles were analyzed with dedicated software (Supporting Information). The RNA-Seq data have been submitted to NCBI Gene Expression Omnibus (accession number GSE80497). Functional clustering was performed with DAVID and the Gene Ontology (GO) database. Each cluster was named as a function of the main biological process detected. Ingenuity® Pathway Analysis (IPA®) software (Ingenuity Systems) was used to assess the involvement of differentially expressed genes from canonical pathways and/or networks. A comparative analysis was performed, by comparing the list of genes upregulated in *wdr12*:GFP$^+$ cells relative to the control with the lists of genes known to be overexpressed in the ventricular zones of the cortex in mice and humans. Genes were considered to be differentially expressed if an adjusted p value $<.05$ was obtained [31].

Whole-Mount in Situ Hybridization. Brains were dissected out and processed as previously described [32], but with the proteinase K treatment (10 μg/ml) reduced to 15 minutes. Antisense riboprobes were diluted in a hybridization buffer containing 5% dextran. For histological analysis, 8-μm-thick paraffin sections were prepared as previously described [33]. For Digoxigenin (DIG)-riboprobes, see Supporting Information.

Whole-Brain Imaging Procedure

Samples were fixed in 4% formaldehyde, infused with a hydrogel monomer solution (4% acrylamide and 0.005% bis-acrylamide) for 2 days and polymerized for 3 hours. They were cleared by incubation in 8% SDS for 1 week. They were then incubated with antibodies in a solution containing 10% Dimethyl sulfoxide (DMSO), 2% Normal Goat Serum (NGS), and 0.05% sodium azide, for 2 weeks at room temperature. Samples were mounted in a fructose-based high-refractive index solution and imaged with a Leica TCS SP8 two-photon microscope equipped with a CLARITY specific objective. See Supporitng Information for more details.

Results

Isolation of a Driver Active in OT NE Cells

In teleosts, the OT grows continuously through the addition of columns of cells at its periphery in a "conveyor belt" process [21, 28, 34]. A population of NE cells has been identified at the OT margin [21], in a zone referred to hereafter as the external tectal marginal zone (TMZe) [35]. These cells form a ribbon of proliferative cells linking the OT to adjacent regions and with morphological features similar to those of an ependymal sheet. Once the progeny of these NE cells reach the tip of the OT periventricular grey zone, they start to proliferate more rapidly, generating the round transit-amplifying progenitors (TAPs) that form the internal TMZ (TMZi) [22, 27] (Fig. 1A).

In a previous study [27], we found that ribosome biogenesis gene transcripts were abundant in OT NE cells (Fig. 1B). We noticed that two of these genes, *wdr12* and *nop58*, were near-neighbors in the medaka genome, being separated by only 3 kb. We screened for regulatory elements at this locus (Fig. 1C) and isolated a putative driver containing the *wdr12* promoter and 2.2 kb of upstream sequences. This element drove identical patterns of green fluorescent protein (GFP) expression in the CNS at stage 37 in five independent lines (not shown). We established a *wdr12*:GFP line from one of the founders.

GFP was strongly expressed in the TMZe, but some fluorescence was also observed in the TMZi. We quantified relative fluorescence levels and the mean diameters of the nuclei in the two regions. We found that the TMZe, which houses cells with larger nuclei, had fluorescence levels 1.6 times higher than those of the TMZi (Supporting Information Fig. S1). Thus, GFP was strongly expressed in NE cells, and the GFP was inherited by subsequent amplifying cells and/or differentiating neurons. Colabeling with the cell proliferation marker Proliferating Cell Nuclear Antigen (PCNA) (96.3% $\pm$ 0.6 of GFP$^+$ cells) and the pluripotency-associated marker SRY (Sex-Determining Region Y)-Box 2 (SOX2) (82.1% $\pm$ 5.7 of GFP$^+$ cells) confirmed that most OT GFP$^+$ cells were stem/progenitor cells (Fig. 1D, 1E). These cells also displayed apical labeling with the cell polarity marker atypical Proteine kinase C (aPKC) (Fig. 1F). By contrast, GFP$^+$ cells in the OT displayed only low levels of colabeling with the neuronal marker HuC/D (7.2% $\pm$ 0.5 of GFP$^+$ cells) and with the marker of young migrating neurons polysialylated neuronal cell adhesion molecule (PSA-NCAM) (Fig. 1; Supporting Information Fig. S1). GFP$^+$ cells displayed no labeling for the glial markers glial fibrillary acidic protein (GFAP), glutamine synthetase (GS), and S100. Similar results were obtained with adult fish (not shown). These results identify postembryonic tectal GFP$^+$ cells in the *wdr12*:GFP medaka line as bona fide NE cells [36] but they also highlight the heterogeneity of this cell population.

GFP$^+$ Cells Are Found in Most Proliferation Zones of the Juvenile Brain

We then used the *wdr12*:GFP line to map all the populations of GFP$^+$ cells in the medaka juvenile brain, with an improved protocol for whole-mount immunostaining and a modified version of the "CLARITY" protocol [37]. One-month-old fish were used because they have all the features of adult fish [38], and the size of their brains facilitates the clearing procedure. We validated this new clearing protocol with the PCNA antibody (Supporting Information Fig. S2).

Cleared *wdr12*:GFP brains were counterstained with DiI, for visualization of the distribution of GFP$^+$ cells at single-cell resolution. The following labeling pattern was obtained (from anterior to posterior): in the pallium, GFP$^+$ cells were found in the dorsomedial ventricular zone (VZ), the pallial posterolateral edge, and the ventral part of the subpallium (Figs. 2A1–A3, 3A–3C). The VZ of the preoptic area (Fig. 2A11) was highly fluorescent, as was the ventral habenula (Fig. 2A7) and the adjacent VZ of the dorsal thalamus (Fig. 2A10). Other diencephalic VZs were labeled: the VZ of the ventromedial nucleus in the prethalamus (Fig. 2A10) and the VZ of the ventral, dorsal, and caudal parts of the hypothalamus (Fig. 2A12). In the posterior tuberculum, GFP$^+$ cells were present only in the tuberal nuclei (Fig. 2A5). The TMZe and the cerebellar proliferation zones were intensely labeled (Fig. 2A8, 2A9). In the caudal rhombencephalon, the VZs of the vagal lobe and the solitary tract nucleus contained numerous GFP$^+$ cells (Fig. 2A6). A few of the labeled cells in the rhombencephalon were differentiated neurons displaying complex dendritic arborization.

Overall, this pattern of GFP expression in VZs closely matched the map of proliferation zones. We assessed the correlation between GFP and cell proliferation, by 3D reconstructions of the whole brain for analysis of the distributions of both GFP and PCNA labeling (Fig. 2B; Supporting Information Movie1). GFP was detected in all zones of proliferation (compare Fig. 2B, 2C), and the correlation between GFP and PCNA labeling was strong (Pearson's coefficient = 0.8 and Manders overlap coefficient = 0.86).

Qualitative assessments of the correlation between PCNA and GFP expression during embryonic development yielded similar conclusions. GFP was expressed in the same areas as PCNA, at all stages considered: from the early proliferating neuroepithelium to restricted zones of proliferation at later stages (Supporting Information Fig. S3A). We detected GFP$^+$ cells in almost all germinal areas of the juvenile brain, the paraventricular organ being the only notable exception.

Detection of New Regions Containing Postembryonic NE Cells in the wdr12:GFP Line

We studied the VZ of the anterior thalamic nucleus and the margin of the caudal cerebellar lobe, two zones of proliferation that have never, to our knowledge, been investigated in detail. The GFP$^+$ cells in these regions had the same antigenic profile as their OT counterparts: PCNA$^+$, SOX2$^+$, polarized (aPKC$^+$ and ZO-1$^+$), and negative for markers of radial glial

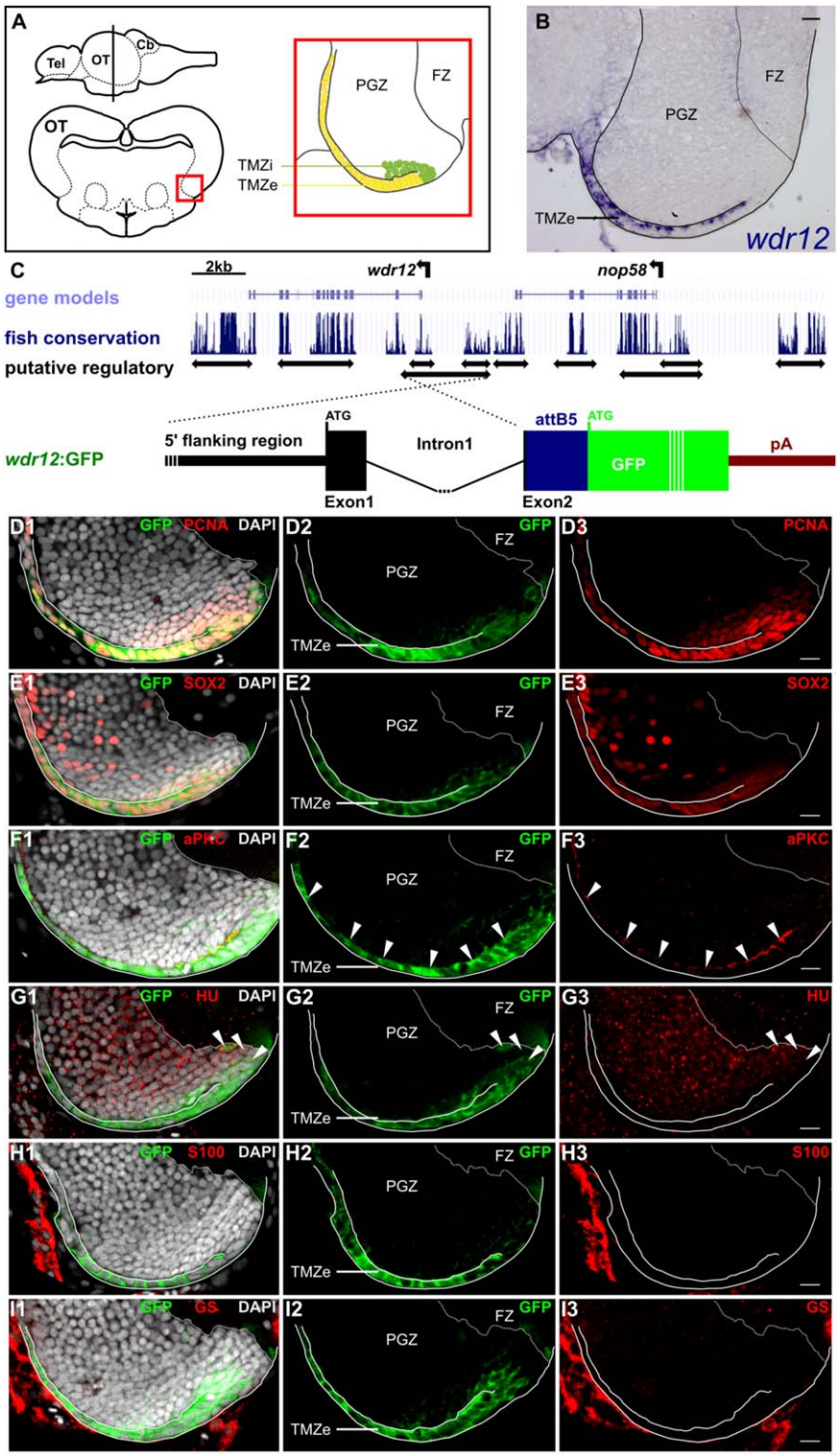

Figure 1. Isolation of a driver active in the neuroepithelial (NE) cells of the OT. **(A)**: Diagram of the OT proliferation zone, with the NE cells in yellow (TMZe) and the transitory amplifying progenitors in green (TMZi). **(B)**: In situ hybridization for *wdr12* on cross-section in 1-month-old medaka brain. **(C)**: The Medaka *wdr12/nop58* locus (from UCSC genome browser (chr2:21879500-21902550, NIG/UT MEDAKA1/oryLat2 Assembly)). Ten putative regulatory elements conserved in fish were assayed (top panel). The *wdr12:gfp* construct contains 2.205 kb upstream from the ORF, 41 bp of exon 1, 811 bp of intron 1, and 30 bp of exon 2 (bottom panel). This construct can produce either GFP alone or a fusion protein containing the first 14 amino acids of wdr12, depending on where translation starts (GFP contains its own Kozac sequence). (D–I) Comparison of the expression of *wdr12:*GFP with that of markers of cell proliferation (PCNA, D1–D3), progenitors (SOX2, E1–E3), cell polarity (aPKC, F1–F3), neurons (Hu, G1–G3), and glial cells (S100, H1–H3; GS, I1–I3) on cross-sections of juvenile medaka (1–2 months old) brain. (D-I): Panel 1 depicts the green channel (GFP) + red channel (marker) + gray channel (DAPI), panel 2 depicts the green channel only and panel 3 the red channel only. White straight line indicates the position of the ventricle. White arrowheads identify GFP^+ cells also labeled for aPKC (F), Hu (G). Scale bar = 100 μm (B); 10 μm (D-I). See Supporting Information Table S1 for anatomical structure abbreviations. Abbreviations: aPKC, atypical Protein Kinase C; Cb, cerebellum; DAPI, 4',6-Diamidine-2'-phenylindole dihydrochloride; GFP, green fluorescent protein; GS, glutamine synthetase; FZ, fibrous zone; OT, optic tectum; PCNA, Proliferating Cell Nuclear Antigen (PCNA); PGZ, periventricular grey zone; SOX2, SRY (Sex-Determining Region Y)-Box 2; Tel, telencephalon; TMZe, external tectal marginal zone; TMZi, internal tectal marginal zone.

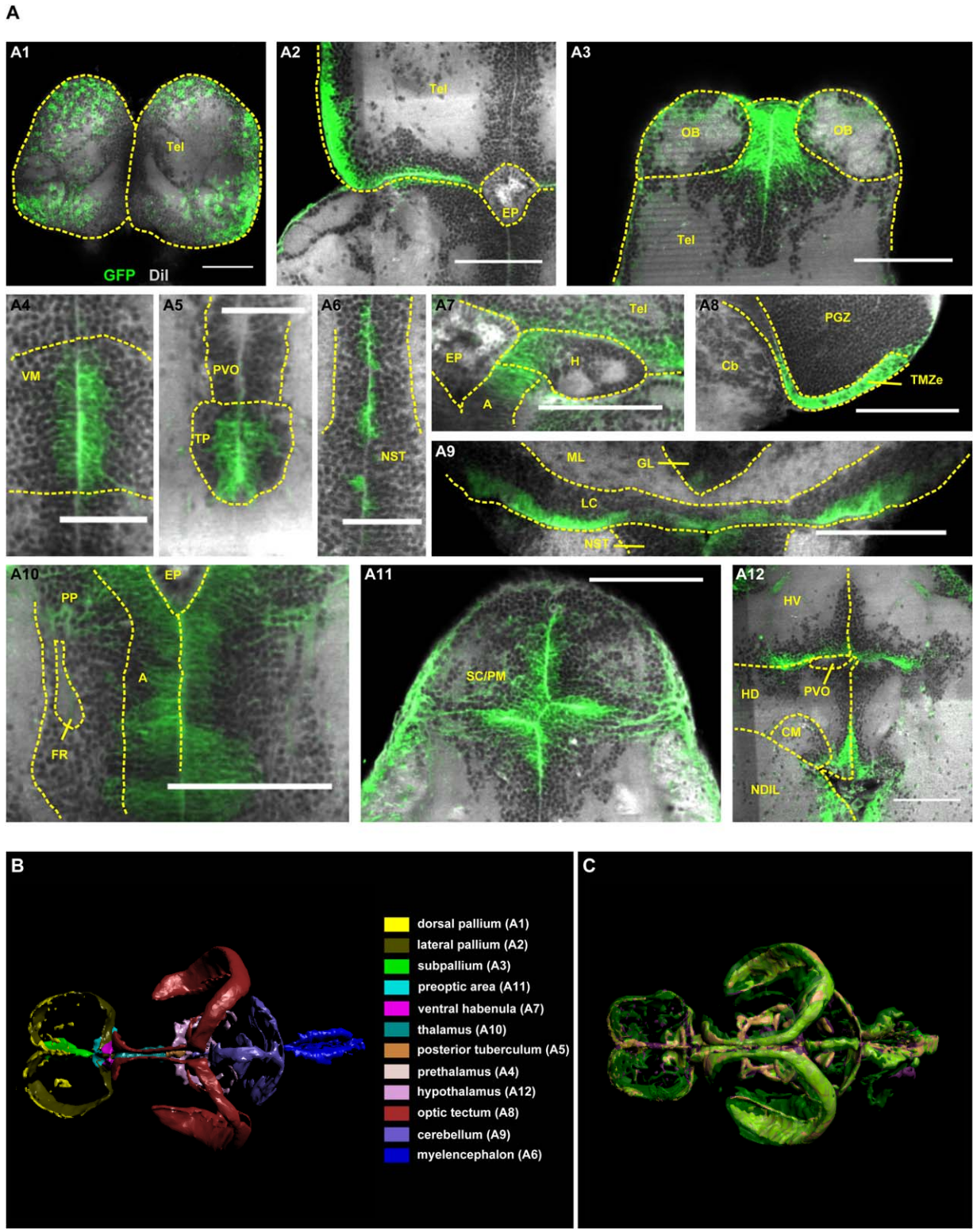

Figure 2. Wdr12:GFP^{+} cells are found in most zones of proliferation in the juvenile brain. **(A)**: Horizontal sections of a cleared 1-month-old *wdr12*:GFP fish brain stained as indicated in (A1). Twelve ventricular zones (VZs) harbor GFP^{+} cells: the dorsomedial pallium (A1: this panel is a maximal projection of the expression observed at the surface of the pallium), the posterolateral edge of the pallium (A2), the subpallium (A3), the preoptic area (A11), the ventral habenula (A7), the dorsal thalamus (A10), the posterior tuberculum (A5), the ventromedial thalamic nucleus (A4), the ventral, dorsal, and caudal hypothalamus (A12), the TMZe (A8), the tip of the cerebellar caudal lobe (A9), and the solitary tract (A6). **(B)**: Volume rendering of a 1-month-old medaka brain cleared and stained for PCNA. The 12 zones of proliferation are segmented in different colors. **(C)**: Volume rendering of a 1-month-old *wdr12*:GFP fish brain cleared and stained for GFP (volume in green) and PCNA (volume in violet). The yellow volume represents the overlap between the two types of staining. Scale bar = 100 μm (A1–A3, A7–A12); 50 μm (A4–A6). See Supporting Information Table S1 for anatomical structure abbreviations. Abbreviations: A, anterior nucleus of diencephalon; Cb, cerebellum; CM, corpus mamillare; EP, epiphysis; FR, fasciculus retroflexus; GFP, green fluorescent protein; GL, cerebellar granule cell layer; H, habenula; HD, dorsal periventricular hypothalamus; HV, ventral periventricular hypothalamus; LC, cerebellar caudal lobe; ML, cerebellar molecular layer; NDIL, diffuse nucleus of inferior lobe; NST, nucleus of the solitary tract; OB, olfactory bulb; PGZ, periventricular grey zone; PM, magnocellular preoptic nucleus; PP, periventricular pretectal nucleus; PVO, paraventricular organ; SC, suprachiasmatic nucleus; Tel, telencephalon; TP, posterior tuberal nucleus; TMZe, external tectal marginal zone; VM, ventromedial nucleus. [To view the 3D model of Figure 2 please download the PDF version of this article available at wileyonlinelibrary.com]

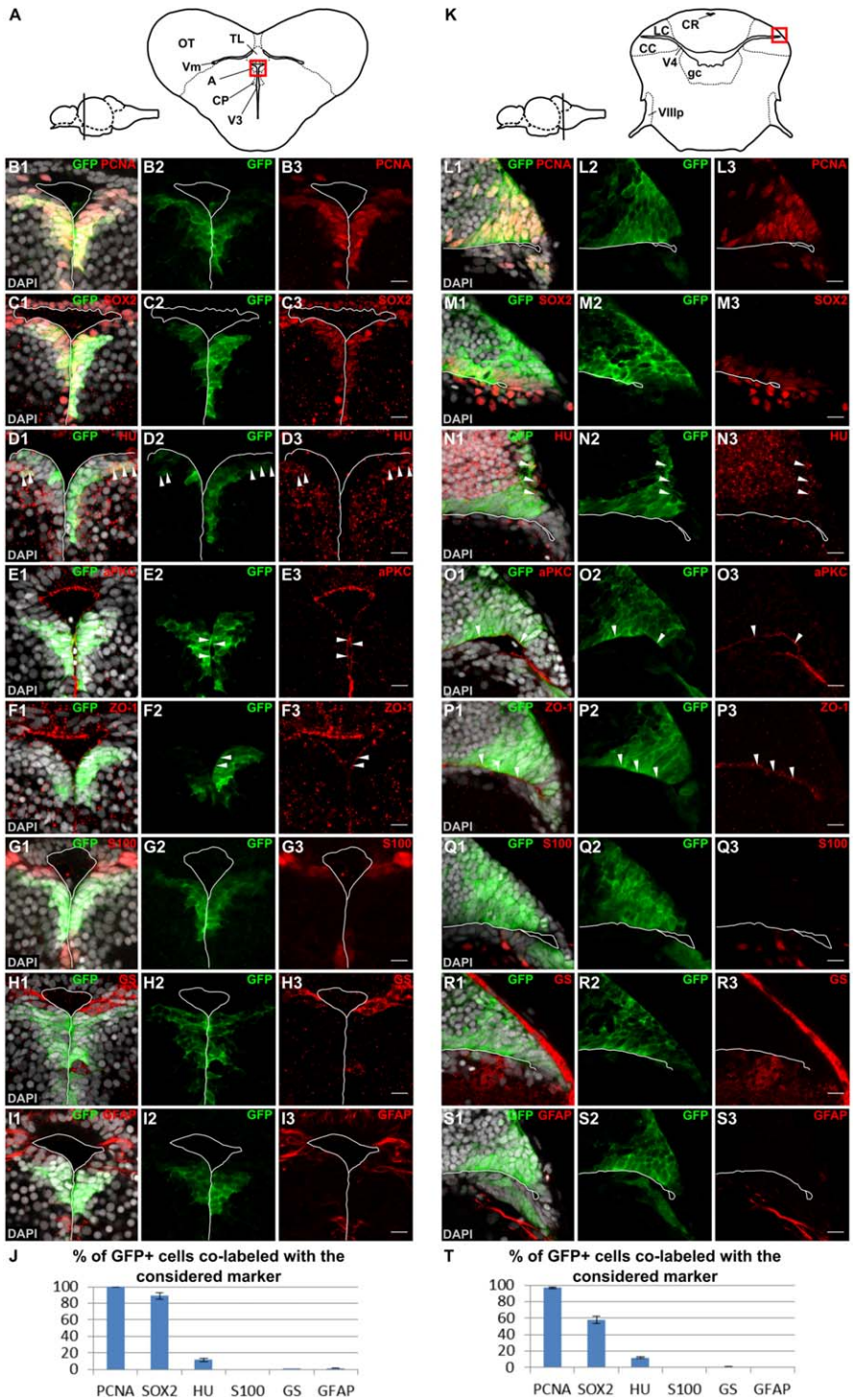

Figure 3. Identification of new regions housing postembryonic neuroepithelial (NE) cells in the *wdr12*:GFP line. **(A–J)**: Characterization of the *wdr12*:GFP^{+} cell population in the ventricular zone (VZ) of the anterior nucleus of the diencephalon (red square in the scheme in A). **(B–I)**: Comparison of the expression of *wdr12*:GFP with that of markers of cell proliferation (PCNA, B1–B3), progenitors (SOX2, C1–C3), neurons (Hu, D1–D3), cell polarity (aPKC, E1–E3; ZO-1, F1–F3), and glial cells (S100, G1–G3; GS, H1–H3; GFAP, I1–I3) on cross-sections of juvenile medaka (1–2 months old) brain. (J): Quantification of colabeling for GFP and PCNA ($n = 520$ cells), SOX2 ($n = 270$ cells), Hu ($n = 359$ cells), S100 ($n = 301$ cells), GS ($n = 605$ cells), or GFAP ($n = 372$ cells). **(K–T)**: Characterization of the *wdr12*:GFP^{+} cell population in the VZ of the caudal lobe of the cerebellum (red square in the scheme in K). **(L–S)**: Comparison of the expression of *wdr12*:GFP with that of markers of cell proliferation (PCNA, L1–L3), progenitors (SOX2, M1–M3), neurons (Hu, N1–N3), cell polarity (aPKC, O1–O3; ZO-1, P1–P3), and glial cells (S100, Q1–Q3; GS, R1–R3; GFAP, S1–S3) on cross-sections of juvenile medaka (1–2 months old) brain. **(T)**: Quantification of the colabeling of GFP and PCNA ($n = 682$ cells), SOX2 ($n = 515$ cells), Hu ($n = 1114$ cells), S100 ($n = 253$ cells), GS ($n = 742$ cells), or GFAP ($n = 1{,}334$ cells). (B–I) and (L–S): Panel 1 depicts the green channel (GFP) + red channel (marker) + gray channel (DAPI), panel 2 depicts the green channel only and panel 3 the red channel only. White straight line indicates the position of the ventricle. White arrowheads identify GFP^{+} cells also labeled for Hu (D, N), aPKC (E, O), or ZO-1 (F, P). Scale bar = 10 μm (B–I; L–S) (panel 3). See Supporting Information Table S1 for anatomical structure abbreviations. Abbreviations: aPKC, atypical Protein Kinase C; A, anterior nucleus of diencephalon; CC, crista cerebellaris; CP, central posterior nucleus; CR, cerebellar recessus; DAPI, 4′,6-Diamidine-2′-phenylindole dihydrochloride; gc, griseum central; GFP, green fluorescent protein; GFAP, glial fibrillary acidic protein; GS, glutamine synthetase; LC, cerebellar caudal lobe; OT, optic tectum; PCNA, Proliferating Cell Nuclear Antigen; TL, torus longitudinalis; VIIIp, posterior vestibular nerve; Vm, mesencephalic ventricle; V3, third ventricle; V4, fourth ventricle; SOX2, SRY (Sex-Determining Region Y)-Box 2; ZO-1, Zonula occludens-1.

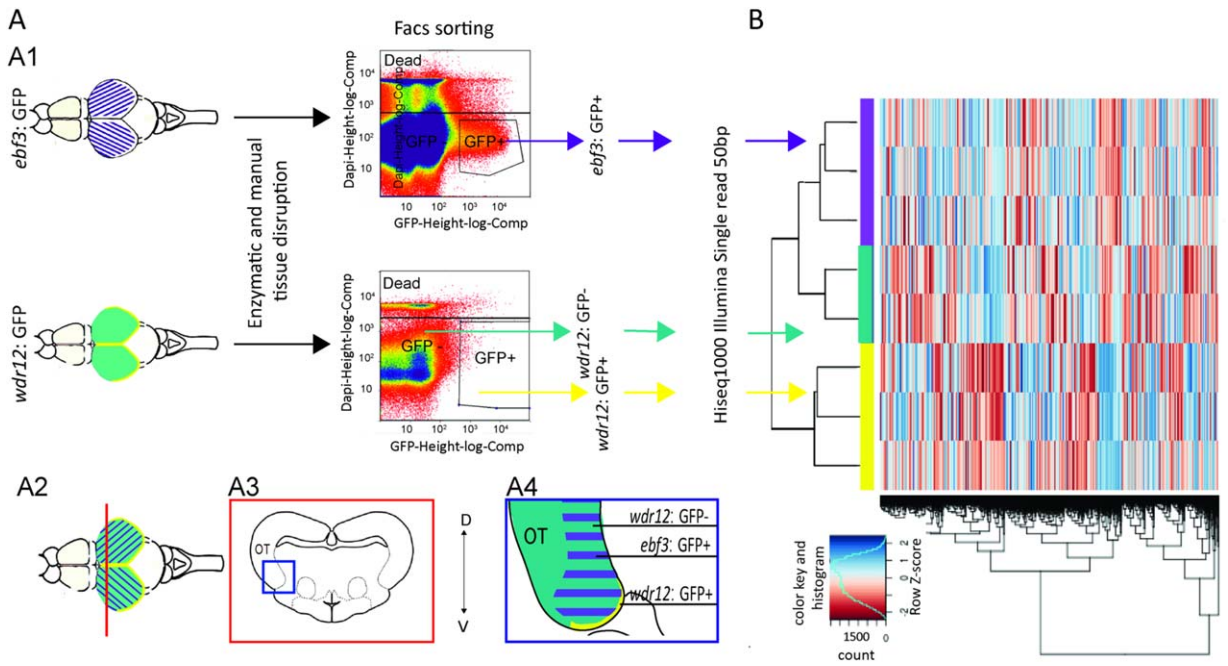

Figure 4. Cell sorting and RNA-seq on OT *wdr12*:GFP$^+$ cells. **(A1)**: Experimental design: 30 OT were dissected from 1-month-old *wdr12*: GFP and *ebf3*:GFP fish and disrupted. We then isolated *wdr12*:GFP$^+$, *wdr12*:GFP$^-$ cells, and *ebf3*:GFP$^+$ cells by cell sorting (FACS). The sorted cells were subjected to Ilumina High-Seq 1000 sequencing. **(A2)**: Dorsal view of adult medaka brain. **(A3)**: Cross-section diagram. **(A4)**: Localization of *wdr12*:GFP$^+$, *wdr12*:GFP$^-$ cells, and *ebf3*:GFP$^+$ cells in the ventral OT. **(B)**: Heat-map representation of expression levels for genes differentially expressed in *wdr12*:GFP$^+$, *wdr12*:GFP$^-$, and *ebf3*:GFP$^+$ cell populations. Red/blue indicates higher/lower levels of expression, as indicated by the scale bar. See Supporting Information Table S1 for anatomical structure abbreviations. Abbreviations: FACS, fluorescence activated cell sorting; GFP, green fluorescent protein; OT, optic tectum.

cells and neurons (GFAP$^-$, GS$^-$, Hu$^-$) (Fig. 3). The proportion of GFP$^+$ cells also positive for SOX2$^+$ was smaller in the cerebellum than in the OT and diencephalon. We then investigated the dorsomedial pallium, as its VZ contained many small clusters of GFP$^+$ cells (Supporting Information Fig. S3B), and this part of the brain is known to be rich in radial glial cells in zebrafish. Overall, 6.8% $\pm$ 2.3% of the GFP$^+$ cells reacted with antibodies against GFAP. A similar proportion of GFP$^+$ cells were found to be immunoreactive with GS: 6.9% $\pm$ 1.5 of GFP$^+$ cells were double-labeled. We can therefore conclude that fewer than 10% of the GFP$^+$ cells in the dorsomedial pallium are glial. Moreover, PCNA immunolabeling showed that the cells strongly expressing GFP in this region were proliferating (Supporting Information Fig. S3B).

Given that the early neural tube (made of neuroepithelial cells) is GFP$^+$ (Supporting Information Fig. S3A), and that the zones of proliferation, known to consist of NE cells, in the postembryonic fish brain (the subpallial VZ, the lateral pallium, the OT, and the dorsal midline of the cerebellum) were all GFP$^+$ in our transgenic line, we concluded that the NE cells were labeled in the *wdr12*:GFP line.

We observed a similar labeling pattern in the zones of proliferation of the anterior thalamic nucleus and the cerebellar caudal lobe, strongly suggesting that NE cells are present in these previously largely understudied zones. As GFP$^+$ cells were found in most of the zones of proliferation, it seems likely that these zones of the postembryonic medaka brain contain NE cells.

Cell Sorting and RNA-Seq of OT *wdr12*:GFP$^+$ Cells

We then characterized the transcriptomic profile of the OT NE cells, by cell sorting followed by RNA-seq on *wdr12*:GFP$^+$ tectal cells from 1-month-old medakas. As a control, we used *wdr12*:GFP$^-$ cells (a mixture of several cell types: TAPs, postmitotic neurons, and glial cells) and *ebf3*:GFP$^+$ cells (postmitotic progenitors and differentiated neurons) [39] (Fig. 4A; Supporting Information Fig. S4A).

Hierarchical clustering revealed that gene expression profiles were similar between replicates, and samples grouped together on the basis of their cellular identity (Fig. 4B). For further validation, we focused on the POU gene family, for which the pattern of expression during vertebrate neurogenesis has been characterized in detail. Our transcriptomic and WMISH data were highly consistent (Supporting Information Fig. S4B). *Pou4f2* was strongly expressed in differentiated cells, whereas *pou3f4* was specifically expressed in the proliferating zone. *Pou3f2* was expressed in both zones, albeit at different levels in the two controls, with markedly lower levels of expression in *wdr12*:GFP$^-$ cells than in *ebf3*:GFP$^+$ cells. We retained the two controls, given the quantitative difference between them, to establish a list of genes displaying enhanced expression in NE cells. A more than twofold difference in expression was considered significant, with a false discovery rate of less than 5% (see GSE80497). With these criteria, 1,053 genes were found to be upregulated and 1,004 genes downregulated in *wdr12*:GFP$^+$ cells compared to controls.

wdr12:GFP$^+$ Cells Have a Molecular Fingerprint Typical of Active NE Cells

A cluster analysis of functional annotations made with DAVID showed that the genes downregulated and upregulated in OT *wdr12*:GFP$^+$ cells formed 107 and 155 clusters, respectively.

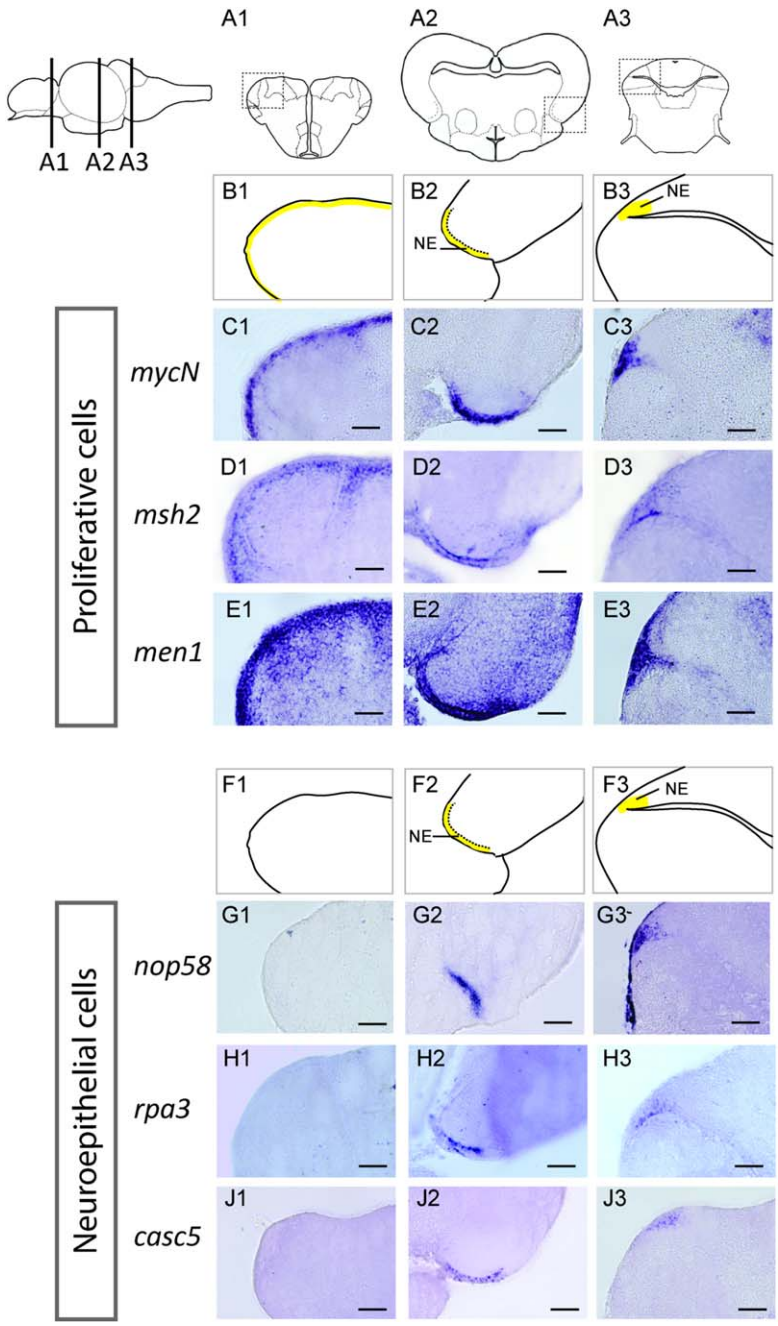

Figure 5. Two classes of proliferation-related genes, one of which is specific to NE cells. **(A)**: Cross-sections of 1-month-old fish brains taken from the telencephalon (1), mesencephalon, (2) and cerebellum (3). Diagrams based on those of Anken and Bourrat [38]. **(B, F)**: Diagram showing the ISH signal (yellow) in the different areas studied: dorsal pallium, optic tectum, and caudal lobe of the cerebellum. **(C–E, G–J)**: Whole-mount in situ hybridization for the *mycN*, *msh2*, *men1*, *nop58*, *rpa3*, and *casc5* genes. See Supporting Information Table S1 for anatomical structure abbreviations. Scale bar = 50 μm. Abbreviation: NE, neuroepithelial cell.

The top 10 clusters are indicated in Supporting Information Figure S4C. As expected, genes involved in processes such as neuronal differentiation were more strongly expressed in control cells, whereas genes involved in cell cycle control or DNA replication were more strongly expressed in *wdr12*:GFP$^+$ cells (22%). The strong expression of proliferation markers, such as *pcna*, *ki67*, and *mcm2,* confirmed that most of the *wdr12*:GFP$^+$ cells were proliferating.

Moreover, genes encoding transcription factors expressed in neural proliferation zones, such as *sox2*, *sox3*, *zic1*, and *zic2*, proliferation-associated factors (e.g., *tead3*), and differentiation-inhibiting factors, such as *hes5*, *id1*, and *id2* (Supporting Information Fig. S4D), were among the genes identified as strongly expressed in *wdr12*:GFP$^+$ cells. IPA analysis also revealed the activation of members of signaling pathways known to be important in stem cells, such as the Shh and Notch pathways [40] (Supporting Information Fig. S5 and Table S2). We retrieved all the genes of the core machinery of nucleotide synthesis or ribosome biogenesis reported to be important for midbrain neuroepithelial cells [27, 33] and

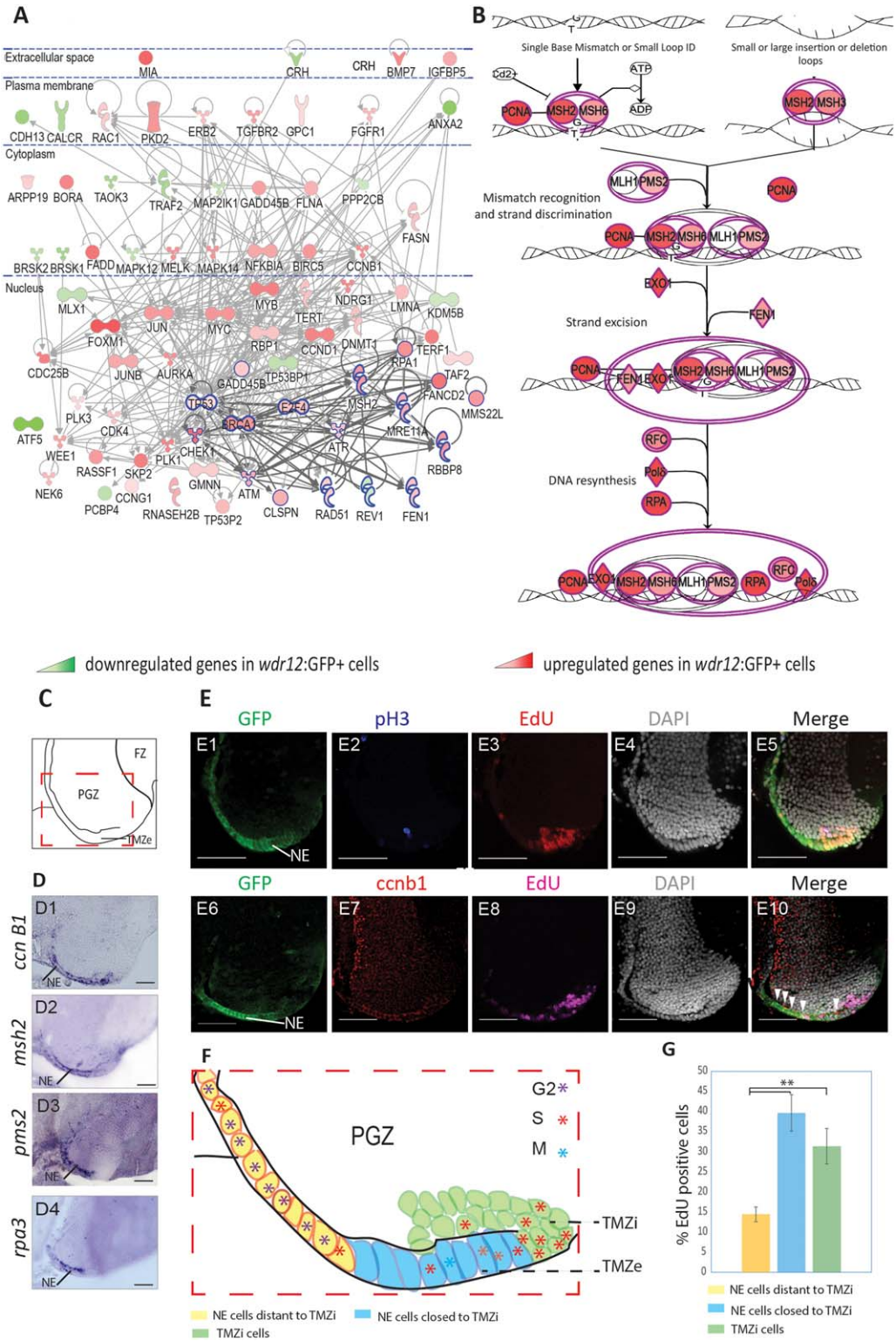

Figure 6. Progressive activation of the proliferation of NE cells and DNA repair. **(A)**: DNA repair network, based on IPA analysis. Blue circles indicate genes involved in DNA repair. Upregulated genes are highlighted in red; and downregulated genes are highlighted in green. **(B)**: IPA canonical pathway analysis of the mismatch repair pathway in *wdr12*:GFP^{+} cells. Red indicates upregulated genes, green indicates downregulated genes, and white symbols depict neighboring genes in this analysis. **(C)**: Diagram of the lateral OT, with NE cells present in the TMZe. **(D1–D4)**: In situ hybridization of *ccnb1, msh2, pms2, and rpa3*. **(E1–E10)**: Confocal cross-sections: *wdr12*:GFP^{+} cells are shown in green, nuclei are labeled with DAPI (gray). (E1–E5): Cells in S phase were labeled with a short pulse of EdU (1 hour), in red. Mitotic cells were labeled with anti-phosphohistone 3 antibody (blue). (E6–E10): Cells in S phase were labeled with a short pulse of EdU (1 hour), in magenta. Cytoplasmic ccnb1 labeling indicates cells in the G2 phase (red). Dual labeling for GFP and ccnb1 is indicated with arrows. Scale bar = 50 μm. **(F)**: Diagram of the different cell cycle stages of NE cells in the TMZ. The cells in the TMZi are shown in green. The yellow NE cells are located at some distance from the TMZi. The blue NE cells are located close to the TMZi. Purple asterisk: G2 phase; red asterisk: S phase; blue asterisk: M phase. Only the shape of the nucleus is represented. **(G)**: Graph showing the percentage of EdU-positive cells in the TMZi (green), in NE cells close to the TMZi (blue) and in NE cells located some distance away from the TMZi (yellow). Values are expressed as means ± SEM. Significant differences are indicated as $^{**}p \leq 0.001$. Abbreviations: DAPI, 4',6-Diamidine-2'-phenylindole dihydrochloride; EdU, 5-Ethynyl-2'-deoxyuridine; FZ, fibrous zone; GFP, green fluorescent protein; NE, neuroepithelial cells; pH3, phosphohistone 3; PCNA, Proliferating Cell Nuclear Antigen; PGZ, periventricular grey zone; TMZe, external tectal marginal zone; TMZi, internal tectal marginal zone.

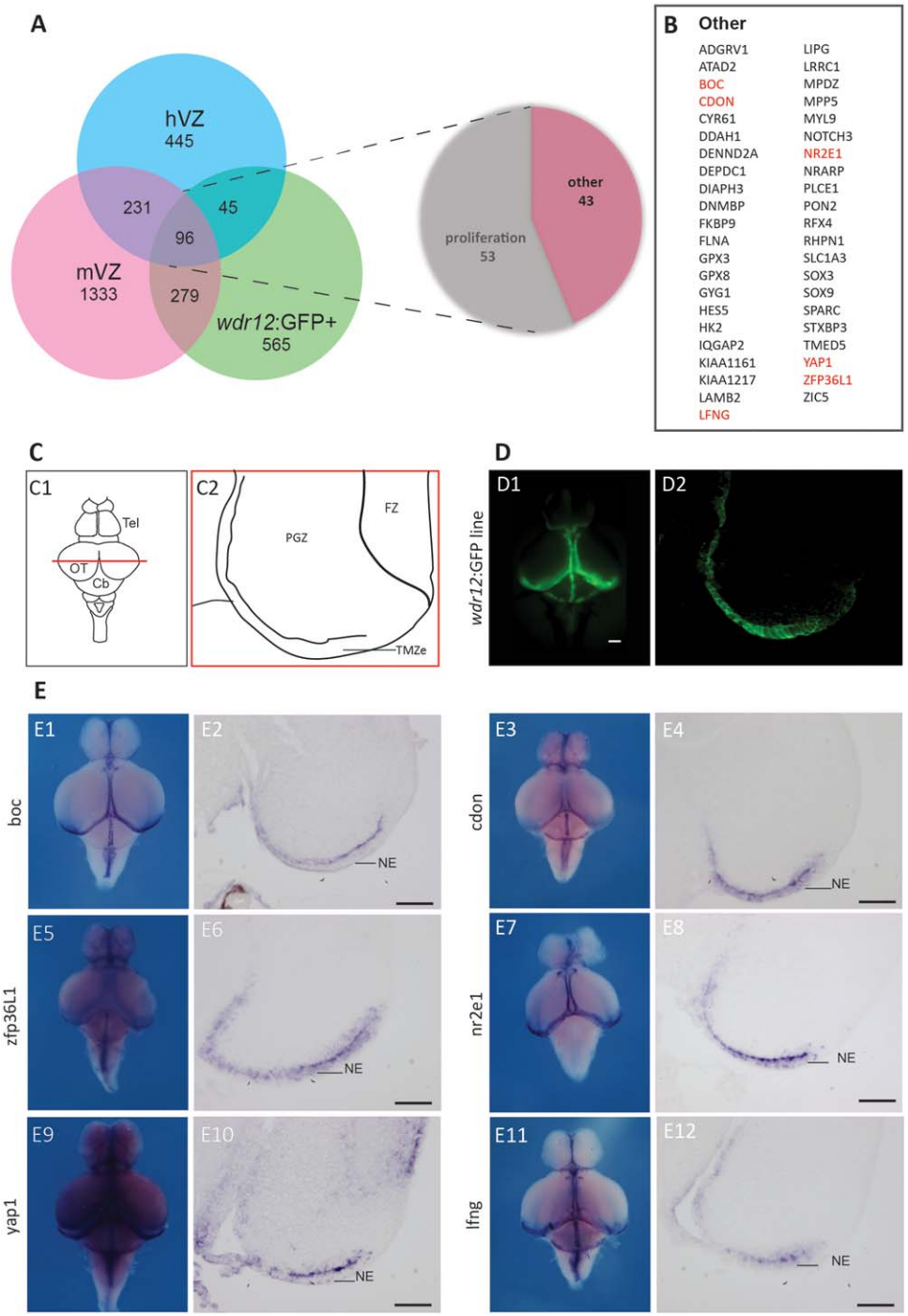

Figure 7. Genes upregulated in *wdr12*:GFP$^+$ cells, the mouse VZ, and the human VZ could be used as neuroepithelial markers. **(A)**: Venn diagram showing the genes upregulated *in wdr12*:GFP$^+$ cells, mouse VZ, and human VZ. **(B)**: List of genes not related to proliferation upregulated in *wdr12*:GFP$^+$ cells, mouse VZ, and human VZ. **(D)**: Immunohistochemistry for GFP in 1-month-old *wdr12*:GFP fish brain (D1) and on a vibratome cross-section of the OT. **(E1–E12)**: In situ hybridization of *yap1, lfng, zfp36L1, boc, cdon*, and *nr2e1*. Scale bar = 50 μm. Abbreviations: Cb, cerebellum; FZ, GFP, green fluorescent protein; hVZ, human ventricular zone; mVZ, mouse ventricular zone; NE, neuroepithelial cells; OT, optic tectum; PGZ, periventricular grey zone; Tel, telencephalon; TMZe, external tectal marginal zone.

additional members for these pathways. We also found 10 microcephaly-associated genes (*mcph1, casc5, aspm, cenpj, phc1, cdk6*, *mfsd2a*, *atr*, *rbbp8,* and *nin*), several of which are known to be strongly expressed in mammalian neuroepithelia [41–44] (see GSE80497).

Specificity of Proliferation-Related Genes

NE cells populate most of the zones of proliferation in the postembryonic medaka brain. It is therefore possible that these cells have a common molecular signature, even if present in different regions. These cells displayed high levels of

expression for genes involved in proliferative processes (cell cycle control, DNA repair, cytokinesis, DNA replication or ribosome biogenesis). We therefore carried out WMISH on juvenile medaka brains, for 26 proliferation-related genes upregulated in OT *wdr12*:GFP$^+$ cells. Histological analyses revealed that only one gene, *orc3,* was not specifically expressed in the TMZ; this gene seemed to be expressed at the brain surface instead (data not shown). Our analysis identified two classes of genes (Fig. 5). The genes of the first class (15 genes) were expressed in the TMZ, at the midline (not shown) and at the border of the caudal lobe of the cerebellum (Fig. 5B–5E). They were also widely expressed in the VZ of the dorsal telencephalon, in which most proliferative cells are radial glial cells. The expression profile of these genes thus appears to be typical of proliferative cells but not specific to NE cells.

The genes of the second class (nine genes) were not expressed in the VZ of the dorsal telencephalon and displayed a narrow pattern of expression in the OT NE (TMZe), at the midline (not shown) and at the border of the caudal lobe of the cerebellum (Fig. 5F–5J and data not shown). These observations indicate a certain degree of specificity and suggest that the overexpression of these genes in *wdr12*:GFP$^+$ cells could be related to other properties of these cells, in addition to their ability to proliferate.

Upregulation of the G2 Phase and DNA Repair Genes in OT NE Cells

G1 cyclins (*cyclin d1, d2*) are expressed at the beginning of the G1 phase, and their levels vary only slightly during the cell cycle. The expression of these molecules was upregulated in *wdr12*:GFP$^+$ cells. M-phase cyclins (*cyclin b1, b2,* and *b3*) were also found to be upregulated in these cells. Cyclin b1 is expressed mostly during the G2/M transition [45] and is essential for the activation of mitosis. WMISH confirmed that the cyclin b1 gene (*ccnb1*) was strongly expressed in NE cells, suggesting that some of these cells were in the G2 or M phase (Fig. 6D1). The gene encoding cyclin g1, which is involved in G2/M arrest in response to DNA damage [46] (see GSE80497), was upregulated, as was *FoxM1*, which is upregulated in cells with long G2 phases [47].

Overall, 8% of the genes upregulated in *wdr12*:GFP$^+$ cells were associated with the G2 phase or with DNA repair (Fig. 6A), including the *p53*, *atm*, and *atr* genes [48]. Most DNA repair genes were upregulated, including genes encoding proteins involved in DNA mismatch repair (Fig. 6B) and in double-strand break (DSB) repair by homologous recombination (10 of the 14 genes of this pathway are overexpressed in *wdr12*: GFP$^+$ cells, data not shown). WMISH for *msh2*, *pms2*, and *rpa3* in the tectum showed that the expression of these genes was restricted to the NE cells (Fig. 6D).

We evaluated the cell cycle dynamics of *wdr12*:GFP$^+$ cells. S-phase cells were labeled by a short (1-hour) EdU pulse. CCNB1 remains inactive and mostly cytoplasmic in G2, whereas it is rapidly imported into the nucleus and becomes active at the beginning of the M phase [49–51]. We used these features to identify cells in the G2 phase. Cells undergoing mitosis were labeled with an anti-phosphohistone 3 (PH3) antibody (Fig. 6E1–6E5). On cross-sections of the lateral part of the OT, *wdr12*:GFP$^+$/CCNB1$^+$ cells were identified at some distance from the TMZi (Fig. 6E6–6E10). CCNB1 appeared to be cytoplasmic in these cells, suggesting that they had long G2 phases. By contrast, most EdU-positive cells occupied a lateral position, close to the TMZi (Fig. 6E3, 6E8, 6F). Indeed, only 14.5% $\pm$ 1.8 of the NE cells distant from the TMZi (yellow) were EdU-positive, whereas 39.7% $\pm$ 4.5 of NE cells close to the TMZi (blue) were EdU-positive (Fig. 6G). PH3 labeling showed that only a few NE cells were undergoing mitosis (3.0% $\pm$0.5), mostly close to the tectum margin (Fig. 6E1–6E5). The OT NE population is, thus, heterogeneous, with some cells close to the TMZi cycling quickly, whereas others, located further away, proliferate more slowly, possibly due to a longer G2 phase (Fig. 6F).

Identification of Neuroepithelial Markers through Comparative Analysis

We attempted to find markers specific for NE cells by comparing the lists of genes overexpressed in OT NE cells, in the VZ of the cortex in human fetuses 13–16 weeks after conception and in E14.5 mouse embryos, which are known to contain many NE cells (Fig. 7A) [31]. We found that 96 genes were overexpressed in human VZ, mouse VZ, and *wdr12*:GFP$^+$ cells. As expected, a high percentage of the overexpressed genes were involved in cell proliferation (53 genes, 55%) (Supporting Information Table S3). We focused on the remaining 43 genes and performed WMISH experiments for six of these genes (Fig. 7B, 7E). For five of these six genes, the expression pattern observed was similar to that of GFP in the *wdr12*: GFP line, with expression in the OT and cerebellum (Fig. 7D). The exception was *nr2e1*, which was not expressed in the cerebellum. Histological analyses revealed a highly restricted pattern of expression for these genes in the NE cells of the OT and cerebellum. Furthermore, with the exception of *yap1*, these genes were not expressed in the VZ of the dorsal pallium (Fig. 5B and data not shown). These findings thus identify several markers potentially belonging to a putative conserved molecular signature of NE cells.

Discussion

The wdr12:GFP Line as a Tool for Studying Neurogenesis in Teleosts

Unlike mammals, teleosts continue to grow throughout their lives. Various attempts have been made to determine whether the mechanisms governing adult neurogenesis in these fish are the same as those regulating their brain growth during development. Multiple approaches, requiring specific molecular markers, are needed to address this issue. In this study, we developed a tool that labels NE cells in the medaka brain. Our findings clarify several important features of post-embryonic fish neurogenesis.

NE Cells Are Widespread in the Medaka Brain

Our results are consistent with NE cells being widespread in the postembryonic medaka brain. They may arise directly from embryonic progenitors [52], as suggested by the expression of *wdr12*:GFP in zones of proliferation in the dorsal telencephalon during development. Our results are not consistent with those previously obtained for the zebrafish pallium, in which neurogenesis is based on glial cells [13, 53, 54]. Teleost fish may have evolved different modes of pallial neurogenesis. Indeed, zebrafish and medaka, despite their similar life cycles, belong to lineages that diverged at least 200 million years ago. Likewise, we cannot rule out the possibility that some nonglial GFP$^+$ cells are committed neuroblasts corresponding to the state 3 progenitors of the

zebrafish pallium [14]. Indeed, in zebrafish, nonglial progenitors, which account for most of the label-retaining cells [55], are generally considered to be amplifying cells [13, 53]. But the possibility that NE cells are present in the zebrafish pallium, at smaller numbers than in medaka, cannot be excluded. Recent lineage studies have identified such cells in the zebrafish lateral and posterior telencephalon [25]. Furthermore, cell type characterizations based on ultrastructure studies have yielded results inconsistent with the presence of neuroblasts [23]. In killifish, putative neuroblasts (doublecortin+ (DCX+) cells) are detected three to four cell diameters away from the pallial ventricle, rather than in the ventricular location of the *wdr12*:GFP$^+$ cells in medaka.

The wdr12:GFP$^+$ Cell Population Is Heterogeneous

The *wdr12*:GFP$^+$ cell population is heterogeneous, like all stem cell populations analyzed to date. This heterogeneity is visible at different levels. First, there are morphological differences between TMZe (NE) and TMZi cells. Second, OT NE cells are themselves heterogeneous in terms of their proliferation state, as reported for mouse radial glial cells [7]. Third, OT NE cells are heterogeneous in terms of their organization within tissues: the NE cells in the diencephalon and cerebellum appear to be pseudostratified, whereas those in the OT form a monolayer similar to the ependymal structure linking different brain areas. Our results raise the intriguing possibility that the stem cell niche in the fish OT consists not only of "typical" NE cells but also of ependymal NE cells. Ependymal tissues have been implicated in brain regeneration in previous studies [56]. In adult newts, the ablation of midbrain dopaminergic neurons induces a burst of ependymal cell proliferation, which leads to dopaminergic neuron production [57]. In the mouse spinal cord, ependymal cells have been shown to be involved in regeneration after lesions [58]. These examples correspond to different vertebrate clades. It is therefore possible that brain ependymal cells are a more widespread than originally thought "generic" form of neural stem cells. If so, studies in teleosts, and the fine characterization of this cell population in well-defined models, such as the medaka optic tectum, are particularly valuable.

Long G2 Phases and Boosted DNA Repair Mechanisms in OT NE Cells

The strong expression of G2-associated markers observed in RNA-seq experiments raised the intriguing possibility that NE cells might have long G2 phases, at least in the OT. Further evidence in support of this hypothesis is provided by the presence of CCNB1 in their cytoplasm and their expression of FoxM1, a transcription factor coordinating the regulators of the G2/M phase of the cell cycle. Indeed, cells arrested in G2 due to DNA damage require FoxM1 activity to re-enter the cell cycle [47].

To our knowledge, long G2 pauses in stem cells have been observed only in organisms with a high regeneration potential, such as hydra, planarians, axolotl, and super-healing Murphy Roths Large (MRL) mice, which display efficient skin regeneration [59–62]. As reported by Harper et al. [63], G2 pausing may, in the long term, decrease cell death rates among stem cells.

We also found that the expression of DNA repair-related genes was significantly upregulated in OT NE cells (mismatch DNA repair or homologous recombination DSB repair genes) [48]. DNA repair mechanisms may be enhanced in active cells with long G2 phases, to eliminate any mutations accumulated. This process has been described in hematopoietic stem cells: quiescent stem cells use nonhomologous DSB with low-fidelity repair, whereas active progenitors use homologous DSB to maintain genome integrity and repair any mutations accumulating during quiescence [64, 65]. DNA repair-related genes have also been shown to be important in the neuroepithelial cells of *Drosophila*, with RPAs. Indeed, these molecules, which are essential for single-strand DNA repair, are also overexpressed in the neuroepithelial cells of the optic lobe in *Drosophila* and have been shown to participate in the maintenance of these cells [66].

Factors of Biomedical Relevance in NE Cell Biology

Many genes known to be involved in primary microcephalies were found to be overexpressed in NE cells. Most encode centrosome-linked proteins involved in the core mechanisms of cell division [67]. For example, *aspm* and *mcph1* encode proteins involved in spindle positioning and orientation, respectively. Mutations of these genes lead to asymmetric cell division and premature neural differentiation in mammals [68–70]. *Casc5* encodes a kinetochore scaffold protein involved in both chromatin attachment to the mitotic apparatus and control of the spindle assembly checkpoint. Loss-of-function mutations of this gene accelerate entry into mitosis [71]. *Plk4*, another gene present in our list of genes overexpressed in *wdr12*:GFP$^+$ cells, has related functions. One recent study [72] showed that neuroepithelial cells were more sensitive to centrosome defects than other types of epithelial cells. It is therefore tempting to speculate that these genes are important members of genetic networks preventing the premature differentiation of NE cells and/or maintaining the pool of NE cells throughout life.

Medaka NE Cell Marker Genes Compared with Those of Other Species

The genes overexpressed in medaka OT NE cells and in the VZ of the cortex in human and mouse embryos included *Hes 5* and *Yap 1*, known to stimulate proliferation and to inhibit the differentiation of NE cells [73, 74]. Another gene of interest is *nr2e1—Nuclear receptor TLX* or *tailless* in *Drosophila melanogaster*. Its expression is conserved in the neural stem cells of vertebrates and *Drosophila*, and it has been shown to be required for their self-renewal. Moreover, *Tll* is required for correct neuroepithelium morphogenesis and neuroepithelial cell survival during the development of the optic lobe in *Drosophila* [75]. Our comparison also identified several less well-known genes, such as *Rfx4*, the product of which regulates *Musashi 1* expression in mouse neural progenitor cells [76]; *Lfng*, which is expressed in the hindbrain neuroepithelial cells during zebrafish development and helps to maintain the pool of progenitor cells [77]; and *LIPG*, which encodes an endothelial lipase expressed in the neuroepithelium of the brain and the neural tube of E10.5 mice [78]. Finally, we retrieved two genes encoding cell surface integral membrane proteins: *cdon*, and *boc* (*brother of cdon*). The proteins encoded by these genes are components of the hedgehog (Hh) receptor complex. They may upregulate or downregulate the Hh pathway, depending on the context. For example, in mouse embryos, these proteins are essential to transduce Hh signaling during neural ventral patterning, whereas, in zebrafish and chicken, *cdon*, which is expressed at the basolateral pole of NE cells, encodes a protein that acts as a negative regulator of Hh during optic vesicle development [79, 80].

Our comparative studies thus contribute to the characterization of a general molecular signature of NE cells in bilaterian

nervous systems. Such approaches cannot replace functional analyses, but they can identify interesting candidates, as genes conserved over large evolutionary distances are likely to be important regulators of the NE progenitor state.

Conclusion

This study highlights the importance of NE cells during post-embryonic neurogenesis in medaka and the mechanisms likely to be crucial for the biology of these cells. These data have important implications not only for our understanding of teleost neurogenesis but also, given that at least some aspects of the processes described here are likely to be widespread in vertebrates, for novel treatments in regenerative medicine, and for our understanding of some neural diseases, such as microcephaly.

Acknowledgments

We thank Elliot Henry, Arnim Jenett, Elodie de Job, and Laurie Riviere for technical assistance, and Stephen Brown for careful reading of the manuscript; Laurence Etwiller for providing the *ebf3*:GFP line and Axel Newe for assistance with the creation of the 3D pdf; Maud Sylvain for assistance with genomic data handling. This research received financial support from the FINEST project (ANR-11-BSV2-0029). E.D. was funded by an ARC long-term postdoctoral fellowship. We thank ANR and ARC foundation for financial support.

Author Contributions

E.D. and M.S.: conception and design, collection and/or assembly of data, data analysis and interpretation, and manuscript writing; T.B.: data analysis and interpretation; B.R. and P.A.: data analysis; S.B., Y.J., J.J., J.E., A.H., and M.B.: collection and/or assembly of data; C.T., A.P., E.R., and F.S.: conception and design; F.B.: manuscript writing and final approval of manuscript; J.S.J.: conception and design, data analysis and interpretation, manuscript writing, and final approval of manuscript.

Disclosure of Potential Conflict of Interest

The authors indicate no potential conflict of interest.

References

1 Bayer SA, Yackel JW Puri PS. Neurons in the rat dentate gyrus granular layer substantially increase during juvenile and adult life. Science 1982;216:890–892.
2 Grandel H Brand M. Comparative aspects of adult neural stem cell activity in vertebrates. Dev Genes Evol 2013;223:131–147.
3 Alvarez-Buylla A, García-Verdugo JM Tramontin AD. A unified hypothesis on the lineage of neural stem cells. Nat Rev Neurosci 2001;2:287–293.
4 Merkle FT, Tramontin AD, García-Verdugo JM et al. Radial glia give rise to adult neural stem cells in the subventricular zone. Proc Natl Acad Sci USA 2004;101:17528–17532.
5 Xu L, Tang X, Wang Y et al. Radial glia, the keystone of the development of the hippocampal dentate gyrus. Mol Neurobiol 2015;51:131–141.
6 Kriegstein A Alvarez-Buylla A. The glial nature of embryonic and adult neural stem cells. Annu Rev Neurosci 2009;32:149–184.
7 Codega P, Silva-Vargas V, Paul A et al. Prospective identification and purification of quiescent adult neural stem cells from their in vivo niche. Neuron 2014;82:545–559.
8 Beckervordersandforth R, Deshpande A, Schäffner I et al. In vivo targeting of adult neural stem cells in the dentate gyrus by a split-cre approach. Stem Cell Rep 2014;2:153–162.
9 Giachino C, Basak O, Lugert S et al. Molecular diversity subdivides the adult forebrain neural stem cell population. Stem Cells 2014;32:70–84.
10 Merkle FT, Mirzadeh Z Alvarez-Buylla A. Mosaic organization of neural stem cells in the adult brain. Science 2007;317:381–384.
11 Suh H, Consiglio A, Ray J et al. In vivo fate analysis reveals the multipotent and self-renewal capacities of Sox2+ neural stem cells in the adult hippocampus. Cell Stem Cell 2007;1:515–528.
12 Pellegrini E, Mouriec K, Anglade I et al. Identification of aromatase-positive radial glial cells as progenitor cells in the ventricular layer of the forebrain in zebrafish. J Comp Neurol 2007;501:150–167.
13 Rothenaigner I, Krecsmarik M, Hayes JA et al. Clonal analysis by distinct viral vectors identifies bona fide neural stem cells in the adult zebrafish telencephalon and characterizes their division properties and fate. Dev Camb Engl 2011;138:1459–1469.
14 Chapouton P, Skupien P, Hesl B et al. Notch activity levels control the balance between quiescence and recruitment of adult neural stem cells. J Neurosci Off J Soc Neurosci 2010;30:7961–7974.
15 März M, Chapouton P, Diotel N et al. Heterogeneity in progenitor cell subtypes in the ventricular zone of the zebrafish adult telencephalon. Glia 2010;58:870–888.
16 Coskun V, Wu H, Blanchi B et al. CD133+ neural stem cells in the ependyma of mammalian postnatal forebrain. Proc Natl Acad Sci USA 2008;105:1026–1031.
17 Luo Y, Coskun V, Liang A et al. Single-cell transcriptome analyses reveal signals to activate dormant neural stem cells. Cell 2015;161:1175–1186.
18 Grandel H, Kaslin J, Ganz J et al. Neural stem cells and neurogenesis in the adult zebrafish brain: origin, proliferation dynamics, migration and cell fate. Dev Biol 2006;295:263–277.
19 Zupanc GKH Sîrbulescu RF. Adult neurogenesis and neuronal regeneration in the central nervous system of teleost fish. Eur J Neurosci 2011;34:917–929.
20 Götz M, Huttner WB. The cell biology of neurogenesis. Nat Rev Mol Cell Biol 2005;6:777–788.
21 Alunni A, Hermel J-M, Heuzé A et al. Evidence for neural stem cells in the medaka optic tectum proliferation zones. Dev Neurobiol 2010;70:693–713.
22 Ito Y, Tanaka H, Okamoto H et al. Characterization of neural stem cells and their progeny in the adult zebrafish optic tectum. Dev Biol 2010;342:26–38.
23 Lindsey BW, Darabie A Tropepe V. The cellular composition of neurogenic periventricular zones in the adult zebrafish forebrain. J Comp Neurol 2012;520:2275–2316.
24 Kaslin J, Ganz J, Geffarth M et al. Stem cells in the adult zebrafish cerebellum: initiation and maintenance of a novel stem cell niche. J Neurosci Off J Soc Neurosci 2009;29:6142–6153.
25 Dirian L, Galant S, Coolen M et al. Spatial regionalization and heterochrony in the formation of adult pallial neural stem cells. Dev Cell 2014;30:123–136.
26 Hölzel M, Rohrmoser M, Schlee M et al. Mammalian WDR12 is a novel member of the Pes1-Bop1 complex and is required for ribosome biogenesis and cell proliferation. J Cell Biol 2005;170:367–378.
27 Recher G, Jouralet J, Brombin A et al. Zebrafish midbrain slow-amplifying progenitors exhibit high levels of transcripts for nucleotide and ribosome biogenesis. Dev Camb Engl 2013;140:4860–4869.
28 Nguyen V, Deschet K, Henrich T et al. Morphogenesis of the optic tectum in the medaka (*Oryzias latipes*): a morphological and molecular study, with special emphasis on cell proliferation. J Comp Neurol 1999;413:385–404.
29 Iwamatsu T. Stages of normal development in the medaka *Oryzias latipes*. Mech Dev 2004;121:605–618.
30 Manoli M, Driever W. Fluorescence-activated cell sorting (FACS) of fluorescently tagged cells from zebrafish larvae for RNA isolation. Cold Spring Harb Protoc 2012;2012.
31 Fietz SA, Lachmann R, Brandl H et al. Transcriptomes of germinal zones of human and mouse fetal neocortex suggest a role of extracellular matrix in progenitor self-renewal. Proc Natl Acad Sci USA 2012;109:11836–11841.
32 Xu Q, Holder N, Patient R et al. Spatially regulated expression of three receptor tyrosine

kinase genes during gastrulation in the zebrafish. Dev Camb Engl 1994;120:287–299.
33 Brombin A, Grossier J-P, Heuzé A et al. Genome-wide analysis of the POU genes in medaka, focusing on expression in the optic tectum. Dev Dyn Off Publ Am Assoc Anat 2011;240:2354–2363.
34 Devès M Bourrat F. Transcriptional mechanisms of developmental cell cycle arrest: problems and models. Semin Cell Dev Biol 2012;23:290–297.
35 Joly J-S, Recher G, Brombin A et al. A conserved developmental mechanism builds complex visual systems in insects and vertebrates. Curr Biol 2016;26:R1001–R1009.
36 Than-Trong E, Bally-Cuif L. Radial glia and neural progenitors in the adult zebrafish central nervous system. Glia 2015;63:1406–1428.
37 Chung K, Deisseroth K. CLARITY for mapping the nervous system. Nat Methods 2013; 10:508–513.
38 Anken R, Bourrat F. Brain Atlas of the Medaka Fish (*Oryzias latipes*). Paris: INRA Ed., 1998.
39 Mongin E, Auer TO, Bourrat F et al. Combining computational prediction of cis-regulatory elements with a new enhancer assay to efficiently label neuronal structures in the medaka fish. Plos One 2011;6:e19747.
40 Alunni A, Krecsmarik M, Bosco A et al. Notch3 signaling gates cell cycle entry and limits neural stem cell amplification in the adult pallium. Dev Camb Engl 2013;140:3335–3347.
41 Izraeli S, Lowe LA, Bertness VL et al. The SIL gene is required for mouse embryonic axial development and left-right specification. Nature 1999;399:691–694.
42 Jackson AP, Eastwood H, Bell SM et al. Identification of microcephalin, a protein implicated in determining the size of the human brain. Am J Hum Genet 2002;71:136–142.
43 Fish JL, Kosodo Y, Enard W et al. Aspm specifically maintains symmetric proliferative divisions of neuroepithelial cells. Proc Natl Acad Sci USA 2006;103:10438–10443.
44 Nicholas AK, Khurshid M, Désir J et al. WDR62 is associated with the spindle pole and is mutated in human microcephaly. Nat Genet 2010;42:1010–1014.
45 Cogswell JP, Godlevski MM, Bonham M et al. Upstream stimulatory factor regulates expression of the cell cycle-dependent cyclin B1 gene promoter. Mol Cell Biol 1995;15: 2782–2790.
46 Kimura SH, Nojima H, Cyclin G. associates with MDM2 and regulates accumulation and degradation of p53 protein. Genes Cells Dev Mol Cell Mech 2002;7:869–880.
47 Alvarez-Fernández M, Halim VA, Krenning L et al. Recovery from a DNA-damage-induced G2 arrest requires Cdk-dependent activation of FoxM1. EMBO Rep 2010;11:452–458.
48 Iyama T, Wilson DM. DNA repair mechanisms in dividing and non-dividing cells. DNA Repair 2013;12:620–636.
49 Gavet O, Pines J. Activation of cyclin B1-Cdk1 synchronizes events in the nucleus and the cytoplasm at mitosis. J Cell Biol 2010; 189:247–259.
50 Pines J, Hunter T. Human cyclins A and B1 are differentially located in the cell and undergo cell cycle-dependent nuclear transport. J Cell Biol 1991;115:1–17.
51 Pines J, Hunter T. The differential localization of human cyclins A and B is due to a cytoplasmic retention signal in cyclin B. EMBO J 1994;13:3772–3781.
52 Stigloher C, Chapouton P, Adolf B et al. Identification of neural progenitor pools by E(Spl) factors in the embryonic and adult brain. Brain Res Bull 2008;75:266–273.
53 Barbosa JS, Sanchez-Gonzalez R, Di Giaimo R et al. Neurodevelopment. Live imaging of adult neural stem cell behavior in the intact and injured zebrafish brain. Science 2015;348:789–793.
54 Dray N, Bedu S, Vuillemin N et al. Large-scale live imaging of adult neural stem cells in their endogenous niche. Dev Camb Engl 2015;142:3592–3600.
55 Ganz J, Kaslin J, Hochmann S et al. Heterogeneity and Fgf dependence of adult neural progenitors in the zebrafish telencephalon. Glia 2010;58:1345–1363.
56 Tanaka EM, Ferretti P. Considering the evolution of regeneration in the central nervous system. Nat Rev Neurosci 2009;10:713–723.
57 Berg DA, Kirkham M, Wang H et al. Dopamine controls neurogenesis in the adult salamander midbrain in homeostasis and during regeneration of dopamine neurons. Cell Stem Cell 2011;8:426–433.
58 Sabelström H, Stenudd M, Réu P et al. Resident neural stem cells restrict tissue damage and neuronal loss after spinal cord injury in mice. Science 2013;342:637–640.
59 Bedelbaeva K, Snyder A, Gourevitch D et al. Lack of p21 expression links cell cycle control and appendage regeneration in mice. Proc Natl Acad Sci USA 2010;107:5845–5850.
60 Buzgariu W, Crescenzi M Galliot B. Robust G2 pausing of adult stem cells in Hydra. Differ Res Biol Divers 2014;87:83–99.
61 Eisenhoffer GT, Kang H, Sánchez Alvarado A. Molecular analysis of stem cells and their descendants during cell turnover and regeneration in the planarian Schmidtea mediterranea. Cell Stem Cell 2008;3:327–339.
62 Rao N, Jhamb D, Milner DJ et al. Proteomic analysis of blastema formation in regenerating axolotl limbs. BMC Biol 2009;7:83.
63 Harper LJ, Costea DE, Gammon L et al. Normal and malignant epithelial cells with stem-like properties have an extended G2 cell cycle phase that is associated with apoptotic resistance. BMC Cancer 2010;10:166.
64 Burkhalter MD, Rudolph KL Sperka T. Genome instability of ageing stem cells-Induction and defence mechanisms. Ageing Res Rev 2015;23:29–36.
65 Mohrin M, Bourke E, Alexander D et al. Hematopoietic stem cell quiescence promotes error-prone DNA repair and mutagenesis. Cell Stem Cell 2010;7:174–185.
66 Zhou L, Luo H. Replication protein a links cell cycle progression and the onset of neurogenesis in Drosophila optic lobe development. J Neurosci Off J Soc Neurosci 2013; 33:2873–2888.
67 Barbelanne M, Tsang WY. Molecular and cellular basis of autosomal recessive primary microcephaly. Biomed Res Int 2014;2014: 547986.
68 Gruber R, Zhou Z, Sukchev M et al. MCPH1 regulates the neuroprogenitor division mode by coupling the centrosomal cycle with mitotic entry through the Chk1-Cdc25 pathway. Nat Cell Biol 2011;13:1325–1334.
69 Higgins J, Midgley C, Bergh A-M et al. Human ASPM participates in spindle organisation, spindle orientation and cytokinesis. BMC Cell Biol 2010;11:85.
70 Zhou Z-W, Tapias A, Bruhn C et al. DNA damage response in microcephaly development of MCPH1 mouse model. DNA Repair 2013;12:645–655.
71 Cheeseman IM, Hori T, Fukagawa T et al. KNL1 and the CENP-H/I/K complex coordinately direct kinetochore assembly in vertebrates. Mol Biol Cell 2008;19:587–594.
72 Dzafic E, Strzyz PJ, Wilsch-Bräuninger M et al. Centriole amplification in zebrafish affects proliferation and survival but not differentiation of neural progenitor cells. Cell Rep 2015;13:168–182
73 Li Y, Hibbs MA, Gard AL et al. Genome-wide analysis of N1ICD/RBPJ targets in vivo reveals direct transcriptional regulation of Wnt, SHH, and hippo pathway effectors by Notch1. Stem Cells 2012;30:741–752.
74 Benítez-Santana T, Simion M, Orraze G et al. Effect of nutrient availability on progenitor cells in zebrafish (*Danio rerio*). Dev Neurobiol 2017;77:26–38.
75 Guillermin O, Perruchoud B, Sprecher SG et al. Characterization of tailless functions during Drosophila optic lobe formation. Dev Biol 2015;405:202–213.
76 Kawase S, Kuwako K, Imai T et al. Regulatory factor X transcription factors control Musashi1 transcription in mouse neural stem/progenitor cells. Stem Cells Dev 2014; 23:2250–2261.
77 Nikolaou N, Watanabe-Asaka T, Gerety S et al. Lunatic fringe promotes the lateral inhibition of neurogenesis. Dev Camb Engl 2009; 136:2523–2533.
78 Lindegaard MLS, Nielsen JE, Hannibal J et al. Expression of the endothelial lipase gene in murine embryos and reproductive organs. J Lipid Res 2005;46:439–444.
79 Cardozo MJ, Sánchez-Arrones L, Sandonis A et al. Cdon acts as a Hedgehog decoy receptor during proximal-distal patterning of the optic vesicle. Nat Commun 2014;5:4272.
80 Allen BL, Song JY, Izzi L et al. Overlapping roles and collective requirement for the coreceptors GAS1, CDO, and BOC in SHH pathway function. Dev Cell 2011;20:775–787.


See www.StemCells.com for supporting information available online.

Chapter 2: Identification of a candidate involved in ribosome biogenesis specifically expressed in neuroepithelial progenitor cells

1. Introduction

In previous studies, we stressed out the putative specific role of ribosome biogenesis factors in cell proliferation since many ribosome biogenesis transcripts are preferentially accumulated in the slow amplifying progenitors of the optic tectum (**Recher et al., 2013**). The main goal of my PhD was to understand how RBFs could specifically regulate progenitor cell homeostasis.

In the first part of the results, I illustrated the role of *fbl* in the correlation between ribosome biogenesis and cell cycle regulation. In particular, I highlighted the importance of Fbl in S-phase progression and neural differentiation.

In parallel, my project focused on the identification of a candidate playing a specific role in cell cycle regulation. To this aim, I performed a whole mount *in situ* hybridization screen that allowed the identification of supplemental RBFs accumulated in the proliferative zone of the brain. I choose to focus my work on one of them, *pa2g4*, since this gene show a very restricted expression pattern in neuroepithelial progenitors and was described in the literature as a cell cycle regulator. I generated transgenic lines to perform the inducible specific overexpression of *pa2g4* to get insight into its functions in neural progenitors cells.

2. Results

2.1. Several additional ribosome biogenesis factor transcripts are accumulated in NePCs

Among clusters of genes upregulated or downregulated in the neuroepithelial population, RNA sequencing data revealed the accumulation of ribosome biogenesis transcripts. In addition to the previously reported factors identified by the datamining of the ZFIN database, nine putative ribosome biogenesis factors were upregulated in the NePCs population compared to the other proliferative cells and differentiated neurons (Table 4). We first verified their role in ribosome biogenesis using literature. *ddx56* is involved in the 60S large subunit assembly as well as the control of association and dissociation of the snoRNA (**Zirwes et al., 2000**). The many other factors are involved in earlier step of the pathway. Indeed, *wdr3* and *exosc2* are both involved in the maturation of rRNA (**Koga et**

al., 2014). Similarly, *ebna1bp*, *heatr1* and *pa2g4* are all playing and important role in pre-rRNA processing and cell cycle regulation (**Dez et al., 2007; Squatrito et al., 2004**). Indeed, *ebna1p* is regulating cellular proliferation and *heatr1* is specifically involved in the central nervous system cell survival (**Azuma et al., 2006**). *pa2g4*, also called *ebp1* in mammals and plants, is involved in cancer, cell survival and pre-rRNA processing (**Hu et al., 2014; Mei et al., 2014; Zhou et al., 2010**). On the contrary, *npm3* (called *npm2* in *Danio rerio*) seems to be an inhibitor of ribosome biogenesis (**Huang et al., 2005**). Finally, *nhp2* and *nhp2l1* are members the snoRNP complex and the U4 snRNP complex, respectively (**Lemay et al., 2011**). From this analysis of the bibliography, we conclude that the upregulated genes reported in **Dambroise et al.** are likely to have a role in the biology of NePCs (**Dambroise et al., 2017**).

Genes	NePCs+	NePCs-	Fold change
ddx56	263	49,5	1,67645362
ebna1bp2	1951,3	276,5	2,00801151
exosc2	738,3	155	1,45367253
heatr1	338,3	53,5	1,89165729
nhp2	673	91,5	2,12908258
nhp2l1a	1857	346,5	1,63356449
npm3	1200,3	166	2,08576761
pa2g4b	5729,6	1189,5	1,44114159
wdr3	322,6	78,5	1,26733153

Table 4: Several ribosome biogenesis factors are overexpressed in the proliferative population of medaka juvenile brain.
Data were obtained after cell sorting the neuroepithelial progenitors of medaka juvenile brains, using Tg (*wdr12:GFP*) transgenic line. The fold change correspond to the ratio between wdr12:GFP positive cells and wdr12:GFP negative cells.

2.2. Isolation of a putative cell cycle regulator in tectal progenitors

2.2.1 *nhp2*, *heatr1*, *wdr3* and *pa2g4* ribosome biogenesis genes display restricted expression in the proliferative cells of the brain

As all of the nine RBFs accumulated in the wdr12:GFP positive cell population are involved in the processing of rRNA and ribosomal subunit, I further analyzed their expression pattern, using ISH in zebrafish juvenile brains and 2dpf and 3dpf embryos. Among the nine candidates, I highlighted a restricted expression pattern for four of them. In particular,

nhp2, *heatr1*, *wdr3* and *pa2g4* are preferentially expressed at the periphery (i.e in the proliferative zone) of the OT (*fig 44*, white arrows) and the retina (*fig 44*, black arrows). Those genes were also expressed in the proliferative population of additional brain structures such as the cerebellum and the telencephalon. However, we did not observed any expression of *nhp2l*, *ebna1p* and *ddx56* either in the juvenile brain or the embryos. *npm2* and *exosc2* were expressed in the optic tectum but were not restricted to the peripheral region (data not shown). Taken together, these data confirm that *nhp2*, *heatr1*, *wdr3* and *pa2g4* are preferentially expressed in the proliferative population of the OT.

2.2.2 Pa2g4 could be involved in the connection between cell cycle regulation and ribosome biogenesis

We, then, focused our studies on the *pa2g4* gene as its expression pattern show the most restricted and biased expression in the OT. Many studies have highlighted the role of *pa2g4* in cell cycle regulation. In particular, post-natal developmental defects are observed in KO-mice, following decrease in cell proliferation (**Zhang et al., 2008**). Similarly, *ebp1* seems to be a dose-dependent cell cycle activator in plants as RNA interference knockdown led to shorter leafs and overexpression studies gave rise to bigger plants (**Horváth et al., 2006**). However, in human fibroblasts and Leishmania parasites, it has been demonstrated that *pa2g4* would be a cell proliferation inhibitor (**Liu et al., 2009; Norris-Mullins et al., 2014**). Strikingly, two isoforms can be found in rat cell lines playing opposite role in cell growth and survival (**Okada et al., 2007**). In addition to its physiological roles, *pa2g4* is also involved in cancer progression. Pa2g4 displays an oncogenic role in some brain, cervical and mouth cancers (**Kim et al., 2010; Liu et al., 2015; Mei et al., 2014**). In contrast, it could also act as a tumor suppressor in hepatocellular carninomas, and in prostate and bladder cancers (**He et al., 2013; Hu et al., 2014; Zhou et al., 2010**). Its involvement in ribosome biogenesis has been illustrated in a few studies. Given that its overexpression leads to the reduction of 28S and 18S rRNA, *pa2g4* would be involved in the regulation of the intermediate and late steps of rRNA processing. Moreover, it is associated with mature and precursor rRNA, highlighting a putative contribution to 60S subunit maturation and rRNA processing (**Squatrito et al., 2004**). Strikingly, analysis of its interaction network showed many interactions with ribosome biogenesis factors and ribosomal proteins (**https://string-db.org/**), emphasizing its participation to ribosome biogenesis.

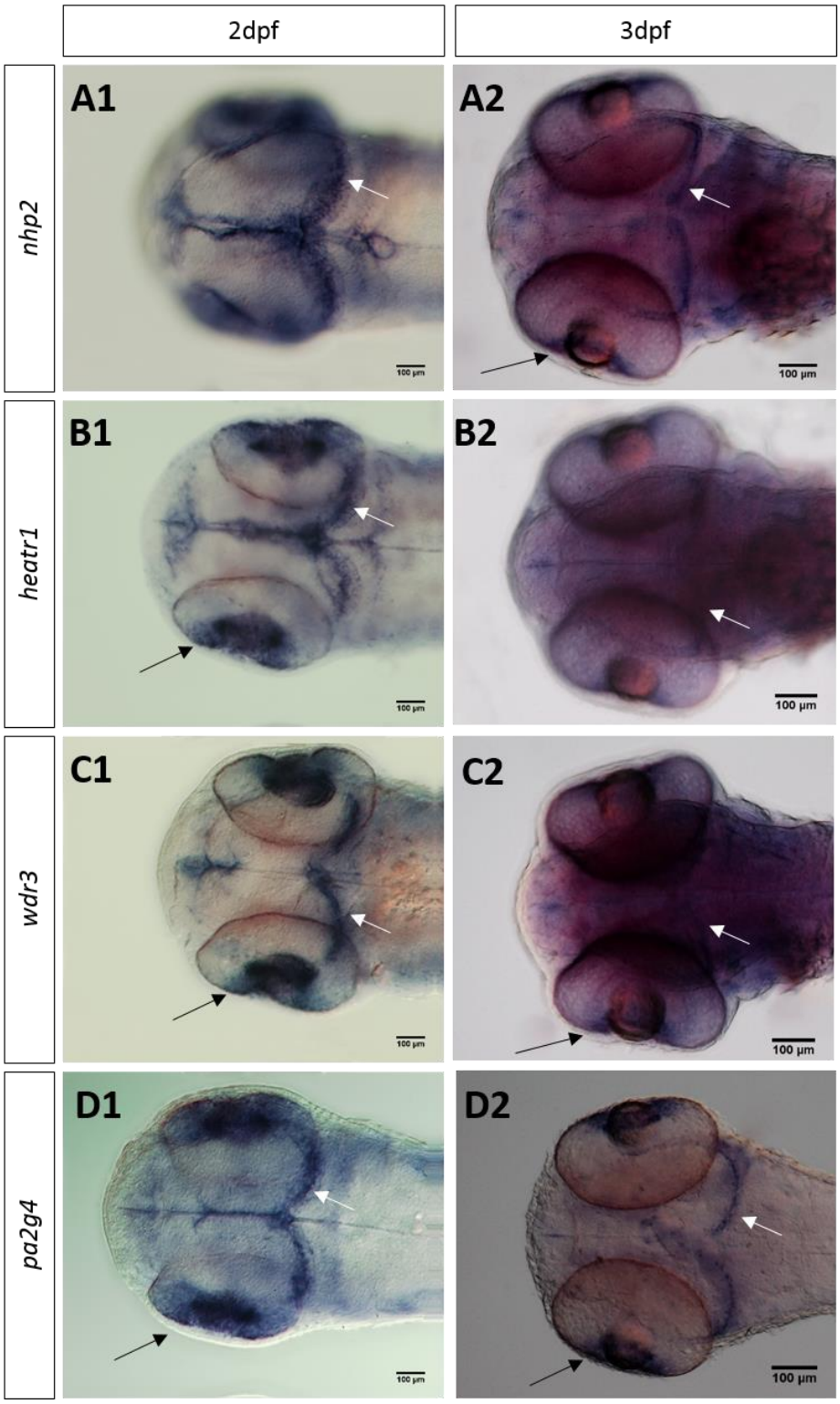

Figure 44: An ISH screen of ribosome biogenesis genes reveals novel external tectal marginal zone (TMZe) specific genes

(A) ISH for *nhp2* at 2dpf **(A1)** and at 3dpf **(A2)**. **(B)** ISH for *heatr1* at 2dpf **(B1)** and 3dpf **(B2)**. **(C)** ISH targeting *wdr3* at 2dpf **(C1)** and 3dpf **(C2)**. **(D)** ISH for *pa2g4* at 2dpf **(D1)** and 3dpf **(D2)**. Expression is boosted in the TMZe, where slow amplifying progenitors which are neuroepithelial, are localized (white arrows). Black arrows: restricted expression in the proliferative population of the retina. Scale bars: 100 µm.

In particular, it interacts with Nucleophosmin in rat cell lines in order to block apoptosis and play a major role in ITS2 cleavage during rRNA processing (Okada et al., 2007). Therefore, pa2g4 seems to be a key cell proliferation regulator, playing a major role as a link between cell cycle regulation and ribosome biogenesis. In the tectum, where cell homeostasis is tightly regulated, pa2g4 could play a specific role in the cell cycle regulation and ribosome biogenesis.

2.2.3 *pa2g4* mRNAs and proteins are accumulated in brain proliferative cells

Two paralogs for pa2g4 have been annotated in *Danio rerio* genome: *pa2g4a* and *pa2g4b*. We studied the expression of the two paralogs. Since similar expression patterns were observed for both paralogs I will only describe the expression pattern of *pa2g4a*. Its expression pattern was assessed by WMISH at different developmental stages (*fig 45*). *pa2g4*a expression mimicked the expression of other TMZe genes. It is widely expressed after somitogenesis (1dpf) in many proliferative tissues, especially in the dorsal part of the midbrain (*fig 45A*). Indeed, at this stage, the midbrain is expanding and proliferation zones are not yet restricted to the periphery of the OT (**Joly et al., 2016**). Upon development, *pa2g4* expression became more restricted, following the partitioning of the proliferation zone at the margin of the OT (*fig 45 B-C*). Interestingly, it was not expressed in other regions than the brain (data not shown). Furthermore, we also detected *pa2g4* expression in proliferative regions of the juvenile zebrafish brain (*fig 45 D-E*). Protein localization was also assessed by WMIHC (*fig 46*). Interestingly, Pa2g4 protein was detected all around the tectum. However, the protein was clearly more present at the periphery of the OT at 2dpf (*fig 46A*), 3dpf (data not shown) and in juveniles (*fig 46B*). Strikingly, Pa2g4 protein displayed cytoplasmic subcellular localization whereas ribosome biogenesis occurs mainly in the nucleolus. This could highlight a putative role in the latest steps of ribosome production. I further characterized the cell population expressing preferentially the protein at juvenile stages. Pa2g4 colocalized with the proliferative marker PCNA (*fig 47A*) and the epithelial marker zonula occludens 1 (ZO-1, *fig 47B*). In addition, it did not colocalize with the glial marker glutamine synthetase (GS) or Elavl3 expressed in differentiated neurons (*fig 47C*). Thus, Pa2g4 is preferentially accumulated in the neuroepithelial progenitor cell population of the OT.

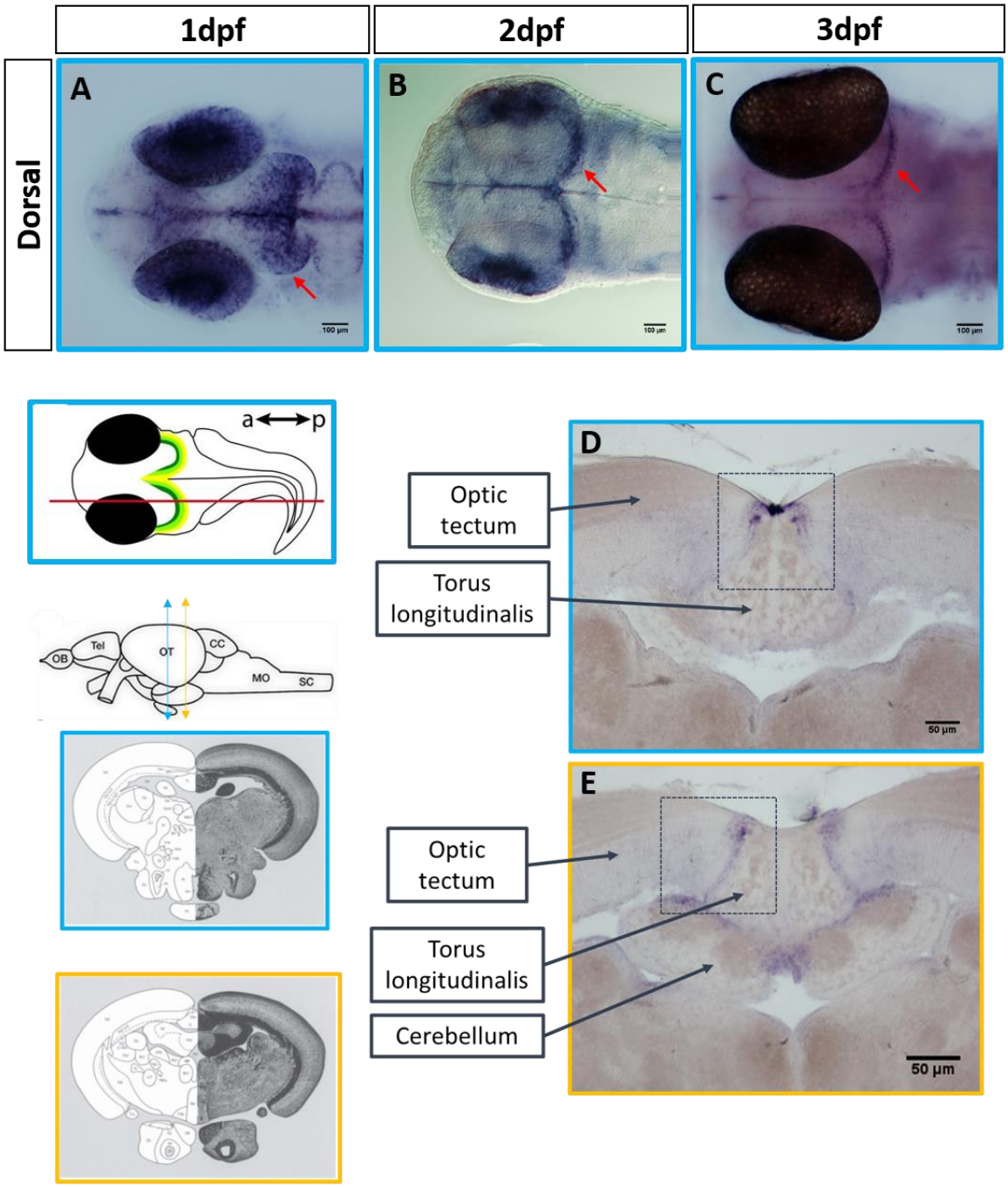

<u>Figure 45</u>: *pa2g4* is expressed in the TMZe at embryonic and juvenile stages

(A-C) *pa2g4* expression pattern during development. Dorsal view of **A**. 1dpf, **B**. 2dpf, **C**. 3dpf zebrafish embryos. Red arrows indicate OT expression. Drawing in the lower panel shows orientation of the embryos. Scale bars: 100 µm. **(D-E)** *pa2g4* expression in juvenile zebrafish transverse brains. D. Medial midbrain section **E.** posterior midbrain section. Dashed squares highlight the restricted expression in the proliferative cells of the OT. Blue and yellow borders and arrows highlight section planes. Scale bars: 50 µm

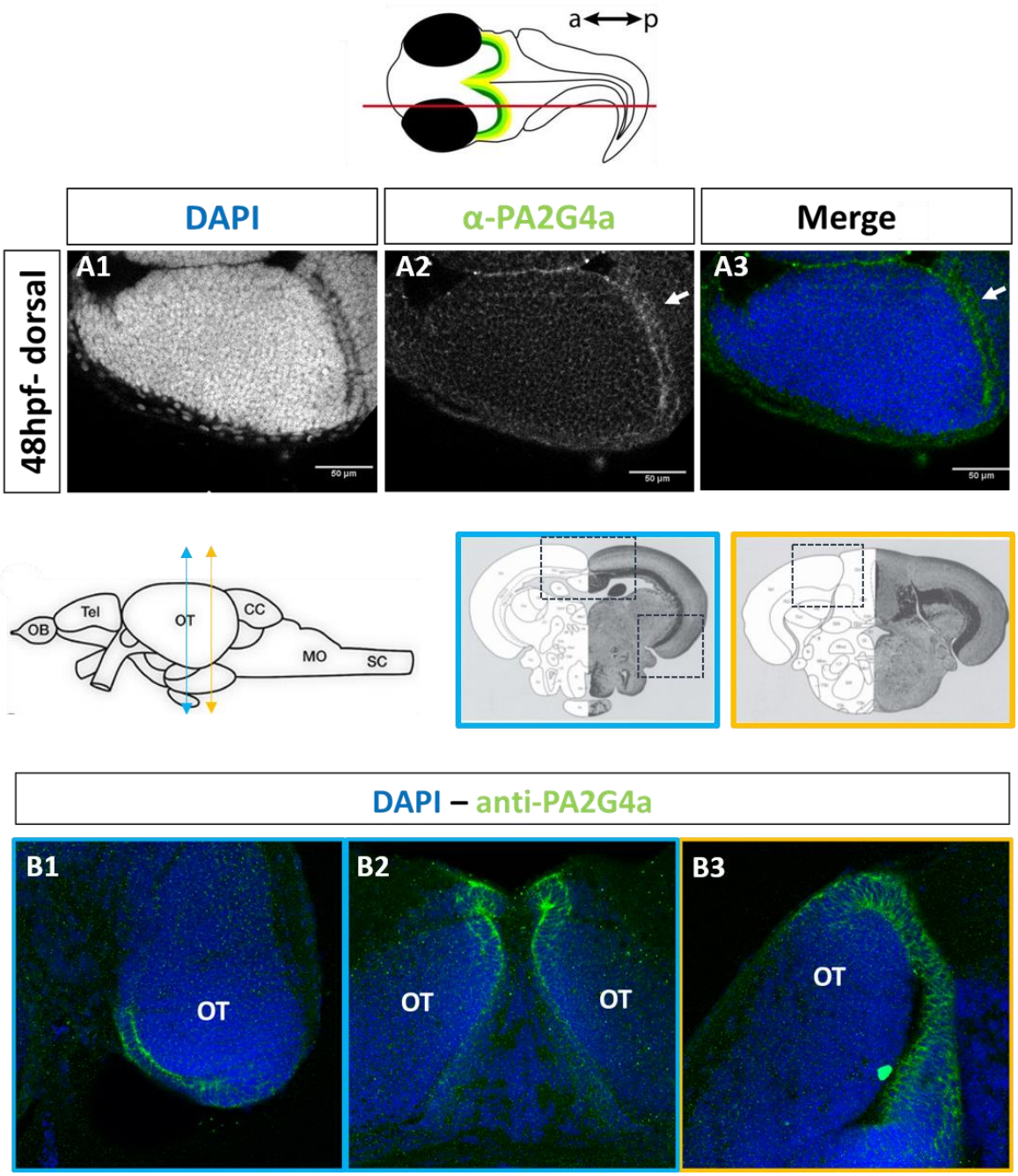

<u>Figure 46:</u> Pa2g4 immunostaining confirm peripheral restricted expression in the OT at embryonic and juvenile stages

A. Dorsal view of Pa2g4 localization in the OT of 2dpf embryos. **A1.** Nuclear staining (DAPI), **A2.** Pa2g4 staining, **A3.** Merged. Grey: blue: nuclei, green: Pa2g4 protein. White arrows indicate the accumulation of the protein in the proliferative zone of the OT. Scale bars: 50 µm. **B.** Transverse sections of juvenile OT. **B1** and **B2** correspond a medial section, two different proliferative zones of the OT are shown. **B3:** Posterior section. Blue: nuclei Green: Pa2g4 protein.

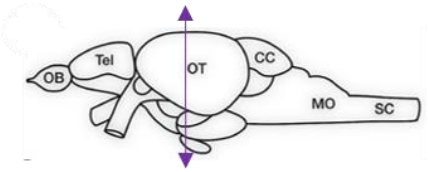
OB
Tel
OT
CC
MO
SC

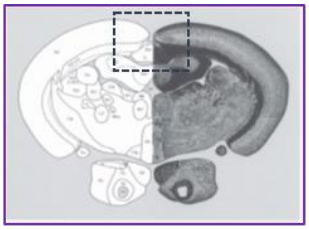

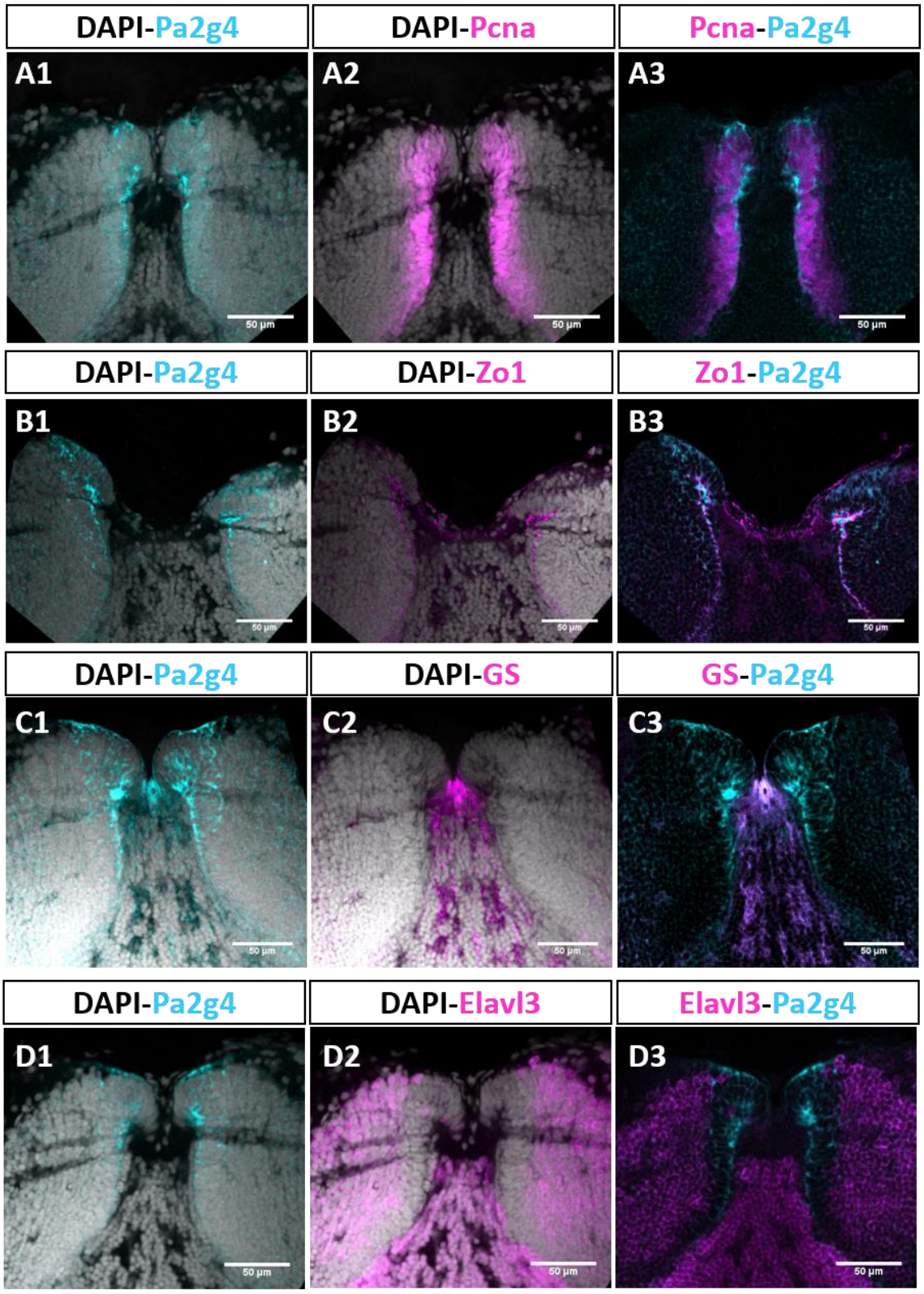
DAPI-Pa2g4
DAPI-Pcna
Pcna-Pa2g4
A1
A2
A3
DAPI-Pa2g4
DAPI-Zo1
Zo1-Pa2g4
B1
B2
B3
DAPI-Pa2g4
DAPI-GS
GS-Pa2g4
C1
C2
C3
DAPI-Pa2g4
DAPI-Elavl3
Elavl3-Pa2g4
D1
D2
D3
50 µm

Figure 47: Pa2g4 is expressed in the TMZe proliferative cells with neuroepithelial features

(A-D) IHC of PA2g4 (cyan) and markers of different cell types of the OT performed on vibratome sections (30 µm) of juvenile zebrafish brains. Nuclei are stained with DAPI (grey) **(A)** Pa2g4 (cyan) is coexpressed with the proliferative marker (PCNA-magenta). **(B)** Pa2g4 is expressed in neuroepithelial cells since it is coexpressed with the epithelial marker zonula occludens 1 (Zo1-magenta). **(C)** Pa2g4 is not present in glial cells as illustrated with the colabelling of Pa2g4 and the glial marker glutamine synthetase (GS-magenta). **(D)** Pa2g4 does not colocalize with the neural marker (Elavl3- magenta). Scale bars= 50 µm.

2.3. Development of biological tools necessary for the inducible and specific functional study of *pa2g4*

2.3.1 Strategy for the specific functional study of *pa2g4*

Given its expression pattern, *pa2g4* could be a key regulator playing a role in cell cycle and ribosome biogenesis. To analyze the potential functions of this gene in the neurogenesis of the tectum, we will overexpress Pa2g4 in the different areas of the zebrafish optic tectum (i.e the slow amplifying progenitors, and the differentiated neurons) using the inducible UAS/ERT2-GAL4 system. Therefore, we decided to generate several transgenic lines allowing the inducible and spatially restricted overexpression of the candidate gene (*fig 48*). First, I designed transgenes carrying specific regulator elements driving the expression of the inducible *gal4*. In parallel, I generated a UAS reporter transgene allowing the overexpression of Pa2g4 upon Gal4 mediated-activation. Overexpressing cells will be followed thanks to the fusion of *pa2g4* with *p2a-gfp*. So far, I generated the inducible gal4 transgenic lines which I will further describe in the rest of this chapter. The production of the UAS reporter transgenic line is ongoing.

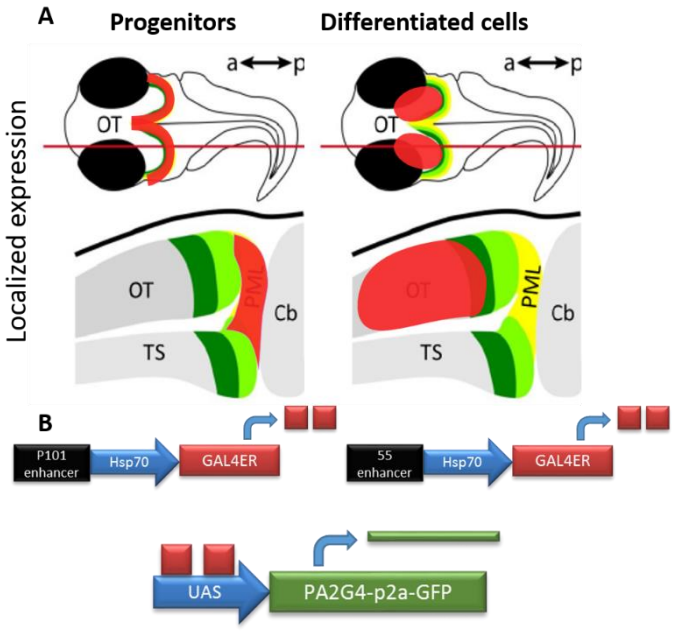

Figure 48: Strategy for the inducible and specific functional study of *pa2g4*

(A) Schematic drawing of Pa2g4 overexpression in the OT. Left panel: proliferative cells are highlighted in red. Right panel: differentiated neurons are highlighted in red. **(B)** Design of the transgenes driving *pa2g4* expression in proliferative or neurons cells. Upper panel: regulator sequences drive the expression of the inducible ERT2-GAL4. Lower panel: the UAS promoter is activated by GAL4 binding and drives the expression of *pa2g4-p2a-GFP*.

2.3.2 Tg(*enh101:ert2-gal4*) is specifically expressed in neuroepithelial progenitor cells

In our group, an enhancer (*enh101*) able to drive the expression of the downstream gene in neuroepithelial slow amplifying progenitors has been isolated and characterized (Aurélie Heuzé, personal communication). I took advantage of this enhancer to generate a new transgenic line carrying the transgene *101: ert2-gal4* that I further characterized by crossing with a Tg(*UAS:NTR-mcherry*) reporter line. I induced *ert2-gal4* expression at 2dpf and subsequently labelled mCherry expressing cells at 3dpf. Tg(enh*101: ert2-gal4*) was able to induce the expression of the mCherry at the margins of the OT (*fig 49A*). PCNA (*fig 49A*) and Elavl3 (*fig 49B*) labelling revealed the restricted enhancer activity of the transgene in the proliferative cells. Thus, Tg (*enh101:ert2-gal4*) recapitulates the expression pattern in the proliferative population. I checked that the Pa2g4 protein colocalizes with the 101:GFP positive cells to ensure that the overexpression will be confined to cells that express *pa2g4* constitutively (*fig 49C*).

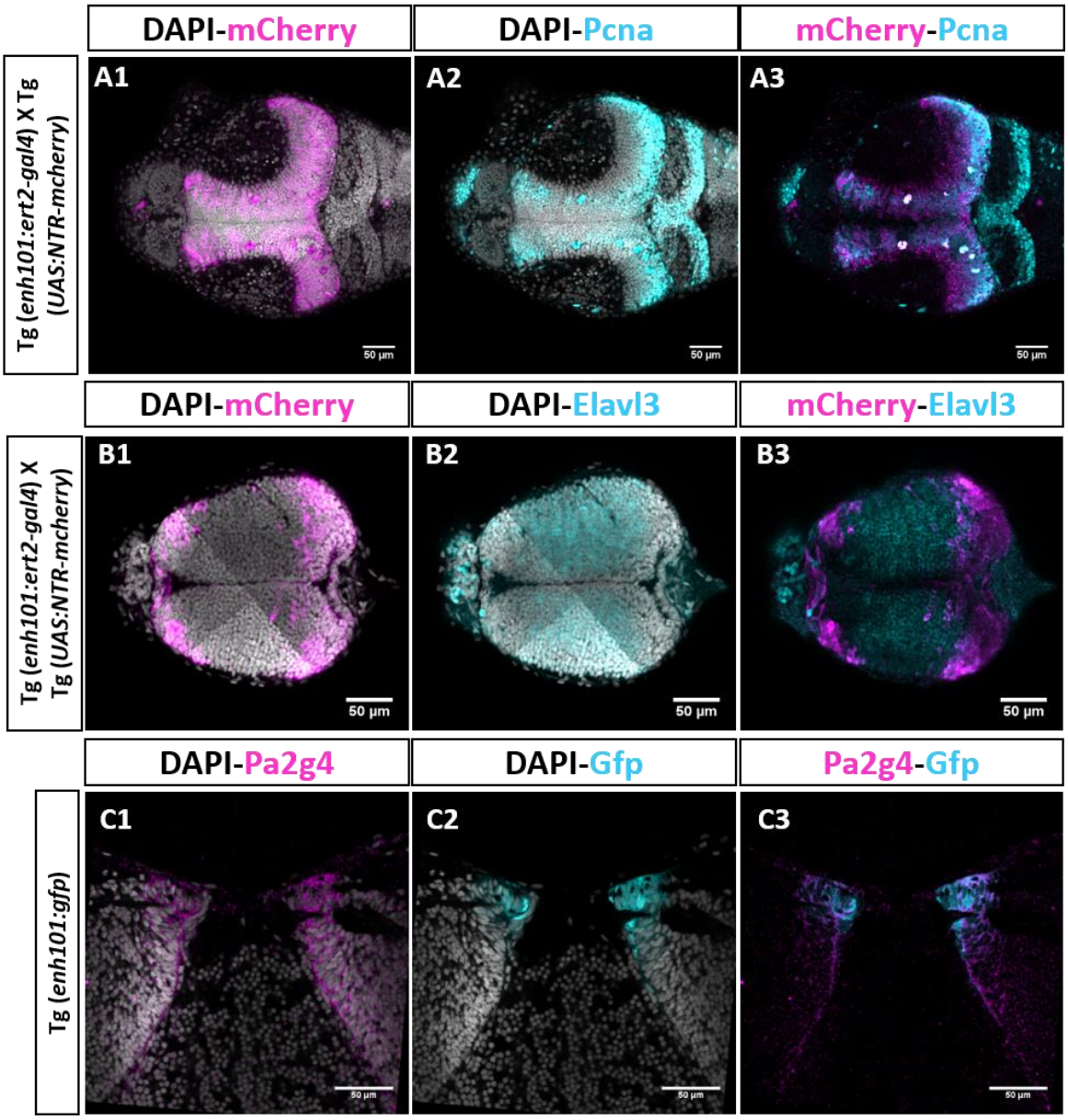

Figure 49: Tg(*enh101:ert2-gal4*) drive expression in the TMZe

(A-B) Tg(*enh101:ert2-gal4*) (gift of Aurélie Heuzé) drives the expression of the inducible Gal4 in the proliferative population of the OT at 3dpf (**A**:PCNA-positive, **B**: Elavl3-negative). Magenta: *enh101:ERT2GAL4* expressing cells, Cyan: differentiated neurons/proliferative cells, Grey: nuclei. **(C)** Pa2g4 is accumulated in the 101 positive cells. Horizontal optical sections. Anterior is on the left, posterior is on the right. Scale bars: 50 µm.

2.3.3 Tg(*enh55:ert2-gal4*) is specifically expressed in the differentiated neurons cells

To allow the overexpression of *pa2g4* in the differentiated cells, we isolated an enhancer (*enh55*) and tested its ability to drive the expression in the differentiated neurons. From this enhancer, we generated two transgenic lines. One of them allows the expression of the GFP reporter gene. It has been used to characterize the transcription activity of the enhancer and to determine the position of the differentiated cells. At 3dpf, in Tg(*enh55:GFP*), GFP is

specifically expressed in the center of the OT (*fig 50A*). Following the validation of this enhancer, we further generated an additional transgenic line allowing the expression of the inducible *ert2-gal4* construct. Similarly to the GFP reporter line, Tg(*enh55:ert2-gal4*) recapitulates the activity of the enhancer as illustrated with its colocalization with Elavl3 labelling (*fig 50B*). Fewer mCherry cells are labelling in this transgenic in comparison to Tg(*enh55:GFP*). We hypothesized that this could be due to an insufficient *ert2-gal4* induction.

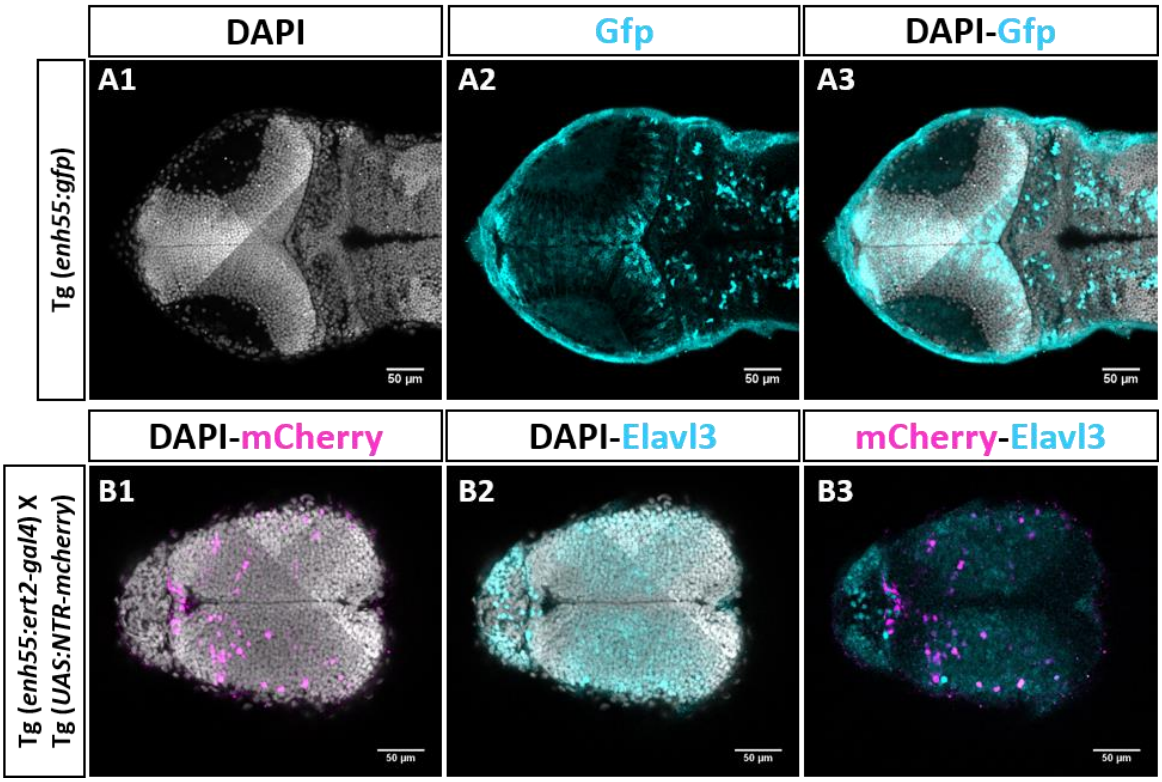

Figure 50: Characterization of the enhancer 55

(A) Tg(*enh55:GFP*) drives the expression of the fluorescent reporter gene GFP in the center of the of the OT at 3dpf. Cyan: GFP, grey: DAPI **(B)** Tg(*enh55:ert2-gal4*) drives the expression of the inducible Gal4 in differentiated neurons of the OT at 3dpf. When crossed with the UAS reporter line (*UAS:NTR-mcherry*) and induced with 4-OHT, mCherry (magenta) colocalizes with Elavl3. Horizontal optical sections. Anterior is on the left, posterior is on the right. Scale bars: 50 µm.

In conclusion, we isolated an enhancer able to drive the expression of the reporter in the differentiated neurons of the OT, and generated a transgenic line driving the expression of the inducible *ert2-gal4* in neural cells.

3. Perspectives

From transcriptomic data generated in medaka juvenile brain after cell sorting, we isolated an interesting candidate, *pa2g4*, that could be one of the key regulators of cell cycle and

ribosome biogenesis. We demonstrated that the expression of this gene, similarly to the neuroepithelial markers described in **Dambroise, Simion et al.,** is restricted to the proliferative zone of the OT at both embryonic and juvenile stages. We also highlighted the accumulation of the protein in our population of interest in juvenile brains. In this study, we then aimed to demonstrate the specific role of pa2g4a in both cell proliferation regulation and ribosome biogenesis in slow amplifying progenitors. To this aim, we generated several transgenic lines allowing the inducible and restricted overexpression of our gene of interest.

I generated biological tools allowing the specific function study of pa2g4. However, so far, no analyzes has been started as I do not have yet obtained the UAS reporter line.

On the short term, F0 injection of the UAS plasmid will be performed to allow the validation of the strategy. As *pa2g4* is involved in cell proliferation, I expect to get a specific cell cycle disruption in the proliferative population and not in the differentiated neurons. I expect to see a boost or a decrease of proliferation of fast-amplifying progenitors, and potential delays of differentiation. This will be studied by counting repeatedly several days after injection the number of cells in clones deriving from the mosaic expression of injected DNA. To further study the phenotype, I will characterize the cell types in different conditions using IHC after fixation of specimens at a chosen time following tamoxifen exposure. To analyze the impact on cell cycle, I will also use FACS to measure DNA content in the different cell types. I will also assess ribosome biogenesis using polysome profiling after cell sorting the diverse cell types.

On the other hand, we obtained a mutant for one of the two paralogs *(pa2g4b*) from the ZIRC. However, homozygous do not show any phenotype. We hypothesized that this could be due to a putative redundant role of the two paralogs. On the long term, we propose to generate a stable specific knock-out of the second paralog (*pa2g4a*) in the pa2g4b mutant line. This cell specific KO of *pa2g4a* would be generated using the CRISPR/Cas9 system, in particular the vector system developed by Ablain and colleagues (**Ablain et al., 2015**).

Since Pa2g4 has been described as either a cell cycle activator or cell cycle repressor depending on the species or the environment, further function study in the embryonic zebrafish optic tectum will give additional information to understand the role of this proliferation associated gene.

CHAPTER 3: Publication submitted in eLife: Fibrillarin is essential for S-phase progression and neuronal specification in zebrafish dorsal midbrain

Fibrillarin is essential for S-phase progression and neuronal specification in zebrafish dorsal midbrain

Stéphanie Bouffard[1], Alessandro Brombin[1,2], Emilie Dambroise[1,3], Sylvain Lempereur[4,5], Isabelle Hatin[6], Matthieu Simion[1], Raphael Corre[1,7], Franck Bourrat[1], Jean-Stéphane Joly[1,4], Françoise Jamen[1]

1- INRA CASBAH Group, Neurosciences Paris-Saclay Institute, CNRS, Université Paris-Saclay, Université Paris-Sud, Gif-sur-Yvette, France
2- Current address: MRC Human Genetics Unit, MRC Institute of Genetics and Molecular Medicine, University of Edinburgh, Edinburgh, UK
3- Current address : INSERM U1163, Université Paris Descartes, Sorbonne Paris Cité, Institut Imagine, Paris, France
4- Tefor Core Facility, TEFOR Infrastructure, NeuroPSI, CNRS, Gif-sur-Yvette, France
5- Université Paris-Est, LIGM, ESIEE, Noisy-le-Grand, France
6- Institut de Biologie Intégrative de la Cellule (I2BC), CEA, CNRS, Université Paris-Sud, Bâtiment 400, 91400 Orsay, France
7- Current address: Institut Gustave Roussy, UMR8200, CNRS, Villejuif, France

Abstract

Fibrillarin (Fbl) is a highly conserved protein playing an essential role in ribosome biogenesis and more particularly in the methylation of rRNA and rDNA histones. Zebrafish optic tectum (OT) is an ideal model to study neurogenesis because its pluripotent and differentiated cells are found in concentric partitioned domains. We previously reported an accumulation of ribosome biogenesis factor transcripts, including *fbl* mRNAs, in tectal progenitors. We show here that Fbl depletion results in tectal morphogenesis defects, impaired neural differentiation and massive apoptosis. *fbl* mutant larvae display defects in ribosome biogenesis. Strikingly, DNA content analyses revealed a disruption of cell distribution within the S-phase. *fbl* would, therefore, be involved in cell cycle regulation,

by controlling S-phase progression in tectum progenitors in particular. We discuss the mechanisms potentially underlying the S-phase disruption.

Introduction

Recently, translation has emerged as an essential step in the regulation of gene expression. Our understanding of gene expression regulation in stem and progenitor cell is gradually shifting from a simple model focusing on transcriptional control to a more complex view with additional levels of regulation, including translation. The ribosome itself stood out as a direct regulator of translation through the "specialized ribosome" and "ribosome code" concepts (Mauro and Edelman 2007). According to these new notions, ribosomes are heterogeneous, due to the existence of cell-specific ribosome biogenesis pathways. Different ribosomes "filter" the mRNA to be translated (**Mauro and Edelman, 2007**). In particular, it has been suggested that a specific ribosome biogenesis pathway occurs in stem cells and progenitors, providing new insight into stem cell homeostasis (Brombin, Joly, and Jamen 2015; Buszczak, Signer, and Morrison 2014). Thus, ribosome biogenesis is not only involved in the formation of a specialized translation machinery, but is also correlated with cell cycle regulation.

Fibrillarin (Fbl) is an essential nucleolar protein with a sequence and function conserved throughout evolution (Rodriguez-Corona et al. 2015; Shubina, Musinova, and Sheval 2016). It functions as a catalytic center of the box C/D small nucleolar ribonucleoprotein complex responsible for the correct 2'-O-methylation of ribosomal RNA (rRNA). rRNA methylation is crucial for the precise cleavage and maturation of rRNA, essential for its correct folding and association with ribosomal proteins (Mullineux and Lafontaine 2012). Fbl is also involved in the methylation of histones at rDNA loci, and plays a major role in the regulation of rDNA transcription (Tessarz et al. 2014).

In recent decades, many functional studies on Fbl have highlighted its importance in several cellular process. In particular, loss-of-function analyses in yeast and mice have shown that Fbl plays a crucial role in cell survival and early development (Schimmang et al. 1989); (Newton et al. 2003). In addition, **Watanabe-Susaki et al.** showed that Fbl was important for cell homeostasis and stem cell identity, through the regulation of pluripotency and the ability of pluripotent stem cells to differentiate (Watanabe-Susaki et al. 2014). Fbl plays a particularly important role in cell cycle regulation, as demonstrated by the abnormally high levels of this protein in several cancers, including human breast cancer (Marcel et al. 2013; Su et al. 2014), squamous cell cervical carcinoma (Choi et al. 2007) and prostatic intraepithelial neoplasia (Koh et al. 2011). **Marcel et al**. also showed that *Fbl* overexpression contributed to tumorigenesis. In breast cancer cell lines, *fbl* overexpression leads to aberrant rRNA methylation, changes in ribosome activity, poor translation fidelity and an increase in the initiation of internal ribosome entry site (IRES)-dependent translation for the products of cancer-related genes, such as IGF1R, c-Myc and FGF1/2 (**Marcel et al., 2013)**. Conversely, the repression of *fbl* with siRNA decreases the proliferation of breast cancer cells (**Su et al., 2014)**. Understanding the integrated roles of Fbl in cell cycle regulation, cell proliferation and ribosome biogenesis has, therefore, become a real challenge.

The zebrafish optic tectum (OT) displays oriented growth during development, leading to the formation of ordered columns of cells with different levels of differentiation, from the periphery towards the center of the structure. This cellular model is thus ideal for studies of the specific role of Fbl in cell cycle regulation and cell homeostasis (**Joly et al., 2016**). At early stages of development, the proliferative neural population is located throughout

the alar plate. Following somitogenesis, progenitor cells differentiate into functional neurons, which are found at the center of the OT. However, proliferation persists in a small zone of the midbrain, at the periphery of the optic tectum. This zone, homologous to the proliferative zone of the retina, is called the tectal marginal zone (TMZ; **Joly et al., 2016**). Using live imaging, we previously identified two types of progenitors on the basis of their rates of proliferation in the transparent embryo (Recher et al. 2013). The neuroepithelial progenitors located at the external edge of the TMZ (TMZe) are slow-amplifying progenitors (SAPs). SAPs divide and give rise to fast-amplifying progenitors (FAPs) located in the intermediate layer (TMZi, **Joly et al., 2016**). Each cell population is characterized by the preferential expression of various genes. In particular, genes encoding ribosome biogenesis factors, such as components of the box C/D complex, and *fbl* in particular, are strongly expressed in SAPs, whereas these "housekeeping" genes are less strongly expressed in FAPs (Recher et al. 2013).

These striking observations led us to suggest that Fbl might be involved in cell cycle regulation in the slow-amplifying progenitors. We therefore performed an *in vivo* functional analysis of Fbl by characterizing zebrafish null mutants for *fbl*. Homozygous mutant embryos had smaller brains and a deregulated cell cycle. Our findings reveal, for the first time, the specific role of Fbl in midbrain development and the regulation of S-phase progression.

Results

Neuroepithelial slow-amplifying progenitor (SAPs) expressed high levels of *fibrillarin* transcripts and proteins.

We first characterized the *fibrillarin (fbl)* gene expression pattern during zebrafish embryogenesis, by whole-mount *in situ* hybridization (WMISH). We found that *fbl* was

ubiquitously expressed during gastrulation (6 hours post-fertilization (hpf), *fig 1A*). At the onset of neurulation, Fbl mRNAs begins to accumulate in the eyes, brain and somites (*fig 1B*). From 1 day post-fertilization (dpf), *fbl* expression begins to be restricted to the OT, retina, gut and somites (*fig 1C2-C3*). At the long-pec (2 dpf) and protruding mouth (3 dpf) stages, high levels of *fbl* expression are observed at the periphery of the OT, in the external tectal marginal zone (TMZe) in which SAPs divide. This gene is also expressed at the extreme edge of the retina, in the CMZ, in which the progenitors and stem cells are localized (*fig 1D-E*). Hence, *fbl* has an expression pattern similar to that of SAP-specific genes (**Recher et al., 2013**). These results demonstrated that *fbl* pattern of expression is progressively restricted during zebrafish embryogenesis. In particular, *fbl* is preferentially expressed in the proliferating cells of the OT and retina, which are thought to be sister cell types (**Joly et al., 2016**). Immunohistochemistry (IHC) analysis revealed the presence of Fbl protein in all tectal cells, within the nucleoli, but this protein preferentially accumulated

at the extreme edge of the OT, where the SAPs are found (*fig 1F*). These findings indicate that Fbl may play an essential role in tectal cell proliferation.

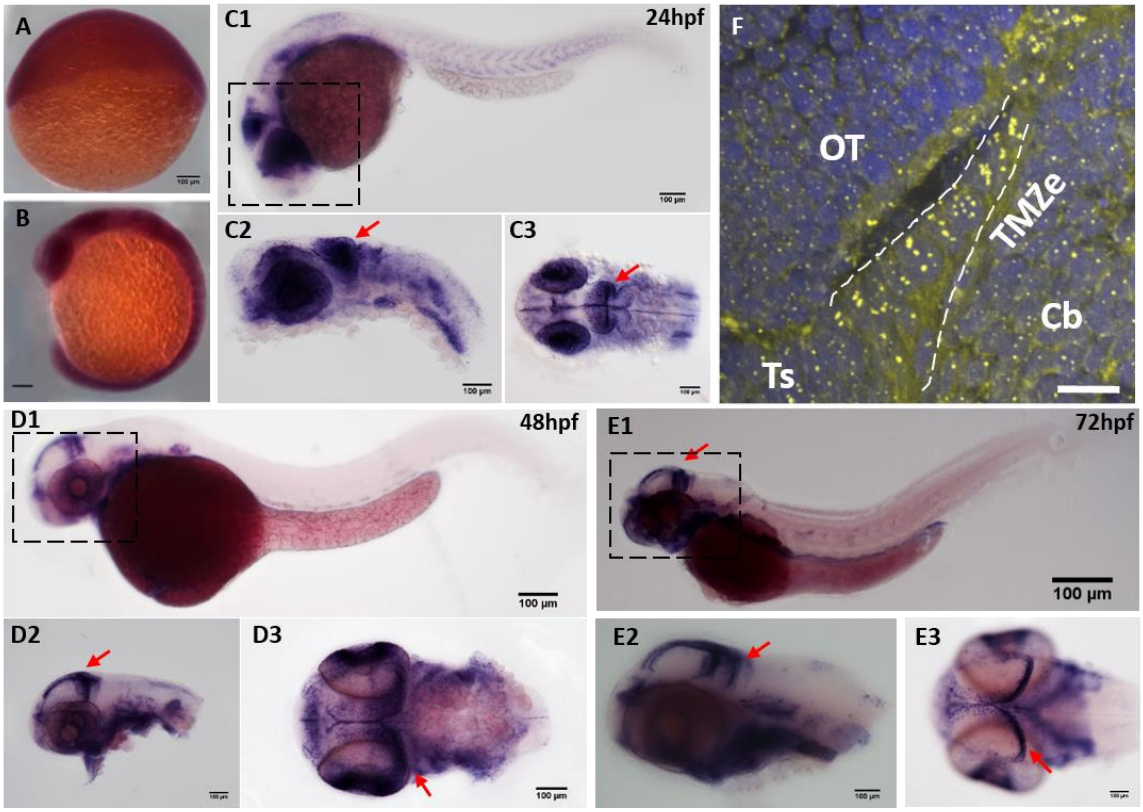

Figure 1: *fbl* expression is restricted to neural progenitors during zebrafish development
(A-E) *In situ* hybridization showing the progressive restriction of *fbl* expression during the development of zebrafish embryos **(A)** *fbl* is ubiquitously expressed at 6 hpf. **(B)**. *fbl* expression begins to be restricted to highly proliferative regions (eyes, midbrain, and somites) during neurulation **(C)** At 1dpf, *fbl* transcripts are abundant in the optic tectum (red arrows) and the retina. C1-C2: lateral views, C3: dorsal view **(D-E)** At 2 dpf **(D)** and 3 dpf **(E)**, *fbl* is preferentially expressed in the neuroepithelial progenitors of the TMZe at the periphery of the OT (red arrows), and in the ciliary marginal zone of the retina. Additional expression can be detected in the digestive system D1-D2 and E1-E2: lateral views, D3 and E3: dorsal views. Scale bars: 100 µm. Anterior is to the left.
(F) Immunostaining showing Fbl protein on a sagittal section of a 2 dpf embryo. The Fbl protein, which is localized in the nucleoli, is present in all cells (yellow dots) but the punctate domains of expression are larger in TMZe neuroepithelial progenitors (surrounded by white dashed lines) than in other cells in the optic tectum (OT), cerebellum or *torus semicircularis*. Scale bars: 25 µm. Cb: cerebellum; OT: optic tectum; *Ts: torus semicircularis*;; TMZe: external tectal marginal zone.

Mutation of the zebrafish *fbl* gene leads to a smaller brain volume and larval death

We investigated the function of Fbl in tectal cell proliferation, in a mutant line previously generated by inserting a 6 kb retroviral sequence into the 5'UTR of the *fbl* gene (Amsterdam et al. 2004). Heterozygous embryos develop normally. By contrast, homozygous *fbl*^{hi2581} mutant embryos begin to display phenotypic differences relative to their control siblings as early as 1dpf *(fig 2A*). From this stage onwards, tissue

disorganization was observed, particularly in the head (*fig 2A2*, black arrow). At 2 dpf (*fig 2A3-A4*) and 3dpf (*fig 2A5-A6*), homozygous mutants exhibited disrupted melanocyte lineage, smaller eyes and heads, pericardiac edema, and a larger and rounder yolk with a thinner yolk extension than the wild type. At 4 dpf, the brain abnormalities became more pronounced, probably due to general defects along the whole body axis of the embryo (data not shown). The *fbl*^{hi2581} larvae had a smaller body, with an increasingly curved tail, and they died by day 4 or 5 post-fertilization.

We quantified brain defects at 3 dpf, by measuring the volume of the central nervous system (CNS; including brain and eyes) by staining lipidic structures with DiI, obtaining 3D images by confocal microscopy and manually segmenting the brain (*fig 2B*).

CNS volume was significantly smaller in *fbl*^{hi2581} larvae than in their siblings not homozygous for the mutation at the same developmental stage. More precisely, CNS volume in the mutants was one third that in their siblings or the wild-type larvae (*fig. 2C*). We also quantified the eye volume in *fbl* mutant, siblings and wild-type larvae. Interestingly, the eye volume of the mutant larvae were five times reduced in comparison with the siblings and wild-type larvae (*fig 2D*). Collectively, these data suggest a role of Fbl in the development of the brain and the eye.

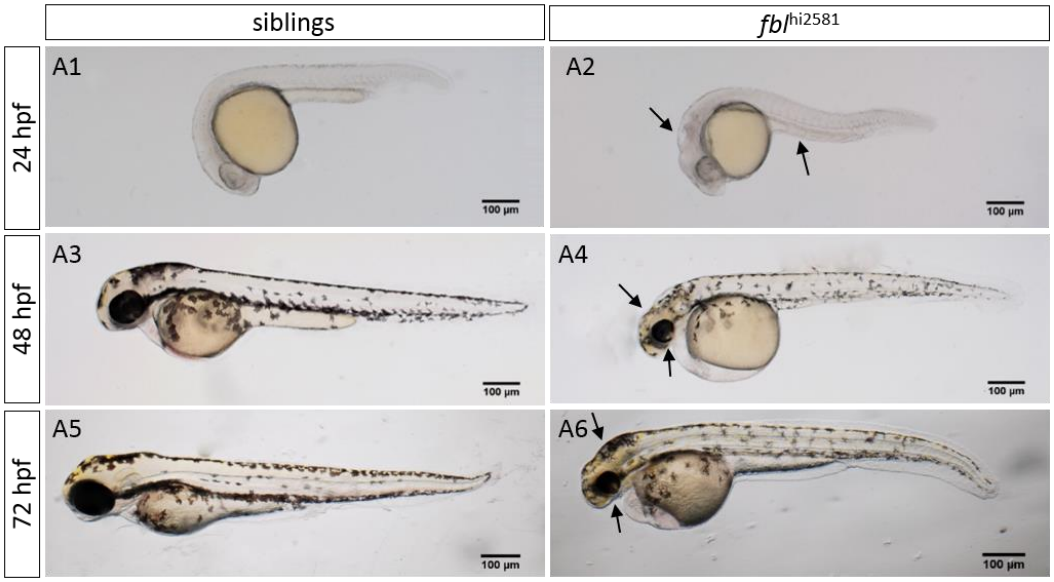
siblings
fbl hi2581
24 hpf
48 hpf
72 hpf
A1
A2
A3
A4
A5
A6
100 µm

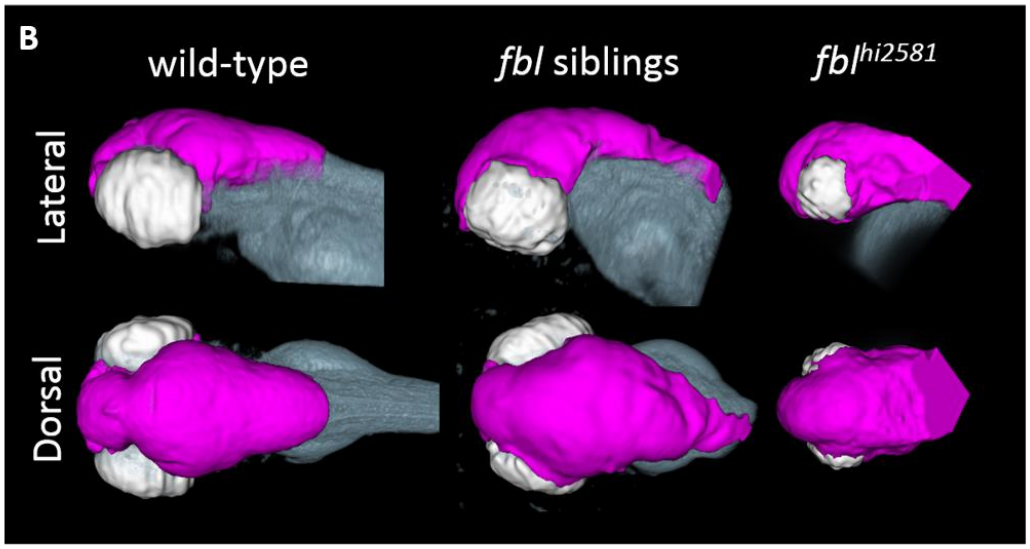
B
wild-type
fbl siblings
fbl hi2581
Lateral
Dorsal

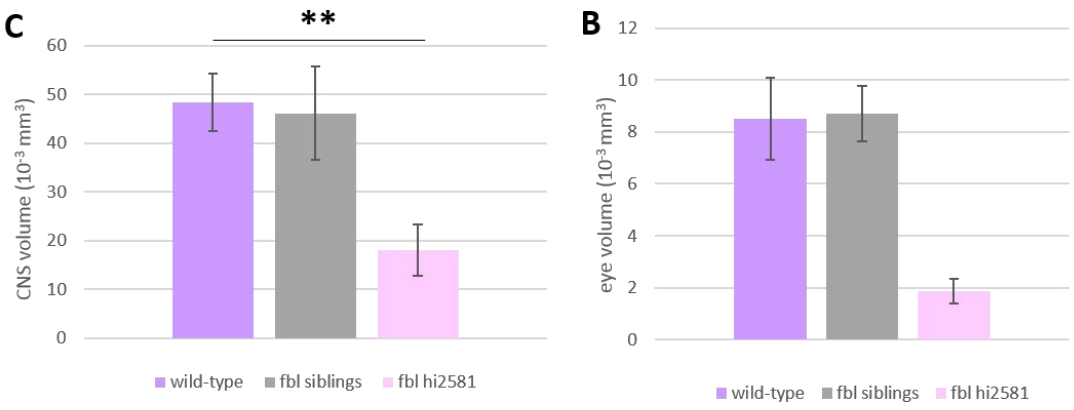
C
**
CNS volume (10-3 mm3)
60
50
40
30
20
10
0
wild-type
fbl siblings
fbl hi2581
B
eye volume (10-3 mm3)
12
10
8
6
4
2
0
wild-type
fbl siblings
fbl hi2581

Figure 2: The *fbl* ^{hi2581} mutation is lethal at larval stages and mostly affects midbrain structures from 1 dpf.
(A1-A2) *fbl*^{hi2581} mutants start to display phenotypic abnormalities as early as the 1 dpf stage. Mutant embryos have disorganized tissues in the brain (black arrow). At 2 dpf **(A3-A4)** and 3 dpf **(A5-A6)** mutant larvae development is impaired, mostly in the midbrain and retina (black arrows). In addition, mutant embryos have impaired pigmentation, a thinner yolk extension, a larger, rounder yolk and pericardiac edema. Black arrows highlight midbrain defects. **(B)** Volume rendering of the DiI-positive domains (grey) and surface rendering of a manual segmentation of the CNS (magenta) and eye (white) based on the DiI signal in 3dpf wild-type, *fbl* siblings and *fbl*^{hi2581} mutant embryos. *fbl* mutant larvae display apparent reduction of the CNS volume compared to their siblings or wild-type larvae Lateral views: anterior to the left, dorsal to the top. Dorsal view: anterior to the left, right to the top. **(C)** Quantification of mean CNS volume highlights a significant difference between *fbl* mutants, their siblings and wild-type larvae. Statistical analyses were performed on six samples per condition. *p*-value: 0.003 (Kruskal-Wallis test). (**D**) Quantification of mean eye volume highlights a significant difference between *fbl* mutants, their siblings and wild-type larvae. Statistical analyses were performed on six samples per condition. *p*-value: 0.003 (Kruskal-Wallis test). Purple: wild-type, gray: *fbl* siblings, pink: *fbl*^{hi2581}. Scale bar: 100 µm. Anterior is to the left.

Ribosome biogenesis is affected in *fbl*^{hi2581} mutant embryos

Fbl is involved in the methylation of rRNA and rDNA histones. We therefore hypothesized that *fbl* loss of function would lead to lower levels of rDNA transcription and a disruption of ribosome biogenesis. Ribosome biogenesis begins with transcription of the 47S intermediate rRNA, which contains a 5' externally transcribed sequence (ETS) and two internally transcribed sequences (ITS1 and ITS2). The intermediate 47S rRNA is processed after its transcription: the 5' ETS is cleaved first, followed by the ITS1 and ITS2, to generate the mature 18S, 5.8S and 28S rRNAs. The 5' ETS, ITS1 and ITS2 are used to estimate relative rRNA transcription levels.

We used RT-qPCR to investigate rDNA transcription and rRNA processing by quantifying the levels of 5'ETS, 18S, ITS1 and ITS2 rRNA. At 3dpf, 18S mature rRNA levels were significantly lower (93% lower) in *fbl*^{hi2581} larvae, whereas we did not observed any significant differences in *fbl* siblings larvae and wild-type larvae (*fig 3A*). Surprisingly, 5' ETS rRNA levels were slightly higher in *fbl*^{hi2581} larvae than in the wild type. However, ITS1 and ITS2 rRNA levels did not differ between the three genotypes (*fig 3A*). Overall, these data indicate that 47S rDNA transcription is not impaired in *fbl*^{hi2581} mutant embryos, but that rRNA processing is greatly impaired, as demonstrated by the relative levels of mature 18S rRNA.

As 18S rRNA processing is considered to be a rate-limiting step in ribosome biogenesis (Laferté et al. 2006), we hypothesized that impaired rRNA processing in *fbl*^{hi2581} mutant embryos and possible subsequent alterations to rRNA posttranslational modifications would result in an overall decrease in ribosome biogenesis. We used polysome profiling to evaluate ribosome biogenesis in 3 dpf *fbl* mutant embryos, control siblings and wild-type embryos (*fig 3B-C*). Fewer polysomes were observed. The polysomal fraction, which corresponds to ribosomes bound to mRNA, provides an indication of the translational activity of the ribosomes. Polysome peaks were smaller for the mutant larvae than for their siblings and wild-type larvae, indicating that smaller numbers of ribosomes were bound to mRNA in the mutants (*fig 3B*). Thus, for every seven ribosomes binding mRNA in wild-type and sibling embryos, only five were bound to mRNA in *fbl*^{hi2581} embryos. We measured the area under each peak, and calculated the ratio between the 80S and polysome peaks (*fig 3B-C*). The polysome ratio was lower in the mutants than in the wild-type embryos, highlighting lower levels of ribosomal activity.

We performed similar experiments at 2 dpf, when the embryos were less affected. Despite the similarity of the defects observed (data not shown), differences in ribosome biogenesis between wild-type and mutant embryos were less marked. This is not surprising and highlights the worsening of the phenotype as development proceeds. Collectively, these data suggest that *fbl* mutation leads to an impaired ribosome biogenesis at late steps of the pathway and lower levels of ribosome activity.

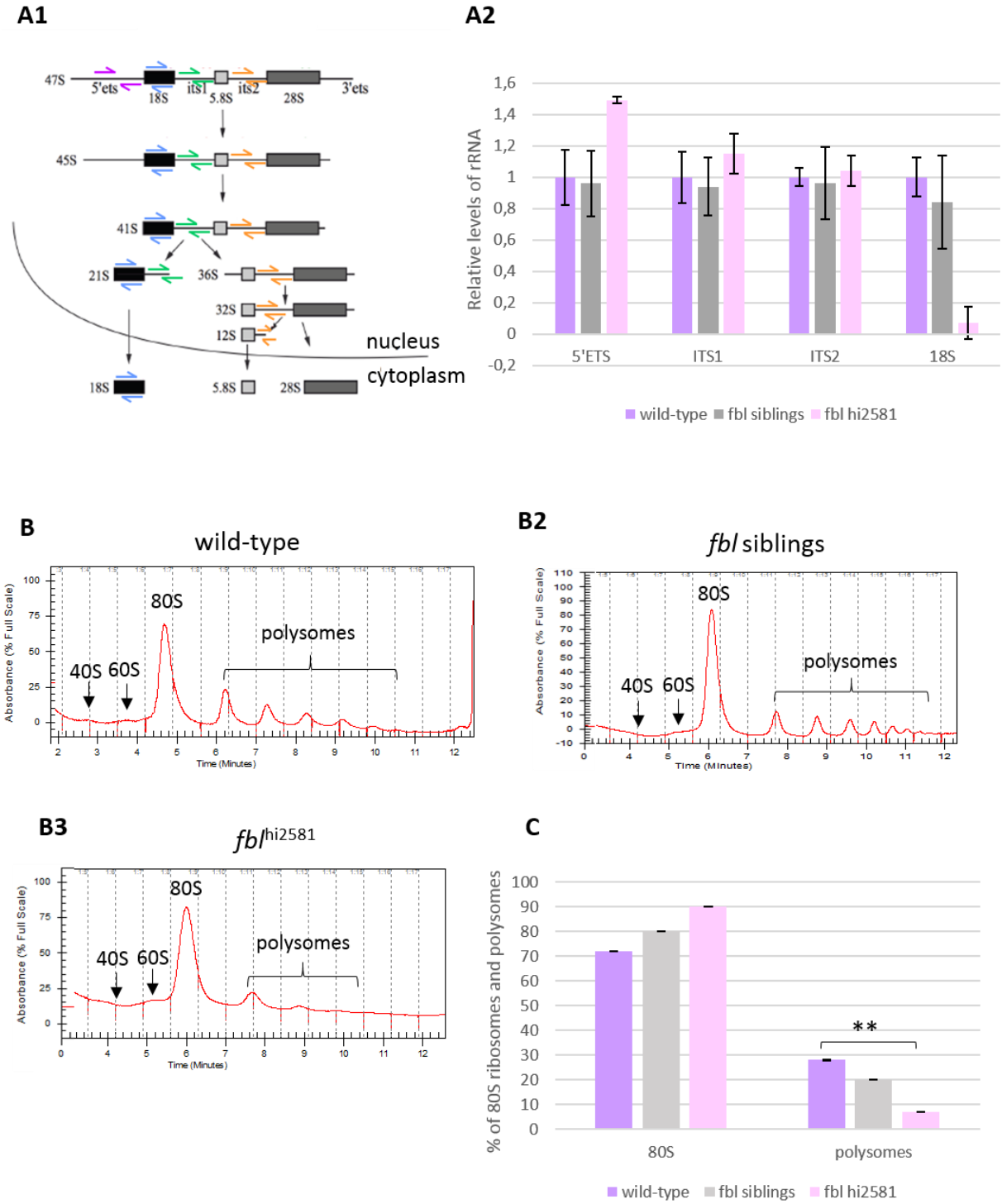
A1
47S
5'ets
18S
its1
5.8S
its2
28S
3'ets
45S
41S
21S
36S
32S
12S
nucleus
cytoplasm
18S
5.8S
28S
A2
Relative levels of rRNA
1,6
1,4
1,2
1
0,8
0,6
0,4
0,2
0
-0,2
5'ETS
ITS1
ITS2
18S
wild-type
fbl siblings
fbl hi2581
B
wild-type
Absorbance (% Full Scale)
80S
polysomes
40S
60S
Time (Minutes)
B2
fbl siblings
Absorbance (% Full Scale)
80S
polysomes
40S
60S
Time (Minutes)
B3
fbl hi2581
Absorbance (% Full Scale)
80S
polysomes
40S
60S
Time (Minutes)
C
% of 80S ribosomes and polysomes
100
90
80
70
60
50
40
30
20
10
0
**
80S
polysomes
wild-type
fbl siblings
fbl hi2581

Figure 3: Ribosome biogenesis is impaired in *fbl* mutant embryos
(A) RT-qPCR quantification of 5'ETS, ITS1, ITS2 and 18S rRNAs in mutant, siblings and wild-type larvae at 3 dpf. **A1**: Scheme of rRNA processing, adapted from (**Le Bouteiller et al., 2013**). Arrows indicate the location of the amplified regions: 18S: purple, 5'ETS: blue, ITS1: green and ITS2: orange. **A2**. Mutant embryos have lower levels of 18S rRNA (93% lower). **(B)** Polysome profiling of 3 dpf wild-type **(B1)**, *fbl* siblings **(B2)** and *fbl*^{hi2581} mutant **(B3)** embryos showed a lower polysome ratio in *fbl*^{hi2581} larvae, indicating impaired ribosomal activity in these larvae. **(C)** Quantification of the relative proportions of 80S and polysomes (ratio of the 80S or polysome area with global area). Statistical analyses were performed on four samples per condition. *p*-value (Kruskal-Wallis test) polysomes: 0.0041. Purple: wild-type, gray: *fbl* siblings, pink: *fbl*^{hi2581}

The dorsal midbrain is the brain structure most strongly affected in *fbl*^{hi2581}

We demonstrated that *fbl*^{hi2581} larvae displayed smaller CNS. To further characterized those brain defects, we analyzed the different regions of the brain by DiI and Elavl3 (marker of neural differentiation) labeling and generated 3D visualization of the stained larvae (supplemental data, movie 1). Several basal domains, such as the telencephalon, olfactory epithelium and hypothalamus, were conserved but disorganized (*fig 4A*). We also detected the presence of the tracts of the anterior (tac) and post-optic commissures (tpoc), which are ventral/basal brain structures (*fig 4A*). Overall, these data suggest that the *fbl* mutation leads to correct differentiation events in the ventral part of the brain, and to the generation of most of the domains of the brain.

Surprisingly, histological analyses revealed that 2 dpf mutants had a smaller tectum than their siblings (*fig 4B*). Moreover, acellular holes were detected in this midbrain structure (*fig 4B2-B4*). However, the proliferative region of the TMZe seemed to be correctly formed, but thicker than stage-matched WT embryos (*fig 4B2*, white arrows). Thus, the mutation strongly affects the midbrain and retina, structures in which the *fbl* gene is preferentially expressed, consistent with a specific role for Fbl in these regions.

Fbl is known to be required for the maintenance of normal nucleolar morphology, but its function in nuclear morphology remains unclear (Amin et al. 2007; Ma et al. 2016). We therefore studied nuclear and nucleolar morphologies in control and mutant embryo midbrains. DAPI staining of the nucleus revealed differences in nuclear shape between *fbl* mutant larvae and their siblings (*fig 4C*, purple). Wild-type embryos had round nuclei at the center of the OT and in FAPs. By contrast the nuclei in the SAPs were more elongated and had larger nucleoli (**Recher et al, 2013**). Surprisingly, in *fbl*^{hi2581} embryos, the nuclei of cells over the entire surface of the tectum were elongated, and resembled those of wild-type SAPs (*fig 4C*).

By contrast, the nuclei of the ventral structure of the midbrain, the torus semicircularis (TS) presented no change in shape (data not shown). On 3D views, we selected the larger axis of the nuclei for measurements. The quantification of nuclear diameters in the OT and TS of wild-type and mutant embryos indicated a specific increase of the area within the OT, with no change in the TS (*fig 4D*). Indeed, wild-type tectal nuclei had a mean longest diameter of 7 µm, whereas *fbl*^{hi2581} tectal nuclei reached diameters of up to 12 µm. By contrast, the nuclei in the TS of both mutant and wild-type embryos had a mean diameter of 6 µm. These findings suggest that the dorsal part of the midbrain was mostly affected in *fbl* mutant embryos.

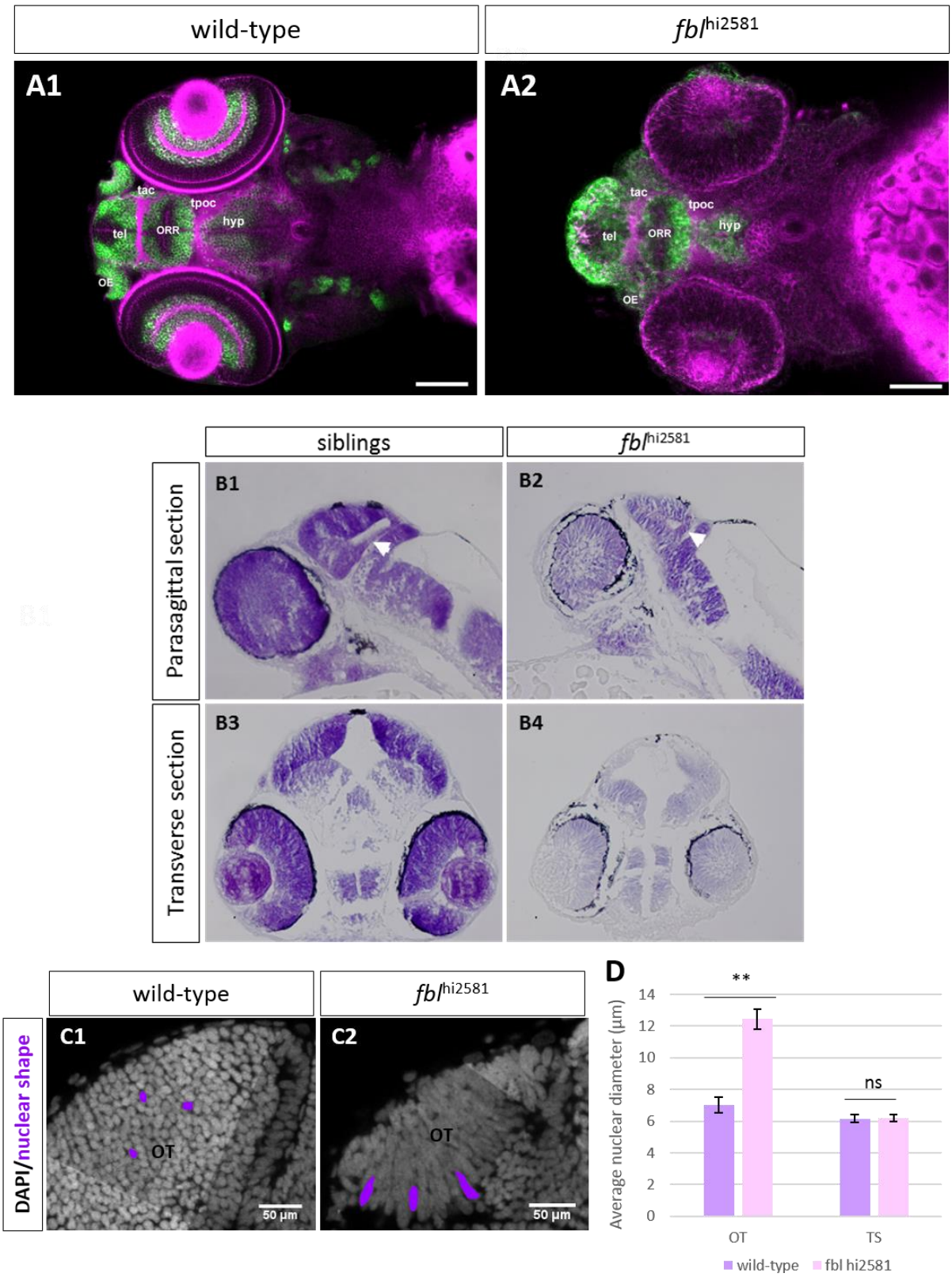
wild-type
fbl hi2581
A1
A2
tac
tpoc
hyp
tel
ORR
OE
siblings
fbl hi2581
Parasagittal section
Transverse section
B1
B2
B3
B4
wild-type
fbl hi2581
DAPI/nuclear shape
C1
C2
OT
50 µm
D
Average nuclear diameter (µm)
**
ns
OT
TS
wild-type
fbl hi2581

Figure 4: ***fbl*** **mutants have specific midbrain and retina defects**
(A) Horizontal optical sections of Elavl3 (marker of neural differentiation) immunolabelling and DiI staining in wild-type **(A1)** and mutant **(A2)** embryos at 3dpf. Pink: DiI labeling, Green: Elavl3 staining. Scale bars: 100 µm. Anterior is to the left. Most brain domains and axon tracts are present but have a disrupted organization in *fbl* mutant embryos. **(B)** Sagittal (A1-A2) and transverse (A3-A4) paraffin sections of wild-type (left) and *fbl*^{hi2581} mutant (right) embryos at 2dpf. Histological analysis with cresyl violet staining revealed smaller tecta and acellular holes in the mutant embryos. The proliferation region (TMZe) is thicker in the mutant embryos (white arrow) **(B2, B4)** than in their siblings **(B1, B3)**. Anterior is to the left. (**C**) Nuclear labeling (DAPI) in the optic tectum of 2dpf wild-type **(C1)** and mutant **(C2)** embryos at 2dpf, showing the larger nuclear diameter in the tectum of mutant larvae. Scale bar: 50 µm **(D)** Quantification of the nuclear diameter of wild-type (purple) and *fbl*^{hi2581} (pink) 2dpf embryos. Nuclear diameters were measured with Fiji software. We measured the longest dimension of 50 nuclei on selected 2D images of the nuclei of 2 dpf embryos. Statistical analyses were performed on the mean diameters of nuclei from five mutant or wild-type embryos. *p*-value (Mann & Whitney test) OT: 0.008; *p*-value TS: 1.000. Hyp: hypothalamus, OE: olfactory epithelium, ORR: optic recess region OT: optic tectum, tac: tract of the anterior commissure, tel: telencephalon, tpoc: tract of the post-optic commissure, *TS: torus semicircularis*

Neuronal specification and differentiation are impaired in mutant embryos

The dorsal midbrain patterning defects observed suggested that neural specification and differentiation might also be impaired in this region. We first addressed this question by quantifying *neuroD1* mRNA levels by RT-qPCR to assess neural specification. Interestingly, we found that *neuroD1* expression levels were 91% lower in mutant embryos than in wild-type embryos (*fig 5A*). Neural specification was, therefore, disrupted in *fbl* mutant embryos.

We also analyzed neural tissue specification in the different regions of the brain, by analyzing the expression pattern of *eomes* and *otx2* by in situ hybridization (ISH), which are involved in the specification of the anterior territories of the developing brain. *otx2* expression is an anterior brain marker in the neural tube but becomes restricted to the developing midbrain later in development, whereas *eomes* is specifically expressed in the forebrain. In mutant embryos, at both 2 dpf (*fig 5B1-B2*) and 3 dpf (data not shown), *eomes* expression was maintained in the developing forebrain. By contrast, *otx2* expression was affected in the dorsal midbrain of mutants, whereas the expression of this gene was unaffected in the most ventral and anterior domains in mutants (*fig 5B3-B4*). These findings

reveal the presence of midbrain-specific defects in neural specification in *fbl* mutant embryos.

We then analyzed neural differentiation, by immunohistochemical staining for Elavl3, a marker of neural differentiation. Neural differentiation begins at 2 dpf in wild-type embryos, and tectal Elavl3-positive neurons are located in the center of the optic tectum. At this stage, no Elavl3 labeling was detected in mutant embryos (*fig 5C*).

We investigated possible links between this phenotype and developmental delay, by analyzing neural differentiation at 3 dpf. In *fbl*^{hi2581} embryos, no Elavl3-positive neurons were detected in the dorsal midbrain at 3 dpf (*fig 5D-5E*), whereas a few Elavl3-positive neurons were detected ventrally in the TS (*fig 5E*) and posteriorly in the spinal cord (data not shown). These data indicate that neural differentiation is specifically impaired in the dorsal midbrain structures of *fbl*^{hi2581} mutant embryos, suggesting that tectal neuronal progenitors are affected.

These results suggest that the neuronal lineage is specifically disrupted in the dorsal midbrain of *fbl* mutants. This finding is consistent with a tissue-specific role of Fbl in midbrain morphogenesis.

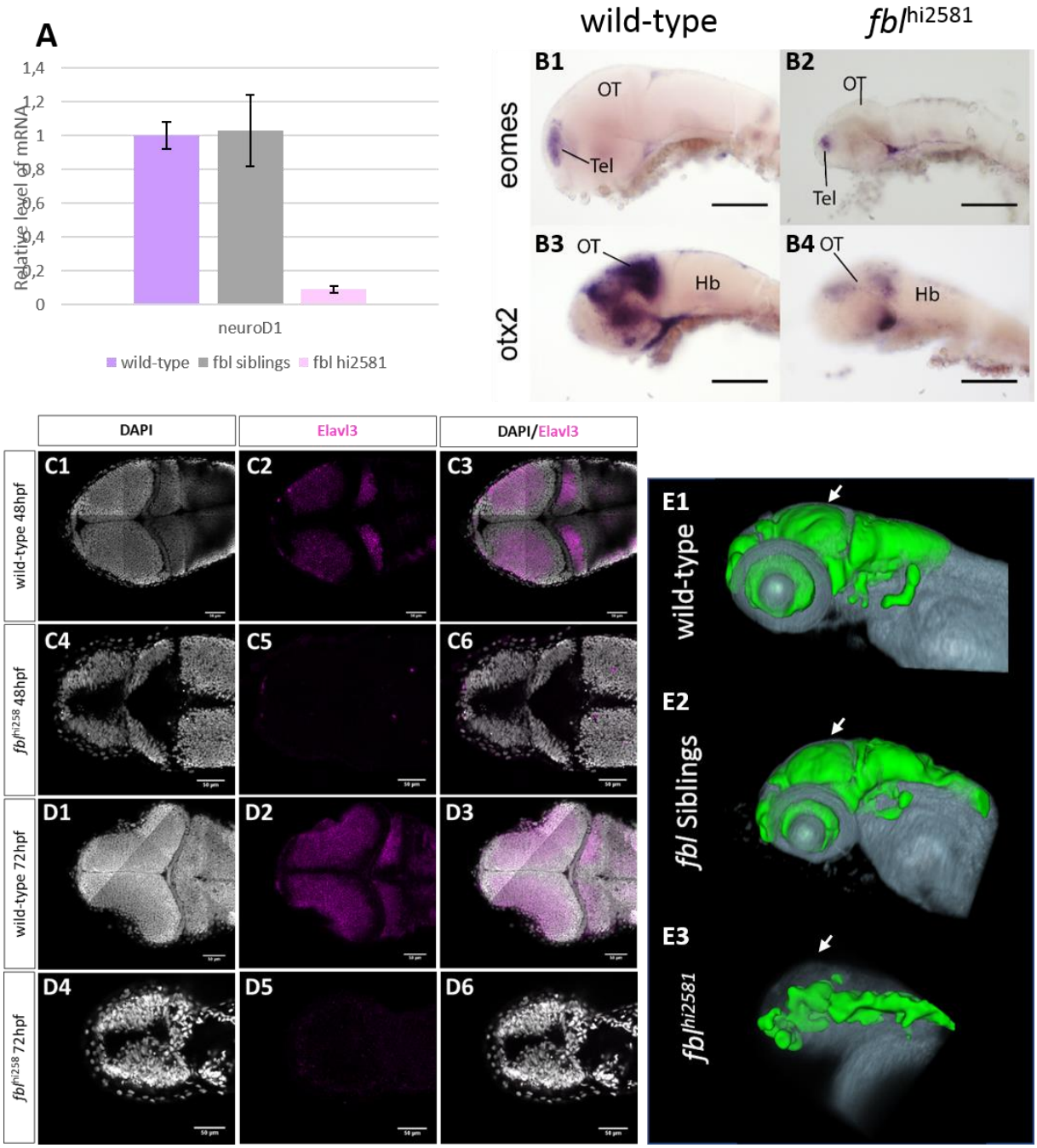

Figure 5: Neural specification and neural differentiation are impaired in *fbl*^{hi2581} mutant embryos.
(A) RT-qPCR quantification of the relative levels of *neuroD1* mRNA. Purple: wild-type, gray: siblings, pink: mutants. **(B)** Expression patterns of *eomes* and *otx2*, two markers of neural specification, in 3 dpf wild-type **(B1, B3)** and *fbl*^{hi2581} mutant embryos **(B2, B4)**. The expression of *eomes* **(B1-B2)**, a marker of forebrain specification, was similar in wild-type and mutant embryos, whereas that of *otx2* **(B3-B4)**, a marker of midbrain specification, disappeared in *fbl*^{hi2581} mutant embryos. Scale bars: 50 µm. Hb: hindbrain, OT: optic tectum, Tel: telencephalon. **(C)** Horizontal optical sections of *elavl3* (marker of neural differentiation) labeling in 2dpf wild-type **(C1-C3)** and mutant **(C4-C6)** embryos and in 3dpf wild-type **(D1-D3)** and mutant **(D4-D6)** embryos. Gray: DAPI staining, pink: Elavl3 staining. Scale bars: 50 µm. Anterior is to the left. (**E**) Volume rendering of the DiI-positive domains (grey) and surface rendering of a manual segmentation of the Elavl3-positive (green) domains in 3dpf wild-type (**E1**), *fbl* siblings (**E2**) and *fbl*^{hi2381} mutant embryos (**E3**). For lateral views, anterior to the left and dorsal to the top. White arrows point out to the midbrain. Neural differentiation is specifically impaired dorsally in *fbl* mutant.

Mutant cells undergo massive apoptosis

We investigated the mechanisms underlying the apparent decrease in tectum neuronal differentiation and the presence of acellular holes in the OT, by evaluating the role of *fbl* in cell survival. We therefore performed TUNEL staining (*fig 6*), to label DNA breaks. At 1 dpf, cell death rates were higher in *fbl*^{hi2581} mutant embryos than in wild-type embryos (*fig 6A*).

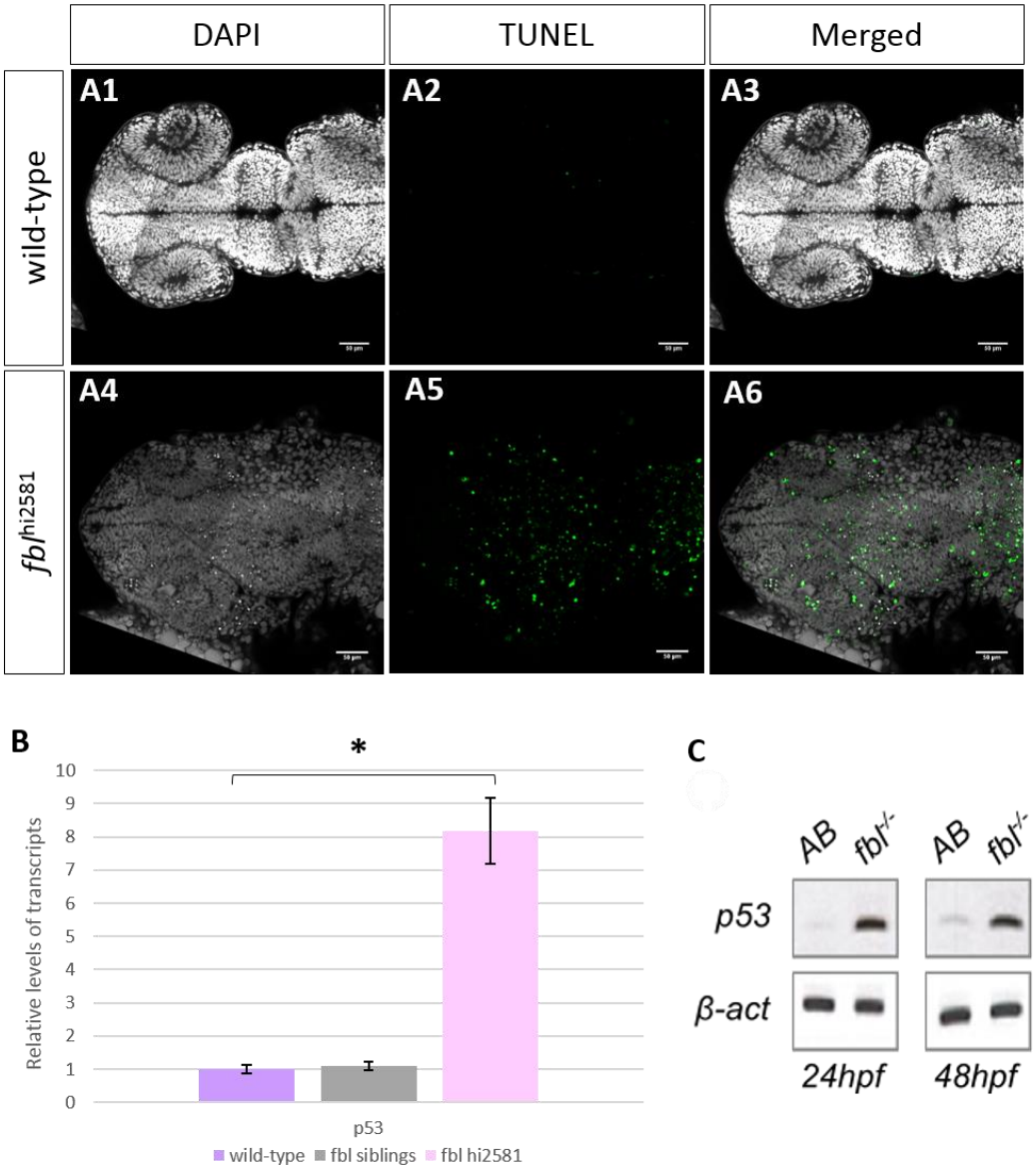

Figure 6: Massive p53-dependent apoptosis in the *fbl* mutant
(A) Horizontal optic sections of TUNEL labeling at 1 dpf in wild-type **(A1-A3)** and mutant **(A4-A6)** embryos. Gray: DAPI staining, Green: TUNEL staining. Scale bar: 50 µm. Anterior is on the left. **(B)** RT-qPCR quantification of relative levels of *tp53* mRNA at 3 dpf shows a strong increase in *tp53* expression in mutants. Purple: wild-type, gray: siblings, pink: mutants. Statistical analyses were performed on biological triplicates, *p*-value (Kruskal-Wallis test): 0.049. **(H)** RT-PCR for *tp53* in 1 dpf and 2 dpf mutant embryos showing a large increase in *tp53* expression. Anterior is to the left.

Cell culture studies have shown that the knockdown of FBL expression induces p53 activation (**Su et al., 2014**). We therefore hypothesized that the apoptosis observed in *fbl* mutant embryos might be p53-mediated. Quantitative RT-PCR revealed that *tp53* transcript levels were significantly higher in mutant embryos than in wild-type embryos at 1 dpf, 2 dpf and 3 dpf (*fig. 6B-C*). These results suggest that the atrophy of the optic tectum in *fbl*^{hi2581} mutant embryos may result from tp53-dependent apoptosis.

The spatial distribution of proliferative cells is disorganized in *fbl* mutant embryos

Hypoplasia may result from an increase in apoptosis and/or an inhibition of proliferation. In 2 dpf wild-type embryos, proliferation is restricted to the periphery of the OT. We analyzed the total proliferating cell population by immunostaining for PCNA (proliferating cell nuclear antigen). Strikingly, at 2 dpf (*fig 7A*) and 3 dpf (data not shown), PCNA labeling was observed in most of the tectal cells of the mutant larvae (*fig 7A1*), whereas it was spatially restricted to a to a subset of tectal cells present at the periphery in the wild type (*fig 7A2*). These findings suggest that all the cells of the OT are proliferating in mutant embryos.

We then analyzed DNA replication by monitoring the incorporation of a thymidine analog (EdU). After a two-hour pulse and fixation, we were able to determine the location of the actively dividing cells. In WT embryos, at 2 dpf, EdU incorporation was observed at the OT margins and in the TMZe. By contrast, EdU-positive cells were found scattered over the entire optic tectum in mutant embryos (*fig 7B2*). We observed the same unrestricted pattern of EdU incorporation at a later stage (3 dpf, data not shown). However, the quantification of EdU-positive cells over the entire OT showed that about 40 to 50% of tectal cells were positive for EdU in both mutant and wild-type embryos (*fig 7C*).

Similarly, pH3 (phospho-histone 3) staining, which labels mitotic cells, showed that mitotic cells were not restricted to the margin in mutant embryos (*fig 7D*). Quantification of the population of mitotic cells within the OT revealed no difference in the proportion of this population between mutant and wild-type embryos at 2 dpf (*fig 7E*).

Collectively, these data reveal the presence of a cell-cycle defect, with a larger population of proliferative cells and an abnormal distribution of actively dividing cells in the tectum of mutant embryos.

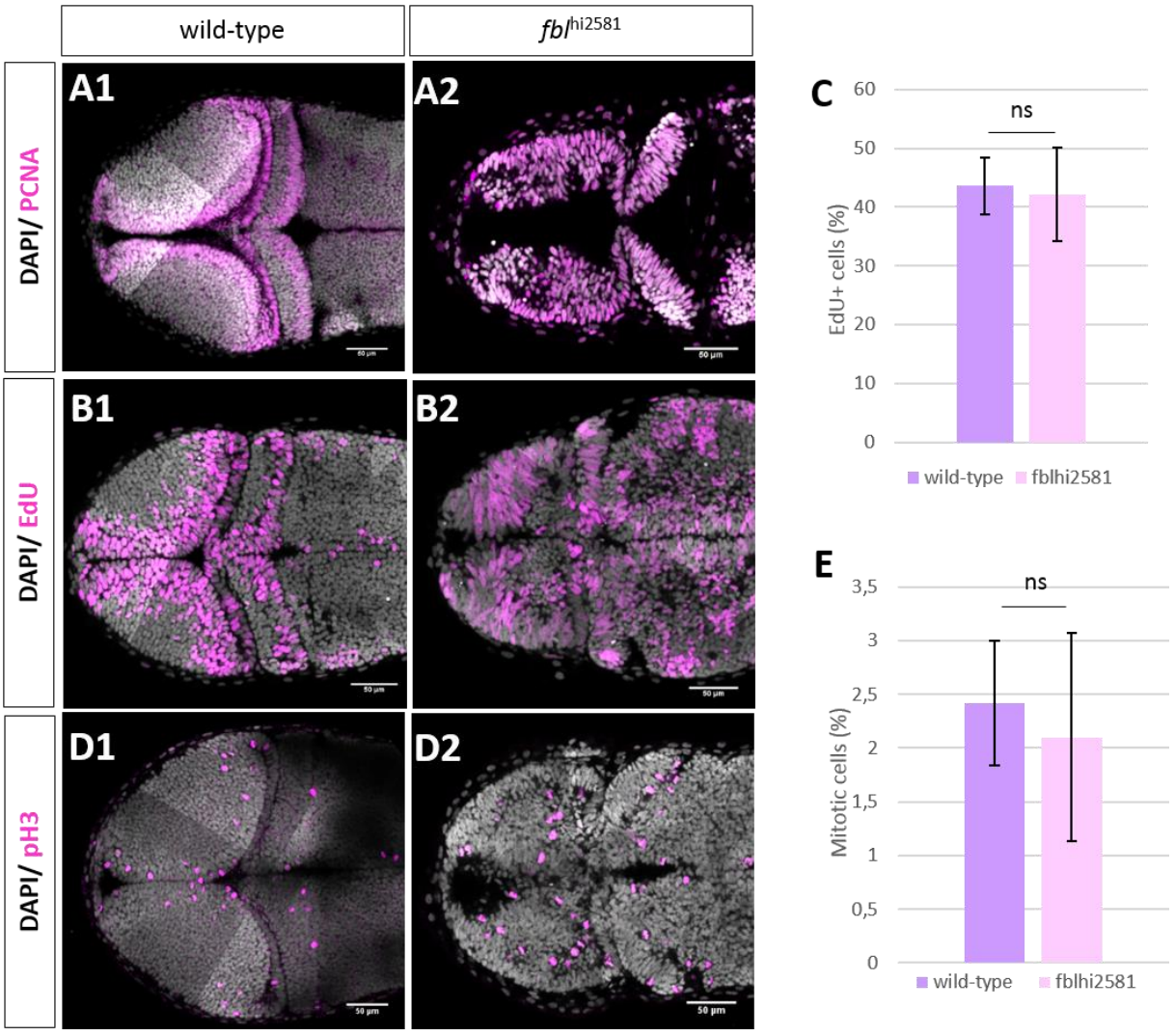

Figure 7: In *fbl* mutants, the pattern of proliferative cells is disorganized
(A) EdU incorporation experiments in 2dpf wild type **(A1)** and mutant **(A2)** embryos after two hour pulse. In wild-type embryos, EdU-positive cells are restricted to the periphery of the OT while in the *fbl*^{hi2581} mutant embryos EdU-positive cells are spread all over the structure. **(B)** EdU-positive cells quantification in wild-type (purple) and mutant (pink) embryos at 2dpf. Statistical analyzes have been performed on four samples per conditions, p-value (Mann & Whitney test): 1.00. **(C)** pH3 staining in 2dpf wild types **(C1)** and mutants **(C2)**. Embryos. Similar abnormal patterns in mutants as for EdU incorporation experiments. **(D)** pH3-positive cells quantification in wild-type (purple) and mutant (pink) embryos at 2dpf. Statistical analyzes have been performed on four samples per conditions, p-value (Mann & Whitney test): 0.53 **(E)** PCNA staining in 2dpf wild type **(H1)** and mutant **(H2)** embryos. Grey: DAPI staining, Pink: EdU, pH3 or PCNA staining. Scale bar: 50 µm. Anterior is to the left.

S-phase progression is impaired in *fbl* mutant embryos

We assessed the cell cycle profiles of mutant cells more accurately and determined whether the rate of cell cycling differed between wild-type and mutant embryos, by analyzing DNA content by Fluorescence-Activated Cell Sorting (FACS). For this purpose, we incorporated EdU for 2 hours at 3dpf, in both mutant and wild-type embryos, and then labeled the DNA with the intercalating agent 7-AAD (7-aminoactinomycin D). We carried out FACS analyses on dissociated cells from the dissected heads of control and mutant embryos. In wild-type embryos (*fig 8A*), 80% of the cells, on average were in G0/G1 phase. Less than 1% of the cells were in G2/M phase and 7-8% were in S-phase. An additional phase, the SubG1, consisting of cell aggregates and dying cells, accounted for 5% of all cells in the heads. The distribution of cells in the different phases of the cell cycle in *fbl* mutant embryos (*fig 8B*) was similar to that in wild-type embryos (*fig 8C*).

We concluded that mutant cells were not blocked in any phase of the cell cycle and seemed to cycle in a similar manner to wild-type embryo cells.

However, 7-AAD/EdU flow cytometry revealed a marked difference in S-phase profiles on histogram plots (*fig 8B*), with lower levels of EdU incorporation in *fbl* mutants than in wild-types larvae. This indicates that either mutant cells incorporate EdU less efficiently than wild-type cells, or that they die in S-phase. We quantified these differences in profile, by analyzing the distribution of cells within S-phase through determinations of the percentages

of cells in early S, mid-S and late S phase (*fig 8D*). In wild-type embryo heads, almost 70% of the S-phase population was in early S-phase. Intriguingly, the proportion of S-phase cells in early S phase was lower, at 50%, in mutant head cells. By contrast, the proportions of mutant cells in the mid- and late S phases were higher than those for wild-type cells (*fig 8D*). Indeed, 18% of wild-type cells were in mid-S phase and 12% were in late S-phase, whereas the corresponding proportions for mutant cells were 28% and 20%.

We investigated the alterations of S-phase in *fbl* mutants further, by evaluating the level of expression of *cdkn1a* (also called $p21^{waf1}$), the product of which is involved in both the regulation of G1 progression and S-phase DNA replication and accumulates during DNA damage repair (Li et al. 1994). Levels of *cdkn1a* expression were markedly higher in mutant embryos than in control and sibling embryos at 3 dpf (*fig 8E*). This suggests that the progression of DNA replication in S-phase is disturbed in the mutant larvae.

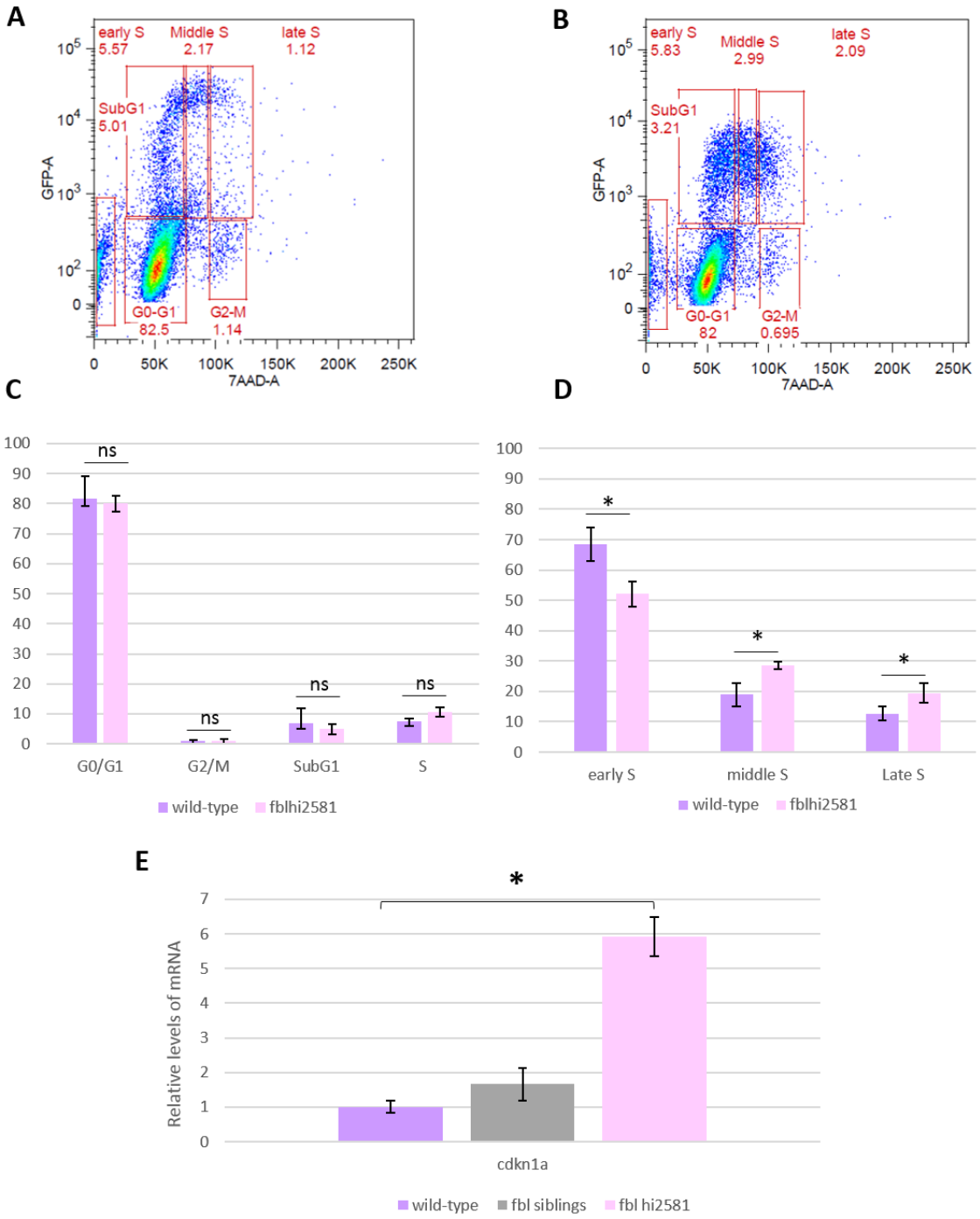

Figure 8: S-phase progression is altered in *fbl* mutant embryos
(A-B) FACS analyses of 3 dpf wild-type and mutant heads after a two-hour pulse of EdU. DNA content was assessed by labeling with 7-AAD. **(C-D)** Quantification and analysis of the distribution of the cells in the different phases of the cell cycle. Statistical analyses were performed on five replicates for the wild-type embryos and four for the mutant embryos, *p*-values (Mann & Whitney test): subG1=0.903; G0/G1= 0.461; S= 0.066; G2/M= 0.713; Early S= 0.016; Mid-S= 0.016; Late S= 0.016. **(E)** RT-qPCR quantification of relative levels of mRNA for *cdkn1a* at 3 dpf showing higher levels of *cdkn1a* expression in mutants, consistent with an alteration of DNA replication. Statistical analyses were performed on biological triplicates, *p*-value (Mann & Whitney test): 0.027. Purple: wild-type, gray: siblings, pink: mutants.

Discussion

Ribosome biogenesis is spatiotemporally dynamic, and different levels of activity are required in cells in different states of differentiation or with different rates of cell cycling. We show here that *fbl* is preferentially expressed in slow-amplifying progenitors (SAPs) of the retina (CMZ) and tectum (TMZe; **Recher et al., 2013**; **Joly et al., 2016**). However, the Fbl protein is not totally absent from differentiated cells and fast-amplifying progenitors (FAPs), but present in various amounts in the different cell types of the OT. We focus here on the role of Fbl in the homeostasis of tectum progenitors. We consider, in particular, the link between ribosome biogenesis and the cell cycle, providing evidence for a putative role of Fbl in S-phase progression.

Why are the defects of fibrillarin mutants mostly found in the tectum and the eyes?

fbl mutant embryos present hypomorphism, particularly of the brain and eye. We also observed severe cellular hypoplasia and an impairment of neuronal differentiation and specification specifically in the dorsal midbrain. The mutation of RBF-coding genes often leads to death of the embryo in early stages of development in mammals (**Newton et al., 2003**), but defects occur later in fish, after gastrulation, during somitogenesis. The large maternal stock of mature ribosomes and RBFs present in the zebrafish oocyte is used up during the first day after fertilization (**Azuma et al., 2006**).

Another possible explanation for the restricted phenotype is differences in the kinetics of early development between the dorsal midbrain and other more posterior or ventral regions. Neurogenesis begins earlier in the ventral part of the brain. After the completion of neural differentiation in the ventral regions, the dorsal part of the brain, including the OT, continues to produce neurons to support its specific sustained growth (**Joly et al., 2016**).

The ventral and dorsal midbrain neural cells may therefore be affected differently by the lack of *fbl*.

In addition, Fbl might have a specific role in neuroepithelial based morphogenesis, present in many proliferative zones of the juvenile fish brain (Dambroise et al. 2017). Indeed, the telencephalon, which grows mainly from glial stem cells and progenitors, seems less affected. In this respect, a more careful examination of other brain regions such as the cerebellum might unravel similar defects as those observed in the tectum and the eye.

Moreover, as TMZe progenitors cycle at a lower rate than TMZi cells (**Recher et al., 2013**), they may remain protected until later in development. In these cells, the dilution of maternal stocks of ribosomes or of correctly methylated ribosomes may be weaker than in more actively dividing cells.

Despite the specific accumulation of Fbl in the SAPs of the TMZe, these cells are not strongly affected, as they continue to divide, display little apoptosis and the neuroepithelial layer connecting the OT to the TS (**Recher et al., 2013**) seems to be unaffected in mutants although thicker. By contrast, the proliferative cells are profoundly disturbed and they have a different distribution, with a massive presence in the center of the tectum at 3 dpf in mutants, whereas these cells are peripheral in the wild type. There are two possible reasons for this difference of localization of progenitors. First, *fbl* loss of function could lead to a developmental delay, as proliferative cells are found throughout the entire structure at earlier stages. However, we think that the second hypothesis is more likely, because no clear signs of differentiation are observed in the tectum of mutants at later stages of development. According to this hypothesis, the *fbl* mutation may lead to the deregulation of mitosis in the FAPs of the TMZi, which would then not be able to undergo mitosis fast enough. Progenitor cells would therefore remain in S-phase for longer and would become

localized at the center of the tectum while additional FAPs would be generated at the periphery of the structure. These cells would then die by apoptosis.

Potential consequences of the impairment of ribosome biogenesis and translational activity in *fbl* mutants.

Fbl is the methyltransferase of the box C/D complex. It is responsible for the methylation of both rRNA and the histones associated with rDNA loci. An absence of Fbl or low levels of this protein lead to abnormally low levels of rDNA transcription and changes of the posttranscriptional modification of rRNAs.

We show here, *in vivo*, that *fbl* mutants display impaired ribosome biogenesis, and, more particularly, low levels of ribosome activity, as illustrated by the low proportion of polysomes. This finding may be explained by translation initiation defects. Indeed, we observed no change in the size of the 80S peak, corresponding to the binding of one ribosome to the target mRNA. We also found that 18S rRNA levels were much lower in fbl^{hi2581} mutant embryos than in the wild type, strongly suggesting that the last steps of the ribosome biogenesis pathway are impaired. It therefore seems likely that the ribosomes can bind to mRNA, but that the translation initiation defects prevent the binding of other ribosomes. However, it remains possible that a feedback loop detects the decrease in translation and subsequently decreases the rates of formation of the two subunits.

The lower level of ribosome activity may be due to lower levels of rRNA methylation, resulting in a lower affinity for specific mRNA targets. The knockdown of *fbl* expression in HeLa cells has been shown to decrease rRNA methylation (**Erales**, personal communication). More detailed exploration of these methylation events may require the profiling of ribose methylation in rRNA by high-throughput sequencing (Marchand et al. 2016).

We also suggest that Fbl may accumulate specifically in SAPs for the production of different ribosomes responsible for the translation of specific targeted mRNAs. Indeed, many RBF-coding genes have tissue-specific patterns of expression in zebrafish (**Brombin et al., 2015**). In particular, rRNA post-transcriptional modifications and ribosomal protein contents differ between the ribosomes of different cell types, particularly between stem and progenitor cells (**Brombin et al., 2015**). Moreover, different types of rRNAs are produced in oocytes and during zebrafish development (Locati et al. 2017). **Kraushar et al.** recently suggested that ribosomes drive the spatiotemporal development of the neocortex (Kraushar et al. 2016). This hypothesis is based on the putative existence of a progenitor-specific ribosome signature during brain development, highlighting the tissue specificity of ribosome biogenesis.

Why is S-phase progression disrupted in *fbl* mutant embryos?

As mentioned above, there are several compelling lines of evidence suggesting that cell division is disturbed in *fbl* mutants. The impairment of ribosome biogenesis often leads to disturbance of the cell cycle (Xu, Xiong, and Sun 2016), and cells are often arrested at the G1/S transition (James et al. 2014) or, in rarer cases, at the G2/M checkpoint (Fumagalli et al. 2012; Negi and Brown 2015).

Surprisingly, FACS analysis of *fbl*^{hi2581} mutant cells revealed that the mutant cells were not blocked at the G1/S or G2/M checkpoints, but that they progressed through the cell cycle, as the distribution of cells in the different phases of the cell cycle was similar to that for wild-type cells (Xu, Xiong, and Sun 2016).

However, the distribution of cells in the various parts of S-phase was disrupted in *fbl*^{hi2581} mutants, suggesting a delay in S-phase and in the replication fork progression. The observed distributions on FACS analysis of mutant and wild-type cells suggests that

replication origins normally activated early in S phase might be activated later in S phase in mutant cells. The low intensity of EdU incorporation is consistent with this hypothesis. The genomic material is replicated during S-phase, for subsequent mitosis. The impairment of pre-rRNA processing might interfere with transcription and, ultimately, with DNA replication (Bermejo, Lai, and Foiani 2012). S-phase progression is tightly regulated by the replication timing process (Fragkos et al. 2015; Lucas and Feng 2003; Méndez 2009; Zink 2006). In particular, the tight regulation of replication timing facilitates the sequential activation of replication origins during S-phase. We suggest that, in the absence of Fbl, the lower levels of ribosomal translation activity due to the disruption of ribosome biogenesis, delay or decrease the translation of many proteins. In particular, proteins involved in DNA replication and origin firing could be lacking, preventing the correct timing of DNA replication and leading to replication stress and genomic instability.

We also observed higher levels of $p21^{waf1}$ expression in mutant cells. In addition to its role in cell cycle exit, $p21^{waf1}$ accumulation leads to a DNA replication block and cell cycle arrest in S-phase (Li et al. 1994; Waga et al. 1994). This protein accumulates when DNA is damaged. The observed accumulation of *tp53* transcripts is also consistent with the presence of DNA breaks. These findings suggest that the intra-S defects in fbl^{hi258} embryos may be linked not only to defective replication, but also to the presence of DNA damage, resulting in replication stress. Other nucleolar proteins, such as nucleostemin, have been implicated in both ribosome biogenesis, and the maintenance of genome integrity.

Further studies are required to deepen our understanding of the origin of the tissue-specific intra-S defects in *fbl* mutants. Such studies should also provide insight into the tissue-specific defects observed in ribosomopathies (Yelick and Trainor 2015).

Material and methods

Zebrafish lines and husbandry

We used the following *Danio rerio* lines for this work: wild-type strain AB and *fbl*^{hi2581} mutants (ZIRC, Eugene, OR, USA). All zebrafish lines were maintained at 28°C in our facility. Embryos were kept at 28°C and staged as described by Kimmel (Kimmel et al. 1995). *fbl*^{hi2581} adult zebrafish were maintained as heterozygotes and inbred to generate homozygous mutant embryos. PCR was conducted on adults, to check for the presence of the insertional mutation. The wild-type *fbl* allele was detected with the following primers: forward 5'-GAGGAAAAGCGGGTCTGAG-3' and reverse 5'-AGTGCGTGGCTAACTCATCC-3'. The *fbl* mutant allele was detected with the following primers: forward 5'-GAGGAAAAGCGGGTCTGAG-3' and reverse 5'-GAAGCCTATAGAGTACGAGCCATAG-3'. All procedures were performed in accordance with European Union Directive 2011/63/EU.

Phenotypic analysis

Immunohistochemistry

Whole-mount immunohistochemistry (WMIHC) was performed as previously described (Inoue and Wittbrodt 2011). Embryos were first incubated in a depigmentation solution (0.5X SSC/5%formamide/3%H_2O_2) at room temperature for 30 minutes. WMIHC for PCNA was performed specifically, with the fast protocol of the Tefor Core Facility (http://tcf.tefor.net; unpublished protocol): following depigmentation, embryos were incubated in unmasking solution (HistoVT One, 06980-05, Nacalai Tesque) at 68°C for 1 hour. Blocking and permeabilization (10% NGS, 10% DMSO, 5% PBS-1 M glycine, 0.5% Triton X-100, 0.1% Tween 20, 0.1% sodium deoxycholate, 0.1% NP40) were performed simultaneously over a period of five hours. The embryos were incubated with antibodies

for three days at 4°C, in staining solution (2% NGS, 20% DMSO, 10 µg/ml heparin, 0.2% Triton X-100, 1X PBS, 0.1% Tween 20, 0.05% sodium azide).

We used mouse anti-PCNA (Dako, 1:150), human anti-FBL (1:1000, autoimmune serum, gift from Danièle Hernandez-Verdun, Jacques Monod Institute, Paris France), rabbit anti-pH3 (Millipore, 1:500) and mouse anti-elavl3 (Molecular Probes, Life Technologies, 1:100) primary antibodies.

The fluorescent secondary antibodies used for detection were AlexaFluor 488- or AlexaFluor 555-conjugated goat anti-rabbit, goat anti-mouse or goat anti-human antibodies (1:200, Molecular Probes, Life Technologies).

Edu labeling

We injected 1 nl of 5-ethynyl-2'-deoxyuridine (EdU, 10 mM, Molecular Probes, Life Technologies) into the pericardiac cavity of 48 hpf and 72 hpf wild-type and mutant embryos, which were fixed two hours later. EdU was detected with the EdU Click-iT Plus EdU Alexa Fluor 488 or 647 Imaging kit (Molecular Probes, Life Technologies), according to the manufacturer's protocol.

TUNEL staining

TUNEL labelling was performed with the Deadend Fluorometric TUNEL system (Promega), according to manufacturer's instructions. Embryos were washed in PBS, counterstained with DAPI (Sigma) and mounted in Vectashield hard-set mounting medium (Vector Laboratories).

Whole-mount *in situ* hybridization

Riboprobes were synthesized as follows: cDNA (PCR-amplified with specific primers was inserted into a pCR II-TOPO vector (Molecular Probes). The sequence and orientation of the inserts were checked by direct sequencing (GATC Biotech). The products of PCR amplification of the inserts with generic SP6-T7 primers were used to synthesize the antisense riboprobes, with T7 or SP6 polymerase (Promega) (chosen on the basis of the sequencing results). Digoxigenin (DIG)-conjugated probes were synthesized with the UTP-DIG nucleotide mix (Roche) and purified with RNA clean-up kit (Macherey-Nagel).

Whole-mount *in situ* hybridization was performed on manually staged (according to Kimmel et al., 1995) dechorionated PTU-treated embryos fixed in 4% paraformaldehyde (PFA)/phosphate-buffered saline (PBS) and stored in methanol at -20°C. Briefly, embryos stored in methanol were rehydrated in a methanol/PBS series, permeabilized with proteinase K (10 mg/ml), prehybridized, and then hybridized overnight at 65°C in hybridization mixture (HM: 50% formamide, 5X standard saline citrate (SSC), 0.1% Tween 20, 100 mg/ml heparin, 100 mg/ml tRNA in water). The embryos were subjected to a series of washes in 50% SSC/formamide and SSC/PBST, and were then incubated in blocking solution for one hour (0.2% Tween 20, 0.2% Triton X-100, 2% sheep serum in PBST) and overnight at 4°C with AP-conjugated anti-DIG antibodies (Roche) diluted 1:4000 in blocking solution. Embryos were then washed in PBST, soaked in staining buffer (TMN: 100 mM NaCl, 100 mM Tris-HCl, pH 9.5, 0.1% Tween 20 in water) and incubated in NBT/BCIP (nitroblue tetrazolium/5-bromo-4-chloro-3-indolyl phosphate) solution (Roche).

Cresyl violet staining

PFA-fixed embryos were dehydrated in ethanol solutions of increasing concentration and incubated in butanol before embedding in paraffin. Serial sections were prepared with a Leica rotary microtome and mounted according to standard procedures. Slides were rehydrated by incubation in xylene and ethanol solutions, and stained with cresyl violet solution. Sections were destained with glacial acetic acid and dehydrated with ethanol.

Imaging

Bright-field imaging was performed with a Nikon AZ100 macroscope (Camera: Nikon Digital Sight DSRi1; Objectives: AZ-Plan Fluor 5x (O.N.: 0.5/D.T.: 15 mm)). Fluorescence imaging was performed using a confocal laser scanning microscope (Leica SP8) with internal photomultiplier tubes (Airy: 1; Objectives: Fluotar VISIR 25x/0.95 WATER; Plan-APOCHROMAT 40x/1.10 WATER).

Segmentation

The 3D-visualisation and segmentation of zebrafish specimens we generated using 3D Slicer 4 (Fedorov et al. 2012) on a HP computer with a 2.9GHz Intel Core 17-4910MQ CPU and 32Gb of RAM.

We performed the 3D visualisation of DiI using the volume rendering module of 3D Slicer which transforms brightness values into opacity values. Using this module, we rendered dark voxels transparent, bright voxels more opaque. We visualized the segmentations with a surface rendering, using the Create surface function of the Segment editor module of 3D Slicer.

For segmentation, we downsampled the data to a voxel size of 3.5x3.5x3.5µm using a python script which is calling SimpleITK (Lowekamp et al. 2013) and numpy.

We segmented the patterns of interest using the segment editor module of 3D Slicer. The nervous system was segmented using the DiI channel by applying a manual threshold and refining the segmentation with the paint and erase tools, restricting it to eyes and brain. For label smoothing, we subsequently applied a median filter of 5x5x5voxels.

Due to its high specificity, we segmented the Elavl3-staining pattern using a manual threshold and a median filter of 5x5x5 voxels only.

For each segmentation, we generated a label map volume, counted the number of voxels and computed the volume for each by multiplying the number of voxels by the size of a voxel.

Molecular analysis

Quantitative real-time PCR

Total RNA was extracted from 72 hpf zebrafish embryos in TRIzol reagent (Invitrogen), purified and treated with DNase, with the Macherey Nagel NucleoSpin® RNAII kit. RNA was quantified with a Nanodrop 2000c spectrophotometer (Thermo Scientific) and the integrity of the RNAs was checked with an Agilent 2100 bioanalyzer and the eukaryote total RNA Nano assay (Agilent Technologies). We reverse-transcribed 1 µg of total RNA in a final reaction volume of 20 µl, with the High Capacity cDNA Reverse Transcription Kit (Life Technologies), RNase inhibitor and random primers, according to the manufacturer's instructions. Quantitative PCR was performed on a QuantStudio™ 12K Flex Real-Time PCR System with a SYBR green detection protocol. We mixed 1.5 ng of cDNA with Fast SYBR® Green Master Mix and 500 nM of each primer, in a final volume of 10 µL. The reaction mixture was subjected to 40 cycles of PCR (95°C/20 s; [95°C/1 s; 60°C/20 s] X40) followed by a fusion cycle, for analysis of the melting curve of the PCR products. Negative controls without reverse transcriptase were introduced, to check for the

absence of genomic DNA contaminants. Primers were designed with the Primer-Blast tool from NCBI and Primer Express 3.0 software (Life Technologies). With the exception of the ribosomal primers, the primers used bound to one exon and one exon-exon junction. Specificity and the absence of multi-locus matching at the primer site were checked by BLAST analysis. The amplification efficiencies of primers were determined from the slopes of standard curves generated with a four-fold dilution series. The amplification specificity of each real-time PCR was confirmed by analyzing the dissociation curves. The Ct values obtained were then used for further analyses, with the *gapdh*, *actb1* and *tbp* genes as references. Each sample was assessed at least in duplicate.

The primers used were as follows:

Gapdh-F1	TTAACGGATTCGGTCGCATT
Gapdh-R1	CCGCCTTCTGCCTTAACCTC
actb1-F1	TACACAGCCATGGATGAGGAAAT
actb1-R1	TCCCTGATGTCTGGGTCGTC
tbp-F1	ATCTCCACAGGGAGCCATGA
tbp-R1	CAGGAGGGACAAGCTGTTGG
5'ETS-F1	CCGGTCTACCTCGAAAGTC
5'ETS-R1	CGAGCAGAGTGGTAGAGGAAG
ITS1-F1	CTCGGAAAACGGTGAACCTG
ITS1-R1	GTGTTCGTTTCAGGGTCCG
ITS2-F1	CCTAAGCGCAGACCGT
ITS2-R1	AGCGCTGGCCTCGGAGATC
18S-F3	ACACGGGGAGGTAGTGACGA
18S-R3	TCGCCCATGGGTTTAGGATA
tp53-F1	GAACCCCGGATGGAGATAACTT
tp53-R1	CAGTTGTCCATTCAGCACCAAG
neurod1-F1	CAACACACCCTAGAGTTCCGACAT

neurod1-R1	CCACGTCTCGTTCGTCTTGG
	TTGCAGAAGCTCAAAACATATTGT
cdkn1a-F1	C
cdkn1a-R1	ACGCAAAGTCGAAGCTCCAG

Polysome profile

We collected 60 wild-type and 100 mutant embryos per sample at 3dpf. Embryos were deyolked, rinsed with ice-cold PBS and dissociated in ice-cold lysis buffer (10 mM Tris-HCl, 5 mM $MgCl_2$, 100 mM KCl, 1% Triton-X100, 2 mM DTT, 100 µg/ml cycloheximide, 200 U/ml RNasin (Promega), and protease inhibitor (Sigma)). Dissociated cells were subjected to sucrose gradient centrifugation (31% sucrose, 50 mM Tris-acetate pH 7.6, 50 mM NH_4Cl, 12 mM $MgCl_2$, 1mM DTT). Gradients were successively frozen and thawed before use. The gradients were then centrifuged for 3 h in an SW41 rotor (4°C, 39000 rpm) and fractionated with the ISCO system.

Cell dissociation and FACS

Injection of 1nL of EdU (10 µM) has been performed in pericardial space of embryos. Following EdU incorporation, embryos were placed in ice-cold embryo medium (5.03 mM NaCl, 0.17 mM KCl, 0.33 mM $CaCl_2$-$2H_2O$, 0.33 mM $MgSO_4$-$7H_2O$) for 10 minutes and transferred to ice-cold Ringer solution for 10 minutes. The tails of the embryos were removed and the heads were placed in 500 µl of FACSMax (Manoli and Driever 2012). Cells were dissociated by manual squishing of the embryos cell strainer (with 40-µm mesh). Cells were collected by centrifugation (500 x *g*, 10 minutes, 4°C) of the suspensions, and fixed by incubation in ethanol 70% at -20°C for 2 days. EdU was detected as described in the "EdU labeling" section. Cells were then incubated in PBS buffer containing 0.1% Triton X-100, RNAse A (SIGMA, 0.5 µg/ml) and 7-AAD (BD Pharmingen 559925, 20µl in 1 ml

buffer), and then incubated for 1 hours in the dark at 37°C before flow cytometry analysis. DNA content was assessed with a BD FACSCalibur analyzer and analyses were performed with FlowJo software.

Statistical analyses

Statistical analysis was performed with Microsoft Excel XLSTAT software. All data are expressed as means ± standard deviations. We calculated two-tailed *p*-values for Kruskal-Wallis non-parametric tests with Bonferroni correction for comparisons between three groups, and Mann-Whitney tests for comparisons of two groups.

Acknowledgments

We wish to thank Julien Hemon, Arnim Jennet, Elodie Machado and Laurie Rivière (Tefor Core Facility) and Charlène Lasgi (Curie Institute, flow cytometry plateform) for technical assistance; Pierre Affaticati (Tefor Core Facility), Odile Bronchain (NeuroPsi), Aurélie Heuzé (CASBAH group), Olivier Namy (I2BC), Vincent Pennaneach (Curie Institute) for fruitful discussion and Frédéric Catez (CRCL) for sharing unpublished data. This work has benefited from the facilities and expertise of TEFOR (TEFOR Infrastructure - Investissement d'avenir - ANR-II-INBS-0014). This research received financial support from the FINEST project (ANR-11-BSV2-0029), INRA PHASE department and from a grant of the "Fondation Leducq". Stéphanie Bouffard was funded by the French minister MENESR.

Author contributions

Stéphanie Bouffard and Françoise Jamen: Conception and design, Collection and assembly of data, Data analysis and interpretation, and manuscript writing; Alessandro Brombin and Emilie Dambroise: conception and design, Collection and assembly of data, Data analysis and interpretation; Sylvain Lempereur, Isabelle Hatin and Raphael Corre: Collection and assembly of data; Franck Bourrat and Matthieu Simion: Data analysis and interpretation; Jean-Stéphane Joly: Conception and design, Data analysis and interpretation and manuscript reviewing.

References

Amin, Mohammed Abdullahel, Sachihiro Matsunaga, Nan Ma, Hideaki Takata, Masami Yokoyama, Susumu Uchiyama, and Kiichi Fukui. 2007. "Fibrillarin, a Nucleolar Protein, Is Required for Normal Nuclear Morphology and Cellular Growth in HeLa Cells." *Biochemical and Biophysical Research Communications* 360 (2): 320–26. doi:10.1016/j.bbrc.2007.06.092.

Amsterdam, Adam, Robert M. Nissen, Zhaoxia Sun, Eric C. Swindell, Sarah Farrington, and Nancy Hopkins. 2004. "Identification of 315 Genes Essential for Early Zebrafish Development." *Proceedings of the National Academy of Sciences of the United States of America* 101 (35): 12792–97. doi:10.1073/pnas.0403929101.

Bermejo, Rodrigo, Mong Sing Lai, and Marco Foiani. 2012. "Preventing Replication Stress to Maintain Genome Stability: Resolving Conflicts between Replication and Transcription." *Molecular Cell* 45 (6): 710–18. doi:10.1016/j.molcel.2012.03.001.

Brombin, Alessandro, Jean-Stéphane Joly, and Françoise Jamen. 2015. "New Tricks for an Old Dog: Ribosome Biogenesis Contributes to Stem Cell Homeostasis." *Current Opinion in Genetics & Development* 34 (October): 61–70. doi:10.1016/j.gde.2015.07.006.

Buszczak, Michael, Robert A. J. Signer, and Sean J. Morrison. 2014. "Cellular Differences in Protein Synthesis Regulate Tissue Homeostasis." *Cell* 159 (2): 242–51. doi:10.1016/j.cell.2014.09.016.

Choi, Y.-W., Y.-W. Kim, S.-M. Bae, S.-Y. Kwak, H.-J. Chun, S. Y. Tong, H. N. Lee, et al. 2007. "Identification of Differentially Expressed Genes Using Annealing Control Primer-Based GeneFishing in Human Squamous Cell Cervical Carcinoma." *Clinical Oncology (Royal College of Radiologists (Great Britain))* 19 (5): 308–18. doi:10.1016/j.clon.2007.02.010.

Dambroise, Emilie, Matthieu Simion, Thomas Bourquard, Stéphanie Bouffard, Barbara Rizzi, Yan Jaszczyszyn, Mickaël Bourge, et al. 2017. "Postembryonic Fish Brain Proliferation Zones Exhibit Neuroepithelial-Type Gene Expression Profile." *Stem Cells (Dayton, Ohio)* 35 (6): 1505–18. doi:10.1002/stem.2588.

Fedorov, Andriy, Reinhard Beichel, Jayashree Kalpathy-Cramer, Julien Finet, Jean-Christophe Fillion-Robin, Sonia Pujol, Christian Bauer, et al. 2012. "3D Slicer as an Image Computing Platform for the Quantitative Imaging Network." *Magnetic Resonance Imaging* 30 (9): 1323–41. doi:10.1016/j.mri.2012.05.001.

Fragkos, Michalis, Olivier Ganier, Philippe Coulombe, and Marcel Méchali. 2015. "DNA Replication Origin Activation in Space and Time." *Nature Reviews. Molecular Cell Biology* 16 (6): 360–74. doi:10.1038/nrm4002.

Fumagalli, Stefano, Vasily V. Ivanenkov, Teng Teng, and George Thomas. 2012. "Suprainduction of P53 by Disruption of 40S and 60S Ribosome Biogenesis Leads to the Activation of a Novel G2/M Checkpoint." *Genes & Development* 26 (10): 1028–40. doi:10.1101/gad.189951.112.

Inoue, Daigo, and Joachim Wittbrodt. 2011. "One for All--a Highly Efficient and Versatile Method for Fluorescent Immunostaining in Fish Embryos." *PloS One* 6 (5): e19713. doi:10.1371/journal.pone.0019713.

James, Allison, Yubo Wang, Himanshu Raje, Raphyel Rosby, and Patrick DiMario. 2014. "Nucleolar Stress with and without P53." *Nucleus (Austin, Tex.)* 5 (5): 402–26. doi:10.4161/nucl.32235.

Kimmel, C. B., W. W. Ballard, S. R. Kimmel, B. Ullmann, and T. F. Schilling. 1995. "Stages of Embryonic Development of the Zebrafish." *Developmental Dynamics: An Official*

Publication of the American Association of Anatomists 203 (3): 253–310. doi:10.1002/aja.1002030302.

Koh, Cheryl M., Tsuyoshi Iwata, Qizhi Zheng, Carlise Bethel, Srinivasan Yegnasubramanian, and Angelo M. De Marzo. 2011. "Myc Enforces Overexpression of EZH2 in Early Prostatic Neoplasia via Transcriptional and Post-Transcriptional Mechanisms." *Oncotarget* 2 (9): 669–83. doi:10.18632/oncotarget.327.

Kraushar, Matthew L., Tatiana Popovitchenko, Nicole L. Volk, and Mladen-Roko Rasin. 2016. "The Frontier of RNA Metamorphosis and Ribosome Signature in Neocortical Development." *International Journal of Developmental Neuroscience: The Official Journal of the International Society for Developmental Neuroscience* 55 (December): 131–39. doi:10.1016/j.ijdevneu.2016.02.003.

Laferté, Arnaud, Emmanuel Favry, André Sentenac, Michel Riva, Christophe Carles, and Stéphane Chédin. 2006. "The Transcriptional Activity of RNA Polymerase I Is a Key Determinant for the Level of All Ribosome Components." *Genes & Development* 20 (15): 2030–40. doi:10.1101/gad.386106.

Li, R., S. Waga, G. J. Hannon, D. Beach, and B. Stillman. 1994. "Differential Effects by the P21 CDK Inhibitor on PCNA-Dependent DNA Replication and Repair." *Nature* 371 (6497): 534–37. doi:10.1038/371534a0.

Locati, Mauro D., Johanna F. B. Pagano, Geneviève Girard, Wim A. Ensink, Marina van Olst, Selina van Leeuwen, Ulrike Nehrdich, et al. 2017. "Expression of Distinct Maternal and Somatic 5.8S, 18S, and 28S RRNA Types during Zebrafish Development." *RNA (New York, N.Y.)*, May. doi:10.1261/rna.061515.117.

Lowekamp, Bradley C., David T. Chen, Luis Ibáñez, and Daniel Blezek. 2013. "The Design of SimpleITK." *Frontiers in Neuroinformatics* 7: 45. doi:10.3389/fninf.2013.00045.

Lucas, Isabelle, and Wenyi Feng. 2003. "The Essence of Replication Timing: Determinants and Significance." *Cell Cycle (Georgetown, Tex.)* 2 (6): 560–63.

Ma, Tian-Hsiang, Li-Wei Lee, Chi-Chang Lee, Yung-Hsiang Yi, Shih-Peng Chan, Bertrand Chin-Ming Tan, and Szecheng J. Lo. 2016. "Genetic Control of Nucleolar Size: An Evolutionary Perspective." *Nucleus (Austin, Tex.)* 7 (2): 112–20. doi:10.1080/19491034.2016.1166322.

Manoli, Martha, and Wolfgang Driever. 2012. "Fluorescence-Activated Cell Sorting (FACS) of Fluorescently Tagged Cells from Zebrafish Larvae for RNA Isolation." *Cold Spring Harbor Protocols* 2012 (8). doi:10.1101/pdb.prot069633.

Marcel, Virginie, Sandra E. Ghayad, Stéphane Belin, Gabriel Therizols, Anne-Pierre Morel, Eduardo Solano-Gonzàlez, Julie A. Vendrell, et al. 2013. "P53 Acts as a Safeguard of Translational Control by Regulating Fibrillarin and RRNA Methylation in Cancer." *Cancer Cell* 24 (3): 318–30. doi:10.1016/j.ccr.2013.08.013.

Marchand, Virginie, Florence Blanloeil-Oillo, Mark Helm, and Yuri Motorin. 2016. "Illumina-Based RiboMethSeq Approach for Mapping of 2'-O-Me Residues in RNA." *Nucleic Acids Research* 44 (16): e135. doi:10.1093/nar/gkw547.

Mauro, Vincent P., and Gerald M. Edelman. 2007. "The Ribosome Filter Redux." *Cell Cycle (Georgetown, Tex.)* 6 (18): 2246–51. doi:10.4161/cc.6.18.4739.

Méndez, Juan. 2009. "Temporal Regulation of DNA Replication in Mammalian Cells." *Critical Reviews in Biochemistry and Molecular Biology* 44 (5): 343–51. doi:10.1080/10409230903232618.

Mullineux, Sahra-Taylor, and Denis L. J. Lafontaine. 2012. "Mapping the Cleavage Sites on Mammalian Pre-RRNAs: Where Do We Stand?" *Biochimie*, RNA in all its forms, 94 (7): 1521–32. doi:10.1016/j.biochi.2012.02.001.

Negi, Sandeep S., and Patrick Brown. 2015. “RRNA Synthesis Inhibitor, CX-5461, Activates ATM/ATR Pathway in Acute Lymphoblastic Leukemia, Arrests Cells in G2 Phase and Induces Apoptosis.” *Oncotarget* 6 (20): 18094–104. doi:10.18632/oncotarget.4093.

Newton, Kathryn, Elisabeth Petfalski, David Tollervey, and Javier F. Cáceres. 2003. “Fibrillarin Is Essential for Early Development and Required for Accumulation of an Intron-Encoded Small Nucleolar RNA in the Mouse.” *Molecular and Cellular Biology* 23 (23): 8519–27.

Recher, Gaëlle, Julia Jouralet, Alessandro Brombin, Aurélie Heuzé, Emilie Mugniery, Jean-Michel Hermel, Sophie Desnoulez, et al. 2013. “Zebrafish Midbrain Slow-Amplifying Progenitors Exhibit High Levels of Transcripts for Nucleotide and Ribosome Biogenesis.” *Development (Cambridge, England)* 140 (24): 4860–69. doi:10.1242/dev.099010.

Rodriguez-Corona, Ulises, Margarita Sobol, Luis Carlos Rodriguez-Zapata, Pavel Hozak, and Enrique Castano. 2015. “Fibrillarin from Archaea to Human.” *Biology of the Cell* 107 (6): 159–74. doi:10.1111/boc.201400077.

Schimmang, T., D. Tollervey, H. Kern, R. Frank, and E. C. Hurt. 1989. “A Yeast Nucleolar Protein Related to Mammalian Fibrillarin Is Associated with Small Nucleolar RNA and Is Essential for Viability.” *The EMBO Journal* 8 (13): 4015–24.

Shubina, M. Y., Y. R. Musinova, and E. V. Sheval. 2016. “Nucleolar Methyltransferase Fibrillarin: Evolution of Structure and Functions.” *Biochemistry. Biokhimiia* 81 (9): 941–50. doi:10.1134/S0006297916090030.

Su, H., T. Xu, S. Ganapathy, M. Shadfan, M. Long, T. H.-M. Huang, I. Thompson, and Z.-M. Yuan. 2014. “Elevated SnoRNA Biogenesis Is Essential in Breast Cancer.” *Oncogene* 33 (11): 1348–58. doi:10.1038/onc.2013.89.

Tessarz, Peter, Helena Santos-Rosa, Sam C. Robson, Kathrine B. Sylvestersen, Christopher J Nelson, Michael L. Nielsen, and Tony Kouzarides. 2014. “Glutamine Methylation in Histone H2A Is an RNA Polymerase I Dedicated Modification.” *Nature* 505 (7484): 564–68. doi:10.1038/nature12819.

Waga, S., G. J. Hannon, D. Beach, and B. Stillman. 1994. “The P21 Inhibitor of Cyclin-Dependent Kinases Controls DNA Replication by Interaction with PCNA.” *Nature* 369 (6481): 574–78. doi:10.1038/369574a0.

Watanabe-Susaki, Kanako, Hitomi Takada, Kei Enomoto, Kyoko Miwata, Hisako Ishimine, Atsushi Intoh, Manami Ohtaka, et al. 2014. “Biosynthesis of Ribosomal RNA in Nucleoli Regulates Pluripotency and Differentiation Ability of Pluripotent Stem Cells.” *Stem Cells (Dayton, Ohio)* 32 (12): 3099–3111. doi:10.1002/stem.1825.

Xu, Xilong, Xiufang Xiong, and Yi Sun. 2016. “The Role of Ribosomal Proteins in the Regulation of Cell Proliferation, Tumorigenesis, and Genomic Integrity.” *Science China. Life Sciences* 59 (7): 656–72. doi:10.1007/s11427-016-0018-0.

Yelick, Pamela C., and Paul A. Trainor. 2015. “Ribosomopathies: Global Process, Tissue Specific Defects.” *Rare Diseases (Austin, Tex.)* 3 (1): e1025185. doi:10.1080/21675511.2015.1025185.

Zink, Daniele. 2006. “The Temporal Program of DNA Replication: New Insights into Old Questions.” *Chromosoma* 115 (4): 273–87. doi:10.1007/s00412-006-0062-8.

GENERAL CONCLUSION

1. Teleost optic tectum as a model to study ribosome biogenesis specific role in neural cell cycle proliferation

The optic tectum is a life-long growing structure of the teleost dorsal midbrain. Its oriented growth allows the tightly regulated spatial distribution of cells at different state. At embryonic stages, the optic tectum is first highly proliferative (**Joly et al., 2016**). Upon development, the proliferative population becomes restricted to the periphery of the structure, while differentiated neurons are generated in the center. More precisely, the proliferative population is subdivided into two classed of cells: the slowly-amplifying and the fastly-amplifying progenitors (SAPs and FAPs respectively, **Recher et al., 2013**). This particular organization is ideal to study cell homeostasis and cell cycle regulation.

In particular, during my PhD I participated to the description of the molecular signature of the SAPs (**Dambroise and Simion et al., 2017**). Interestingly, ribosome biogenesis factors are preferentially expressed in those stem-cell like cells.

2. Ribosome biogenesis and cell cycle progression

Ribosome biogenesis is an essential process, necessary for cellular growth and cell proliferation. The increased demand for protein synthesis in highly proliferative cells such as embryonic progenitors and stem cells is met by regulation of the ribosome biogenesis rate (**Thomas et al., 2000; Conlon and Raff., 1999**). A functional and efficient ribosome production is necessary for progression through the cell cycle phases. Thus, cell proliferation should be closely coordinated with ribosome biogenesis. Indeed, many studies have highlighted the importance of several pathways in both processes (**Derenzini et al., 2017**).

In this context, the main goal of my PhD was to study the functional relationship between ribosome biogenesis and neural progenitor proliferation. Therefore, I performed a functional analysis of *fbl*, the methyltransferase involved in rRNA maturation using zebrafish mutants. Strikingly, I did not observe a block in one of the phase of cell cycle. However, cell cycle length could still be disrupted. To further analyze this feature, I suggest to perform cumulative EdU incorporation with pH3 and PCNA labelling. This will allow to decipher the length of each of the cell phases.

Interestingly, I demonstrated that *fbl* is essential for S-phase progression since mutant cells showed disturbed EdU incorporation and disrupted distribution within S-phase. We

hypothesized that *fbl* mutant could have defects in DNA replication upon impaired ribosome biogenesis.

However, with our experiments we cannot conclude yet about this mechanism. To further analyze this hypothesis, I propose to first study DNA replication forks in *fbl* mutants. A fast and simple way to do these analyzes would be to phenocopy the phenotype we observe using the DNA replication inhibitor aphidicolin (**Vesela et al., 2017**). Additionally, analysis of the DNA fibers by molecular combing, following EdU incorporation, would allow to measure the length of the replication forks (**Kaykov et al., 2016**).

Moreover, using qPCR analyzes, we revealed the increased expression of both t*p53* and $p21^{waf1}$ suggesting a replicative or nucleolar stress. The impaired S-phase progression as well as lower EdU intensity incorporated suggest a replicative stress. To verify this hypothesis, it would be interesting to analyze the genomic instability using the γH2AX marker of DNA breaks. Furthermore, following S-phase defects such as double strand breaks, single stranded regions of DNA or resected double strand breaks, the ATM/ATR pathways is activated via the phosphorylation of the checkpoint kinase 1 (Chk1). Therefore, it would be important to assess the activation of this pathway using western blot analyzes of the phosphorylated form Chk1, and qPCR of the different intermediates of the pathways such as *c-myc* and *cdc25a*.

On the other hand, accumulation of free ribosomal proteins (RPs), due to disruption in ribosome assembly or ribosome biogenesis, leads to a cellular stress called "nucleolar stress". More precisely, upon ribosomal stress, increase in the level of free RPs leads to the sequestration of MDM2, preventing the latter to interact with p53 to target its degradation. Therefore, any decrease in the translational machinery formation is recognized by the cell and prevent cell cycle progression. This often leads to cell cycle arrest through the induction of p21 by p53 stabilization and subsequent apoptosis.

Despite the apparent absence of ribosome subunit defects illustrated by polysome profiling, we cannot exclude the nucleolar stress hypothesis. To observe nucleolar stress, the analysis by Western Blot of the expression of two ribosomal proteins accumulated upon nucleolar stress (Rpl11 and Rpl5) will be performed. In addition, labelling of the nucleoli, using the nucleolar marker Nucleolin will be performed.

3. Ribosome biogenesis and tumorigenesis

The importance of ribosome biogenesis in tumor progression has been evidenced by many studies. Not only quantitative variations in ribosome level, but also qualitative modification in ribosomal proteins or ribosomal RNA are responsible for cancer cell formation and progression. In particular, **Su et al.** revealed the highly important role of Fbl, the methyltransferase responsible for the proper methylation of rRNA in human cancer since Fbl is overexpressed in breast cancers (**Su et al., 2014**).

In *fbl* mutant embryos, I highlighted a massive decrease of 18S rRNA with impaired ribosome translation activity. Because fbl is responsible for the methylation rRNA and the subsequence adapted cleavages, the decreased production of 18S rRNA with no obvious defects in early steps of the pathway could be explained by the hypomethylation of the rRNA. To assess this question, it would be extremely relevant to study methylation events using the profiling of ribosome methylation in rRNA by high throughput sequencing (**Marchand et al., 2016**).

Besides, a decrease in the number of mature ribosomes may also contribute to tumorigenesis (**Bursal et al., 2014**). Reduction in ribosome biogenesis is responsible for the decreased protein synthesis (**Lodish, 1974; Ruggero, 2013**). In particular, diminished ribosome content leads to the preferential translation of high affinity mRNAs. Subsequently, translation of lower affinity mRNAs such as those encoding for tumor suppressors is decreased. Moreover, usage of alternative RP isoforms, post-translational modification of RPs, mutations of RPs genes, sequence diversity of rRNA and post-transcriptional chemical modifications of rRNA might be associated with tumorigenesis and cancer progression (**Filipovska and Rackham, 2013; Xue and Barna, 2012**). More precisely, **Barna et al.** observed aberrant regulation of cap and IRES-mediated translation (**Barna et al., 2008**). Ribosomal heterogeneity, arising from the presence of specific mutant RPs or aberrant chemical modification of rRNA, has been highlighted in malignant tumors (**De Keersmaecker et al., 2013; Xue and Barna, 2012**).

fbl loss of function could lead to hypomethylated rRNAs targeting different mRNAs to translate. Since ribosomal activity is decreased in the mutant embryos, we expect to see IRES-containing mRNAs preferentially translated in those mutants. I propose to compare IRES-containing mRNA translation in the polysomal fractions.

4. Ribosome biogenesis specificity

While ribosome biogenesis has been considered a "house-keeping" process for many years, it is now widely believed that ribosome biogenesis can be a specific process. This postulation has been confirmed by many studies highlighting the tissue, cell or organ specific role of many ribosome biogenesis factors, or ribosomal proteins. Furthermore, the discovery of ribosomopathies caused by the mutations in genes encoding for either ribosomal proteins, or for factors involved in ribosome synthesis, has reinforced this new concept. Indeed, as mutation in the translational machinery proteins should lead to non-viable organisms, many patients suffering from ribosomopathies show tissue specific symptoms.

Several different mechanisms have been proposed to underlie the tissue specificity of ribosome biogenesis disorders, including the selective translation of specific mRNAs, the extra-ribosomal functions of RPs and RBFs, and the differential requirements for ribosomes in different tissues.The notion of ribosome specificity stresses out the new and original concepts claiming that gene expression regulation is not only regulated at the transcriptional level but also at the translational level. Indeed, cell homeostasis and cell identity would be controlled by the specific or preferential translation of a subset of available mRNAs. This oriented translation is mediated by the slightly different ribosomes depending on the cell, or tissue of interest, having higher affinity for some mRNAs.

The second project of my PhD was to assess the specific role of ribosome biogenesis in neural progenitor. Indeed, many ribosome biogenesis factors show a specific expression in the slowly amplifying progenitors of the optic tectum. I used the results of a transcriptomic approach to isolate a new candidate. Besides *fbl*, *pa2g4* gene expression was spatially restricted to the peripheral layer of the OT. I designed transgenes using regulator sequences to allow the restricted specific overexpression of the gene in order to study its specific role in tectal progenitor homeostasis. I generated several transgenic lines which I characterized. Nowadays, performing tissue or cell specific knock-out is possible with the CRISPR/Cas9 system (**Ablain et al., 2015**) Therefore, I propose to take advantage of the different isolated enhancers to perform cell specific knock-out of *pa2g4a* in the pa2g4b mutants. Indeed, as illustrated with *fbl* mutants, ubiquitous loss of the function often leads to lethality. It would therefore be more relevant to study specifically the function of ribosome biogenesis factor. These analyzes would further emphasize the ribosome biogenesis specificity concept.

MATERIAL AND METHODS

Zebrafish lines and husbandry

For this work, the following *Danio rerio* lines were used: wild-type strain AB; *fbl*^{hi2581} mutants (ZIRC, Eugene, OR, USA); Tg(*UAS:NTR-mcherry*) nicely given by Laure Bally Cuif's group; Tg(*enh101-hsp70:GFP*) developed by Aurélie Heuzé, Gif sur Yvette, France, unpublished; Tg(*enh55-hsp70:GFP*); Tg(*enh55-hsp70:ERT2-GAL4*); Tg(*enh101-hsp70:ERT2-GAL4*). All zebrafish lines were maintained at 28°C in our facility. Embryos were kept at 28°C and staged as described by Kimmel (**Kimmel et al., 1995**). *fbl*^{hi2581} adult zebrafish were maintained as heterozygotes and incrossed to generate homozygous mutant embryos. PCR was conducted on adults for the presence of the insertional mutation. The *fbl* wild type allele was detected using the primers forward 5'-GAGGAAAAGCGGGTCTGAG-3' and reverse 5'-AGTGCGTGGCTAACTCATCC-3'. The *fbl* mutant allele was detected using the primers forward 5'-GAGGAAAAGCGGGTCTGAG-3' and reverse 5'-GAAGCCTATAGAGTACGAGCCATAG-3'. All procedures were performed in accordance with European Union Directive 2011/63/EU.

Phenotype analysis

Immunohistochemistry

Whole-mount IHC (WMIHC) was performed as previously described (**Inoue and Wittbrodt, 2011**). Embryos were beforehand incubated in a depigmentation solution (0.5X SSC/5%formamide/3%H_20_2) at room temperature for thirty minutes. PCNA WMIHC was specifically performed using fast protocol from Tefor Core Facility (http://tcf.tefor.net; unpublished protocol): following depigmentation, embryos were first incubated in unmasking solution (HistoVT One, 06980-05, Nacalai Tesque) at 68°C for 1hour. Blocking and permeabilization (10% NGS, 10%DMSO, 5% PBS-glycine 1M, 0.5% Triton X-100, 0.1% Tween20, 0.1% sodium deoxycholate, 0.1% NP40) were simultaneously achieved during five hours. Antibody incubations were performed during 3 days at 4°C, in staining solution (2% NGS, 20% DMSO, 10µg/ml heparin, 0.2% Triton X-100, 1X PBS, 0.1% Tween20, 0.05% azide).

Primary antibodies used: mouse anti-PCNA (Dako, 1:150); human anti-FBL (1:1000, autoimmune serum, gift from Danièle Hernandez-Verdun, Jacques Monod Institute, Paris France); rabbit anti-pH3 (Millipore, 1:500); mouse anti-elavl3 (Molecular probes, Life technologies, 1:100); mouse anti-GS (Millipore, 1:500); chicken anti-GFP (Aves labs,

1:500); rabbit anti-Dsred (Clontech, 1:500); rabbit anti-pa2g4a (GeneTex, 1:100); mouse anti-ZO-1 (Invitrogen, 1:500); rabbit anti-caspase 3 (BD pharmingen, 1:500).
Fluorescent secondary antibodies used for detection were: AlexaFluor 488 or AlexaFluor 555 goat anti-rabbit, goat anti-mouse, goat anti-chicken or goat anti-human (1:200, Molecular probes, Life technologies).

Edu labelling

48hpf and 72hpf wild-type and mutant embryos were injected with 1nl of 5-Ethynyl-2'-deoxyuridine (EdU, 10mM, Molecular probes, life technologies) in the pericardiac cavity and fixed 2 hours later. EdU was detected with the EdU Click-iT Plus EdU Alexa Fluor 488 or 647 Imaging kit (Molecular probes, Life technologies), according to the manufacturer's protocol.

TUNEL staining

TUNEL labelling was performed using the Deadend Fluorometric TUNEL system (Promega) according to manufacturer's instructions. Embryos were washed in PBS, counterstained with DAPI (Sigma) and mounted with Vectashield hard-set mounting medium (Vector Laboratories).

Whole mount in situ hybridization

Riboprobes were synthesized as follow: cDNA (PCR amplified with specific primers, see Table 5) was inserted into a pCR II-TOPO vector (Molecular probes). Sequences and orientation of the inserts were checked by direct sequencing (GATC Biotech). The products of PCR amplification of the inserts with generic SP6-T7 primers were used to synthesize the antisense riboprobes, with the T7 or SP6 polymerase (Promega) (chosen on the basis of the sequencing results). Digoxigenin (DIG)-conjugated probes were synthesized with the UTP-DIG nucleotide mix (Roche) and purified then with the RNA clean up kit (Macherey-Nagel). Information about DIG riboprobes used for in situ hybridization is indicated in

Whole-mount in situ hybridization was performed on manually staged (accoriding to Kimmel et al., 1995) dechorionated PTU-treated embryos fixed in 4% paraformaldehyde (PFA)/phosphate buffered saline (PBS) and stored in methanol at -20°C. Briefly, methanol-stored embryos were rehydrated in a methanol/PBS series, permeabilized with proteinase K (10 mg/ml), pre-hybridized, and then hybridized overnight at 65°C in hybridization mixture (HM: 50% formamide, 5X standard saline citrate (SSC), 0.1% Tween 20, 100

mg/ml heparin, 100 mg/ml tRNA in water). After a series of washes in 50% SSC/formamide and SSC/PBST, embryos were incubated in blocking solution (0.2% Tween 20, 0.2% Triton X-100, 2% sheep serum in PBST) and incubated overnight at 4°C with AP-conjugated anti-DIG antibodies (Roche) diluted 1:4000 in blocking solution. Embryos were then washed in PBST, soaked in staining buffer (TMN: 100mM NaCl, 100 mM Tris-HCl, pH 9.5, 0.1% Tween 20 in water) and then incubated in NBT/BCIP (nitroblue tetrazolium/5-bromo-4-chloro-3-indolyl phosphate) solution (Roche).

Juvenile brains were dissected out and processed as previously described (**Xu et al., 1994**) but with the proteinase K treatment (10 mg/ml) reduced to 15 minutes. Antisense riboprobes were diluted in a hybridization buffer containing 5% dextran. For histological analysis, 30-µm thick agarose sections were prepared using vibratome.

Targeted transcripts	ENSEMBL ID	Primers (5'->3')
pa2g4a	ENSDARG00000039578	GGCAGCCAAACCAGGAGTAT
		CACCACTCCAAGACGAGCTT
pa2g4b	ENSDARG00000070657	CGCATCACCAGTGGACTCTT
		CAAAACACGCCAAGGGGAAG
wdr43	ENSDARG00000011079	AAACCTCTCGCCTCACACTG
		ACCAGACCTCCCGATGATGA
ebna1bp2	ENSDARG00000054980	ACATGTGAAGTATTTTGTGGCCG
		AAACTTTTGCAACTTTGGTAACGC
nhp2	ENSDARG00000069422	GTGTTGTGCCTTGCATCCTG
		GTGTTGTGCCTTGCATCCTG
nhp2l1a	ENSDARG00000069878	AAACCCTGAACCGGGGAATC
		CGATGCGCATGGAATCATCC
npm2a	ENSDARG00000076391	TTTTCACAGGGCGCGAAAAG
		TGCATTACACTTCCTTTGTTTGTCT
ddx56	ENSDARG00000020913	GCTGTAGTTCTGGTCCCCAC
		TCACCGCCTGTTTAGTCACC
exosc2	ENSDARG00000028688	GGTTGTGCCTGGAGATGTGA
		CCTCCATGATCTCCGGCTTC
fbl	ENSDARG00000053912	TGGTAAGGAGGATGCTCTGG
		TATGGCTCCAGTGTGAGCTG
otx2	ENSDARG0000001123	ACTCCTCGAAAGCAGAGACG
		GAGGCACCGTAACCTTGTGT

Table 5: Primers used for riboprobe synthesis

Cresyl violet staining

PFA-fixed embryos were dehydrated in ethanol solutions of increasing concentrations and incubated in butanol before embedding in paraffin. Serial sections were prepared with a Leica rotary microtome and mounted according to standard procedures. Slides were rehydrated into xylene and ethanol, and stained with cresyl violet solution. Sections were lighten with glacial acetic acid and dehydrated with ethanol.

Imaging

Brightfield imaging was performed with a macroscope Nikon AZ100 (Camera: Nikon Digital Sight DSRi1; Objectives: AZ-Plan Fluor 5x (O.N. : 0,5/D.T. : 15 mm)). Fluorescent imaging was performed using a Confocal Laser Scanning microscope (Leica SP8) with internal PhotoMultiplier Tubes (Airy: 1; Objectives: Fluotar VISIR 25x/0.95 WATER; Plan-APOCHROMAT 40x/1.10 WATER).

Molecular analysis

Quantitative real-time PCR

Total RNA was extracted from 72hpf Zebrafish embryos with TRIzol reagent (Invitrogen) followed by purification and DNase treatment with the Macherey Nagel NucleoSpin® RNAII kit. RNA amounts were determined by the Nanodrop 2000c spectrophotometer (Thermo Scientific) and the integrity of the RNAs verified using the Agilent 2100 bioanalyzer with the eukaryote total RNA Nano assay (Agilent Technologies). 1µg of total RNA was reverse-transcribed in a 20 µl final reaction volume using the High Capacity cDNA Reverse Transcription Kit (Life Technologies) with RNase inhibitor and random primers following the manufacturer's instructions. Quantitative PCR was performed on a QuantStudio™ 12K Flex Real-Time PCR System with a SYBR green detection protocol. 1.5 ng of cDNA were mixed with Fast SYBR® Green Master Mix and 500 nM of each primer in a final volume of 10µL. The reaction mixture was submitted to 40 cycles of PCR (95°C/20 sec; [95°C/1 sec; 60°C/20 sec] X40) followed by a fusion cycle in order to analyze the melting curve of the PCR products. Negative controls without the reverse transcriptase were introduced to verify the absence of genomic DNA contaminants. Primers were designed by using the Primer-Blast tool from NCBI and the Primer Express 3.0 software (Life Technologies). Primers were defined in one exon and one exon-exon junction except for the ribosomal primers. Specificity and the absence of multi-locus matching at the primer site were verified by BLAST analysis. The amplification efficiencies of primers were generated using the slopes of standard curves obtained by a four-fold dilution series. Amplification specificity for each real-time PCR reaction was confirmed by analysis of the dissociation curves. Determined Ct values were then exploited for further analysis, with the 3 genes, gapdh, actb1 and tbp as references. Each sample measurement was made at least in duplicate.

The primers used are as followed:

0866-DRGapdh-F1	TTAACGGATTCGGTCGCATT
0867-DRGapdh-R1	CCGCCTTCTGCCTTAACCTC
0870-DRactb1-F1	TACACAGCCATGGATGAGGAAAT
0871-DRactb1-R1	TCCCTGATGTCTGGGTCGTC
1169-DRtbp-F1	ATCTCCACAGGGAGCCATGA
1170-DRtbp-R1	CAGGAGGGACAAGCTGTTGG
1173-DRb2m-F1	GTACAGGGGAAAGTCTCCACTCC
1174-DRb2m-R1	AGGTCGGTCTGCTTGGTGTC
1145-DR5'ETS-F1	CCGGTCTACCTCGAAAGTC
1146-DR5'ETS-R1	CGAGCAGAGTGGTAGAGGAAG
1149-DRITS1-F1	CTCGGAAAACGGTGAACCTG
1150-DRITS1-R1	GTGTTCGTTTCAGGGTCCG
1151-DRITS2-F1	CCTAAGCGCAGACCGT
1152-DRITS2-R1	AGCGCTGGCCTCGGAGATC
1177-DR18S-F3	ACACGGGGAGGTAGTGACGA
1178-DR18S-R3	TCGCCCATGGGTTTAGGATA
1119-DRtp53-F1	GAACCCCGGATGGAGATAACTT
1120-DRtp53-R1	CAGTTGTCCATTCAGCACCAAG
1121-DRmyca-F1	ACCGTGACTCTGACGCCACT
1122-DRmyca-R1	CACCGGCATTTTGACACTTG
1123-DRmycb-F1	GCGAATCCGATGACGAAGAT
1124-DRmycb-R1	GCGTTCGCGTCAGACTTTTT
1125-DRigf1rb-F1	TCGACTTGGAACAGAGCCTGA
1126-DRigf1rb-R1	GCCCGAACACGGACAGAATA
1127-DRigf1ra-F1	GCCACCCCCTAAACGGAAT
1128-DRigf1ra-R1	ACTCGGGGTTCACAGAAGCA
1131-DRvegfab-F1	CCCCCACCGTCACATACAAC
1132-DRvegfab-R1	TTTCATCCGACACTGGCATTC
1135-DRapaf1-F1	CCCTGTTGAGGAAAGACAATCG
1136-DRapaf1-R1	CTCAGAATCGCCTGGACAGAG
1137-DRxiap-F1	CGTCCCCCTGACAACACCTA
1138-DRxiap-R1	CACGGTCTTGTTCACCTGTGC
1139-DRneurod1-F1	CAACACACCCTAGAGTTCCGACA T
1140-DRneurod1-R1	CCACGTCTCGTTCGTCTTGG
1143-DRelavl3-F1	CAAAACAATCAAGGTGTCTTACG C
1144-DRelavl3-R1	TTTACCAGGATGCGTGAGGTG
1153-DRcdkn1a-F1	TTGCAGAAGCTCAAAACATATTG TC
1154-DRcdkn1a-R1	ACGCAAAGTCGAAGCTCCAG
1155-DRcdkn1bbF1	AGCTCCTGTCTCGACTCATCGT
1156-DRcdkn1bbR1	GGCACTGAGGTCATCGAAGC
1157-DRcdkn1caF1	CACGCCGCAAATTACAGACTT
1158-DRcdkn1caR1	GATGTGCCGGCTTGAAGGTA
1159-DRcdkn2abF1	CGAGGATGAACTGACCACAGC
1160-DRcdkn2abR1	CGTTACCCATCATCATCACCTGT
1161-DRmdm2-F1	GAGGACCCGGGGATACAGAT
1162-DRmdm2-R1	CAATCACGCACCAAGACAGG
1165-DRvegfaa-F2	ATGCGTCCCGACAGAGACAC
1166-DRvegfaa-R2	TCTTGGCTTTTCACATCTTTCTTT C
1167-DRmap2-F2	AGGCTGCCATCAGTGGAAGA
1168-DRmap2-R2	CGAGGAACTTGCACCTCTCG
1181-DRfgf2-F3	AACGCAGACGGACGACTGTT
1182-DRfgf2-R3	GCCACGTACCAGTCGGGATA

Polysome profile

60 wild-type and 100 mutant embryos per sample were collected at 72hpf. Embryos were deyolked and rinsed with ice cold PBS and then dissociated in ice-cold lysis buffer (10mM Tris-HCl, 5 mM MgCl2, 100 mM KCL, 1% TritonX-100, 2 mM DTT, 100µg/ml cycloheximide, 200U/ml RNasin (Promega), and protease inhibitor (Sigma)). Dissociated cells were applied on saccharose gradient (31% saccharose, 50mM Tris-acetate pH7.6, 50mM NH_4Cl, 12mM $MgCl_2$, 1mM DTT). Gradient were successively freezed and unfreezed before use. Centrifugation was performed for 3h in a SW41 rotor (4°C, 39000 rpm). Gradients were thereafter fractioned with ISCO.

Cell dissociation and FACS

Following EdU incorporation, embryos were placed in ice-cold embryo medium (5.03 mM NaCl, 0.17 mM KCl, 0.33 mM $CaCl_2$-$2H_20$, 0.33 mM $MgS0_4$-$7H_20$) for 10 minutes and transferred to ice-cold Ringer for 10 minutes. The tails of the embryos were removed and the heads were placed in 500 µl of FACSMax (**Manoli and Driever, 2012**). Cells were dissociated by manual squishing of the embryos on adapted cell strainer. Cells were collected by centrifugation (500 *g*, 10 minutes, 4°C) of the suspensions, and fixed in ethanol at -20°C for 2 days. EdU revelation was further proceed as described in the chapter "EdU labelling". DNA content studies were performed using the BD FACSCalibur analyzer and analyzes were accomplished with FlowJo software.

Transgenesis

Microinjection of zebrafish embryos

Embryos at one cell stage were injected with 1 nl of the transgenesis mix (15ng/µl transgenesis construction + 8ng/µl of tol2 mRNA) using a PicoSpritzer injector.

Constructions for transgenesis

pDEST AMA plasmids were designed for transgenesis in fish (Amagen platform, Gif sur Yvette, France). They bear recognition sequences for the Tol2 transposase (**Suster et al., 2009**) to improve genomic integration. Moreover, they bear a transgenesis marker (AMA). Thanks to this, CFP is expressed in the fish lens upon genomic integration. Enhancers and promoters were inserted using Gateway Cloning Technology (Life technologies) and the desired reporter cloned in the vector via restriction/ligation.

The transgenic reporter line carrying enh55 driving the expression of either GFP or ERT2-GAL4 as well as the transgenic line carrying Tg(*enh101: ERT2-GAL4*) were generated using the pDest_AMA_12H_GAL4FF_GFP (Amagen platform, Gif sur Yvette, France) and pDEST_AMA1 Enhancer101_12H_hsp70_eGFP (Aurélie Heuzé, unpublished) as templates.

Statistical analyzes

Statistical analysis was performed with Microsoft Excel XLSTAT software. All data are expressed as mean standard deviation. To calculate the two-sided p-values, Kruskal & Wallis non-parametric test with a Bonferroni correction was used in the case of three groups, and Mann & Whitney test was applied in only two groups were compared.

REFERENCES

A

Aaku-Saraste, E., Hellwig, A., and Huttner, W.B. (1996). Loss of occludin and functional tight junctions, but not ZO-1, during neural tube closure--remodeling of the neuroepithelium prior to neurogenesis. Dev. Biol. *180*, 664–679.

Abbas, T., Keaton, M.A., and Dutta, A. (2013). Genomic instability in cancer. Cold Spring Harb. Perspect. Biol. *5*, a012914.

Ablain, J., Durand, E.M., Yang, S., Zhou, Y., and Zon, L.I. (2015). A CRISPR/Cas9 Vector System for Tissue-Specific Gene Disruption in Zebrafish. Dev. Cell *32*, 756–764.

Abrous, D.N., Koehl, M., and Le Moal, M. (2005). Adult neurogenesis: from precursors to network and physiology. Physiol. Rev. *85*, 523–569.

Adolf, B., Chapouton, P., Lam, C.S., Topp, S., Tannhäuser, B., Strähle, U., Götz, M., and Bally-Cuif, L. (2006). Conserved and acquired features of adult neurogenesis in the zebrafish telencephalon. Dev. Biol. *295*, 278–293.

Affaticati, P., Yamamoto, K., Rizzi, B., Bureau, C., Peyriéras, N., Pasqualini, C., Demarque, M., and Vernier, P. (2015). Identification of the optic recess region as a morphogenetic entity in the zebrafish forebrain. Sci. Rep. *5*, 8738.

Aittaleb, M., Rashid, R., Chen, Q., Palmer, J.R., Daniels, C.J., and Li, H. (2003). Structure and function of archaeal box C/D sRNP core proteins. Nat. Struct. Mol. Biol. *10*, 256–263.

Alawi, F., and Lin, P. (2011). Dyskerin is required for tumor cell growth through mechanisms that are independent of its role in telomerase and only partially related to its function in precursor rRNA processing. Mol. Carcinog. *50*, 334–345.

Ali, S.A., Zaidi, S.K., Dacwag, C.S., Salma, N., Young, D.W., Shakoori, A.R., Montecino, M.A., Lian, J.B., van Wijnen, A.J., Imbalzano, A.N., et al. (2008). Phenotypic transcription factors epigenetically mediate cell growth control. Proc. Natl. Acad. Sci. U. S. A. *105*, 6632–6637.

Altman, J. (1962). Are new neurons formed in the brains of adult mammals? Science *135*, 1127–1128.

Alunni, A., Hermel, J.-M., Heuzé, A., Bourrat, F., Jamen, F., and Joly, J.-S. (2010). Evidence for neural stem cells in the medaka optic tectum proliferation zones. Dev. Neurobiol. *70*, 693–713.

Alunni, A., Krecsmarik, M., Bosco, A., Galant, S., Pan, L., Moens, C.B., and Bally-Cuif, L. (2013). Notch3 signaling gates cell cycle entry and limits neural stem cell amplification in the adult pallium. Dev. Camb. Engl. *140*, 3335–3347.

Amin, M.A., Matsunaga, S., Ma, N., Takata, H., Yokoyama, M., Uchiyama, S., and Fukui, K. (2007). Fibrillarin, a nucleolar protein, is required for normal nuclear morphology and cellular growth in HeLa cells. Biochem. Biophys. Res. Commun. *360*, 320–326.

Amin, M.A., Matsunaga, S., Uchiyama, S., and Fukui, K. (2008). Depletion of nucleophosmin leads to distortion of nucleolar and nuclear structures in HeLa cells. Biochem. J. *415*, 345–351.

Amsterdam, A., Sadler, K.C., Lai, K., Farrington, S., Bronson, R.T., Lees, J.A., and Hopkins, N. (2004). Many ribosomal protein genes are cancer genes in zebrafish. PLoS Biol. *2*, E139.

Anastassova-Kristeva, M. (1977). The nucleolar cycle in man. J. Cell Sci. *25*, 103–110.

Apicelli, A.J., Maggi, L.B., Hirbe, A.C., Miceli, A.P., Olanich, M.E., Schulte-Winkeler, C.L., Saporita, A.J., Kuchenreuther, M., Sanchez, J., Weilbaecher, K., et al. (2008). A non-tumor suppressor role for basal p19ARF in maintaining nucleolar structure and function. Mol. Cell. Biol. *28*, 1068–1080.

Aris, J.P., and Blobel, G. (1991). cDNA cloning and sequencing of human fibrillarin, a conserved nucleolar protein recognized by autoimmune antisera. Proc. Natl. Acad. Sci. U. S. A. *88*, 931–935.

Armistead, J., Khatkar, S., Meyer, B., Mark, B.L., Patel, N., Coghlan, G., Lamont, R.E., Liu, S., Wiechert, J., Cattini, P.A., et al. (2009). Mutation of a gene essential for ribosome biogenesis, EMG1, causes Bowen-Conradi syndrome. Am. J. Hum. Genet. *84*, 728–739.

Azuma, M., Toyama, R., Laver, E., and Dawid, I.B. (2006). Perturbation of rRNA synthesis in the bap28 mutation leads to apoptosis mediated by p53 in the zebrafish central nervous system. J. Biol. Chem. *281*, 13309–13316.

B

Bachellerie, J.-P., Cavaillé, J., and Hüttenhofer, A. (2002). The expanding snoRNA world. Biochimie *84*, 775–790.

Baier, H. (2013). Synaptic laminae in the visual system: molecular mechanisms forming layers of perception. Annu. Rev. Cell Dev. Biol. *29*, 385–416.

Baker, D.L., Youssef, O.A., Chastkofsky, M.I.R., Dy, D.A., Terns, R.M., and Terns, M.P. (2005). RNA-guided RNA modification: functional organization of the archaeal H/ACA RNP. Genes Dev. *19*, 1238–1248.

Baranick, B.T., Lemp, N.A., Nagashima, J., Hiraoka, K., Kasahara, N., and Logg, C.R. (2008). Splicing mediates the activity of four putative cellular internal ribosome entry sites. Proc. Natl. Acad. Sci. *105*, 4733–4738.

Barna, M., Pusic, A., Zollo, O., Costa, M., Kondrashov, N., Rego, E., Rao, P.H., and Ruggero, D. (2008). Suppression of Myc oncogenic activity by ribosomal protein haploinsufficiency. Nature *456*, 971–975.

Belin, S., Beghin, A., Solano-Gonzàlez, E., Bezin, L., Brunet-Manquat, S., Textoris, J., Prats, A.-C., Mertani, H.C., Dumontet, C., and Diaz, J.-J. (2009). Dysregulation of ribosome biogenesis and translational capacity is associated with tumor progression of human breast cancer cells. PloS One *4*, e7147.

Bellodi, C., Krasnykh, O., Haynes, N., Theodoropoulou, M., Peng, G., Montanaro, L., and Ruggero, D. (2010). Loss of function of the tumor suppressor DKC1 perturbs p27 translation control and contributes to pituitary tumorigenesis. Cancer Res. *70*, 6026–6035.

Beltrame, M., and Tollervey, D. (1995). Base pairing between U3 and the pre-ribosomal RNA is required for 18S rRNA synthesis. EMBO J. *14*, 4350–4356.

Bermejo, R., Lai, M.S., and Foiani, M. (2012). Preventing Replication Stress to Maintain Genome Stability: Resolving Conflicts between Replication and Transcription. Mol. Cell *45*, 710–718.

Birch, J.L., and Zomerdijk, J.C.B.M. (2008). Structure and function of ribosomal RNA gene chromatin. Biochem. Soc. Trans. *36*, 619–624.

Bogengruber, E., Briza, P., Doppler, E., Wimmer, H., Koller, L., Fasiolo, F., Senger, B., Hegemann, J.H., and Breitenbach, M. (2003). Functional analysis in yeast of the Brix protein superfamily involved in the biogenesis of ribosomes. FEMS Yeast Res. *3*, 35–43.

Boisvert, F.-M., van Koningsbruggen, S., Navascués, J., and Lamond, A.I. (2007). The multifunctional nucleolus. Nat. Rev. Mol. Cell Biol. *8*, 574–585.

Bolli, N., Payne, E.M., Grabher, C., Lee, J.-S., Johnston, A.B., Falini, B., Kanki, J.P., and Look, A.T. (2010). Expression of the cytoplasmic NPM1 mutant (NPMc+) causes the expansion of hematopoietic cells in zebrafish. Blood *115*, 3329–3340.

Bond, A.M., Ming, G.-L., and Song, H. (2015). Adult Mammalian Neural Stem Cells and Neurogenesis: Five Decades Later. Cell Stem Cell *17*, 385–395.

Boothby, C.B., and Bower, B.D. (1973). Cartilage hair hypoplasia. Arch. Dis. Child. *48*, 918–921.

Boulon, S., Marmier-Gourrier, N., Pradet-Balade, B., Wurth, L., Verheggen, C., Jády, B.E., Rothé, B., Pescia, C., Robert, M.-C., Kiss, T., et al. (2008). The Hsp90 chaperone controls the biogenesis of L7Ae RNPs through conserved machinery. J. Cell Biol. *180*, 579–595.

Boulon, S., Westman, B.J., Hutten, S., Boisvert, F.-M., and Lamond, A.I. (2010). The nucleolus under stress. Mol. Cell *40*, 216–227.

Brimacombe, R., Mitchell, P., Osswald, M., Stade, K., and Bochkariov, D. (1993). Clustering of modified nucleotides at the functional center of bacterial ribosomal RNA. FASEB J. Off. Publ. Fed. Am. Soc. Exp. Biol. *7*, 161–167.

Brombin, A., Joly, J.-S., and Jamen, F. (2015). New tricks for an old dog: ribosome biogenesis contributes to stem cell homeostasis. Curr. Opin. Genet. Dev. *34*, 61–70.

Bursac, S., Brdovcak, M.C., Donati, G., and Volarevic, S. (2014). Activation of the tumor suppressor p53 upon impairment of ribosome biogenesis. Biochim. Biophys. Acta BBA - Mol. Basis Dis. *1842*, 817–830.

Buszczak, M., Signer, R.A.J., and Morrison, S.J. (2014). Cellular differences in protein synthesis regulate tissue homeostasis. Cell *159*, 242–251.

Butler, A.B., and Hodos, W. (2005). Comparative Vertebrate Neuroanatomy: Evolution and Adaptation (Hoboken, N.J: Wiley-Liss).

Byrd, C.A., and Brunjes, P.C. (1998). Addition of new cells to the olfactory bulb of adult zebrafish. Ann. N. Y. Acad. Sci. *855*, 274–276.

Byrd, C.A., and Brunjes, P.C. (2001). Neurogenesis in the olfactory bulb of adult zebrafish. Neuroscience *105*, 793–801.

C

Cahill, N.M., Friend, K., Speckmann, W., Li, Z.-H., Terns, R.M., Terns, M.P., and Steitz, J.A. (2002). Site-specific cross-linking analyses reveal an asymmetric protein distribution for a box C/D snoRNP. EMBO J. *21*, 3816–3828.

Cajal, S.R. y (1913). Estudios sobre la degeneración y regeneración del sistema nerviosa (Imprenta de Hijos de Nicolás Moya).

Carroll, K., and Wickner, R.B. (1995). Translation and M1 double-stranded RNA propagation: MAK18 = RPL41B and cycloheximide curing. J. Bacteriol. *177*, 2887–2891.

Castro, D.S., Skowronska-Krawczyk, D., Armant, O., Donaldson, I.J., Parras, C., Hunt, C., Critchley, J.A., Nguyen, L., Gossler, A., Göttgens, B., et al. (2006). Proneural bHLH and Brn proteins coregulate a neurogenic program through cooperative binding to a conserved DNA motif. Dev. Cell *11*, 831–844.

Cavaillé, J., Nicoloso, M., and Bachellerie, J.P. (1996). Targeted ribose methylation of RNA in vivo directed by tailored antisense RNA guides. Nature *383*, 732–735.

Cavaillé, J., Buiting, K., Kiefmann, M., Lalande, M., Brannan, C.I., Horsthemke, B., Bachellerie, J.P., Brosius, J., and Hüttenhofer, A. (2000). Identification of brain-specific and imprinted small nucleolar RNA genes exhibiting an unusual genomic organization. Proc. Natl. Acad. Sci. U. S. A. *97*, 14311–14316.

Cavodeassi, F., and Houart, C. (2012). Brain regionalization: of signaling centers and boundaries. Dev. Neurobiol. *72*, 218–233.

Celesia, G.G. (2015). Hearing disorders in brainstem lesions. Handb. Clin. Neurol. *129*, 509–536.

Cerveny, K.L., Varga, M., and Wilson, S.W. (2012). Continued growth and circuit building in the anamniote visual system. Dev. Neurobiol. *72*, 328–345.

Chagnon, P., Michaud, J., Mitchell, G., Mercier, J., Marion, J.-F., Drouin, E., Rasquin-Weber, A., Hudson, T.J., and Richter, A. (2002). A Missense Mutation (R565W) in Cirhin (FLJ14728) in North American Indian Childhood Cirrhosis. Am. J. Hum. Genet. *71*, 1443–1449.

Chapouton, P., Adolf, B., Leucht, C., Tannhäuser, B., Ryu, S., Driever, W., and Bally-Cuif, L. (2006). her5 expression reveals a pool of neural stem cells in the adult zebrafish midbrain. Dev. Camb. Engl. *133*, 4293–4303.

Chapouton, P., Skupien, P., Hesl, B., Coolen, M., Moore, J.C., Madelaine, R., Kremmer, E., Faus-Kessler, T., Blader, P., Lawson, N.D., et al. (2010). Notch activity levels control the balance between quiescence and recruitment of adult neural stem cells. J. Neurosci. Off. J. Soc. Neurosci. *30*, 7961–7974.

Chapouton, P., Webb, K.J., Stigloher, C., Alunni, A., Adolf, B., Hesl, B., Topp, S., Kremmer, E., and Bally-Cuif, L. (2011). Expression of hairy/enhancer of split genes in neural progenitors and neurogenesis domains of the adult zebrafish brain. J. Comp. Neurol. *519*, 1748–1769.

Chatr-Aryamontri, A., Breitkreutz, B.-J., Heinicke, S., Boucher, L., Winter, A., Stark, C., Nixon, J., Ramage, L., Kolas, N., O'Donnell, L., et al. (2013). The BioGRID interaction database: 2013 update. Nucleic Acids Res. *41*, D816-823.

Chaudhuri, S., Vyas, K., Kapasi, P., Komar, A.A., Dinman, J.D., Barik, S., and Mazumder, B. (2007). Human ribosomal protein L13a is dispensable for canonical ribosome function but indispensable for efficient rRNA methylation. RNA N. Y. N *13*, 2224–2237.

Chen, M., and von Mikecz, A. (2000). Specific inhibition of rRNA transcription and dynamic relocation of fibrillarin induced by mercury. Exp. Cell Res. *259*, 225–238.

Chen, M., Rockel, T., Steinweger, G., Hemmerich, P., Risch, J., and von Mikecz, A. (2002). Subcellular recruitment of fibrillarin to nucleoplasmic proteasomes: implications for processing of a nucleolar autoantigen. Mol. Biol. Cell *13*, 3576–3587.

Choi, Y.-W., Kim, Y.-W., Bae, S.-M., Kwak, S.-Y., Chun, H.-J., Tong, S.Y., Lee, H.N., Shin, J.C., Kim, K.T., Kim, Y.J., et al. (2007). Identification of differentially expressed genes using annealing control primer-based GeneFishing in human squamous cell cervical carcinoma. Clin. Oncol. R. Coll. Radiol. G. B. *19*, 308–318.

Christensen, M.E., Beyer, A.L., Walker, B., and LeStourgeon, W.M. (1977). Identification of NG, NG-dimethylarginine in a nuclear protein from the lower eukaryote Physarum polycephalum homologous to the major proteins of mammalian 40S ribonucleoprotein particles. Biochem. Biophys. Res. Commun. *74*, 621–629.

Christian, K.M., Song, H., and Ming, G. (2014). Functions and Dysfunctions of Adult Hippocampal Neurogenesis.

Ciganda, M., and Williams, N. (2011). Eukaryotic 5S rRNA biogenesis. Wiley Interdiscip. Rev. RNA *2*, 523–533.

Clos, J., Buttgereit, D., and Grummt, I. (1986). A purified transcription factor (TIF-IB) binds to essential sequences of the mouse rDNA promoter. Proc. Natl. Acad. Sci. U. S. A. *83*, 604–608.

Coller, H.A., Grandori, C., Tamayo, P., Colbert, T., Lander, E.S., Eisenman, R.N., and Golub, T.R. (2000). Expression analysis with oligonucleotide microarrays reveals that MYC regulates genes involved in growth, cell cycle, signaling, and adhesion. Proc. Natl. Acad. Sci. U. S. A. *97*, 3260–3265.

Colombo, E., Alcalay, M., and Pelicci, P.G. (2011). Nucleophosmin and its complex network: a possible therapeutic target in hematological diseases. Oncogene *30*, 2595–2609.

Conlon, I., and Raff, M. (1999). Size Control in Animal Development. Cell *96*, 235–244.

D

De la Cruz, J., Kressler, D., Tollervey, D., and Linder, P. (1998). Dob1p (Mtr4p) is a putative ATP-dependent RNA helicase required for the 3' end formation of 5.8S rRNA in Saccharomyces cerevisiae. EMBO J. *17*, 1128–1140.

Daftuar, L., Zhu, Y., Jacq, X., and Prives, C. (2013). Ribosomal proteins RPL37, RPS15 and RPS20 regulate the Mdm2-p53-MdmX network. PloS One *8*, e68667.

Dai, M.-S., Sun, X.-X., and Lu, H. (2008). Aberrant expression of nucleostemin activates p53 and induces cell cycle arrest via inhibition of MDM2. Mol. Cell. Biol. *28*, 4365–4376.

Dambroise, E., Simion, M., Bourquard, T., Bouffard, S., Rizzi, B., Jaszczyszyn, Y., Bourge, M., Affaticati, P., Heuzé, A., Jouralet, J., et al. (2017). Postembryonic Fish Brain Proliferation Zones Exhibit Neuroepithelial-Type Gene Expression Profile. Stem Cells Dayt. Ohio *35*, 1505–1518.

Darnell, D., and Gilbert, S.F. (2017). Neuroembryology. Wiley Interdiscip. Rev. Dev. Biol. *6*.

Dauwerse, J.G., Dixon, J., Seland, S., Ruivenkamp, C.A.L., van Haeringen, A., Hoefsloot, L.H., Peters, D.J.M., Boers, A.C., Daumer-Haas, C., Maiwald, R., et al. (2011). Mutations in genes encoding subunits of RNA polymerases I and III cause Treacher Collins syndrome. Nat. Genet. *43*, 20–22.

De Keersmaecker, K., Atak, Z.K., Li, N., Vicente, C., Patchett, S., Girardi, T., Gianfelici, V., Geerdens, E., Clappier, E., Porcu, M., et al. (2013). Exome sequencing identifies mutation in CNOT3 and ribosomal genes RPL5 and RPL10 in T-cell acute lymphoblastic leukemia. Nat. Genet. *45*, 186–190.

Deisenroth, C., and Zhang, Y. (2010). Ribosome biogenesis surveillance: probing the ribosomal protein-Mdm2-p53 pathway. Oncogene *29*, 4253–4260.

Del Bene, F. (2011). Interkinetic nuclear migration: cell cycle on the move. EMBO J. *30*, 1676–1677.

Del Bene, F., Wehman, A.M., Link, B.A., and Baier, H. (2008). Regulation of neurogenesis by interkinetic nuclear migration through an apical-basal notch gradient. Cell *134*, 1055–1065.

Delaporta, P., Sofocleous, C., Stiakaki, E., Polychronopoulou, S., Economou, M., Kossiva, L., Kostaridou, S., and Kattamis, A. (2014). Clinical phenotype and genetic analysis of RPS19, RPL5, and RPL11 genes in Greek patients with Diamond Blackfan Anemia. Pediatr. Blood Cancer *61*, 2249–2255.

Demirci, H., Murphy, F., Belardinelli, R., Kelley, A.C., Ramakrishnan, V., Gregory, S.T., Dahlberg, A.E., and Jogl, G. (2010). Modification of 16S ribosomal RNA by the KsgA methyltransferase restructures the 30S subunit to optimize ribosome function. RNA N. Y. N *16*, 2319–2324.

Derenzini, M., Montanaro, L., Chillà, A., Tosti, E., Vici, M., Barbieri, S., Govoni, M., Mazzini, G., and Treré, D. (2005). Key role of the achievement of an appropriate ribosomal RNA complement for G1-S phase transition in H4-II-E-C3 rat hepatoma cells. J. Cell. Physiol. *202*, 483–491.

Derenzini, M., Montanaro, L., and Trerè, D. (2017). Ribosome biogenesis and cancer. Acta Histochem. *119*, 190–197.

Devès, M., and Bourrat, F. (2012). Transcriptional mechanisms of developmental cell cycle arrest: problems and models. Semin. Cell Dev. Biol. *23*, 290–297.

Dez, C., Dlakić, M., and Tollervey, D. (2007). Roles of the HEAT repeat proteins Utp10 and Utp20 in 40S ribosome maturation. RNA N. Y. N *13*, 1516–1527.

Dimova, D.K., and Dyson, N.J. (2005). The E2F transcriptional network: old acquaintances with new faces. Oncogene *24*, 2810–2826.

Dirian, L., Galant, S., Coolen, M., Chen, W., Bedu, S., Houart, C., Bally-Cuif, L., and Foucher, I. (2014). Spatial regionalization and heterochrony in the formation of adult pallial neural stem cells. Dev. Cell *30*, 123–136.

Dixon, J., Hovanes, K., Shiang, R., and Dixon, M.J. (1997). Sequence Analysis, Identification of Evolutionary Conserved Motifs and Expression Analysis of Murine tcof1 Provide Further Evidence for a Potential Function for the Gene and Its Human Homologue, TCOF1. Hum. Mol. Genet. *6*, 727–737.

Dixon, J., Jones, N.C., Sandell, L.L., Jayasinghe, S.M., Crane, J., Rey, J.-P., Dixon, M.J., and Trainor, P.A. (2006). Tcof1/Treacle is required for neural crest cell formation and proliferation deficiencies that cause craniofacial abnormalities. Proc. Natl. Acad. Sci. *103*, 13403–13408.

Doetsch, F., Caillé, I., Lim, D.A., García-Verdugo, J.M., and Alvarez-Buylla, A. (1999). Subventricular zone astrocytes are neural stem cells in the adult mammalian brain. Cell *97*, 703–716.

Donati, G., Brighenti, E., Vici, M., Mazzini, G., Treré, D., Montanaro, L., and Derenzini, M. (2011). Selective inhibition of rRNA transcription downregulates E2F-1: a new p53-independent mechanism linking cell growth to cell proliferation. J. Cell Sci. *124*, 3017–3028.

Dousset, T., Wang, C., Verheggen, C., Chen, D., Hernandez-Verdun, D., and Huang, S. (2000). Initiation of nucleolar assembly is independent of RNA polymerase I transcription. Mol. Biol. Cell *11*, 2705–2717.

Dragon, F., Gallagher, J.E.G., Compagnone-Post, P.A., Mitchell, B.M., Porwancher, K.A., Wehner, K.A., Wormsley, S., Settlage, R.E., Shabanowitz, J., Osheim, Y., et al. (2002). A large nucleolar U3 ribonucleoprotein required for 18S ribosomal RNA biogenesis. Nature *417*, 967–970.

Drygin, D., Rice, W.G., and Grummt, I. (2010). The RNA polymerase I transcription machinery: an emerging target for the treatment of cancer. Annu. Rev. Pharmacol. Toxicol. *50*, 131–156.

D’Souza, B., Miyamoto, A., and Weinmaster, G. (2008). The many facets of Notch ligands. Oncogene *27*, 5148–5167.

Dundr, M., Hoffmann-Rohrer, U., Hu, Q., Grummt, I., Rothblum, L.I., Phair, R.D., and Misteli, T. (2002). A kinetic framework for a mammalian RNA polymerase in vivo. Science *298*, 1623–1626.

E

Ebersberger, I., Simm, S., Leisegang, M.S., Schmitzberger, P., Mirus, O., von Haeseler, A., Bohnsack, M.T., and Schleiff, E. (2014). The evolution of the ribosome biogenesis pathway from a yeast perspective. Nucleic Acids Res. *42*, 1509–1523.

Eichler, D.C., and Craig, N. (1994). Processing of eukaryotic ribosomal RNA. Prog. Nucleic Acid Res. Mol. Biol. *49*, 197–239.

Eifert, C., Farnworth, M., Schulz-Mirbach, T., Riesch, R., Bierbach, D., Klaus, S., Wurster, A., Tobler, M., Streit, B., Indy, J.R., et al. (2015). Brain size variation in extremophile fish: local adaptation versus phenotypic plasticity. J. Zool. *295*, 143–153.

Eivers, E., Demagny, H., and De Robertis, E.M. (2009). Integration of BMP and Wnt signaling via vertebrate Smad1/5/8 and Drosophila Mad. Cytokine Growth Factor Rev. *20*, 357–365.

Ekström, P., Johnsson, C.M., and Ohlin, L.M. (2001). Ventricular proliferation zones in the brain of an adult teleost fish and their relation to neuromeres and migration (secondary matrix) zones. J. Comp. Neurol. *436*, 92–110.

Eriksson, P.S., Perfilieva, E., Björk-Eriksson, T., Alborn, A.-M., Nordborg, C., Peterson, D.A., and Gage, F.H. (1998). Neurogenesis in the adult human hippocampus. Nat. Med. *4*, 1313–1317.

Essers, P.B., Pereboom, T.C., Goos, Y.J., Paridaen, J.T., and Macinnes, A.W. (2014). A comparative study of nucleostemin family members in zebrafish reveals specific roles in ribosome biogenesis. Dev. Biol. *385*, 304–315.

Eymin, B., Claverie, P., Salon, C., Leduc, C., Col, E., Brambilla, E., Khochbin, S., and Gazzeri, S. (2006). p14ARF activates a Tip60-dependent and p53-independent ATM/ATR/CHK pathway in response to genotoxic stress. Mol. Cell. Biol. *26*, 4339–4350.

F

Faigle, R., and Song, H. (2013). Signaling mechanisms regulating adult neural stem cells and neurogenesis. Biochim. Biophys. Acta BBA - Gen. Subj. *1830*, 2435–2448.

Falcone Ferreyra, M.L., Pezza, A., Biarc, J., Burlingame, A.L., and Casati, P. (2010). Plant L10 ribosomal proteins have different roles during development and translation under ultraviolet-B stress. Plant Physiol. *153*, 1878–1894.

Falini, B., Bolli, N., Liso, A., Martelli, M.P., Mannucci, R., Pileri, S., and Nicoletti, I. (2009). Altered nucleophosmin transport in acute myeloid leukaemia with mutated NPM1: molecular basis and clinical implications. Leukemia *23*, 1731–1743.

Feder, M., Pas, J., Wyrwicz, L.S., and Bujnicki, J.M. (2003). Molecular phylogenetics of the RrmJ/fibrillarin superfamily of ribose 2'-O-methyltransferases. Gene *302*, 129–138.

Ferreira-Cerca, S., Pöll, G., Gleizes, P.-E., Tschochner, H., and Milkereit, P. (2005). Roles of eukaryotic ribosomal proteins in maturation and transport of pre-18S rRNA and ribosome function. Mol. Cell *20*, 263–275.

Filipovska, A., and Rackham, O. (2013). Specialization from synthesis: How ribosome diversity can customize protein function. FEBS Lett. *587*, 1189–1197.

Filipowicz, W., and Pogacić, V. (2002). Biogenesis of small nucleolar ribonucleoproteins. Curr. Opin. Cell Biol. *14*, 319–327.

Fish, J.L., Dehay, C., Kennedy, H., and Huttner, W.B. (2008). Making bigger brains-the evolution of neural-progenitor-cell division. J. Cell Sci. *121*, 2783–2793.

Flach, J., Bakker, S.T., Mohrin, M., Conroy, P.C., Pietras, E.M., Reynaud, D., Alvarez, S., Diolaiti, M.E., Ugarte, F., Forsberg, E.C., et al. (2014). Replication stress is a potent driver of functional decline in ageing haematopoietic stem cells. Nature *512*, 198–202.

Foucher, I., Mione, M., Simeone, A., Acampora, D., Bally-Cuif, L., and Houart, C. (2006). Differentiation of cerebellar cell identities in absence of Fgf signalling in zebrafish Otx morphants. Dev. Camb. Engl. *133*, 1891–1900.

Fragkos, M., Ganier, O., Coulombe, P., and Méchali, M. (2015). DNA replication origin activation in space and time. Nat. Rev. Mol. Cell Biol. *16*, 360–374.

Frederiksen, K., and McKay, R.D. (1988). Proliferation and differentiation of rat neuroepithelial precursor cells in vivo. J. Neurosci. Off. J. Soc. Neurosci. *8*, 1144–1151.

Freed, E.F., and Baserga, S.J. (2010). The C-terminus of Utp4, mutated in childhood cirrhosis, is essential for ribosome biogenesis. Nucleic Acids Res. *38*, 4798–4806.

Freed, E.F., Prieto, J.-L., McCann, K.L., McStay, B., and Baserga, S.J. (2012). NOL11, Implicated in the Pathogenesis of North American Indian Childhood Cirrhosis, Is Required for Pre-rRNA Transcription and Processing. PLOS Genet. *8*, e1002892.

Fumagalli, S., Ivanenkov, V.V., Teng, T., and Thomas, G. (2012). Suprainduction of p53 by disruption of 40S and 60S ribosome biogenesis leads to the activation of a novel G2/M checkpoint. Genes Dev. *26*, 1028–1040.

G

Galant, S., Furlan, G., Coolen, M., Dirian, L., Foucher, I., and Bally-Cuif, L. (2016). Embryonic origin and lineage hierarchies of the neural progenitor subtypes building the zebrafish adult midbrain. Dev. Biol. *420*, 120–135.

Galardi, S., Fatica, A., Bachi, A., Scaloni, A., Presutti, C., and Bozzoni, I. (2002). Purified Box C/D snoRNPs Are Able To Reproduce Site-Specific 2′-O-Methylation of Target RNA In Vitro. Mol. Cell. Biol. *22*, 6663–6668.

Gammill, L.S., and Bronner-Fraser, M. (2003). Neural crest specification: migrating into genomics. Nat. Rev. Neurosci. *4*, 795–805.

Ganot, P., Jády, B.E., Bortolin, M.L., Darzacq, X., and Kiss, T. (1999). Nucleolar factors direct the 2'-O-ribose methylation and pseudouridylation of U6 spliceosomal RNA. Mol. Cell. Biol. *19*, 6906–6917.

Ganz, J., Kaslin, J., Hochmann, S., Freudenreich, D., and Brand, M. (2010). Heterogeneity and Fgf dependence of adult neural progenitors in the zebrafish telencephalon. Glia *58*, 1345–1363.

Gates, M.A., Thomas, L.B., Howard, E.M., Laywell, E.D., Sajin, B., Faissner, A., Götz, B., Silver, J., and Steindler, D.A. (1995). Cell and molecular analysis of the developing and adult mouse subventricular zone of the cerebral hemispheres. J. Comp. Neurol. *361*, 249–266.

Gautier, T., Fomproix, N., Masson, C., Azum-Gélade, M.C., Gas, N., and Hernandez-Verdun, D. (1994). Fate of specific nucleolar perichromosomal proteins during mitosis: cellular distribution and association with U3 snoRNA. Biol. Cell *82*, 81–93.

Geling, A., Itoh, M., Tallafuss, A., Chapouton, P., Tannhäuser, B., Kuwada, J.Y., Chitnis, A.B., and Bally-Cuif, L. (2003). bHLH transcription factor Her5 links patterning to regional inhibition of neurogenesis at the midbrain-hindbrain boundary. Dev. Camb. Engl. *130*, 1591–1604.

Gerbi, S.A., and Borovjagin, A.V. (2013). Pre-Ribosomal RNA Processing in Multicellular Organisms (Landes Bioscience).

Gigova, A., Duggimpudi, S., Pollex, T., Schaefer, M., and Koš, M. (2014). A cluster of methylations in the domain IV of 25S rRNA is required for ribosome stability. RNA N. Y. N *20*, 1632–1644.

Gingold, H., Tehler, D., Christoffersen, N.R., Nielsen, M.M., Asmar, F., Kooistra, S.M., Christophersen, N.S., Christensen, L.L., Borre, M., Sørensen, K.D., et al. (2014). A dual program for translation regulation in cellular proliferation and differentiation. Cell *158*, 1281–1292.

Goessens, G. (1984). Nucleolar structure. Int. Rev. Cytol. *87*, 107–158.

Gómez-Skarmeta, J., de La Calle-Mustienes, E., and Modolell, J. (2001). The Wnt-activated Xiro1 gene encodes a repressor that is essential for neural development and downregulates Bmp4. Dev. Camb. Engl. *128*, 551–560.

Gonzales, B., Henning, D., So, R.B., Dixon, J., Dixon, M.J., and Valdez, B.C. (2005). The Treacher Collins syndrome (TCOF1) gene product is involved in pre-rRNA methylation. Hum. Mol. Genet. *14*, 2035–2043.

Goodfellow, S.J., and Zomerdijk, J.C.B.M. (2013). Basic mechanisms in RNA polymerase I transcription of the ribosomal RNA genes. Subcell. Biochem. *61*, 211–236.

Götz, M., and Huttner, W.B. (2005). The cell biology of neurogenesis. Nat. Rev. Mol. Cell Biol. *6*, 777–788.

Götz, M., Sirko, S., Beckers, J., and Irmler, M. (2015). Reactive astrocytes as neural stem or progenitor cells: In vivo lineage, In vitro potential, and Genome-wide expression analysis. Glia *63*, 1452–1468.

Gould, E., Reeves, A.J., Graziano, M.S.A., and Gross, C.G. (1999). Neurogenesis in the Neocortex of Adult Primates. Science *286*, 548–552.

Grandel, H., and Brand, M. (2013). Comparative aspects of adult neural stem cell activity in vertebrates. Dev. Genes Evol. *223*, 131–147.

Grandel, H., Kaslin, J., Ganz, J., Wenzel, I., and Brand, M. (2006). Neural stem cells and neurogenesis in the adult zebrafish brain: origin, proliferation dynamics, migration and cell fate. Dev. Biol. *295*, 263–277.

Granneman, S., and Tollervey, D. (2007). Building Ribosomes: Even More Expensive Than Expected? Curr. Biol. *17*, R415–R417.

Grisendi, S., Mecucci, C., Falini, B., and Pandolfi, P.P. (2006). Nucleophosmin and cancer. Nat. Rev. Cancer *6*, 493–505.

Group, T.T.C.S.C., Dixon, J., Edwards, S.J., Gladwin, A.J., Dixon, M.J., Loftus, S.K., Bonner, C.A., Koprivnikar, K., and Wasmuth, J.J. (1996). Positional cloning of a gene involved in the pathogenesis of Treacher Collins syndrome. Nat. Genet. *12*, 130–136.

Grummt, I. (2010). Wisely chosen paths--regulation of rRNA synthesis: delivered on 30 June 2010 at the 35th FEBS Congress in Gothenburg, Sweden. FEBS J. *277*, 4626–4639.

Gu, B.-W., Ge, J., Fan, J.-M., Bessler, M., and Mason, P.J. (2013). Slow growth and unstable ribosomal RNA lacking pseudouridine in mouse embryonic fibroblast cells expressing catalytically inactive dyskerin. FEBS Lett. *587*, 2112–2117.

Guérout, N., Li, X., and Barnabé-Heider, F. (2014). Cell fate control in the developing central nervous system. Exp. Cell Res. *321*, 77–83.

Guetg, C., and Santoro, R. (2012). Formation of nuclear heterochromatin: the nucleolar point of view. Epigenetics *7*, 811–814.

H

Haaf, T., Hayman, D.L., and Schmid, M. (1991). Quantitative determination of rDNA transcription units in vertebrate cells. Exp. Cell Res. *193*, 78–86.

Hadjiolova, K.V., Nicoloso, M., Mazan, S., Hadjiolov, A.A., and Bachellerie, J.P. (1993). Alternative pre-rRNA processing pathways in human cells and their alteration by cycloheximide inhibition of protein synthesis. Eur. J. Biochem. *212*, 211–215.

Haimov, O., Sinvani, H., and Dikstein, R. (2015). Cap-dependent, scanning-free translation initiation mechanisms. Biochim. Biophys. Acta *1849*, 1313–1318.

Hallgren, J., Pietrzak, M., Rempala, G., Nelson, P.T., and Hetman, M. (2014). Neurodegeneration-associated instability of ribosomal DNA. Biochim. Biophys. Acta *1842*, 860–868.

Hamperl, S., Wittner, M., Babl, V., Perez-Fernandez, J., Tschochner, H., and Griesenbeck, J. (2013). Chromatin states at ribosomal DNA loci. Biochim. Biophys. Acta *1829*, 405–417.

Hartenstein, V., and Stollewerk, A. (2015). The evolution of early neurogenesis. Dev. Cell *32*, 390–407.

Hayashi, Y., Kuroda, T., Kishimoto, H., Wang, C., Iwama, A., and Kimura, K. (2014). Downregulation of rRNA transcription triggers cell differentiation. PloS One *9*, e98586.

He, H., Ling, X., Zhu, J., Fu, X., Han, Z., Liang, Y., Deng, Y., Lin, Z., Chen, G., Chen, Y., et al. (2013). Down-regulation of the ErbB3 binding protein 1 in human bladder cancer promotes tumor progression and cell proliferation. Mol. Biol. Rep. *40*, 3799–3805.

Heiss, N.S., Knight, S.W., Vulliamy, T.J., Klauck, S.M., Wiemann, S., Mason, P.J., Poustka, A., and Dokal, I. (1998). X-linked dyskeratosis congenita is caused by mutations in a highly conserved gene with putative nucleolar functions. Nat. Genet. *19*, 32–38.

Heix, J., Vente, A., Voit, R., Budde, A., Michaelidis, T.M., and Grummt, I. (1998). Mitotic silencing of human rRNA synthesis: inactivation of the promoter selectivity factor SL1 by cdc2/cyclin B-mediated phosphorylation. EMBO J. *17*, 7373–7381.

Henke, R.M., Meredith, D.M., Borromeo, M.D., Savage, T.K., and Johnson, J.E. (2009). Ascl1 and Neurog2 form novel complexes and regulate Delta-like3 (Dll3) expression in the neural tube. Dev. Biol. *328*, 529–540.

Henras, A.K., Plisson-Chastang, C., O'Donohue, M.-F., Chakraborty, A., and Gleizes, P.-E. (2015). An overview of pre-ribosomal RNA processing in eukaryotes. Wiley Interdiscip. Rev. RNA *6*, 225–242.

Hermanns, P., Bertuch, A.A., Bertin, T.K., Dawson, B., Schmitt, M.E., Shaw, C., Zabel, B., and Lee, B. (2005). Consequences of mutations in the non-coding RMRP RNA in cartilage-hair hypoplasia. Hum. Mol. Genet. *14*, 3723–3740.

Hernandez-Verdun, D., Roussel, P., and Gautier, T. (1993). Nucleolar proteins during mitosis. 79–90.

Hernandez-Verdun, D., Roussel, P., Thiry, M., Sirri, V., and Lafontaine, D.L.J. (2010). The nucleolus: structure/function relationship in RNA metabolism. Wiley Interdiscip. Rev. RNA *1*, 415–431.

Hernandez-Verdun, D., Louvet, E., and Muro, E. (2013). Time-lapse, photoactivation, and photobleaching imaging of nucleolar assembly after mitosis. Methods Mol. Biol. Clifton NJ *1042*, 337–350.

Higa-Nakamine, S., Suzuki, T., Uechi, T., Chakraborty, A., Nakajima, Y., Nakamura, M., Hirano, N., Suzuki, T., and Kenmochi, N. (2012). Loss of ribosomal RNA modification causes developmental defects in zebrafish. Nucleic Acids Res. *40*, 391–398.

Horos, R., Ijspeert, H., Pospisilova, D., Sendtner, R., Andrieu-Soler, C., Taskesen, E., Nieradka, A., Cmejla, R., Sendtner, M., Touw, I.P., et al. (2012). Ribosomal deficiencies

in Diamond-Blackfan anemia impair translation of transcripts essential for differentiation of murine and human erythroblasts. Blood *119*, 262–272.

Horváth, B.M., Magyar, Z., Zhang, Y., Hamburger, A.W., Bakó, L., Visser, R.G.F., Bachem, C.W.B., and Bögre, L. (2006). EBP1 regulates organ size through cell growth and proliferation in plants. EMBO J. *25*, 4909–4920.

Hovhanyan, A., Herter, E.K., Pfannstiel, J., Gallant, P., and Raabe, T. (2014). Drosophila mbm is a nucleolar myc and casein kinase 2 target required for ribosome biogenesis and cell growth of central brain neuroblasts. Mol. Cell. Biol. *34*, 1878–1891.

Hu, B., Xiong, Y., Ni, R., Wei, L., Jiang, D., Wang, G., Wu, D., Xu, T., Zhao, F., Zhu, M., et al. (2014). The downregulation of ErbB3 binding protein 1 (EBP1) is associated with poor prognosis and enhanced cell proliferation in hepatocellular carcinoma. Mol. Cell. Biochem. *396*, 175–185.

Huang, C., Chan, J.A., and Schuurmans, C. (2014). Proneural bHLH genes in development and disease. Curr. Top. Dev. Biol. *110*, 75–127.

Huang, N., Negi, S., Szebeni, A., and Olson, M.O.J. (2005). Protein NPM3 interacts with the multifunctional nucleolar protein B23/nucleophosmin and inhibits ribosome biogenesis. J. Biol. Chem. *280*, 5496–5502.

Hughes, J.M. (1996). Functional base-pairing interaction between highly conserved elements of U3 small nucleolar RNA and the small ribosomal subunit RNA. J. Mol. Biol. *259*, 645–654.

Huttner, W.B., and Kosodo, Y. (2005). Symmetric versus asymmetric cell division during neurogenesis in the developing vertebrate central nervous system. Curr. Opin. Cell Biol. *17*, 648–657.

I

Iadevaia, V., Caldarola, S., Biondini, L., Gismondi, A., Karlsson, S., Dianzani, I., and Loreni, F. (2010). PIM1 kinase is destabilized by ribosomal stress causing inhibition of cell cycle progression. Oncogene *29*, 5490–5499.

Ide, S., Miyazaki, T., Maki, H., and Kobayashi, T. (2010). Abundance of ribosomal RNA gene copies maintains genome integrity. Science *327*, 693–696.

Imayoshi, I., Sakamoto, M., Yamaguchi, M., Mori, K., and Kageyama, R. (2010). Essential roles of Notch signaling in maintenance of neural stem cells in developing and adult brains. J. Neurosci. Off. J. Soc. Neurosci. *30*, 3489–3498.

Ingolia, N.T., Lareau, L.F., and Weissman, J.S. (2011). Ribosome profiling of mouse embryonic stem cells reveals the complexity and dynamics of mammalian proteomes. Cell *147*, 789–802.

Inoue, D., and Wittbrodt, J. (2011). One for all--a highly efficient and versatile method for fluorescent immunostaining in fish embryos. PloS One *6*, e19713.

Ito, H., Ishikawa, Y., Yoshimoto, M., and Yamamoto, N. (2007). Diversity of brain morphology in teleosts: brain and ecological niche. Brain. Behav. Evol. *69*, 76–86.

Ito, Y., Tanaka, H., Okamoto, H., and Ohshima, T. (2010). Characterization of neural stem cells and their progeny in the adult zebrafish optic tectum. Dev. Biol. *342*, 26–38.

J

Jack, K., Bellodi, C., Landry, D.M., Niederer, R.O., Meskauskas, A., Musalgaonkar, S., Kopmar, N., Krasnykh, O., Dean, A.M., Thompson, S.R., et al. (2011). rRNA pseudouridylation defects affect ribosomal ligand binding and translational fidelity from yeast to human cells. Mol. Cell *44*, 660–666.

Jackson, R.J., Hellen, C.U.T., and Pestova, T.V. (2010). The mechanism of eukaryotic translation initiation and principles of its regulation. Nat. Rev. Mol. Cell Biol. *11*, 113–127.

James, A., Wang, Y., Raje, H., Rosby, R., and DiMario, P. (2014). Nucleolar stress with and without p53. Nucl. Austin Tex *5*, 402–426.

Jangani, M., Poolman, T.M., Matthews, L., Yang, N., Farrow, S.N., Berry, A., Hanley, N., Williamson, A.J.K., Whetton, A.D., Donn, R., et al. (2014). The methyltransferase WBSCR22/Merm1 enhances glucocorticoid receptor function and is regulated in lung inflammation and cancer. J. Biol. Chem. *289*, 8931–8946.

Jansen, R.P., Hurt, E.C., Kern, H., Lehtonen, H., Carmo-Fonseca, M., Lapeyre, B., and Tollervey, D. (1991). Evolutionary conservation of the human nucleolar protein fibrillarin and its functional expression in yeast. J. Cell Biol. *113*, 715–729.

Jobert, L., Skjeldam, H.K., Dalhus, B., Galashevskaya, A., Vågbø, C.B., Bjørås, M., and Nilsen, H. (2013). The human base excision repair enzyme SMUG1 directly interacts with DKC1 and contributes to RNA quality control. Mol. Cell *49*, 339–345.

Joly, J.-S., Recher, G., Brombin, A., Ngo, K., and Hartenstein, V. (2016). A Conserved Developmental Mechanism Builds Complex Visual Systems in Insects and Vertebrates. Curr. Biol. CB *26*, R1001–R1009.

Junéra, H.R., Masson, C., Géraud, G., and Hernandez-Verdun, D. (1995). The three-dimensional organization of ribosomal genes and the architecture of the nucleoli vary with G1, S and G2 phases. J. Cell Sci. *108 (Pt 11)*, 3427–3441.

K

Kageyama, R., Ohtsuka, T., and Kobayashi, T. (2008). Roles of Hes genes in neural development. Dev. Growth Differ. *50 Suppl 1*, S97-103.

Kaplan, F.S., Murray, J., Sylvester, J.E., Gonzalez, I.L., O'Connor, J.P., Doering, J.L., Muenke, M., Emanuel, B.S., and Zasloff, M.A. (1993). The topographic organization of repetitive DNA in the human nucleolus. Genomics *15*, 123–132.

Kaslin, J., Kroehne, V., Benato, F., Argenton, F., and Brand, M. (2013). Development and specification of cerebellar stem and progenitor cells in zebrafish: from embryo to adult. Neural Develop. *8*, 9.

Kaslin, J., Kroehne, V., Ganz, J., Hans, S., and Brand, M. (2017). Distinct roles of neuroepithelial-like and radial glia-like progenitor cells in cerebellar regeneration. Dev. Camb. Engl. *144*, 1462–1471.

Kaykov, A., Taillefumier, T., Bensimon, A., and Nurse, P. (2016). Molecular Combing of Single DNA Molecules on the 10 Megabase Scale. Sci. Rep. *6*.

Kellis, M., Birren, B.W., and Lander, E.S. (2004). Proof and evolutionary analysis of ancient genome duplication in the yeast Saccharomyces cerevisiae. Nature *428*, 617–624.

Killen, M.W., Stults, D.M., Adachi, N., Hanakahi, L., and Pierce, A.J. (2009). Loss of Bloom syndrome protein destabilizes human gene cluster architecture. Hum. Mol. Genet. *18*, 3417–3428.

Kim, C.K., Nguyen, T.L.X., Joo, K.M., Nam, D.-H., Park, J., Lee, K.-H., Cho, S.-W., and Ahn, J.-Y. (2010). Negative regulation of p53 by the long isoform of ErbB3 binding protein Ebp1 in brain tumors. Cancer Res. *70*, 9730–9741.

Kim, J.-H., You, K.-R., Kim, I.H., Cho, B.-H., Kim, C.-Y., and Kim, D.-G. (2004). Over-expression of the ribosomal protein L36a gene is associated with cellular proliferation in hepatocellular carcinoma. Hepatology *39*, 129–138.

Kim, S.H., Macfarlane, S., Kalinina, N.O., Rakitina, D.V., Ryabov, E.V., Gillespie, T., Haupt, S., Brown, J.W.S., and Taliansky, M. (2007). Interaction of a plant virus-encoded protein with the major nucleolar protein fibrillarin is required for systemic virus infection. Proc. Natl. Acad. Sci. U. S. A. *104*, 11115–11120.

Kim, S.-K., Ahn, H.-S., Back, H.-J., Cho, B., Choi, E.-J., Chung, N.-G., Hwang, P.-H., Jeoung, D.-C., Kang, H.-J., Kim, H., et al. (2012). Clinical and hematologic manifestations in patients with Diamond Blackfan anemia in Korea. Korean J. Hematol. *47*, 131–135.

Kimmel, C.B., Ballard, W.W., Kimmel, S.R., Ullmann, B., and Schilling, T.F. (1995). Stages of embryonic development of the zebrafish. Dev. Dyn. Off. Publ. Am. Assoc. Anat. *203*, 253–310.

Kirsche, W. (1967). [On postembryonic matrix zones in the brain of various vertebrates and their relationship to the study of the brain structure]. Z. Mikrosk. Anat. Forsch. *77*, 313–406.

Kiss-László, Z., Henry, Y., Bachellerie, J.P., Caizergues-Ferrer, M., and Kiss, T. (1996). Site-specific ribose methylation of preribosomal RNA: a novel function for small nucleolar RNAs. Cell *85*, 1077–1088.

Kiss-László, Z., Henry, Y., and Kiss, T. (1998). Sequence and structural elements of methylation guide snoRNAs essential for site-specific ribose methylation of pre-rRNA. EMBO J. *17*, 797–807.

Kizil, C., Kaslin, J., Kroehne, V., and Brand, M. (2012). Adult neurogenesis and brain regeneration in zebrafish. Dev. Neurobiol. *72*, 429–461.

Klein, J., and Grummt, I. (1999). Cell cycle-dependent regulation of RNA polymerase I transcription: the nucleolar transcription factor UBF is inactive in mitosis and early G1. Proc. Natl. Acad. Sci. U. S. A. *96*, 6096–6101.

Klein, D.J., Schmeing, T.M., Moore, P.B., and Steitz, T.A. (2001). The kink-turn: a new RNA secondary structure motif. EMBO J. *20*, 4214–4221.

Knippenberg, P.H. van (1986). Structural and Functional Aspects of the N 6,N 6 Dimethyladenosines in 16S Ribosomal RNA. In Structure, Function, and Genetics of Ribosomes, B. Hardesty, and G. Kramer, eds. (Springer New York), pp. 412–424.

Kobayashi, T. (2011). Regulation of ribosomal RNA gene copy number and its role in modulating genome integrity and evolutionary adaptability in yeast. Cell. Mol. Life Sci. CMLS *68*, 1395–1403.

Koga, M., Satoh, T., Takasaki, I., Kawamura, Y., Yoshida, M., and Kaida, D. (2014). U2 snRNP is required for expression of the 3' end of genes. PloS One *9*, e98015.

Koh, C.M., Gurel, B., Sutcliffe, S., Aryee, M.J., Schultz, D., Iwata, T., Uemura, M., Zeller, K.I., Anele, U., Zheng, Q., et al. (2011a). Alterations in nucleolar structure and gene expression programs in prostatic neoplasia are driven by the MYC oncogene. Am. J. Pathol. *178*, 1824–1834.

Koh, C.M., Iwata, T., Zheng, Q., Bethel, C., Yegnasubramanian, S., and De Marzo, A.M. (2011b). Myc enforces overexpression of EZH2 in early prostatic neoplasia via transcriptional and post-transcriptional mechanisms. Oncotarget *2*, 669–683.

Komar, A.A., and Hatzoglou, M. (2005). Internal ribosome entry sites in cellular mRNAs: mystery of their existence. J. Biol. Chem. *280*, 23425–23428.

Komili, S., Farny, N.G., Roth, F.P., and Silver, P.A. (2007). Functional specificity among ribosomal proteins regulates gene expression. Cell *131*, 557–571.

Kondrashov, N., Pusic, A., Stumpf, C.R., Shimizu, K., Hsieh, A.C., Xue, S., Ishijima, J., Shiroishi, T., and Barna, M. (2011). Ribosome-mediated specificity in Hox mRNA translation and vertebrate tissue patterning. Cell *145*, 383–397.

Kraushar, M.L., Popovitchenko, T., Volk, N.L., and Rasin, M.-R. (2016). The frontier of RNA metamorphosis and ribosome signature in neocortical development. Int. J. Dev. Neurosci. Off. J. Int. Soc. Dev. Neurosci. *55*, 131–139.

Krauzlis, R.J., Lovejoy, L.P., and Zénon, A. (2013). Superior colliculus and visual spatial attention. Annu. Rev. Neurosci. *36*, 165–182.

Kriegstein, A., and Alvarez-Buylla, A. (2009). The glial nature of embryonic and adult neural stem cells. Annu. Rev. Neurosci. *32*, 149–184.

Krogan, N.J., Cagney, G., Yu, H., Zhong, G., Guo, X., Ignatchenko, A., Li, J., Pu, S., Datta, N., Tikuisis, A.P., et al. (2006). Global landscape of protein complexes in the yeast Saccharomyces cerevisiae. Nature *440*, 637–643.

Kuhn, A., Stefanovsky, V., and Grummt, I. (1993). The nucleolar transcription activator UBF relieves Ku antigen-mediated repression of mouse ribosomal gene transcription. Nucleic Acids Res. *21*, 2057–2063.

Kuhn, A., Vente, A., Dorée, M., and Grummt, I. (1998). Mitotic phosphorylation of the TBP-containing factor SL1 represses ribosomal gene transcription. J. Mol. Biol. *284*, 1–5.

Kuo, J.S., Patel, M., Gamse, J., Merzdorf, C., Liu, X., Apekin, V., and Sive, H. (1998). Opl: a zinc finger protein that regulates neural determination and patterning in Xenopus. Dev. Camb. Engl. *125*, 2867–2882.

Kuroyanagi, Y., Okuyama, T., Suehiro, Y., Imada, H., Shimada, A., Naruse, K., Takeda, H., Kubo, T., and Takeuchi, H. (2010). Proliferation zones in adult medaka (Oryzias latipes) brain. Brain Res. *1323*, 33–40.

Kusnadi, E.P., Hannan, K.M., Hicks, R.J., Hannan, R.D., Pearson, R.B., and Kang, J. (2015). Regulation of rDNA transcription in response to growth factors, nutrients and energy. Gene *556*, 27–34.

L

Laferté, A., Favry, E., Sentenac, A., Riva, M., Carles, C., and Chédin, S. (2006). The transcriptional activity of RNA polymerase I is a key determinant for the level of all ribosome components. Genes Dev. *20*, 2030–2040.

Lafontaine, D.L., and Tollervey, D. (2000). Synthesis and assembly of the box C+D small nucleolar RNPs. Mol. Cell. Biol. *20*, 2650–2659.

Lafontaine, D.L., and Tollervey, D. (2001). The function and synthesis of ribosomes. Nat. Rev. Mol. Cell Biol. *2*, 514–520.

Lafontaine, D.L.J., Bousquet-Antonelli, C., Henry, Y., Caizergues-Ferrer, M., and Tollervey, D. (1998). The box H+ACA snoRNAs carry Cbf5p, the putative rRNA pseudouridine synthase. Genes Dev. *12*, 527–537.

Lapik, Y.R., Fernandes, C.J., Lau, L.F., and Pestov, D.G. (2004). Physical and functional interaction between Pes1 and Bop1 in mammalian ribosome biogenesis. Mol. Cell *15*, 17–29.

Le Bouteiller, M., Souilhol, C., Beck-Cormier, S., Stedman, A., Burlen-Defranoux, O., Vandormael-Pournin, S., Bernex, F., Cumano, A., and Cohen-Tannoudji, M. (2013). Notchless-dependent ribosome synthesis is required for the maintenance of adult hematopoietic stem cells. J. Exp. Med. *210*, 2351–2369.

Learned, R.M., Learned, T.K., Haltiner, M.M., and Tjian, R.T. (1986). Human rRNA transcription is modulated by the coordinate binding of two factors to an upstream control element. Cell *45*, 847–857.

Lechertier, T., Grob, A., Hernandez-Verdun, D., and Roussel, P. (2009). Fibrillarin and Nop56 interact before being co-assembled in box C/D snoRNPs. Exp. Cell Res. *315*, 928–942.

Lemay, V., Hossain, A., Osheim, Y.N., Beyer, A.L., and Dragon, F. (2011). Identification of novel proteins associated with yeast snR30 small nucleolar RNA. Nucleic Acids Res. *39*, 9659–9670.

Lenkowski, J.R., and Raymond, P.A. (2014). Müller glia: Stem cells for generation and regeneration of retinal neurons in teleost fish. Prog. Retin. Eye Res. *40*, 94–123.

Li, R., Waga, S., Hannon, G.J., Beach, D., and Stillman, B. (1994). Differential effects by the p21 CDK inhibitor on PCNA-dependent DNA replication and repair. Nature *371*, 534–537.

Liang, X., Liu, Q., and Fournier, M.J. (2007). rRNA modifications in an intersubunit bridge of the ribosome strongly affect both ribosome biogenesis and activity. Mol. Cell *28*, 965–977.

Liang, X.-H., Liu, Q., and Fournier, M.J. (2009). Loss of rRNA modifications in the decoding center of the ribosome impairs translation and strongly delays pre-rRNA processing. RNA N. Y. N *15*, 1716–1728.

Lin, J., Lai, S., Jia, R., Xu, A., Zhang, L., Lu, J., and Ye, K. (2011). Structural basis for site-specific ribose methylation by box C/D RNA protein complexes. Nature *469*, 559–563.

Lindsey, B.W., and Tropepe, V. (2006). A comparative framework for understanding the biological principles of adult neurogenesis. Prog. Neurobiol. *80*, 281–307.

Lindström, M.S. (2009). Emerging functions of ribosomal proteins in gene-specific transcription and translation. Biochem. Biophys. Res. Commun. *379*, 167–170.

Liu, L., Li, X.D., Chen, H.Y., Cui, J.S., and Xu, D.Y. (2015). Significance of Ebp1 and p53 protein expression in cervical cancer. Genet. Mol. Res. GMR *14*, 11860–11866.

Liu, Z., Oh, S.-M., Okada, M., Liu, X., Cheng, D., Peng, J., Brat, D.J., Sun, S., Zhou, W., Gu, W., et al. (2009). Human BRE1 is an E3 ubiquitin ligase for Ebp1 tumor suppressor. Mol. Biol. Cell *20*, 757–768.

Llorens-Bobadilla, E., Zhao, S., Baser, A., Saiz-Castro, G., Zwadlo, K., and Martin-Villalba, A. (2015). Single-Cell Transcriptomics Reveals a Population of Dormant Neural Stem Cells that Become Activated upon Brain Injury. Cell Stem Cell *17*, 329–340.

Lo, S.-J., Fan, L.-C., Tsai, Y.-F., Lin, K.-Y., Huang, H.-L., Wang, T.-H., Liu, H., Chen, T.-C., Huang, S.-F., Chang, C.-J., et al. (2013). A novel interaction of nucleophosmin with BCL2-associated X protein regulating death evasion and drug sensitivity in human hepatoma cells. Hepatol. Baltim. Md *57*, 1893–1905.

Locati, M.D., Pagano, J.F.B., Girard, G., Ensink, W.A., van Olst, M., van Leeuwen, S., Nehrdich, U., Spaink, H.P., Rauwerda, H., Jonker, M.J., et al. (2017). Expression of Distinct Maternal and Somatic 5.8S, 18S, and 28S rRNA Types during Zebrafish Development. RNA N. Y. N.

Lodish, H.F. (1974). Model for the regulation of mRNA translation applied to haemoglobin synthesis. Nature *251*, 385–388.

Long, E.O., and Dawid, I.B. (1980). Repeated genes in eukaryotes. Annu. Rev. Biochem. *49*, 727–764.

Long, Y., Song, G., Yan, J., He, X., Li, Q., and Cui, Z. (2013). Transcriptomic characterization of cold acclimation in larval zebrafish. BMC Genomics *14*, 612.

Lopes, A.M., Miguel, R.N., Sargent, C.A., Ellis, P.J., Amorim, A., and Affara, N.A. (2010). The human RPS4 paralogue on Yq11.223 encodes a structurally conserved ribosomal protein and is preferentially expressed during spermatogenesis. BMC Mol. Biol. *11*, 33.

Love, N.K., Keshavan, N., Lewis, R., Harris, W.A., and Agathocleous, M. (2014). A nutrient-sensitive restriction point is active during retinal progenitor cell differentiation. Dev. Camb. Engl. *141*, 697–706.

Loza-Muller, L., Rodríguez-Corona, U., Sobol, M., Rodríguez-Zapata, L.C., Hozak, P., and Castano, E. (2015). Fibrillarin methylates H2A in RNA polymerase I trans-active promoters in Brassica oleracea. Front. Plant Sci. *6*.

Lucas, I., and Feng, W. (2003). The essence of replication timing: determinants and significance. Cell Cycle Georget. Tex *2*, 560–563.

Luo, Y., Coskun, V., Liang, A., Yu, J., Cheng, L., Ge, W., Shi, Z., Zhang, K., Li, C., Cui, Y., et al. (2015). Single-Cell Transcriptome Analyses Reveal Signals to Activate Dormant Neural Stem Cells. Cell *161*, 1175–1186.

M

Ma, H., and Pederson, T. (2007). Depletion of the nucleolar protein nucleostemin causes G1 cell cycle arrest via the p53 pathway. Mol. Biol. Cell *18*, 2630–2635.

MacInnes, A.W., Amsterdam, A., Whittaker, C.A., Hopkins, N., and Lees, J.A. (2008). Loss of p53 synthesis in zebrafish tumors with ribosomal protein gene mutations. Proc. Natl. Acad. Sci. *105*, 10408–10413.

Malatesta, P., Appolloni, I., and Calzolari, F. (2008). Radial glia and neural stem cells. Cell Tissue Res. *331*, 165–178.

Manoli, M., and Driever, W. (2012). Fluorescence-activated cell sorting (FACS) of fluorescently tagged cells from zebrafish larvae for RNA isolation. Cold Spring Harb. Protoc. *2012*.

Mansour-Robaey, S., and Pinganaud, G. (1990). Quantitative and morphological study of cell proliferation during morphogenesis in the trout visual system. J. Hirnforsch. *31*, 495–504.

Marcel, V., Ghayad, S.E., Belin, S., Therizols, G., Morel, A.-P., Solano-Gonzàlez, E., Vendrell, J.A., Hacot, S., Mertani, H.C., Albaret, M.A., et al. (2013). p53 acts as a safeguard of translational control by regulating fibrillarin and rRNA methylation in cancer. Cancer Cell *24*, 318–330.

Marchand, V., Blanloeil-Oillo, F., Helm, M., and Motorin, Y. (2016). Illumina-based RiboMethSeq approach for mapping of 2'-O-Me residues in RNA. Nucleic Acids Res. *44*, e135.

Marcus, R.C., Delaney, C.L., and Easter, S.S. (1999). Neurogenesis in the visual system of embryonic and adult zebrafish (Danio rerio). off. Vis. Neurosci. *16*, 417–424.

Marmier-Gourrier, N., Cléry, A., Schlotter, F., Senty-Ségault, V., and Branlant, C. (2011). A second base pair interaction between U3 small nucleolar RNA and the 5'-ETS region is required for early cleavage of the yeast pre-ribosomal RNA. Nucleic Acids Res. *39*, 9731–9745.

Marygold, S.J., Roote, J., Reuter, G., Lambertsson, A., Ashburner, M., Millburn, G.H., Harrison, P.M., Yu, Z., Kenmochi, N., Kaufman, T.C., et al. (2007). The ribosomal protein genes and Minute loci of Drosophila melanogaster. Genome Biol. *8*, R216.

Mason, P.J., and Bessler, M. (2011). The genetics of dyskeratosis congenita. Cancer Genet. *204*, 635–645.

Massenet, S., Bertrand, E., and Verheggen, C. (2016). Assembly and trafficking of box C/D and H/ACA snoRNPs. RNA Biol. 1–13.

Mauro, V.P., and Edelman, G.M. (2007). The ribosome filter redux. Cell Cycle Georget. Tex *6*, 2246–2251.

Mayer, C., Schmitz, K.-M., Li, J., Grummt, I., and Santoro, R. (2006). Intergenic transcripts regulate the epigenetic state of rRNA genes. Mol. Cell *22*, 351–361.

McLeod, C.J., Wang, L., Wong, C., and Jones, D.L. (2010). Stem cell dynamics in response to nutrient availability. Curr. Biol. CB *20*, 2100–2105.

McMahon, M., Contreras, A., and Ruggero, D. (2015). Small RNAs with big implications: new insights into H/ACA snoRNA function and their role in human disease. Wiley Interdiscip. Rev. RNA *6*, 173–189.

Mei, Y., Zhang, P., Zuo, H., Clark, D., Xia, R., Li, J., Liu, Z., and Mao, L. (2014). Ebp1 activates podoplanin expression and contributes to oral tumorigenesis. Oncogene *33*, 3839–3850.

Mejia Otero, C., Assassi, S., Hudson, M., Mayes, M.D., Estrada-Y-Martin, R., Pedroza, C., Mills, T.W., Walker, J., Baron, M., Stevens, W., et al. (2017). Antifibrillarin Antibodies Are Associated with Native North American Ethnicity and Poorer Survival in Systemic Sclerosis. J. Rheumatol.

Melén, K., Tynell, J., Fagerlund, R., Roussel, P., Hernandez-Verdun, D., and Julkunen, I. (2012). Influenza A H3N2 subtype virus NS1 protein targets into the nucleus and binds primarily via its C-terminal NLS2/NoLS to nucleolin and fibrillarin. Virol. J. *9*, 167.

Méndez, J. (2009). Temporal regulation of DNA replication in mammalian cells. Crit. Rev. Biochem. Mol. Biol. *44*, 343–351.

Mitchell, J.R., Wood, E., and Collins, K. (1999). A telomerase component is defective in the human disease dyskeratosis congenita. Nature *402*, 551–555.

Mizuseki, K., Kishi, M., Matsui, M., Nakanishi, S., and Sasai, Y. (1998). Xenopus Zic-related-1 and Sox-2, two factors induced by chordin, have distinct activities in the initiation of neural induction. Dev. Camb. Engl. *125*, 579–587.

Mochizuki, Y., He, J., Kulkarni, S., Bessler, M., and Mason, P.J. (2004). Mouse dyskerin mutations affect accumulation of telomerase RNA and small nucleolar RNA, telomerase activity, and ribosomal RNA processing. Proc. Natl. Acad. Sci. U. S. A. *101*, 10756–10761.

Mokrejs, M., Masek, T., Vopálensky, V., Hlubucek, P., Delbos, P., and Pospísek, M. (2010). IRESite--a tool for the examination of viral and cellular internal ribosome entry sites. Nucleic Acids Res. *38*, D131-136.

Montanaro, L., Chillà, A., Trerè, D., Pession, A., Govoni, M., Derenzini, M., and Tazzari, P.L. (2002). Increased Mortality Rate and Not Impaired Ribosomal Biogenesis is Responsible for Proliferative Defect in Dyskeratosis Congenita Cell Lines. J. Invest. Dermatol. *118*, 193–198.

Montanaro, L., Treré, D., and Derenzini, M. (2008). Nucleolus, ribosomes, and cancer. Am. J. Pathol. *173*, 301–310.

Montanaro, L., Treré, D., and Derenzini, M. (2012). Changes in ribosome biogenesis may induce cancer by down-regulating the cell tumor suppressor potential. Biochim. Biophys. Acta *1825*, 101–110.

Moody, S.A., Klein, S.L., Karpinski, B.A., Maynard, T.M., and Lamantia, A.-S. (2013). On becoming neural: what the embryo can tell us about differentiating neural stem cells. Am. J. Stem Cells *2*, 74–94.

Mullineux, S.-T., and Lafontaine, D.L.J. (2012). Mapping the cleavage sites on mammalian pre-rRNAs: Where do we stand? Biochimie *94*, 1521–1532.

N

Nakazawa, Y., Arai, H., and Fujita, N. (2011). The novel metastasis promoter Merm1/Wbscr22 enhances tumor cell survival in the vasculature by suppressing Zac1/p53-dependent apoptosis. Cancer Res. *71*, 1146–1155.

Naora, H., Takai, I., Adachi, M., and Naora, H. (1998). Altered Cellular Responses by Varying Expression of a Ribosomal Protein Gene: Sequential Coordination of Enhancement and Suppression of Ribosomal Protein S3a Gene Expression Induces Apoptosis. J. Cell Biol. *141*, 741–753.

Neumüller, R.A., Richter, C., Fischer, A., Novatchkova, M., Neumüller, K.G., and Knoblich, J.A. (2011). Genome-wide analysis of self-renewal in Drosophila neural stem cells by transgenic RNAi. Cell Stem Cell *8*, 580–593.

Newman, D.R., Kuhn, J.F., Shanab, G.M., and Maxwell, E.S. (2000). Box C/D snoRNA-associated proteins: two pairs of evolutionarily ancient proteins and possible links to replication and transcription. RNA N. Y. N *6*, 861–879.

Newton, K., Petfalski, E., Tollervey, D., and Cáceres, J.F. (2003). Fibrillarin is essential for early development and required for accumulation of an intron-encoded small nucleolar RNA in the mouse. Mol. Cell. Biol. *23*, 8519–8527.

Nguyen, V., Deschet, K., Henrich, T., Godet, E., Joly, J.S., Wittbrodt, J., Chourrout, D., and Bourrat, F. (1999). Morphogenesis of the optic tectum in the medaka (Oryzias latipes): a morphological and molecular study, with special emphasis on cell proliferation. J. Comp. Neurol. *413*, 385–404.

Ni, L., and Snyder, M. (2001). A genomic study of the bipolar bud site selection pattern in Saccharomyces cerevisiae. Mol. Biol. Cell *12*, 2147–2170.

Niehrs, C. (2004). Regionally specific induction by the Spemann-Mangold organizer. Nat. Rev. Genet. *5*, 425–434.

Niehrs, C. (2010). On growth and form: a Cartesian coordinate system of Wnt and BMP signaling specifies bilaterian body axes. Dev. Camb. Engl. *137*, 845–857.

Ninkovic, J., and Götz, M. (2014). A time and place for understanding neural stem cell specification. Dev. Cell *30*, 114–115.

Noack Watt, K.E., Achilleos, A., Neben, C.L., Merrill, A.E., and Trainor, P.A. (2016). The Roles of RNA Polymerase I and III Subunits Polr1c and Polr1d in Craniofacial Development and in Zebrafish Models of Treacher Collins Syndrome. PLoS Genet. *12*, e1006187.

Noller, H.F., Hoffarth, V., and Zimniak, L. (1992). Unusual resistance of peptidyl transferase to protein extraction procedures. Science *256*, 1416–1419.

Nomura, M., Nogi, Y., and Oakes, M. (2013). Transcription of rDNA in the Yeast Saccharomyces cerevisiae (Landes Bioscience).

Norris-Mullins, B., VanderKolk, K., Vacchina, P., Joyce, M.V., and Morales, M.A. (2014). LmaPA2G4, a homolog of human Ebp1, is an essential gene and inhibits cell proliferation in L. major. PLoS Negl. Trop. Dis. *8*, e2646.

O

Ochs, R.L., Lischwe, M.A., Spohn, W.H., and Busch, H. (1985). Fibrillarin: a new protein of the nucleolus identified by autoimmune sera. Biol. Cell *54*, 123–133.

O'Donohue, M.-F., Choesmel, V., Faubladier, M., Fichant, G., and Gleizes, P.-E. (2010). Functional dichotomy of ribosomal proteins during the synthesis of mammalian 40S ribosomal subunits. J. Cell Biol. *190*, 853–866.

Ohtake, Y., and Wickner, R.B. (1995). Yeast virus propagation depends critically on free 60S ribosomal subunit concentration. Mol. Cell. Biol. *15*, 2772–2781.

Oie, S., Matsuzaki, K., Yokoyama, W., Tokunaga, S., Waku, T., Han, S.-I., Iwasaki, N., Mikogai, A., Yasuzawa-Tanaka, K., Kishimoto, H., et al. (2014). Hepatic rRNA transcription regulates high-fat-diet-induced obesity. Cell Rep. *7*, 807–820.

Okada, M., Jang, S.-W., and Ye, K. (2007). Ebp1 association with nucleophosmin/B23 is essential for regulating cell proliferation and suppressing apoptosis. J. Biol. Chem. *282*, 36744–36754.

O'Leary, M.N., Schreiber, K.H., Zhang, Y., Duc, A.-C.E., Rao, S., Hale, J.S., Academia, E.C., Shah, S.R., Morton, J.F., Holstein, C.A., et al. (2013). The ribosomal protein Rpl22 controls ribosome composition by directly repressing expression of its own paralog, Rpl22l1. PLoS Genet. *9*, e1003708.

Oliveira-Carlos, V., Ganz, J., Hans, S., Kaslin, J., and Brand, M. (2013). Notch receptor expression in neurogenic regions of the adult zebrafish brain. PloS One *8*, e73384.

Omer, A.D., Ziesche, S., Ebhardt, H., and Dennis, P.P. (2002). In vitro reconstitution and activity of a C/D box methylation guide ribonucleoprotein complex. Proc. Natl. Acad. Sci. U. S. A. *99*, 5289–5294.

Osheim, Y.N., French, S.L., Keck, K.M., Champion, E.A., Spasov, K., Dragon, F., Baserga, S.J., and Beyer, A.L. (2004). Pre-18S ribosomal RNA is structurally compacted into the SSU processome prior to being cleaved from nascent transcripts in Saccharomyces cerevisiae. Mol. Cell *16*, 943–954.

Osumi, N., Shinohara, H., Numayama-Tsuruta, K., and Maekawa, M. (2008). Concise review: Pax6 transcription factor contributes to both embryonic and adult neurogenesis as a multifunctional regulator. Stem Cells Dayt. Ohio *26*, 1663–1672.

Ozair, M.Z., Kintner, C., and Brivanlou, A.H. (2013). Neural induction and early patterning in vertebrates. Wiley Interdiscip. Rev. Dev. Biol. *2*, 479–498.

P

Palade, G.E. (1955). A small particulate component of the cytoplasm. J. Biophys. Biochem. Cytol. *1*, 59–68.

Panov, K.I., Friedrich, J.K., and Zomerdijk, J.C. (2001). A step subsequent to preinitiation complex assembly at the ribosomal RNA gene promoter is rate limiting for human RNA polymerase I-dependent transcription. Mol. Cell. Biol. *21*, 2641–2649.

Parain, K., Mazurier, N., Bronchain, O., Borday, C., Cabochette, P., Chesneau, A., Colozza, G., El Yakoubi, W., Hamdache, J., Locker, M., et al. (2012). A large scale screen for neural stem cell markers in Xenopus retina. Dev. Neurobiol. *72*, 491–506.

Parenteau, J., Durand, M., Morin, G., Gagnon, J., Lucier, J.-F., Wellinger, R.J., Chabot, B., and Elela, S.A. (2011). Introns within ribosomal protein genes regulate the production and function of yeast ribosomes. Cell *147*, 320–331.

Peculis, B.A., and Steitz, J.A. (1993). Disruption of U8 nucleolar snRNA inhibits 5.8S and 28S rRNA processing in the Xenopus oocyte. Cell *73*, 1233–1245.

Pera, E.M., Acosta, H., Gouignard, N., Climent, M., and Arregi, I. (2014). Active signals, gradient formation and regional specificity in neural induction. Exp. Cell Res. *321*, 25–31.

Pestov, D.G., Strezoska, Z., and Lau, L.F. (2001). Evidence of p53-dependent cross-talk between ribosome biogenesis and the cell cycle: effects of nucleolar protein Bop1 on G(1)/S transition. Mol. Cell. Biol. *21*, 4246–4255.

Pfister, A.S., Keil, M., and Kühl, M. (2015). The Wnt Target Protein Peter Pan Defines a Novel p53-independent Nucleolar Stress-Response Pathway. J. Biol. Chem. *290*, 10905–10918.

Phair, R.D., and Misteli, T. (2000). High mobility of proteins in the mammalian cell nucleus. Nature *404*, 604–609.

Phipps, K.R., Charette, J.M., and Baserga, S.J. (2011). The small subunit processome in ribosome biogenesis—progress and prospects. Wiley Interdiscip. Rev. RNA *2*, 1–21.

Pianese, G., and Teuscher, R. (1896). Beitrag zur Histologie und Aetiologie des Carcinoms: histologische und experimentelle Untersuchungen (Jena: G. Fischer).

Pierfelice, T., Alberi, L., and Gaiano, N. (2011). Notch in the vertebrate nervous system: an old dog with new tricks. Neuron *69*, 840–855.

Pinto, L., and Götz, M. (2007). Radial glial cell heterogeneity--the source of diverse progeny in the CNS. Prog. Neurobiol. *83*, 2–23.

Ponti, D., Troiano, M., Bellenchi, G.C., Battaglia, P.A., and Gigliani, F. (2008). The HIV Tat protein affects processing of ribosomal RNA precursor. BMC Cell Biol. *9*, 32.

Preti, M., O'Donohue, M.-F., Montel-Lehry, N., Bortolin-Cavaillé, M.-L., Choesmel, V., and Gleizes, P.-E. (2013). Gradual processing of the ITS1 from the nucleolus to the cytoplasm during synthesis of the human 18S rRNA. Nucleic Acids Res. *41*, 4709–4723.

R

Rahmann, H. (1968). [Autoradiographic studies on the DNA metabolism (mitosis frequency) in the CNS of Brachydanio rerio Ham. Buch. (Cyprinidae, Pisces)]. J. Hirnforsch. *10*, 279–284.

Raible, F., and Brand, M. (2004). Divide et Impera--the midbrain-hindbrain boundary and its organizer. Trends Neurosci. *27*, 727–734.

Rakitina, D.V., Taliansky, M., Brown, J.W.S., and Kalinina, N.O. (2011). Two RNA-binding sites in plant fibrillarin provide interactions with various RNA substrates. Nucleic Acids Res. *39*, 8869–8880.

Ramagopal, S. (1990). Induction of cell-specific ribosomal proteins in aggregation-competent nonmorphogenetic Dictyostelium discoideum. Biochem. Cell Biol. Biochim. Biol. Cell. *68*, 1281–1287.

Ramagopal, S., and Ennis, H.L. (1981). Regulation of synthesis of cell-specific ribosomal proteins during differentiation of Dictyostelium discoideum. Proc. Natl. Acad. Sci. U. S. A. *78*, 3083–3087.

Ramialison, M., Reinhardt, R., Henrich, T., Wittbrodt, B., Kellner, T., Lowy, C.M., and Wittbrodt, J. (2012). Cis-regulatory properties of medaka synexpression groups. Dev. Camb. Engl. *139*, 917–928.

Rapacioli, M., Palma, V., and Flores, V. (2016). Morphogenetic and Histogenetic Roles of the Temporal-Spatial Organization of Cell Proliferation in the Vertebrate Corticogenesis as Revealed by Inter-specific Analyses of the Optic Tectum Cortex Development. Front. Cell. Neurosci. *10*, 67.

Rashid, R., Aittaleb, M., Chen, Q., Spiegel, K., Demeler, B., and Li, H. (2003). Functional requirement for symmetric assembly of archaeal box C/D small ribonucleoprotein particles. J. Mol. Biol. *333*, 295–306.

Raska, I., Koberna, K., Malínský, J., Fidlerová, H., and Masata, M. (2004). The nucleolus and transcription of ribosomal genes. Biol. Cell *96*, 579–594.

Raymond, P.A., and Easter, S.S. (1983). Postembryonic growth of the optic tectum in goldfish. I. Location of germinal cells and numbers of neurons produced. J. Neurosci. Off. J. Soc. Neurosci. *3*, 1077–1091.

Recher, G., Jouralet, J., Brombin, A., Heuzé, A., Mugniery, E., Hermel, J.-M., Desnoulez, S., Savy, T., Herbomel, P., Bourrat, F., et al. (2013). Zebrafish midbrain slow-amplifying progenitors exhibit high levels of transcripts for nucleotide and ribosome biogenesis. Dev. Camb. Engl. *140*, 4860–4869.

Reicherter, K., Veeramani, A.I., and Jagadeesh, S. (2011). Cartilage-hair hypoplasia caused by novel compound heterozygous RMRP mutations. Indian Pediatr. *48*, 559–561.

Reichow, S.L., Hamma, T., Ferré-D'Amaré, A.R., and Varani, G. (2007). The structure and function of small nucleolar ribonucleoproteins. Nucleic Acids Res. *35*, 1452–1464.

Reuter, R., Tessars, G., Vohr, H.W., Gleichmann, E., and Lührmann, R. (1989). Mercuric chloride induces autoantibodies against U3 small nuclear ribonucleoprotein in susceptible mice. Proc. Natl. Acad. Sci. U. S. A. *86*, 237–241.

Richter, C.A., Amin, S., Linden, J., Dixon, J., Dixon, M.J., and Tucker, A.S. (2010). Defects in middle ear cavitation cause conductive hearing loss in the Tcof1 mutant mouse. Hum. Mol. Genet. *19*, 1551–1560.

Rodriguez-Corona, U., Sobol, M., Rodriguez-Zapata, L.C., Hozak, P., and Castano, E. (2015). Fibrillarin from Archaea to human. Biol. Cell *107*, 159–174.

Romanova, L., Kellner, S., Katoku-Kikyo, N., and Kikyo, N. (2009). Novel role of nucleostemin in the maintenance of nucleolar architecture and integrity of small nucleolar ribonucleoproteins and the telomerase complex. J. Biol. Chem. *284*, 26685–26694.

Roussel, P., André, C., Comai, L., and Hernandez-Verdun, D. (1996). The rDNA transcription machinery is assembled during mitosis in active NORs and absent in inactive NORs. J. Cell Biol. *133*, 235–246.

Ruggero, D. (2013). Translational Control in Cancer Etiology. Cold Spring Harb. Perspect. Biol. *5*, a012336.

Ruggero, D., Grisendi, S., Piazza, F., Rego, E., Mari, F., Rao, P.H., Cordon-Cardo, C., and Pandolfi, P.P. (2003). Dyskeratosis Congenita and Cancer in Mice Deficient in Ribosomal RNA Modification. Science *299*, 259–262.

Russell, J., and Zomerdijk, J.C.B.M. (2005). RNA-polymerase-I-directed rDNA transcription, life and works. Trends Biochem. Sci. *30*.

Russo, A., and Russo, G. (2017). Ribosomal Proteins Control or Bypass p53 during Nucleolar Stress. Int. J. Mol. Sci. *18*.

Russo, A., Esposito, D., Catillo, M., Pietropaolo, C., Crescenzi, E., and Russo, G. (2013). Human rpL3 induces G_1/S arrest or apoptosis by modulating p21 (waf1/cip1) levels in a p53-independent manner. Cell Cycle Georget. Tex *12*, 76–87.

S

Sabelström, H., Stenudd, M., Réu, P., Dias, D.O., Elfineh, M., Zdunek, S., Damberg, P., Göritz, C., and Frisén, J. (2013). Resident neural stem cells restrict tissue damage and neuronal loss after spinal cord injury in mice. Science *342*, 637–640.

Sakai, D., and Trainor, P.A. (2009). Treacher Collins syndrome: unmasking the role of Tcof1/treacle. Int. J. Biochem. Cell Biol. *41*, 1229–1232.

Santoro, R., Li, J., and Grummt, I. (2002). The nucleolar remodeling complex NoRC mediates heterochromatin formation and silencing of ribosomal gene transcription. Nat. Genet. *32*, 393–396.

Sasano, Y., Hokii, Y., Inoue, K., Sakamoto, H., Ushida, C., and Fujiwara, T. (2008). Distribution of U3 small nucleolar RNA and fibrillarin during early embryogenesis in Caenorhabditis elegans. Biochimie *90*, 898–907.

Sauer, F.C. (1935). Mitosis in the neural tube. J. Comp. Neurol. *62*, 377–405.

Savino, R., and Gerbi, S.A. (1990). In vivo disruption of Xenopus U3 snRNA affects ribosomal RNA processing. EMBO J. *9*, 2299–2308.

Savino, T.M., Bastos, R., Jansen, E., and Hernandez-Verdun, D. (1999). The nucleolar antigen Nop52, the human homologue of the yeast ribosomal RNA processing RRP1, is recruited at late stages of nucleologenesis. J. Cell Sci. *112 (Pt 12)*, 1889–1900.

Schimmang, T., Tollervey, D., Kern, H., Frank, R., and Hurt, E.C. (1989). A yeast nucleolar protein related to mammalian fibrillarin is associated with small nucleolar RNA and is essential for viability. EMBO J. *8*, 4015–4024.

Schlosser, I., Hölzel, M., Mürnseer, M., Burtscher, H., Weidle, U.H., and Eick, D. (2003). A role for c-Myc in the regulation of ribosomal RNA processing. Nucleic Acids Res. *31*, 6148–6156.

Schmidt, R., Strähle, U., and Scholpp, S. (2013). Neurogenesis in zebrafish – from embryo to adult. Neural Develop. *8*, 3.

Schneider, D.A. (2012). RNA polymerase I activity is regulated at multiple steps in the transcription cycle: recent insights into factors that influence transcription elongation. Gene *493*, 176.

Schultz, A., Nottrott, S., Watkins, N.J., and Lührmann, R. (2006). Protein-protein and protein-RNA contacts both contribute to the 15.5K-mediated assembly of the U4/U6 snRNP and the box C/D snoRNPs. Mol. Cell. Biol. *26*, 5146–5154.

Schwanhäusser, B., Busse, D., Li, N., Dittmar, G., Schuchhardt, J., Wolf, J., Chen, W., and Selbach, M. (2011). Global quantification of mammalian gene expression control. Nature *473*, 337–342.

Seo, S., and Kroll, K.L. (2006). Geminin's double life: chromatin connections that regulate transcription at the transition from proliferation to differentiation. Cell Cycle Georget. Tex *5*, 374–379.

Seri, B., García-Verdugo, J.M., McEwen, B.S., and Alvarez-Buylla, A. (2001). Astrocytes give rise to new neurons in the adult mammalian hippocampus. J. Neurosci. Off. J. Soc. Neurosci. *21*, 7153–7160.

Seri, B., García-Verdugo, J.M., Collado-Morente, L., McEwen, B.S., and Alvarez-Buylla, A. (2004). Cell types, lineage, and architecture of the germinal zone in the adult dentate gyrus. J. Comp. Neurol. *478*, 359–378.

Shadel, G.S., Buckenmeyer, G.A., Clayton, D.A., and Schmitt, M.E. (2000). Mutational analysis of the RNA component of Saccharomyces cerevisiae RNase MRP reveals distinct nuclear phenotypes. Gene *245*, 175–184.

Sharma, K., and Tollervey, D. (1999). Base pairing between U3 small nucleolar RNA and the 5' end of 18S rRNA is required for pre-rRNA processing. Mol. Cell. Biol. *19*, 6012–6019.

Sharma, S., and Lafontaine, D.L.J. (2015). "View From A Bridge": A New Perspective on Eukaryotic rRNA Base Modification. Trends Biochem. Sci. *40*, 560–575.

Shaw, P.J., Beven, A.F., Leader, D.J., and Brown, J.W. (1998). Localization and processing from a polycistronic precursor of novel snoRNAs in maize. J. Cell Sci. *111 (Pt 15)*, 2121–2128.

Shin, J., Berg, D.A., Zhu, Y., Shin, J.Y., Song, J., Bonaguidi, M.A., Enikolopov, G., Nauen, D.W., Christian, K.M., Ming, G., et al. (2015). Single-Cell RNA-Seq with Waterfall Reveals Molecular Cascades underlying Adult Neurogenesis. Cell Stem Cell *17*, 360–372.

Shubina, M.Y., Musinova, Y.R., and Sheval, E.V. (2016). Nucleolar Methyltransferase Fibrillarin: Evolution of Structure and Functions. Biochem. Biokhimiia *81*, 941–950.

Signer, R.A.J., Magee, J.A., Salic, A., and Morrison, S.J. (2014). Haematopoietic stem cells require a highly regulated protein synthesis rate. Nature *509*, 49–54.

Simmons, A.M., Tanyu, L.H., Horowitz, S.S., Chapman, J.A., and Brown, R.A. (2008). Developmental and regional patterns of GAP-43 immunoreactivity in a metamorphosing brain. Brain. Behav. Evol. *71*, 247–262.

Sirri, V., Hernandez-Verdun, D., and Roussel, P. (2002). Cyclin-dependent kinases govern formation and maintenance of the nucleolus. J. Cell Biol. *156*, 969–981.

Sloan, K.E., Schneider, C., and Watkins, N.J. (2012). Comparison of the yeast and human nuclear exosome complexes. Biochem. Soc. Trans. *40*, 850–855.

Sloan, K.E., Mattijssen, S., Lebaron, S., Tollervey, D., Pruijn, G.J.M., and Watkins, N.J. (2013a). Both endonucleolytic and exonucleolytic cleavage mediate ITS1 removal during human ribosomal RNA processing. J. Cell Biol. *200*, 577–588.

Sloan, K.E., Bohnsack, M.T., and Watkins, N.J. (2013b). The 5S RNP couples p53 homeostasis to ribosome biogenesis and nucleolar stress. Cell Rep. *5*, 237–247.

Smirnov, E., Cmarko, D., Mazel, T., Hornáček, M., and Raška, I. (2016). Nucleolar DNA: the host and the guests. Histochem. Cell Biol. *145*, 359–372.

Snaar, S., Wiesmeijer, K., Jochemsen, A.G., Tanke, H.J., and Dirks, R.W. (2000). Mutational analysis of fibrillarin and its mobility in living human cells. J. Cell Biol. *151*, 653–662.

Sobol, M., Yildirim, S., Philimonenko, V.V., Marášek, P., Castaño, E., and Hozák, P. (2013). UBF complexes with phosphatidylinositol 4,5-bisphosphate in nucleolar organizer regions regardless of ongoing RNA polymerase I activity. Nucl. Austin Tex *4*, 478–486.

Southall, T.D., Gold, K.S., Egger, B., Davidson, C.M., Caygill, E.E., Marshall, O.J., and Brand, A.H. (2013). Cell-type-specific profiling of gene expression and chromatin binding without cell isolation: assaying RNA Pol II occupancy in neural stem cells. Dev. Cell *26*, 101–112.

Spriggs, K.A., Bushell, M., and Willis, A.E. (2010). Translational regulation of gene expression during conditions of cell stress. Mol. Cell *40*, 228–237.

Squatrito, M., Mancino, M., Donzelli, M., Areces, L.B., and Draetta, G.F. (2004). EBP1 is a nucleolar growth-regulating protein that is part of pre-ribosomal ribonucleoprotein complexes. Oncogene *23*, 4454–4465.

Stefanovsky, V.Y., Pelletier, G., Bazett-Jones, D.P., Crane-Robinson, C., and Moss, T. (2001). DNA looping in the RNA polymerase I enhancesome is the result of non-cooperative in-phase bending by two UBF molecules. Nucleic Acids Res. *29*, 3241–3247.

Sterling, P. (1988). The retina. An approachable part of the brain. Cell *53*, 175–176.

Stiewe, T., and Pützer, B.M. (2000). Role of the p53-homologue p73 in E2F1-induced apoptosis. Nat. Genet. *26*, 464–469.

Su, H., Xu, T., Ganapathy, S., Shadfan, M., Long, M., Huang, T.H.-M., Thompson, I., and Yuan, Z.-M. (2014). Elevated snoRNA biogenesis is essential in breast cancer. Oncogene *33*, 1348–1358.

Sugihara, Y., Honda, H., Iida, T., Morinaga, T., Hino, S., Okajima, T., Matsuda, T., and Nadano, D. (2010). Proteomic analysis of rodent ribosomes revealed heterogeneity

including ribosomal proteins L10-like, L22-like 1, and L39-like. J. Proteome Res. *9*, 1351–1366.

Suster, M.L., Kikuta, H., Urasaki, A., Asakawa, K., and Kawakami, K. (2009). Transgenesis in zebrafish with the tol2 transposon system. Methods Mol. Biol. Clifton NJ *561*, 41–63.

Szewczak, L.B.W., DeGregorio, S.J., Strobel, S.A., and Steitz, J.A. (2002). Exclusive interaction of the 15.5 kD protein with the terminal box C/D motif of a methylation guide snoRNP. Chem. Biol. *9*, 1095–1107.

T

Takagi, M., Absalon, M.J., McLure, K.G., and Kastan, M.B. (2005). Regulation of p53 translation and induction after DNA damage by ribosomal protein L26 and nucleolin. Cell *123*, 49–63.

Takahashi, T., Nowakowski, R.S., and Caviness, V.S. (1995). The cell cycle of the pseudostratified ventricular epithelium of the embryonic murine cerebral wall. J. Neurosci. Off. J. Soc. Neurosci. *15*, 6046–6057.

Tallafuss, A., and Bally-Cuif, L. (2003). Tracing of her5 progeny in zebrafish transgenics reveals the dynamics of midbrain-hindbrain neurogenesis and maintenance. Dev. Camb. Engl. *130*, 4307–4323.

Teng, T., Thomas, G., and Mercer, C.A. (2013). Growth control and ribosomopathies. Curr. Opin. Genet. Dev. *23*, 63–71.

Terns, M.P., and Terns, R.M. (2002). Small nucleolar RNAs: versatile trans-acting molecules of ancient evolutionary origin. Gene Expr. *10*, 17–39.

Tessarz, P., Santos-Rosa, H., Robson, S.C., Sylvestersen, K.B., Nelson, C.J., Nielsen, M.L., and Kouzarides, T. (2014). Glutamine methylation in Histone H2A is an RNA Polymerase I dedicated modification. Nature *505*, 564–568.

Than-Trong, E., and Bally-Cuif, L. (2015). Radial glia and neural progenitors in the adult zebrafish central nervous system. Glia *63*, 1406–1428.

Therizols, G., Laforêts, F., Marcel, V., Catez, F., Bouvet, P., and Diaz, J.-J. (2015). Ribosomal RNA Methylation and Cancer. In Epigenetic Cancer Therapy, (Elsevier), pp. 115–139.

Thiel, C.T., Mortier, G., Kaitila, I., Reis, A., and Rauch, A. (2007). Type and level of RMRP functional impairment predicts phenotype in the cartilage hair hypoplasia-anauxetic dysplasia spectrum. Am. J. Hum. Genet. *81*, 519–529.

Thomas, G. (2000). An encore for ribosome biogenesis in the control of cell proliferation. Nat. Cell Biol. *2*, E71-72.

Tollervey, D. (1996). Trans-acting factors in ribosome synthesis. Exp. Cell Res. *229*, 226–232.

Tollervey, D., Lehtonen, H., Jansen, R., Kern, H., and Hurt, E.C. (1993). Temperature-sensitive mutations demonstrate roles for yeast fibrillarin in pre-rRNA processing, pre-rRNA methylation, and ribosome assembly. Cell *72*, 443–457.

Topisirovic, I., and Sonenberg, N. (2014). Distinctive tRNA repertoires in proliferating versus differentiating cells. Cell *158*, 1238–1239.

Tozzini, E.T., Baumgart, M., Battistoni, G., and Cellerino, A. (2012). Adult neurogenesis in the short-lived teleost Nothobranchius furzeri: localization of neurogenic niches, molecular characterization and effects of aging. Aging Cell *11*, 241–251.

Tsai, R.Y.L., and Pederson, T. (2014). Connecting the nucleolus to the cell cycle and human disease. FASEB J. Off. Publ. Fed. Am. Soc. Exp. Biol. *28*, 3290–3296.

Tseng, H. (2006). Cell-type-specific regulation of RNA polymerase I transcription: a new frontier. BioEssays News Rev. Mol. Cell. Dev. Biol. *28*, 719–725.

Tseng, H., Chou, W., Wang, J., Zhang, X., Zhang, S., and Schultz, R.M. (2008). Mouse ribosomal RNA genes contain multiple differentially regulated variants. PloS One *3*, e1843.

Tycowski, K.T., Shu, M.D., and Steitz, J.A. (1996). A mammalian gene with introns instead of exons generating stable RNA products. Nature *379*, 464–466.

Tycowski, K.T., You, Z.H., Graham, P.J., and Steitz, J.A. (1998). Modification of U6 spliceosomal RNA is guided by other small RNAs. Mol. Cell *2*, 629–638.

V

Valdez, B.C., Henning, D., So, R.B., Dixon, J., and Dixon, M.J. (2004). The Treacher Collins syndrome (TCOF1) gene product is involved in ribosomal DNA gene transcription by interacting with upstream binding factor. Proc. Natl. Acad. Sci. U. S. A. *101*, 10709–10714.

Vesela, E., Chroma, K., Turi, Z., and Mistrik, M. (2017). Common Chemical Inductors of Replication Stress: Focus on Cell-Based Studies. Biomolecules *7*.

Vieira, C., Pombero, A., García-Lopez, R., Gimeno, L., Echevarria, D., and Martínez, S. (2010). Molecular mechanisms controlling brain development: an overview of neuroepithelial secondary organizers. Int. J. Dev. Biol. *54*, 7–20.

Volarevic, S., Stewart, M.J., Ledermann, B., Zilberman, F., Terracciano, L., Montini, E., Grompe, M., Kozma, S.C., and Thomas, G. (2000). Proliferation, but not growth, blocked by conditional deletion of 40S ribosomal protein S6. Science *288*, 2045–2047.

W

Waga, S., Hannon, G.J., Beach, D., and Stillman, B. (1994). The p21 inhibitor of cyclin-dependent kinases controls DNA replication by interaction with PCNA. Nature *369*, 574–578.

Walne, A.J., and Dokal, I. (2008). Dyskeratosis Congenita: a historical perspective. Mech. Ageing Dev. *129*, 48–59.

Wang, H., Boisvert, D., Kim, K.K., Kim, R., and Kim, S.H. (2000). Crystal structure of a fibrillarin homologue from Methanococcus jannaschii, a hyperthermophile, at 1.6 A resolution. EMBO J. *19*, 317–323.

Wang, H., Chen, X., He, T., Zhou, Y., and Luo, H. (2013). Evidence for tissue-specific Jak/STAT target genes in Drosophila optic lobe development. Genetics *195*, 1291–1306.

Warner, J.R. (1999). The economics of ribosome biosynthesis in yeast. Trends Biochem. Sci. *24*, 437–440.

Watanabe-Susaki, K., Takada, H., Enomoto, K., Miwata, K., Ishimine, H., Intoh, A., Ohtaka, M., Nakanishi, M., Sugino, H., Asashima, M., et al. (2014). Biosynthesis of ribosomal RNA in nucleoli regulates pluripotency and differentiation ability of pluripotent stem cells. Stem Cells Dayt. Ohio *32*, 3099–3111.

Watkins, N.J., and Bohnsack, M.T. (2012). The box C/D and H/ACA snoRNPs: key players in the modification, processing and the dynamic folding of ribosomal RNA. Wiley Interdiscip. Rev. RNA *3*, 397–414.

Watkins, N.J., Newman, D.R., Kuhn, J.F., and Maxwell, E.S. (1998). In vitro assembly of the mouse U14 snoRNP core complex and identification of a 65-kDa box C/D-binding protein. RNA N. Y. N *4*, 582–593.

Weijers, D., Franke-van Dijk, M., Vencken, R.J., Quint, A., Hooykaas, P., and Offringa, R. (2001). An Arabidopsis Minute-like phenotype caused by a semi-dominant mutation in a RIBOSOMAL PROTEIN S5 gene. Dev. Camb. Engl. *128*, 4289–4299.

Weiner, A.M.J., Scampoli, N.L., and Calcaterra, N.B. (2012). Fishing the Molecular Bases of Treacher Collins Syndrome. PLOS ONE *7*, e29574.

Weinstein, D.C., and Hemmati-Brivanlou, A. (1999). Neural induction. Annu. Rev. Cell Dev. Biol. *15*, 411–433.

Weinstein, L.B., and Steitz, J.A. (1999). Guided tours: from precursor snoRNA to functional snoRNP. Curr. Opin. Cell Biol. *11*, 378–384.

Wilkins, B.J., Lorent, K., Matthews, R.P., and Pack, M. (2013). p53-mediated biliary defects caused by knockdown of cirh1a, the zebrafish homolog of the gene responsible for North American Indian Childhood Cirrhosis. PloS One *8*, e77670.

Willardsen, M.I., and Link, B.A. (2011a). Cell biological regulation of division fate in vertebrate neuroepithelial cells. Dev. Dyn. Off. Publ. Am. Assoc. Anat. *240*, 1865–1879.

Willardsen, M.I., and Link, B.A. (2011b). Cell biological regulation of division fate in vertebrate neuroepithelial cells. Dev. Dyn. Off. Publ. Am. Assoc. Anat. *240*, 1865–1879.

Wong, Q.W.-L., Li, J., Ng, S.R., Lim, S.G., Yang, H., and Vardy, L.A. (2014). RPL39L is an example of a recently evolved ribosomal protein paralog that shows highly specific tissue expression patterns and is upregulated in ESCs and HCC tumors. RNA Biol. *11*, 33–41.

Woods, S.J., Hannan, K.M., Pearson, R.B., and Hannan, R.D. (2015). The nucleolus as a fundamental regulator of the p53 response and a new target for cancer therapy. Biochim. Biophys. Acta *1849*, 821–829.

Wulliman, M.F., Rupp, B., and Reichert, H. (2012). Neuroanatomy of the Zebrafish Brain: A Topological Atlas (Birkhäuser).

Wurst, W., and Bally-Cuif, L. (2001). Neural plate patterning: upstream and downstream of the isthmic organizer. Nat. Rev. Neurosci. *2*, 99–108.

X

Xu, Q., Holder, N., Patient, R., and Wilson, S.W. (1994). Spatially regulated expression of three receptor tyrosine kinase genes during gastrulation in the zebrafish. Dev. Camb. Engl. *120*, 287–299.

Xu, X., Xiong, X., and Sun, Y. (2016). The role of ribosomal proteins in the regulation of cell proliferation, tumorigenesis, and genomic integrity. Sci. China Life Sci. *59*, 656–672.

Xue, S., and Barna, M. (2012). Specialized ribosomes: a new frontier in gene regulation and organismal biology. Nat. Rev. Mol. Cell Biol. *13*, 355–369.

Xue, S., and Barna, M. (2015). Cis-regulatory RNA elements that regulate specialized ribosome activity. RNA Biol. *12*, 1083.

Y

Yanagida, M., Hayano, T., Yamauchi, Y., Shinkawa, T., Natsume, T., Isobe, T., and Takahashi, N. (2004). Human fibrillarin forms a sub-complex with splicing factor 2-associated p32, protein arginine methyltransferases, and tubulins alpha 3 and beta 1 that is independent of its association with preribosomal ribonucleoprotein complexes. J. Biol. Chem. *279*, 1607–1614.

Yang, L., Song, T., Chen, L., Kabra, N., Zheng, H., Koomen, J., Seto, E., and Chen, J. (2013). Regulation of SirT1-nucleomethylin binding by rRNA coordinates ribosome biogenesis with nutrient availability. Mol. Cell. Biol. *33*, 3835–3848.

Yelick, P.C., and Trainor, P.A. (2015). Ribosomopathies: Global process, tissue specific defects. Rare Dis. Austin Tex *3*, e1025185.

Yilmaz, Ö.H., Katajisto, P., Lamming, D.W., Gültekin, Y., Bauer-Rowe, K.E., Sengupta, S., Birsoy, K., Dursun, A., Yilmaz, V.O., Selig, M., et al. (2012). mTORC1 in the Paneth cell niche couples intestinal stem-cell function to calorie intake. Nature *486*, 490–495.

Yoon, A., Peng, G., Brandenburger, Y., Brandenburg, Y., Zollo, O., Xu, W., Rego, E., and Ruggero, D. (2006). Impaired control of IRES-mediated translation in X-linked dyskeratosis congenita. Science *312*, 902–906.

Yoshikawa, H., Komatsu, W., Hayano, T., Miura, Y., Homma, K., Izumikawa, K., Ishikawa, H., Miyazawa, N., Tachikawa, H., Yamauchi, Y., et al. (2011). Splicing factor 2-associated protein p32 participates in ribosome biogenesis by regulating the binding of Nop52 and fibrillarin to preribosome particles. Mol. Cell. Proteomics MCP *10*, M110.006148.

Young, S.K., and Wek, R.C. (2016). Upstream Open Reading Frames Differentially Regulate Gene-specific Translation in the Integrated Stress Response. J. Biol. Chem. *291*, 16927–16935.

Yuan, X., Zhou, Y., Casanova, E., Chai, M., Kiss, E., Gröne, H.-J., Schütz, G., and Grummt, I. (2005). Genetic inactivation of the transcription factor TIF-IA leads to nucleolar disruption, cell cycle arrest, and p53-mediated apoptosis. Mol. Cell *19*, 77–87.

Z

Zénon, A., and Krauzlis, R. (2014). [Superior colliculus as a subcortical center for visual selection]. Med. Sci. MS *30*, 637–643.

Zhang, Y., and Lu, H. (2009). Signaling to p53: ribosomal proteins find their way. Cancer Cell *16*, 369–377.

Zhang, Q., Shalaby, N.A., and Buszczak, M. (2014a). Changes in rRNA transcription influence proliferation and cell fate within a stem cell lineage. Science *343*, 298–301.

Zhang, X., Wang, W., Wang, H., Wang, M.-H., Xu, W., and Zhang, R. (2013a). Identification of ribosomal protein S25 (RPS25)-MDM2-p53 regulatory feedback loop. Oncogene *32*, 2782–2791.

Zhang, Y., Lu, Y., Zhou, H., Lee, M., Liu, Z., Hassel, B.A., and Hamburger, A.W. (2008). Alterations in cell growth and signaling in ErbB3 binding protein-1 (Ebp1) deficient mice. BMC Cell Biol. *9*, 69.

Zhang, Y., Duc, A.-C.E., Rao, S., Sun, X.-L., Bilbee, A.N., Rhodes, M., Li, Q., Kappes, D.J., Rhodes, J., and Wiest, D.L. (2013b). Control of hematopoietic stem cell emergence by antagonistic functions of ribosomal protein paralogs. Dev. Cell *24*, 411–425.

Zhang, Y., Ear, J., Yang, Z., Morimoto, K., Zhang, B., and Lin, S. (2014b). Defects of protein production in erythroid cells revealed in a zebrafish Diamond-Blackfan anemia model for mutation in RPS19. Cell Death Dis. *5*, e1352.

Zhao, R., Kakihara, Y., Gribun, A., Huen, J., Yang, G., Khanna, M., Costanzo, M., Brost, R.L., Boone, C., Hughes, T.R., et al. (2008). Molecular chaperone Hsp90 stabilizes Pih1/Nop17 to maintain R2TP complex activity that regulates snoRNA accumulation. J. Cell Biol. *180*, 563–578.

Zheng, L., Du, Z., Lin, C., Mao, Q., Wu, K., Wu, J., Wei, T., Wu, Z., and Xie, L. (2015). Rice stripe tenuivirus p2 may recruit or manipulate nucleolar functions through an interaction with fibrillarin to promote virus systemic movement. Mol. Plant Pathol. *16*, 921–930.

Zhou, H., Mazan-Mamczarz, K., Martindale, J.L., Barker, A., Liu, Z., Gorospe, M., Leedman, P.J., Gartenhaus, R.B., Hamburger, A.W., and Zhang, Y. (2010). Post-transcriptional regulation of androgen receptor mRNA by an ErbB3 binding protein 1 in prostate cancer. Nucleic Acids Res. *38*, 3619–3631.

Zhou, X., Liao, W.-J., Liao, J.-M., Liao, P., and Lu, H. (2015). Ribosomal proteins: functions beyond the ribosome. J. Mol. Cell Biol. *7*, 92–104.

Zhu, Y., Poyurovsky, M.V., Li, Y., Biderman, L., Stahl, J., Jacq, X., and Prives, C. (2009). Ribosomal protein S7 is both a regulator and a substrate of MDM2. Mol. Cell *35*, 316–326.

Zink, D. (2006). The temporal program of DNA replication: new insights into old questions. Chromosoma *115*, 273–287.

Zirwes, R.F., Eilbracht, J., Kneissel, S., and Schmidt-Zachmann, M.S. (2000). A novel helicase-type protein in the nucleolus: protein NOH61. Mol. Biol. Cell *11*, 1153–1167.

Zupanc, G.K.H., Hinsch, K., and Gage, F.H. (2005). Proliferation, migration, neuronal differentiation, and long-term survival of new cells in the adult zebrafish brain. J. Comp. Neurol. *488*, 290–319.

Zurita-Lopez, C.I., Sandberg, T., Kelly, R., and Clarke, S.G. (2012). Human protein arginine methyltransferase 7 (PRMT7) is a type III enzyme forming ω-NG-monomethylated arginine residues. J. Biol. Chem. *287*, 7859–7870.

Titre : Etude des facteurs de la biogenèse des ribosomes dans les progéniteurs neuraux de poisson zèbre

Mots clés : Biogenèse des ribosomes, Cycle cellulaire, Poisson-zèbre, Cellules neuroépithéliales

Résumé :
Alors que la biogénèse des ribosomes a été considérée comme un mécanisme ubiquiste, les étapes de ce processus ont récemment été démontrées comme étant tissu-spécifiques. Le toit optique (OT) du poisson-zèbre est un modèle approprié pour étudier la prolifération cellulaire puisque les cellules à différents états de différenciation se trouvent dans des domaines séparés.

Au cours de mon doctorat, j'ai examiné si les gènes de la biogenèse des ribosomes peuvent avoir des rôles spécifiques dans les cellules progénitrices neuroépithéliales (CPNe). Profitant d'une analyse transcriptomique antérieure, j'ai d'abord examiné les nouveaux candidats accumulés dans les CPNe. J'ai décidé de me concentrer sur *proliferation-associated 2G4* (*pa2G4/ebp1)* qui est exprimé de manière préférentielle dans les CPNe.

Ce gène favorise ou réprime la prolifération cellulaire dans des organismes normaux ou pendant la tumorigénèse. J'ai conçu une stratégie pour l'expression inductible et cellule-spécifique de ce gène.

Fibrillarin (Fbl), une petite méthyltranférase nucléolaire est également préférentiellement exprimée dans CPNe. Ce gène joue un rôle important dans le cancer. J'ai montré que les mutants *fbl* présentaient des défauts OT-spécifiques, en lien avec une apoptose massive et une absence de différenciation neurale. J'ai également démontré une diminution de l'activité de traduction des ribosomes. En outre, les mutants *fbl* montrent une progression de la phase S altérée. Nos données suggèrent que *fbl* est essentiel à la prolifération des progéniteurs neuraux du poisson-zèbre.

Title : Study of ribosome biogenesis factors in zebrafish neural progenitors

Keywords : Ribosome biogenesis, cell cycle, Zebrafish, Neuroepithelial Cells

Abstract :
While ribosome biogenesis has been considered as an ubiquitous mechanism, steps of this process have recently been shown to be tissue specific. Zebrafish optic tectum (OT) is a suitable model to study cell proliferation since cells at different differentiation states are spatially partitioned.

During my PhD, I examined whether ribosome biogenesis genes may have specific roles in neuroepithelial progenitor cells (NePCs). Taking advantage of a previous transcriptomic analysis, I first screened for new candidates accumulated in NePCs. I decided to focus on *proliferation-associated 2G4* (*pa2g4/ebp1)*, which was expressed preferentially in NePCs.

This gene promotes or represses cell proliferation in normal organisms or during tumorigenesis. I designed a strategy for the inducible expression and cell specific expression of this gene.

Fibrillarin (Fbl), a small nucleolar methyltransferase is also preferentially expressed in NePCs. It plays an important role in cancer. I showed that *fbl* mutants displayed specific OT defects linked to a massive apoptosis and an absence of neural differentiation. I also demonstrated deficiencies in the ribosome translational activity. Additionally, *fbl* mutants showed impaired S-phase progression. Our data suggest that *fbl* is essential for the proliferation of zebrafish neural progenitors.